Universidad Autónoma de Madrid

Facultad de Ciencias
Departamento de Física Teórica

Consejo Superior de Investigaciones Científicas

Instituto de Física Teórica
IFT UAM/CSIC

Entanglement Entropy and Non-relativistic Systems in the AdS/CFT correspondence

Carlos Alberto Fuertes Pascual

June 2009

PhD Thesis

Universidad Autónoma de Madrid

Facultad de Ciencias
Departamento de Física Teórica

Consejo Superior de Investigaciones Científicas

Instituto de Física Teórica
IFT UAM/CSIC

Entanglement Entropy and Non-relativistic Systems in the AdS/CFT correspondence

Memoria de Tesis Doctoral presentada ante la Facultad de Ciencias,
Sección de Ciencias Físicas, de la Universidad Autónoma de Madrid,
por **D. Carlos Alberto Fuertes Pascual**.

Trabajo dirigido por el Doctor **D. José Luis Fernández Barbón**,
Investigador Científico del Instituto de Física Teórica
y
Consejo Superior de Investigaciones Científicas.

Madrid, 7 de Mayo de 2009.

Agradecimientos

A todos aquellos que me han acompañado en este viaje. En especial a Pepe, mi director de tesis, por su dedicación, haberme enseñado Física en estado puro, por su guía y paciencia, porque sin él esta tesis no habría sido posible. A mis padres, ellos siempre me inculcaron el amor por el conocer y el trabajo, por las cosas bien hechas y el disfrutar haciéndolas, porque en todo ello reside gran parte de la riqueza de una persona. A mis compañeros del IFT y Autónoma presentes y pasados: Adolfo, Alfonso, Antón, Irene, Jacobo, Josemi, Meggi, Miguel, Sergio, el otro Sergio, Carlos, Guillermo, Johan, Florián, Giovanni, Mª Eugenia, Andrés y todo el resto con los que más o menos contacto he tenido pero que todos y cada uno de ellos hacen del IFT/UAM lo que es. Por esas comidas, el spam, y en definitiva el haber compartido el duro bregar que es sacar un paper y todos los días dar un pasito más hacia la tesis. Al resto de profesores del IFT y del Departamento: Karl, Esperanza, Patrick, Marga, Rafa, Jesús, Toni, Enrique, Luis y todos los que me dieron clase, siempre estuvieron dispuestos a discutir de Física y de los que también he aprendido. A las secretarias del IFT, Isabel, Yolanda, y las de la Autónoma, Juanca y Lola. A aquellos profesores de Salamanca, Fernando, Miguel Ángel y el resto que sentaron las bases en mí e hicieron que terminase aquí haciendo la tesis. A mis amigos, por esas cenas, cafés entre Madrid y Salamanca: Antonio, Jorge, Anna, Luismi. A los de la Complu, Dani, Alberto, Álvaro y Rubén. A arXiv y al proyecto GNU. A mi abuela Luisa y mi abuelo Jose Mari, porque sé que una de sus ilusiones es ver esta tesis terminada, y a mi abuela Gloria que no lo pudo ver pero siempre estuvo ahí con su ejemplo. Que el terminar no sea más que un comenzar.

Contents

Chapter 1

Introduction

During the last decade we have witnessed a revolution in the field of String Theory with the advent of the AdS/CFT correspondence or Maldacena conjecture [1]. String Theory in its inception was born as a model for mesons, later to be discarded in favor of Quantum Chromodynamics (QCD), and finally recognized as a consistent theory of Quantum Gravity. As such, before the Maldacena conjecture, String Theory was viewed as a possible candidate for a unified quantum theory of all known forces including gravity. Nevertheless after the work of Juan Maldacena in 1997 [1], it became apparent that String Theory could be seen independently as a dual theory of some Quantum Field Theory. This is a weak-strong duality. More precisely, the semiclassical approximation of String Theory, supergravity, in asymptotically anti-de-Sitter (AdS) spacetimes is dual to the strongly coupled regime of maximally supersymmetric Yang-Mills theories. And viceversa, the weakly coupled regime of these gauge theories is dual to the strongly coupled regime of String Theory. The AdS/CFT correspondence allows us the treatment of the non-perturbative regime of Quantum Field Theory by means of a weak-coupling, semiclassical limit of a gravity theory and at the same time gives us a non-perturbative definition of String Theory through a weakly coupled Quantum Field Theory. Gauge/gravity duality has become a useful tool for investigating strongly coupled field theories. This approach has already seen many successes giving a new understanding of various field theoretical phenomena in gauge theories like the confinement-deconfinement transition, chiral symmetry breaking, computation of transport coefficients in the plasma phase, etc. Between the most remarkable findings is the unexpected link between the universality of the physics of black holes and predictions of universal bounds on observables in the field theory side. One example is the ratio of the shear viscosity to entropy density [2]. The qualitative agreement between the predicted value of $1/4\pi$ and measured one for the plasmas created at the Relativistic Heavy Ion Collider (RHIC) indicates that the

gauge/gravity duality is useful for studies of QCD.

Nevertheless given the generality of the principles underlying the gauge/gravity correspondence, it seems natural to look for new systems and phenomena that are described by means of the gauge/gravity duality. This is a vastly unexplored territory since most efforts so far has focused on QCD and its supersymmetric cousins. However during the last two years new connections and theoretical studies have been established pointing to the usefulness of the gauge/gravity duality to other strongly correlated systems, particularly those coming from Condensed Matter Physics. The new phenomena include models of cold atom gases at unitarity [3, 4], superconductivity [5], superfluidity [6], quantum liquids [7, 8]. Most of them are related to long time unsolved hard problems in Condensed Matter Physics and as such any new progress would mean exciting new developments.

Quantum criticality

The application of the gauge/gravity duality into Condensed Matter is intimately connected with the existence of *quantum phase transitions* and their associated critical points [9]. They consist of phase transitions at zero temperature linked to a non-analytic change in the physical properties of the system when smoothly varying some parameter of the system, like applied magnetic field, pressure or doping.

As any phase transition, quantum phase transitions can be of different types. Our focus will be on the ones that are second order. For them the spectrum of energy excitations at criticality is gapless. In fact the energy gap Δ vanishes as

$$\Delta \sim J|g - g_c|^{z\nu} \,, \tag{1.0.1}$$

where g is the parameter we vary and g_c its critical value. At the same time the correlation length scale ξ diverges as

$$\xi^{-1} \sim \Lambda|g - g_c|^{\nu} \,. \tag{1.0.2}$$

The ratio of critical exponents in (1.0.1) and (1.0.2) gives the dynamical critical exponent z: the characteristic energy scale vanishes as the zth power of the characteristic inverse length scale

$$\Delta \sim \xi^{-z} \,. \tag{1.0.3}$$

The divergence of the correlation length of the system at the quantum critical point, indicates that the system becomes scale invariant. What is more the system can then be described effectively by a fixed point of a quantum field theory, with dynamical critical exponent z.

There are two possibilities for the $T > 0$ phase diagram of a system near a quantum critical point. The quantum critical point can be isolated or be the end point of a line of second order phase transitions at $T > 0$. In the case of an isolated quantum critical point, for $T > 0$ the systems presents a crossover. In the case of having a line of second order phase transitions, in the immediate vicinity of the line one can describe the system in terms of a classical theory for some order parameter that is narrower in its validity as we approach the quantum critical point.

In either case, the relevance of these quantum critical points comes from the fact that they can paradoxically dominate the phase diagram for $T > 0$. In regions where the deformation away from criticality due to an energy scale Δ is less important that the deformation due to the a finite temperature, i.e. $\Delta < T$, the system can be described by the finite temperature quantum critical point. This observation leads to the counterintuitive fact that the imprint of the zero temperature critical point grows as temperature is increased.

One example is found in the superfluid-insulator transition in two spatial dimensions [10]. One simple model for this is the the Bose Hubbard model at integer filling. It is described by the lattice Hamiltonian

$$H = -t \sum_{\langle ij \rangle} \left(b_i^\dagger b_j + b_j^\dagger b_i \right) + U \sum_i n_i (n_i - 1) \, , \tag{1.0.4}$$

where b_i are the annihilation operator for the different bosons. U is the on-site repulsion between the bosons, and t is the boson hopping matrix element. As a function of the ratio U/t, the system is in one of the two possible regimes, an insulator or a superfluid, both of which have an effective classical description of their dynamics and transport with a clear concept of quasiparticle. At small U/t, we are in the superfluid region and across the Kosterlitz-Thouless transition, we can use the Gross-Pitaevski equation to describe the spin-wave and vortex fluctuations. At large U/t the system behaves as an insulator and we have to consider the particle and hole excitations on the insulator. These are dilute enough at low T to allow a classical gas description via the Boltzmann equation. In the intermediate region we have a quantum phase transition and in its vicinity neither classical description is possible. The theory describing the quantum critical point happens to be a $2+1$ dimensional conformal field theory associated with the Wilson-Fisher fixed point, that can be realized in the familiar $\lambda \phi^4$ theory. In fact one can use this theory to describe the system around the critical point at finite temperature with a crossover to the other regimes. See Fig. 1.1.

The theory of the quantum critical region shows that the transport coefficients, and the relaxation time to local equilibrium, are not proportional to a mean free scattering time between the excitations, as is the case in the Boltzmann theory of quasiparticles [11]. Rather,

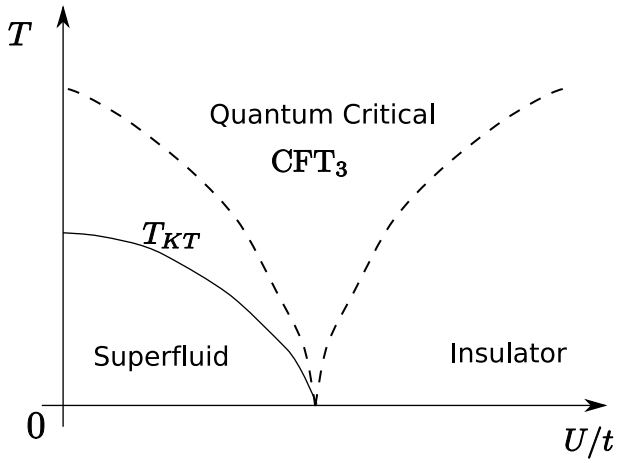

Figure 1.1: Phase diagram of the Bose Hubbard model at integer filling. Dashed lines are crossovers, while the full line is the Kosterlitz-Thouless transition at T_{KT}.

the system behaves like a perfect fluid in which the relaxation time is as short as possible, and is determined universally by the absolute temperature. The transport coefficients of this quantum-critical perfect fluid also do not depend upon the interaction strength, and can be connected to the fundamental constants of nature. Such are the examples of the electrical conductivity σ or momentum transport that related to the shear viscosity η (more precisely the ratio of viscosity to entropy density s), i.e.

$$\sigma = \frac{e_*^2}{h}\Phi_\sigma \ , \qquad \frac{\eta}{s} = \frac{\hbar}{k_B}\Phi_\eta \ , \tag{1.0.5}$$

with Φ_σ and Φ_η some numbers of order unity. e_* is the charge of the carriers.

Due to the lack of a quasiparticle picture and the strongly coupled regime, a direct computation of the observables from the QFT action is difficult. The only known approaches to extract some analytic predictions come from large N and $(d' - \varepsilon)$ expansions. However, both expansions are neither straightforward nor rigorous, and require a physically motivated resummation of the bare perturbative expansion to all orders. One would like to have exact solutions to quantum critical points where one could check the above results, as well as new tools that provide us with intuition on the possible phenomenology.

The AdS/CFT correspondence

Here is where the AdS/CFT correspondence makes its appearance as a handy tool to explore the surroundings of these quantum critical points.

We have seen that near quantum critical points, the systems can be described by means of

conformal field theories (at zero or finite temperature). What the AdS/CFT correspondence claims is that for certain type of CFTs in $d+1$ dimensions, one can give a weakly coupled description in terms of a classical gravity theory in AdS_{d+2}. More generically we have that a gravity theory in a spacetime in $d+2$ dimensions asymptoting to AdS_{d+2} is going to be dual to some $d+1$-dimensional QFT in its strong coupling regime and large N limit, with N a number of degrees of freedom, and that has an UV conformal fixed point. By means of this strong-weak duality one can then hope to explore and gain intuition of the QFT side, which is otherwise by conventional methods of difficult study.

The AdS/CFT correspondence is still a conjecture, no rigorous proof is known up to date.[1] Nonetheless overwhelming evidence in its favor has been gathered. We will do not try to motivate it once again, see for example [13], but will just highlight the backbone and the interplay of the different elements of the correspondence.

The AdS/CFT correspondence can be understood as a realization of the 'master field' approach [14] to the large N limit of gauge theories. In the large N limit one expects that the path integral be dominated by some saddle points whose contribution can be recast as saddle points of an effective classical action for some master field which, in principle, is unrelated to the UV gauge theory degrees of freedom. What the Maldacena conjecture tells us is that the classical saddle points belong to a gravitational theory in one more dimension. The extra dimension becomes a geometrization of the field theory energy scale and allows scale dependent phenomena such as confinement and temperature to be conceptualised in new ways.

In order to build controlled instances of the duality and the precise dictionary, one starts with a String Theory construction. It usually involves a stack of branes. The worldvolume theory at low energies is a gauge theory. On the other hand a sufficient number of branes will back-react on the geometry and a decoupling near-horizon limit gives you a spacetime that is then conjecture to encode the same physics as the worldvolume theory at low energies, the gauge theory. The paramount example is the duality between $\mathcal{N}=4$ SU(N) SYM in four dimensions and type IIB superstring on $\mathrm{AdS}_5 \times S^5$.

As a consequence of this type of constructions one ends up with a spacetime whose isometries match the global symmetries of the dual QFT. Additional R-symmetries are mapped to the isometries of compact manifolds. In the case of $\mathcal{N}=4$ SU(N) SYM, it is a CFT and hence the necessity of having AdS. The $SU(4)$ R-symmetry corresponds to the S^5.

One also obtains that the couplings and parameters of both the QFT and the gravity theory are completely fixed as a function of each other. In the gauge theory one has basically

[1] in spite of remarkable progress in this direction under the umbrella of integrability in the particular case of $\mathcal{N}=4$ SYM - $\mathrm{AdS}_5 \times S^5$ duality, see for an account [12] and references therein.

the Yang-Mills coupling $g_{\rm YM}$ and the rank of the gauge group N. In the large N limit they appear in the combination of the t'Hooft parameter $\lambda = g^2_{\rm YM}N$. On the other hand, the gravity theory has three parameters: the AdS radius R, the gravitational constant $G_N^{(d+2)}$ and the string length ℓ_s. For the particular case of $\mathcal{N} = 4$ SU(N) SYM one obtains

$$\frac{R^4}{l_s^4} = \lambda \ , \qquad \frac{R^8}{G_N^{(10)}} \sim N^2 \ . \tag{1.0.6}$$

From this we see that when the YM theory is weakly coupled ($\lambda \ll 1$), the spacetime is highly curved and viceversa. When the spacetime is weakly curved we can use the supergravity approximation to String Theory but the dual QFT is strongly coupled. From the second relation we also learn that in general we will have that

$$N_{\rm eff} \sim \frac{R^d}{G_N^{(d+2)}} \tag{1.0.7}$$

where $N_{\rm eff}$ is the number of effective gauge degrees of freedom and $G_N^{(d+2)}$ refers to the Newton's constant upon dimensional reduction along the compact manifold.

The duality also instructs us a very detailed relation between field in the gravity side and operators of the dual QFT. They can usually be identified by the rule that the non-normalizable modes of the fields at the boundary of the spacetime act as sources of their respective dual operators. In particular we have the equality of the partition functions between the gravity theory and the gauge theory, such that

$$Z_{\rm string}[\phi(x)|_{\rm boundary} = \phi_0(\vec{x})] = \langle e^{\int d^{d+1}\phi_0(\vec{x})\mathcal{O}(\vec{x}))}\rangle_{\rm QFT} \ . \tag{1.0.8}$$

Moreover conserved global currents in the QFT are dual to gauge fields. In the same way, the conservation of the energy-momentum tensor of the QFT (dual to the metric field) requires that the dual theory must contain gravity. Correlation functions can be computed by functional by taking functional derivatives on (1.0.8). They reduce to finding the solution to equations of motion of fields in the bulk that propagate from the boundary into the bulk, interact and go back to the boundary.

In order to put the theory at finite temperature, one introduces a black hole in the bulk with a Hawking temperature equal to the desired temperature of the dual QFT, but without modifying the asymptotics of the spacetime. One can still use (1.0.8) to compute correlation function at finite temperature, but in the case of real time (retarded or advanced Green's functions) one has to extend the prescription to pay attention to the boundary conditions for the fields at the horizon [15].

From the point of view of applications to Condensed Matter, this is very useful since it allows the computation of transport coefficients, such as σ and η, by just solving wave

equations in the black hole background. The dissipation and irreversibility associated with these transport coefficients emerges naturally from the irreversibility of matter falling past the horizon of the black hole. Even a simple saddlepoint treatment of the gravity theory already yields a CFT dynamics which has non-zero and non-singular transport coefficients, has positive entropy production, and relaxes to local thermal equilibrium. These are the features which make the AdS/CFT correspondence so attractive: they are unprecedented in previous mean-field theories of quantum many body systems.

Pioneered by the work of [16, 17], focused primarily on transport dynamics and coefficients, the application of the AdS/CFT to quantum phase transitions has been seen to be a useful tool. The main obstacle however is the disparity between the typical emergent gauge theories in the Condensed Matter systems, that are at most U(1) or even SU(2), and the large N approximation unavoidable in a dual gravity treatment. The results are not high precision predictions that can be blindly compared directly to experiment. Nonetheless they can be seen to provide invaluable insight by means of exactly solvable models of quantum critical points and, more importantly, to put at our disposal a new tool to explore the phenomenology of these systems.

It is in this line of thought where this thesis develops. We will put to work the AdS/CFT correspondence to study different aspects of these quantum critical points. In the first part we will use the duality to explore the structure of the ground states of critical points with $z = 1$. We will investigate it by means of the entanglement entropy. Thanks to the holographic prescription of Ryu and Takayanagi [18], we will be able to browse over the properties of the entanglement entropy in strongly coupled theories, see chapter 2 for a review. In particular we will elucidate the relation between the locality of the interactions and the area law in chapter 3. In chapter 4 we will systematically explore the different possible behaviour of the entanglement entropy in generic gravitational duals with $z = 1$.

In the second part of this thesis we will tackle a different aim and go after the study of extensions of the applicability of the AdS/CFT correspondence to other types of quantum critical points. So far the only class of backgrounds that have been thoroughly studied in the literature correspond to theories with a dynamical critical exponent $z = 1$. They are precisely the ones that asymptote to AdS: the scale invariance is under transformations that treat space and time in an equal footing. However there are other (somewhat exotic) critical points with $z \neq 1$. One particular example arises as an isolated critical point at $T = 0$ in three-dimensional non-relativistic Fermi gas near a Feshbach resonance. This fixed point was shown [19] to have a non-relativistic conformal symmetry (the Schrödinger group) with $z = 2$. What we will do in the second part is study precisely the recent constructions of dual

gravitational theories implementing the Schrödinger group [3, 4], see chapter 5 for a review. In particular we will study its Hamiltonian formulation (chapter 6), its correlation functions (chapter 7) and in the end we will undertand in terms of a simple statistical model its known thermodynamics which are different from fermions at unitarity (chapter 8). Finally, summary and concluding remarks are given in chapter 9.

The work presented in this thesis is based on the author's papers [20, 21, 22, 23, 24].

Part I: Entanglement Entropy

Chapter 2

Entanglement Entropy

In this chapter we will introduce the concept of entanglement entropy and its uses in the context of quantum field theory (QFT) as well as a prescription to compute it in holographic duals of QFTs. We will mainly review results available in the literature. In the first section we will give a general overview of entanglement entropy. Then we will focus of how to compute it and what is known about it in QFT. These results apply to (conformal) theories in 1+1 dimensions and free theories in higher dimensions. Then we will present a prescription to calculate the entanglement entropy from holographic duals, expanding much more what can be learnt in interacting theories. We will present the evidence in favor of this holographic ansatz as well as the results one obtains for (strongly interacting) conformal field theories in arbitrary dimension.

2.1 Entanglement entropy: an overview

Among the postulates of Quantum Mechanics, there is a basic postulate on many-body states: the Hilbert space of a many-body state is the tensor product of the Hilbert space of the individual components [25]. This postulate sets the possible structure of many-body quantum states and makes it radically different from the classical one. The key new ingredient breaking our classical intuition is the possibility of having *entanglement*. Entanglement can be defined as the failure of a multi-particle state to factorize into a tensor product of pure single particle states, i.e.

$$|\psi\rangle = \sum_{i,j,\ldots,k} c_{ij\ldots k} |\psi_i\rangle \otimes |\psi_j\rangle \otimes \cdots \otimes |\psi_k\rangle \neq |a\rangle \otimes |b\rangle \otimes \cdots \otimes |c\rangle \ . \tag{2.1.1}$$

The existence of entangled states is at the heart of some of the deepest puzzles of Quantum Mechanics and its most promising applications.

The most immediate depart from the classical world allowed by entanglement is the violation of Einstein's locality principle [26]. In Einstein's own words: "But on one supposition we should, in my opinion, absolutely hold fast: The real factual situation of the system S_1 is independent of what is done with the system S_2, which is spatially separated from the former." This violation can be experimentally demonstrated through the violation of Bell's inequalities that incidentally also shows the breakdown of the assumption of local realism. On the other hand entanglement arises as a new precious resource that is at the basis of quantum information and quantum computing [25]. It enables phenomena such as quantum teleportation, superdense coding, ... As such there is a new practical need coming from these emerging fields to better study, classify and quantify the entanglement in multi-partite system and its availability to transformation and distillation.

Having said this, we can consider entanglement as a key characteristic that sets aside classical versus quantum many-body states. Traditionally one characterizes a state by its correlation functions, response under external perturbations, etc. However we can directly study the proper "quantum structure" of a state by its entanglement. The quantum complexity of a state can be given in terms of its entanglement structure. Hence the logical question to pose is: can we measure or give a precise number to the entanglement encoded in a state? or even better, how can we generically characterize its entanglement structure?

For the case of pure bipartite systems the answer is well known. Furthermore it is unique upon imposing some natural requirements to the entanglement measure [27]. If we consider a pure state of a two-body system, given by the two parts A and B, that we denote by $|\psi_{AB}\rangle$, and we have an orthonormal basis for each subsystem $\{|\varphi_{A,i}\rangle\}$ and $\{|\phi_{B,j}\rangle\}$, we can write down what is called its Schmidt decomposition as

$$|\psi_{AB}\rangle = \sum_i \alpha_i |\varphi_{A,i}\rangle |\phi_{B,i}\rangle \ . \tag{2.1.2}$$

Then the corresponding reduced density operators are

$$\rho_B = \mathrm{tr}_A(|\psi_{AB}\rangle) = \sum_i \alpha_i^2 |\phi_{B,i}\rangle\langle\phi_{B,i}| \tag{2.1.3}$$

and

$$\rho_A = \mathrm{tr}_B(|\psi_{AB}\rangle) = \sum_i \alpha_i^2 |\varphi_{A,i}\rangle\langle\varphi_{A,i}| \ . \tag{2.1.4}$$

Both reduced density matrices have the same structure. The key observation is that for a pure state the reduced density is pure. We can impose that the entanglement measure, E, satisfies: 1) E is invariant under local operations, 2) E is continuous and 3) E is additive, in the sense that when several copies of the system are present $E(|\psi_{AB}\rangle \otimes |\phi_{AB}\rangle) = E(|\psi_{AB}\rangle) +$

$E(|\phi_{AB}\rangle)$. The unique measure satisfying these properties is called the *entanglement entropy* and corresponds to the von Neumann entropy of the reduced density matrices,

$$S(\rho_A) = -\mathrm{tr}_A\, \rho_A \ln \rho_A = -\sum_i \alpha_i^2 \ln \alpha_i^2 = -\mathrm{tr}_B\, \rho_B \ln \rho_B = S(\rho_B)\ . \tag{2.1.5}$$

As an example one can consider a two particle spin-$\frac{1}{2}$ system in the pure state $|\psi\rangle = \cos\theta|\uparrow\downarrow\rangle - \sin\theta|\uparrow\downarrow\rangle$. The entanglement entropy is given by $S(\rho_A) = -\cos^2\theta \ln\cos^2\theta - \sin^2\theta \ln\sin^2\theta$ that is maximum when $\cos^2\theta = \frac{1}{2}$ corresponding to the expected singlet state. Even more one can show [28] that when one has M copies of the state available, by making operations on only one subsystem one can produce $M' < M$ which are maximally entangled, where the optimal conversion ratio M'/M is given by S_A for large M. One can think of the numerical value of the entanglement entropy as the one corresponding to the number of maximally entangled pairs (each weighted by $\ln 2$) between the two systems.

Intuitively one considers the entropy as a measure of our lack of information of the system, related to the exact microstate out of all the compatible ones to the current macrostate. However in quantum mechanics, even for a pure state, we see the appearance of another entropy which is not related to our lack of knowledge of the exact state of the system. Here the entropy arises becase of the entanglement in the state. When tracing out over one subsystem we lose knowledge about it and due to the entanglement with the rest of the system, we unavoidably lose information on the remaining part.

In the case when one has a many-body or multi-partite system, things are less well understood. When we have a many-body or multi-partite system we are dealing with a quantum system with many degrees of freedom such as spin chains, lattice models of QFTs and QFTs themselves. For them there are different inequivalent proposals for measuring the entanglement, and the classification of entanglement and its quantification is an open problem (see for example [27]).

However one can proceed and use a direct generalization of the bipartite entanglement entropy for a many-body system. When we have a multipartite system we can follow the approach to consider different bipartitions of the whole system and study its associated entanglement entropy. We divide the system into two distinctive regions A and B in coordinate space, like in Fig. 2.1, and introduce the *entanglement entropy* or *geometric entropy* for that bipartition as the von Neuman entropy associated to the reduced density matrix for one of the two regions,

$$S_A = -\mathrm{tr}_A\, \rho_A \ln \rho_A\ . \tag{2.1.6}$$

The result is independent of which of the two regions we take. In the following we will use the word entanglement entropy as a synonym to geometric entropy, to which all our discussion

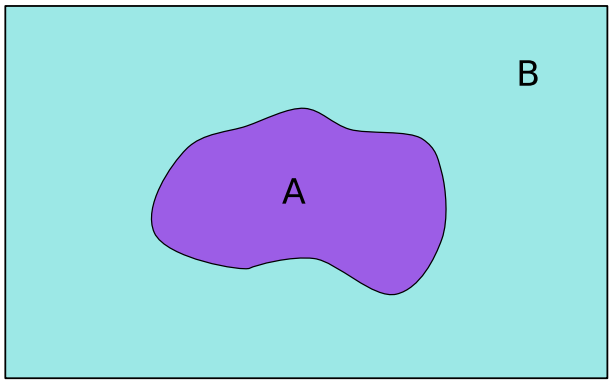

Figure 2.1: Bipartion of a system in two complementary regions A and B.

refers. We assume implicitly that we can introduce a basis of localized degrees of freedom in coordinate space over which we can trace over, as can be done in a quantum field theory.

The basic properties of the entanglement entropy are that (i) $S_A = S_B$ where B is the complement of the region A and (ii) $S_{A_1} + S_{A_2} \geq S_{A_1 \cup A_2} + S_{A_1 \cap A_2}$, that is strong subadditivity, where $A_{1,2}$ are two different regions [25].

Historically the consideration of the geometric entropy was born in the context of black hole physics [29, 30, 31, 32, 33, 30]. One would consider the interior of the black hole as the region over which we trace the degrees of freedom out, while the observer measures the remaining entropy of the outer region. The remarkable finding was that for a free relativistic scalar in flat space, the entanglement entropy was seen to follow an area law [31, 32], in the sense that the entanglement entropy was proportional to the area of the boundary of the region divided by some ultraviolet cutoff area, in a way analogously to the Bekenstein-Hawking entropy of a black hole [34, 35]. This set the pace for some speculation of whether one could ascribe the whole entropy of a black hole to be a consequence of the entanglement [29, 36, 37, 38, 39] — or at least some correction to it as a renormalization of the gravitational constant. After the success of stringy constructions to reproduce the (BPS) black hole entropy as a standard counting of underlying microstates [40], the original proposal of explaining the black entropy as pure entanglement was relaxed and seen more as a subleading contribution. Nonetheless later in the context of AdS/CFT there were some proposals of explaining the entropy of eternal black holes [41] (see also [42]) or deSitter entropy [43] as the entanglement entropy of two copies of the the dual CFT describing the whole system. See also [44] for a work about the entropy of black-holes not centered in AdS in terms of purely entanglement entropy.

Nowadays the study of the properties of the entanglement entropy have enjoyed a revival (initiated in [45, 46, 47, 48]), benefited from the new perspectives and ideas of quantum

information, quantum phase transitions and from the realization of their significance for the understanding of classical numerical methods and their efficiency in simulating quantum many-body physics.

To answer the question of what is the role of entanglement, viewed as genuine quantum correlations, in quantum many-body systems, one is interested in the *scaling* of the entanglement entropy. A priori the scaling of the entanglement entropy with the size of the region is very different from the scaling or the two-point function and is also capable of reflecting to a large extent the critical behaviour of the system and its properties.

Naively one would think that the entanglement entropy is going to be extensive in the volume of the region under consideration. This would be a volume scaling typical of the observed one in thermal states. In fact this is the typical scaling of the entanglement entropy of a randomly chosen state of the whole (unphysical) Hilbert space [49, 50, 51].[1] However, surprisingly for typical ground states one encounters an *area law* or an area law with logarithmic corrections: the scaling of the geometric entropy is merely linear in the boundary area of the region [52].

Area laws say something quite profound on how quantum correlations are distributed in states of local quantum many-body systems. The emergence of an area law support the intuitive idea that short range interactions require that quantum correlations are also short ranged. This on the other hand is by no means obvious from the decay of two-point correlators. Also we can use the entanglement entropy as an observable that signals criticality on the behaviour of the entanglement and quantum correlations in quantum phase transitions [9]. However it is fair to say that the study of entanglement close to a quantum critical point does not provide new understanding to the scaling theory of quantum phase transitions but rather may be useful for a deeper characterization of the ground state of the many-body system at criticality. This situation is now clear in one-dimensional systems but much less in higher dimensions where only rigorous results are known for quasi-free bosons and fermions as well as disordered systems.

From a point of view of quantum information understanding of the scaling of the entropy as a function of the size of the region has important consequences on the efficient simulability of a quantum system by a classical algorithm (see for example [53, 54, 55, 56]). The key

[1] As an example to understand this, one can consider a one-dimensional $\frac{1}{2}$-spin chain. A random state of the chain will consists of products of singlets formed from random pairs of sites as well as unpaired spins. We can consider the entanglement entropy of one half of the chain with respect to the remaining part. The entanglement entropy basically measures the number of singlets formed across the two regions. If the singlets are formed randomly (we take a random state), the number of singlets across the boundary are going to be proportional to the size of the region and thus the entanglement entropy is going to satisfy a volume law.

fact is that area-law states are a polynomial subset of the exponentially large set of many-body states. The simulation of a quantum system can usually be considered to consist on the optimization of $\langle\psi|H|\psi\rangle$ with $|\psi\rangle \in (\mathbb{C}^d)^{\otimes n}$. This problem is impractical due to the fact that we have to deal with an exponential set. However for systems satisfying an area law we can replace it by an optimization problem over a polynomially large set of states that are the ones that by construction satisfy the area law. This is the root of the success of the density-matrix renormalization group (DMRG) method [57, 58] in the treatment of interacting quantum chains, that is based on a decomposition in terms of matrix-product-states (MPS) [59, 60, 61, 62, 63]. The matrix product states form a restrictive basis of states that satisfy an area law by construction in one dimension. Attempts are under way to generalize the DMRG to higher dimensions through what is called PEPS states [64].

In one dimension the area law implies that the entanglement entropy is independent of the block size, $S_\ell \sim$ cte. This has been rigorously proven in the case of a gapped quantum-chain (away from quantum criticality) [65]. In the gapless case, when the correlation length is infinite, i.e. at a critical quantum point, diverging logarithmic corrections appear and the prefactor of the entanglement entropy is universal, related to the central charge of the underlying conformal field theory [66]. That is $S_\ell \sim \ln \ell/a$, where a is the lattice spacing (an UV cutoff) and ℓ is the size of the block. Slightly away from criticality, when the correlation length is finite but much bigger that the lattice spacing, $\xi \gg a$, the entanglement entropy is still logarithmic divergent but saturates to a finite value, $S_\ell \sim \ln \xi/a$.

In higher-dimensions only the case of quasi-free bosons [67, 68, 69] and fermions [70, 71, 72] has been rigorously studied. One basically finds an area law. In lattice systems the bosonic case satisfies an strict area law, $S_\ell \sim \ell^{d-1}$, whereas the fermionic case has logarithmic corrections $S_\ell \sim \ell^{d-1} \ln \ell$ [71, 72], where d is the number of spatial dimensions and ℓ is the scale of the region measured in lattice units. In the case of criticality, the bosonic system still satisfies an strict area law, $S_\ell \sim \ell^{d-1}/a^{d-1}$, provided we introduce an UV cutoff, a. Whereas for critical fermionic systems one still finds logarithmic corrections, $S_\ell \sim \ell^{d-1} k_F^{d-1} \ln \ell/a$, with k_F the Fermi momentum. However when the Fermi-surface is zero-dimensional, one recovers an strict area law $S_\ell \sim \ell^{d-1}/a^{d-1}$ [73]. In the case of continuum interacting systems very little is known analytically but in the known cases it still satisfies the area law [74, 75, 76].

If one computes the entanglement entropy at finite temperature, one finds that it satisfies a volume law. This is immediate from the fact that the system that we start with is in a mixed state. By definition the entanglement entropy is also measuring the thermal entropy of the part of the system that we consider and hence it becomes an extensive quantity, as any thermal entropy.[2] To properly measure the entanglement at finite temperature one

[2] In fact when the region is the whole system the entanglement entropy coincides with the thermal entropy.

introduces the *mutual information* [25]

$$I = S_A + S_B - S_{A\cup B} \tag{2.1.7}$$

At zero temperature it coincides with the entanglement entropy, whereas at finite temperature it cancels the contribution from the thermal entropy. Using methods of quantum information, the mutual information has been demonstrated to obey an area law for systems with a finite correlations length [77].

Entanglement entropy has also arisen as a candidate of an order parameter for exotic phases that are beyond the Ginzburg-Landau paradigm. These phases cannot be characterized by any classical order parameter of any kind. One of these instances that have been found is topological order (in two spatial dimensions)[78, 79, 80, 81, 82] for which entanglement entropy has appeared to be a good indicator. One way to see when topological order is present, is that the ground state of the systems presents a degeneracy dependent on the genus of the spatial manifold where it lives [83]. It also allows the fractionalization of quantum numbers, the presence of anyons (the key ingredient for topological quantum computation [84]), etc. This clearly is a new kind of order in quantum many-body systems that cannot be described by local order parameters. After the work of [79, 80], it is now established that the presence of topological order manifests itself in the entanglement entropy as a subleading universal constant correction, γ, to the area law

$$S_\ell = \alpha\ell - \gamma + \mathcal{O}(\ell^{-1}) \tag{2.1.8}$$

The part $\alpha\ell$ is the typical contribution of the area law in two dimensions, with α a non-universal constant. In contrast, the quantity γ can be expressed as $\ln D$, where D is known as the *total quantum dimension* of the system which is an universal quantity. Using methods of topological field theory one can find exact expressions for γ [85].

2.2 Entanglement entropy in Quantum Field Theory

After having seen an overview of entanglement in the general context of quantum many-body systems, let us focus on how we can compute the entanglement entropy in quantum field theory and what is exactly known.

QFTs can be understood as many-body systems at criticality (or at criticality perturbed with some mass operator). For them the exact statement of the area law is that the behaviour

Also at finite temperature is not longer true that $S_A = S_B$ where B is the complement of the region A, since we have a mixed state.

of the entanglement entropy is

$$S_A = \gamma \frac{|\partial A|}{a^{d-1}} + \text{subleading terms} \tag{2.2.1}$$

That is, we have a non-universal (divergent) contribution, dependent on some UV cutoff of the theory a, and that is proportional to the area of the boundary and to the number of degrees of the theory. The subleading terms are universal terms (they do not depend on any UV cutoff) and in principle depend on the scales of the theory and size of the region. In a strong version of the area law, the universal subleading terms would be also proportional to the area, as is the case of the free theory. Nevertheless as will discuss later this is not always necessarily the case. In order to study the universal subleading terms one introduces the entropic C-function [86, 87, 88],

$$C(\ell) = \ell \frac{dS_A(\ell)}{d\ell} \,, \tag{2.2.2}$$

where ℓ is the size scale of the A. The entropic C-function is equivalent to considering a renormalized entanglement entropy where the divergent (non-universal) piece has been cut off. In our discussion we will consider as synonyms renormalized entanglement entropy and entropic C-function.

In order to compute the entanglement entropy we will use the *replica trick*. If we start from a system in a pure state $|\psi\rangle$, the entanglement entropy of a region A and the rest of the system B is given by

$$S_A = -\mathrm{tr}_A \, \rho_A \ln \rho_A \,. \tag{2.2.3}$$

If we denote the eigenvalues of the reduced density matrix ρ_A as $\{\lambda_j\}$, we can rewrite this expression as

$$S_A = -\sum_j \lambda_j \ln \lambda_j \,. \tag{2.2.4}$$

But now using that

$$\zeta(n) = \sum_j {\lambda_j}^n = \sum_j e^{n \ln \lambda_j} \quad , \qquad \left.\frac{d\zeta(n)}{dn}\right|_{n=1} = \sum_j \lambda_j \ln \lambda_j \quad , \tag{2.2.5}$$

it is immediate that one can rewrite the entanglement entropy as

$$S_A = -\lim_{n\to 1} \frac{\partial}{\partial n} \mathrm{tr}_A \, \rho_A^n \quad . \tag{2.2.6}$$

Since $\mathrm{tr}_A \rho_A^n = \sum_j \lambda_j^n$, with $\lambda_j \in [0,1)$, and $\mathrm{tr}_A \, \rho_A = 1$, it follows that $\mathrm{tr}_A \rho_A^n$ is absolutely convergent and therefore convergent analytic for all $\mathrm{Re}\, n > 1$ and its derivative with respect to n exists.

The replica expression of the entanglement entropy, eq. (2.2.6), can be recast into a path integral of the original theory on an n-sheeted Euclidean space. Consider a complete set of local commuting observables $\left\{\hat{\phi}(x)\right\}$ with eigenvalues $\{\phi(x)\}$ and eigenstates $\otimes_x|\{\phi(x)\}\rangle$. The path integral expression for the density matrix ρ (at time $t=0$) is

$$\begin{aligned}\rho[\phi^+(x'),\phi^-(x'')] &= (Z_1)^{-1}\langle\phi^+(x')|\rho|\phi^-(x'')\rangle \\ &= (Z_1)^{-1}\int \mathcal{D}\phi(x,t)\, e^{-S_E}\prod_x \delta(\phi(x,0^+)-\phi^+(x'))\delta(\phi(x,0^-)-\phi^-(x''))\end{aligned} \tag{2.2.7}$$

where S_E is the Euclidean action of the theory and Z_1 is the usual vacuum partition function of the theory on $\mathbb{R}\times X_d$, with X_d the spatial manifold where the theory lives. The effect of tracing over the degrees of freedom on B can be taken into account by imposing that for $x\in B$, the fields satisfy $\phi(x,0^+)=\phi(x,0^-)$, giving us ρ_A,

$$\rho_A[\phi^+(x'),\phi^-(x'')] = (Z_1)^{-1}\int \mathcal{D}\phi(x,t)\, e^{-S_E}\prod_{x\in A} \delta(\phi(x,0^+)-\phi^+(x'))\delta(\phi(x,0^-)-\phi^-(x'')) \tag{2.2.8}$$

where now $\phi^+(x'),\phi^-(x'')$ are restricted to A. We may then compute $\mathrm{tr}_A\,\rho_A^n$ by making n-copies of the above and sewing them together through $\phi_k^+(x)=\phi_{k+1}^-(x)$ with $1\le k<n$ and $\phi_n^+(x)=\phi_1^-(x)$, for $x\in A$ and integrate over the $\phi_j^+(x)$. The result is that $\mathrm{tr}_A\rho_A^n$ is given in terms of a path integral over an n-sheeted Riemann hypersurface $\mathcal{R}_n$,

$$\mathrm{tr}_A\,\rho_A^n = (Z_1)^{-n}\int_{x\in\mathcal{R}_n}\mathcal{D}\phi\, e^{-S_E} = \frac{Z_n}{(Z_1)^n}\ . \tag{2.2.9}$$

If we were at finite temperature, to calculate $\mathrm{tr}_A\,\rho_A^n$ one should impose periodic boundary conditions in the 'time' direction with period $n\beta$ if $x\in A$ and period β otherwise, and compute the partition function integrating over the fields as in the zero temperature case.

Thus in the end we arrive to

$$S_A = -\lim_{n\to 1}\frac{\partial}{\partial n}\frac{Z_n}{(Z_1)^n}\ , \tag{2.2.10}$$

where Z_n is the partition function of the theory on the n-sheeted Riemann manifold $\mathcal{R}_n$ and Z_1 is the usual partition function on $\mathbb{R}^{d+1}$.

In order to evaluate the path integral on $\mathcal{R}_n$ we can think of it as being equivalent to consider n copies of the theory where we introduce some twist operators $\mathbf{T}_n^{(\partial A)}$. One starts taking n copies of the original theory on respectively n disconnected sheets, with fields $\phi_k(x)$ with $k=1,\ldots,n$. The twist operator $\mathbf{T}_n^{(\partial A)}$ is defined as introducing the following boundary

conditions on the path integral

$$\phi_i^+ = \sum_{j=1}^{n} \Gamma_{ij}\, \phi_j^- \ , \tag{2.2.11}$$

with $\Gamma_{ij} = \delta_{i,j+1} + \delta_{n,1}$ identifying fields of consecutive copies across the set A. And where again the superscript $\pm$ denote the 'two sides' of A, when embedded in the complete Euclidean manifold $\mathbb{R} \times X_d$. Alternatively, for any point $x \in \mathrm{A}$, $\phi^+(x)$ is obtained from $\phi^-(x)$ by transporting the field from the 'lower side' to the 'upper side' of A along a closed path of linking number one with the boundary ∂A. In particular, the construction shows that the twist operator in (2.2.11) is 'instanton-like', i.e. it is always sharply localized in the time direction.

The twist operator $\mathbf{T}_n^{(\partial A)}$ is locally supported on ∂A. The simplest particular case occurs in 1+1 dimensions, where the non-local twist operator is given by a *bilocal* product of two standard (local) twist operators, i.e. (2.2.11) is a two-point function. In $2+1$ dimensions, $\mathbf{T}_n^{(\partial A)}$ is supported on a one-dimensional curve, just like standard Wilson and 't Hooft loop operators. Taking inspiration from the case of Wilson loops, one's natural guess for the ultraviolet contribution to (2.2.11) is

$$\left\langle\, \mathbf{T}_n^{(\partial A)} \,\right\rangle_{\mathrm{UV}} \sim \exp\left(-\alpha_n\, a^{\,1-d}\, |\partial \mathrm{A}|\right) \ , \tag{2.2.12}$$

with a a short-distance cutoff and $|\partial \mathrm{A}|$ the volume of ∂A in the metric of the spatial manifold X_d. Although all previous expressions hold in an arbitrary QFT in a formal sense, Eq. (2.2.12) assumes that a^{-1} is taken beyond any mass scale in the theory, so that we are close to some ultraviolet (UV) fixed point. Since (2.2.11) is almost an n-fold product of partition functions, we expect α_n/n to be finite in the $n \to \infty$ limit. Furthermore, we know that $\alpha_1 = 0$, since the partition function is not 'frustrated' for $n = 1$. The resulting entanglement entropy has the form

$$S_{\mathrm{A}} = \left.\frac{d\alpha_n}{dn}\right|_{n=1} \frac{|\partial \mathrm{A}|}{a^{\,d-1}} + \dots \ , \tag{2.2.13}$$

where the dots stand for less divergent terms, which will depend in general on the size and shape of A and any intrinsic mass scales of the QFT. In Eq. (2.2.13) we see the expected UV scaling of the geometric entropy, i.e. non-extensive behavior and 'area law' with respect to the entangled region [89].

The former argument is not by any means rigorous by gives a glimpse on how the area law arises in the QFTs. Now let us briefly discuss the exact results: in 1+1 CFTs and in free theories in 1+1 and higher dimensions.

2.2.1 1+1 CFTs and massive theories

Let us consider the case of CFT in 1+1 dimensions and the simplest case of $A = [u, v]$, that is an interval of length ℓ. According to our previous discussion we have to compute Z_n, the partition function of the theory on the n-sheeted Riemann manifold, or equivalently the expectation value of two twist operators, $\Phi_n^{+(k)}(u), \Phi_n^{-(k)}(v)$, inserted at u and v respectively in $\mathbb{R}^2$, isomorphic to the complex plane $\mathbb{C}$, i.e.

$$\mathrm{tr}_A\, \rho_A = \prod_{k=0}^{n-1} \langle \Phi_n^{+(k)}(u) \Phi_n^{-(k)}(v) \rangle_{\mathbb{C}} \tag{2.2.14}$$

Since we are in a CFT, in order to determine the correlation functions of the pairs of twist operators all we have to do is to determine its conformal weight Δ_n, since the conformal symmetry fixes completely the rest (assuming the operators are primary as will be the case).

On the other hand the conformal Ward identity [90]

$$\langle T(z)\phi_1(w_1, \bar{w}_1) \dots \phi_n(w_n, \bar{w}_n)\rangle = \sum_{j=1}^{n} \left(\frac{\Delta_j}{(z-w_j)^2} + \frac{1}{z-w_j}\frac{\partial}{\partial w_j} \right) \langle \phi_1(w_1, \bar{w}_1) \dots \phi_n(w_n, \bar{w}_n)\rangle \tag{2.2.15}$$

determines the conformal weight and properties under conformal transformations. $T(w)$ denotes the holomorphic component of the holomorphic tensor. Thus it makes sense to study the expectation value of $\langle T(w)\rangle_{\mathcal{R}_n}$. Through its study one can see that it can be recast in the form of $\langle T(w)\Phi(u)\Phi(v)\rangle_{\mathbb{C}}$ and from there identify these two operators as the twist operators and obtain its conformal weight.

The arguments reduces to the following. In two dimensions we have the conformal mapping $w \to ((w-u)/(w-v))^{1/n}$ that maps the whole of the n-sheeted Riemann surface $\mathcal{R}_n$ to the complex plane $\mathbb{C}$. Under conformal transformations the holomorphic component of the stress tensor $T(w)$ transforms as

$$T(w) = \left(\frac{dz}{dw}\right)^2 T(z) + \frac{c}{12}\{z, w\} \tag{2.2.16}$$

where $\{z, w\}$ is the Schwartzian derivative $(z'''z' - \frac{3}{2}z''^2)/z'^2$ and $T(z)$ is the transformed component. From this we obtain

$$\langle T(w)\rangle_{\mathcal{R}_n} = \frac{c}{12}\{z, w\} = \frac{c(1-n^{-2}))}{24}\frac{(v-u)^2}{(w-u)^2(w-v)^2}\,. \tag{2.2.17}$$

This expression precisely coincides with the expression of the standard form [90] of the correlator of T with two primary operators $\Phi_n^+(u)$ and $\Phi_n^-(v)$ which have the same complex conformal dimensions $\Delta_n = \bar{\Delta}_n = \frac{c}{24}(1-n^{-2})$.

This way one arrives to the result that $\mathrm{tr}_A\,\rho_A$ behaves (apart from a possible overall constant) as the nth power of two-point function of primary operators that we can identify with the twist operators $\Phi_n^{\pm(k)}$ in (2.2.14) with conformal dimension $\Delta_n = \bar{\Delta}_n = \frac{c}{24}(1-n^{-2})$. This implies that

$$\mathrm{tr}_A\,\rho_A = c_n \left(\frac{v-u}{a}\right)^{-\frac{c}{6}(n-\frac{1}{n})} . \tag{2.2.18}$$

a is an UV cutoff introduced to make the final result dimensionless. The constant c_n is not determined by this method. However c_1 must be unity. Differentiating with respect to n and setting $n = 1$ we finally arrive to

$$S_A = \frac{c}{3}\ln\frac{\ell}{a} + c_1' . \tag{2.2.19}$$

The constant c_1' is non-universal.

We see that in the case of two dimension at criticality the area law is corrected by a logarithm (an strict area law would be just proportional to the number of boundary points) and the overall constant is proportional to the central charge, that measures the degrees of freedom in the theory.

Along the same lines, employing different conformal mapping of $\mathcal{R}_n$ to $\mathbb{C}$ one can compute the entanglement entropy of any other configuration. For the case where A consists of several intervals, $[u_1, v_1] \cup \cdots \cup [u_N, v_N]$, the result is

$$S_A = \frac{c}{3}\sum_{1\le i,j\le N}\ln\frac{u_i - v_j}{a} - \frac{c}{3}\sum_{1\le i<j\le N}\ln\frac{u_j-u_i}{a} - \frac{c}{3}\sum_{1\le i<j\le N}\ln\frac{v_j-v_i}{a} + Nc_1' . \tag{2.2.20}$$

In the case of a single interval of length ℓ in a system with periodic boundary conditions with period L the entanglement entropy is

$$S_A = \frac{c}{3}\ln\left[\frac{L}{\pi a}\sin\left(\frac{\pi}{L}\ell\right)\right] + c_1' . \tag{2.2.21}$$

By taking the time direction compact with period the inverse of the temperature β one can also compute the entanglement entropy of an interval of length ℓ finding

$$S_A = \frac{c}{3}\ln\left[\frac{\beta}{\pi a}\sinh\left(\frac{\pi}{\beta}\ell\right)\right] + c_1' . \tag{2.2.22}$$

When we take the limit of high temperature, $\beta \to 0$, it approaches $S_A \simeq \frac{\pi c}{3}\ell T$, which is the same as the thermal entropy for A as expected.

In the case when we the theory under consideration has a finite correlation length, ξ, the theory is no longer conformal and the previous technique using conformal mappings can no

longer be applied to compute the entanglement entropy. However in [66] using an argument paralleling Zamalodchikov's proof of the c-theorem [91], they were able to show that for $\ell \gg \xi$ the scaling (2.2.19) is modified and becomes

$$S_A = \mathcal{A}\,\frac{c}{6}\ln\frac{\xi}{a}\ , \tag{2.2.23}$$

where $\mathcal{A}$ is the number of boundary points that separate A from its complement. Thus in the massive case the area law really holds, saturating to a maximum value provided one introduces an UV cutoff a in the theory.

One can check explicitly this result for the case of a free massive bosonic theory

$$S = \frac{1}{2}\int d^2r\,\left[(\partial_\mu\varphi)^2 + m^2\varphi^2\right]\ . \tag{2.2.24}$$

Here the trick is to realize that for a free theory one has that

$$\frac{\partial}{\partial m^2}\ln Z_n = -\frac{1}{2}\int G_n(\vec{r},\vec{r})\,d^2r\ . \tag{2.2.25}$$

In the case of A being a semi-infinite interval, one can compute the two-point correlation function $G_n(\vec{r},\vec{r})$ in the corresponding n-sheeted geometry that has just one conical singularity at the origin [66]. The end result is that

$$S_A = -\frac{1}{12}\ln m^2a^2\ , \tag{2.2.26}$$

that agrees with the general formula (2.2.23) with $c = 1$ and $m = \xi^{-1}$, as one would naturally expect.

2.2.2 Higher dimensional QFTs

In the case of higher dimensions computing the entanglement is much harder. The main reason is that we are trying to compute something in a theory where we break a lot of symmetries by considering a distinguished region A. Here conformal symmetries are not powerful as in 1+1, they cannot be used as in two dimensions to map $\mathcal{R}_n$ to $\mathbb{R}^{d+1}$. On the other hand, in the non-conformal case, the only treatable case is the free theory in some particular geometries.

One of these geometries is the *strip* given by $A = [-\ell/2, \ell/2]\times\mathbb{R}^{d-1}$. Here we preserve translational invariance along $d-1$ dimensions. Actually for this geometry the computation reduces to the 1+1 case but with the substitution in the mass $m^2 \to m^2 + k_\perp^2$ and the integration over the $k_\perp$ in front of all the equations, where $k_\perp$ is the momentum along $\mathbb{R}^{d-1}$. In this way the entropy for the free massive scalar results in [66]

$$S_A = -\frac{|\partial A|}{12}\int\frac{d^{d-1}k_\perp}{(2\pi)^{d-1}}\ln\frac{k_\perp^2+m^2}{k_\perp^2+a^{-2}} \tag{2.2.27}$$

The behaviour of the integral is given by

$$S_A \simeq \frac{|\partial A|}{a^{d-1}} - \frac{|\partial A|}{m^{1-d}} \tag{2.2.28}$$

and in the massless case by

$$S_A \simeq \frac{|\partial A|}{a^{d-1}} - \frac{|\partial A|}{\ell^{d-1}} \,. \tag{2.2.29}$$

We see that here the entanglement entropy fulfills the area law with a divergent non-universal part and a finite subleading term that also satisfies the area law. Free scalars satisfy a strong area law.

In order to get a rough estimates for the fermionic case in the geometry of the strip, one can just use directly the expressions of the 1+1 CFT case already discussed but with the shift in the mass and integration over $k_\perp$ but now having in mind that we have a Fermi surface with a Fermi momentum k_F. For the momentum k outside and close to the Fermi surface, the gap is given by $m \sim \xi^{-1} \sim k - k_F$. The entanglement can then be roughly estimated for a massless fermion as

$$S_A^{\text{rough}} = \frac{|\partial A|}{(2\pi)^{d-1}} \frac{c}{3} \left\{ \int_{k=k_F+\ell^{-1}}^{a^{-1}} d^{d-1}k_\perp \ln \frac{\xi}{a} + \int_0^{k=k_F+\ell^{-1}} d^{d-1}k_\perp \ln \frac{\ell}{a} \right\} \tag{2.2.30}$$

that for large ℓ gives

$$S_A^{\text{rough}} \sim |\partial A|\, k_F^{d-1}\, \ln \frac{\ell}{a} + \text{subleading terms} \tag{2.2.31}$$

This same estimate but without the Fermi surface reproduces (2.2.29). Thus we can see how the presence of a Fermi surface introduces a logarithmic correction to the area law.

In the case of interacting fields very little is known. There has been some progress in the computation of the entanglement entropy for some $z = 2$ quantum critical points, where z is the dynamical scaling exponent, in two spatial dimensions [74, 75]. On the other hand in [76] the entanglement entropy of the $O(N)$ model in two spatial dimensions was recently computed. These computations are involved but the end result respects the area law. Thus we see the difficulty and limited knowledge we have from a direct QFT point of view of the entanglement entropy.

2.3 Holographic computation of entanglement entropy

After having browsed over the QFT results on entanglement entropy, let us change gears and move to the AdS/CFT correspondence. The AdS/CFT correspondence can be seen as a tool that allows us to compute observables for a strongly coupled QFT from a weakly interacting

gravity theory in the limit where we can use the supergravity approximation. In this context it is interesting to study whether we can give a prescription to calculate the entanglement entropy of a QFT from its holographic dual. An affirmative answer would allow us to explore the entanglement structure of strongly interacting fixed points of QFTs, out of reach via a direct treatment with present techniques.

This question was addressed and answered in the affirmative by Ryu and Takayanagi in [18]. The holographic proposal for the entanglement entropy they presented is the following: Let A denote a purely spatial, d-dimensional domain in a manifold X_{d+1} with a smooth boundary ∂A and let $\bar{A}$ denote the minimal d-dimensional hypersurface in the bulk[3] whose boundary at spatial infinity precisely coincides with ∂A, that is $\partial \bar{A} = \partial A$. Then, the holographic ansatz for the entanglement entropy is

$$S_A = \frac{\mathrm{Vol}(\bar{A})}{4G_N} \,, \tag{2.3.1}$$

where G_N is the Newton's constant in the gravity theory and $\mathrm{Vol}(\bar{A})$ is the volume of $\bar{A}$ computed from the induced volume form of the bulk defined in the Einstein frame. See also [92] for some covariant proposal for the holographic ansatz with the aim to generalize it for a time dependent setting.

We do not have a rigorous derivation of this ansatz in arbitrary dimensions. Nonetheless one physical motivation of this prescription involves going back to one of the original motivations of entanglement entropy, black hole entropies and holographic bounds [93, 94, 95] for information loss. When we compute the entanglement entropy for a pure state in a region A we have to trace over the degrees of freedom corresponding to that region, losing all information contained in it. From a holographic point of view this would correspond to hiding to an observer part of the bulk that holds the information associated to A. One can think then of introducing an imaginary (spatial) horizon inside the bulk and tentatively associate its maximal entropy, given by the Bekenstein-Hawking entropy of that horizon, to the entanglement entropy of A. Then the natural surface to introduce associated to A saturating the holographic bounds is the minimal hypersurface $\bar{A}$ that ends at the boundary of the spacetime on ∂A. This is by no means a proof of the prescription but gives you some suggestive physical motivation for (2.3.1) that has to be checked a posteriori with particular cases where the entanglement entropy is known. Nonetheless see [96] for some general attempt to give a proof of the ansatz.

The only case when one can justify from known facts of the AdS/CFT correspondence the holographic prescription (2.3.1) is in the case when we deal with a 1+1 CFT and its

[3]The bulk must satisfy that its conformal boundary is X_{d+1}.

holographic dual is AdS_3. That furthermore is the case that is completely understood from the CFT point of view. We should be able to reproduce the known results, serving as a check. As already discussed in section 2.2.1, in two dimensions the computation of $\mathrm{tr}_A\,\rho_A^n$ is equivalent to the evaluation of the product of n two point functions $\langle \Phi_n^{+(k)} \Phi_n^{-(k)} \rangle_{\mathbb{C}}$, cf. (2.2.14), each for every copy of the original CFT, where $\Phi_n^{\pm(k)}$ is a twist operator localized at the boundary of A that is this case is a simple spatial interval, $[u, v]$. Instead of considering the n copies of the CFT on n different sheets, one can equivalently consider a CFT in a single sheet ($\mathbb{C}$), but with a central charge that is nc, with c the original central charge. And introduce two twist operators, $\Phi_n^{\pm}$, localized at the boundary points of A. Then using the AdS/CFT dictionary [97] the two point function $\langle \Phi_n^+(u) \Phi_n^-(v) \rangle_{\mathbb{C}}$ is going to be given by

$$\langle \Phi_n^+(u) \Phi_n^-(v) \rangle_{\mathbb{C}} \approx \exp(-c_n L_{\partial A}) \tag{2.3.2}$$

where $L_{\partial A}$ is the bulk geodesic connecting the two boundary points of A and c_n is some constant dependent on n. Then the entanglement entropy is given by

$$S_A \approx \left. \frac{dc_n}{dn} \right|_{n=1} L_{\partial A} \ . \tag{2.3.3}$$

The exact constant of proportionality is then fixed by carrying out the exact computation [18] and comparing to the known expression of the entanglement entropy (2.2.19), leading to

$$S_A = \frac{L_{\partial A}}{4 G_N^{(3)}} \ , \tag{2.3.4}$$

with $G_N^{(3)}$ being Newton's constant in AdS_3.

In higher dimensions, one can repeat the same replica trick and introduce the twist operator $\mathbf{T}_n^{(\partial A)}$, cf. (2.2.11). The twist operator is supported all over ∂A, that now has dimension $d-1$, and the computation of $\mathrm{tr}_A\,\rho_A^n$ is equivalent to computing the expectation value of a non-local operator, $\langle \mathbf{T}_n^{(\partial A)} \rangle$. Then by direct analogy to the treatment of Wilson and 't Hooft loop operators [98], one expects the ansatz

$$\langle \mathbf{T}_n^{(\partial A)} \rangle \approx \exp(-c_n \mathrm{Vol}(\bar{A})) \ , \tag{2.3.5}$$

where $\bar{A}$ is the minimal d-dimensional hypersurface dropped inside the bulk, with boundary conditions $\partial \bar{A} = \partial A$ at the conformal boundary of the spacetime. This again gives

$$S_A \approx \left. \frac{dc_n}{dn} \right|_{n=1} \mathrm{Vol}(\bar{A}) = \frac{\mathrm{Vol}(\bar{A})}{4 G_N^{(d+2)}} \ , \tag{2.3.6}$$

where the constant of proportionality is fixed such that for two dimensions we recover the standard known result.

Considering bulk spaces with AdS_{d+2} asymptotics near the boundary:

$$ds^2/R^2 \longrightarrow u^2\,(d\tau^2 + d\vec{x}^{\,2}) + du^2/u^2\,, \tag{2.3.7}$$

any minimal hypersurface $\overline{\mathrm{A}}$ with a boundary component at infinity is asymptotically perpendicular to the boundary, with a volume divergence at large u of the form

$$\frac{R^d u_a^{d-1}\,|\partial \mathrm{A}|}{4G_N^{(d+2)}} \propto N_{\text{eff}} \frac{|\partial \mathrm{A}|}{a^{\,d-1}}\,, \tag{2.3.8}$$

where $u_a = a^{-1}$ and $N_{\text{eff}} = R^d/G_N^{(d+2)}$ is the effective number of degrees of freedom of the conformal UV fixed point.[4] Hence, the holographic ansatz obtains the expected UV structure (2.2.12) of an area law (see chapter 3 for a detailed discussion of the area law from holography).

Using the same ansatz (2.3.1) one can demonstrate the strong subadditivity of the entanglement entropy [99] (see also [100] for earlier work and [101] for related discussion). cf. [102] for a discussion of the extension of the ansatz for disconnected regions. That the area law and the strong subadditivity are recovered from the holographic ansatz, along an exact matching for 1+1 CFTs, are very strong evidence for the correctness of the prescription.

If the UV fixed point is associated to a holographic model of the form $\mathrm{AdS}_{d+2}\times K$, with K some compact Einstein manifold of dimension $d_K = D-d-2$, this extra structure only enters (2.3.6) through the Kaluza–Klein reduction of Newton's constant ${G_{(d+2)}}^{-1} = {G_{(D)}}^{-1}\,\mathrm{Vol}\,(K)$. Therefore, we can generalize the prescription to the higher-dimensional description via a minimal $(D-2)$-dimensional hypersurface which wraps completely the internal manifold. The Kaluza–Klein ansatz also applies to warped products of AdS-like spaces and compact manifolds, where the radius of curvature of both factors has a non-trivial dependence on the holographic coordinate u. If R and $G_N^{(d+2)}$ denote the asymptotic values of curvature radius and Newton's constant, the ansatz (2.3.6) remains valid, ensuring UV asymptotics controlled by $N_{\text{eff}} \sim R^d/G_N^{(d+2)}$ as before, but with modified behavior at the level of the renormalized entropy. Models arising from ten-dimensional string backgrounds are treated in the same way, provided we remember to use the Einstein-frame metric in the ten-dimensional set up before the Kaluza–Klein reduction.[5]

Nonetheless as it is clear from the beginning, the ansatz (2.3.6) is only going to capture the leading term in a large N expansion of the entanglement entropy, that is the one that goes as $\mathcal{O}(N_{\text{eff}})$. Extending the prescription to take into account subleading terms is an open question but does not render the present holographic ansatz less useful.

[4] For example, for models governed by a large-N gauge theory we have $N_{\text{eff}} \sim N^2$. Other models, such as the theory on a stack of N M2-branes, have $N_{\text{eff}} \sim N^{3/2}$, whereas $N_{\text{eff}} \sim N^3$ for a stack of N M5-branes.

[5] The difference between both frames amounts to a factor of $\exp(-2\phi)$ in the induced volume 8-form.

2.4 Holographic matching of the entanglement entropy for 1+1 CFTs

Here we will sketch how the holographic ansatz (2.3.1) gives you an exact matching for the entanglement entropy of a 1+1 CFT of central charge c.

According to the AdS/CFT correspondence [1], the holographic dual of a 1+1 CFT is given by an AdS_3 space of radius R and where the central charge of the CFT is related to

$$c = \frac{3R}{2G_N^{(3)}} \tag{2.4.1}$$

with $G_N^{(3)}$ denoting Newton's gravitational constant.

Depending on what coordinates we choose for AdS_3, the conformal boundary will have different topologies, corresponding to the topologies of the dual CFT. If we choose global coordinates,

$$\frac{ds^2}{R^2} = -\cosh\rho^2 dt^2 + d\rho^2 + \sinh^2\rho^2 d\theta^2 \ , \tag{2.4.2}$$

we can give the boundary the topology of a cylinder $\mathbb{R}\times S^1$, where $\rho\in[0,\infty)$, $t\in(-\infty,\infty)$ and θ is a compact coordinate in the range $[0,L)$. The boundary is at $\rho\to\infty$. If we choose Poincare coordinates,

$$\frac{ds^2}{R^2} = \frac{-dt^2+dx^2+dz^2}{z^2} \ , \tag{2.4.3}$$

the boundary corresponds to $\mathbb{R}^2$, where $t,x\in(-\infty,\infty)$ and $z\in[0,\infty)$ with the boundary at $z\to 0$.

The finite temperature version is given by the Euclidean BTZ black hole [103],

$$ds^2 = (r^2-r_+^2)d\tau^2 + \frac{R^2}{r^2-r_+^2}dr^2 + r^2 d\varphi^2 \ . \tag{2.4.4}$$

φ has period L, $r\in[0,\infty)$ and τ is compatified with a period $\beta=\frac{LR}{r_+}$ equal to the inverse of the temperature of the CFT.

For simplicity we will choose our region A to be a single connected interval of length ℓ. The holographic prescription, (2.3.4), tells us to compute the entanglement entropy from the length of a geodesic the goes from the boundary into the bulk and back to the boundary right at the ends of the interval A. We see immediately that since the boundary is at spatial infinity, this length is going to be divergent. One always has to introduce in this computations a cutoff in the holographic direction near the boundary. Due to the UV/IR mixing in the holographic correspondence, the introduction of this cutoff in the holographic direction is equivalent to the introduction of an UV cutoff in the dual CFT.

In the case of AdS_3 in global coordinates (2.4.2), corresponding to a CFT on a cylinder of length L, we impose a cutoff at ρ_0 such that $\rho \leq \rho_0$. Using the holographic UV/IR rule, the cutoff in the holographic direction corresponds to an UV cutoff a in the CFT theory, related by

$$e^{\rho_0} \sim \frac{L}{a} \,. \tag{2.4.5}$$

With this cutoff in place the geodesic length L_A is given by [18]

$$\cosh \frac{L_A}{R} = 1 + 2 \sinh^2 \rho_0 \sin^2 \frac{\pi \ell}{L} \,. \tag{2.4.6}$$

Then the expression of the entanglement entropy (2.3.4) becomes

$$S_A \simeq \frac{R}{4G_N^{(3)}} \ln \left(e^{2\rho_0} \sin^2 \frac{\pi \ell}{L} \right) = \frac{c}{3} \ln \left[\frac{L}{\pi a} \sin \left(\frac{\pi \ell}{L} \right) \right] \,, \tag{2.4.7}$$

that agrees with the CFT result (2.2.21).

If we want to recover the result for a CFT in $\mathbb{R}^2$, we switch to Poincare coordinates (2.4.3). In this case a cutoff in the holographic direction z_0 corresponds to an UV cutoff a in the CFT, related by $z_0 \sim a$. The geodesic connecting both ends of A is given by [18]

$$(x, z) = \frac{\ell}{2} (\cos s, \sin s) \qquad \text{with } \epsilon \leq s \leq \pi - \epsilon \tag{2.4.8}$$

and $\epsilon \sim 2a/\ell$. Then the entanglement entropy results in

$$S_A = \frac{R}{2G_N^{(3)}} \int_\epsilon^{\frac{\pi}{2}} \frac{ds}{\sin s} = \frac{c}{3} \ln \frac{\ell}{a} \,. \tag{2.4.9}$$

Again in agreement with the CFT result (2.2.19).

For the finite temperature case, upon the introduction of a cutoff in the radial direction

$$e^{\rho_0} \sim \beta / a \,, \tag{2.4.10}$$

with a the CFT UV cutoff, the geodesic length L_A is given by [18]

$$\cosh \frac{L_A}{R} = 1 + 2 \cosh^2 \rho_0 \sinh^2 \frac{\pi \ell}{\beta} \,. \tag{2.4.11}$$

The entanglement entropy then follows as

$$S_A = \frac{c}{3} \ln \left[\frac{\beta}{\pi a} \sinh \left(\frac{\pi \ell}{\beta} \right) \right] \,, \tag{2.4.12}$$

matching the CFT result (2.2.22). Here in the finite temperature case, the geodesic tends to wrap the horizon, giving for large temperatures (large horizons), an extensive behaviour for the entanglement entropy.

2.5 Holographic entanglement entropy for CFT$_{d+1}$s

In the preceding section we have seen how the holographic ansatz for the entanglement entropy is able to reproduce the exact known results of a 1+1 CFT. Now it is time to put it to use and obtain new results for interacting CFTs in higher dimensions ($d \geq 2$) in the large N limit.

According to the AdS/CFT correspondence a CFT$_{d+1}$ is going to be dual to a gravity theory on AdS$_{d+2}$. The easiest way to argue that this must be case is by a matching of symmetries. The conformal group of the field theory corresponds to a spacetime whose isometries fulfill the conformal algebra, i.e. AdS. Additional symmetries like R-symmetries require the addition of compact manifolds, with appropriate isometries to completely match them all.

We will consider the simplest scenario when the CFT lives in $\mathbb{R}^{d+1}$. This tells us that we must use Poincare coordinates so that the conformal boundary is indeed $\mathbb{R}^{d+1}$,

$$\frac{ds^2}{R^2} = \frac{-dt^2 + d\vec{x}^2 + dz^2}{z^2} \,. \tag{2.5.1}$$

As the region A we will take at the same time the simplest possibility, a strip given by $A = [-\ell/2, \ell/2] \times \mathbb{R}^{d-1}$, extending in the x coordinate. This choice is the simplest for the computations and after all we are mainly interested in the general functional dependence of the entanglement of the size of the region. By translational invariance on $\mathbb{R}^{d-1}$ we know that the entropy will be extensive along these $d-1$ directions. To regulate the divergence coming from this extensivity we will regulate the space to have length L along those directions.

The computation of the minimal area is reduced to the extremization of

$$\text{Area} = R^d L^{d-1} \int_{-\frac{\ell}{2}}^{\frac{\ell}{2}} dx\, z^{-d} \sqrt{1 + \left(\frac{dz}{dx}\right)^2} \tag{2.5.2}$$

Using the conservation of the associated Hamiltonian of the problem with respect to x, the minimal surface is determined in terms of

$$\frac{dz}{dx} = \frac{\sqrt{z_*^{2d} - z^{2d}}}{z^d} \,, \qquad \frac{\ell}{2} = \int_0^{z_*} dz \frac{z^d}{\sqrt{z_*^{2d} - z^{2d}}} = \frac{\sqrt{\pi}\Gamma\left(\frac{d+1}{2d}\right)}{\Gamma\left(\frac{1}{2d}\right)} z_* \,. \tag{2.5.3}$$

z_* is the point in the bulk where the minimal surfaces bounces back to the boundary, i.e. $dz/dx|_{z=z_*} = 0$. Upon introducing an UV cutoff, a, the entanglement entropy is given by [18]

$$S_A = \frac{R^d}{4G_N^{(d+2)}} \left[\frac{2}{d-1} \left(\frac{L}{a}\right)^{d-1} - \frac{2^d \pi^{\frac{d}{2}}}{d-1} \left(\frac{\Gamma\left(\frac{d+1}{2d}\right)}{\Gamma\left(\frac{1}{2d}\right)} \right)^d \left(\frac{L}{\ell}\right)^{d-1} \right] \,. \tag{2.5.4}$$

This expression for the entanglement entropy is given in terms of the gravity constants. In order to rewrite it in terms of the physical CFT observables we need information of the precise correspondence, coming from a String Theory construction that varies in each particular case. Nonetheless we can already see that the structure of the entanglement entropy is going to be of the form

$$S_A \propto N_{\text{eff}} \frac{|\mathbb{R}^{d-1}|}{a^{d-1}} - N_{\text{eff}} \frac{|\mathbb{R}^{d-1}|}{\ell^{d-1}} \,. \tag{2.5.5}$$

$N_{\text{eff}} = R^d/G_N^{d+2}$ is the effective number of freedom of the theory. $|\mathbb{R}^{d-1}|$ refers to the (regulated) volume of $\mathbb{R}^{d-1}$. We see that the renormalized entanglement entropy (the universal part independent of the UV cutoff and proportional to the entropic C-function) also satisfies an area law. The latter can be understood by the following argument: a rescaling of the boundary coordinates, $\vec{x}$, induces a rescaling of ℓ which can be absorbed in a rescaling of z in (2.5.1) leaving the metric invariant. Thus we expect that even an strongly interacting CFT fulfills a strong area law in the large N limit.

Let us consider three explicit examples. The best well known instance of the AdS/CFT correspondence is the duality between $\mathcal{N} = 4$ SU(N) SYM and $\text{AdS}_5 \times S^5$ coming from a type IIB String Theory construction via a stack of D3-branes. The supergravity approximation in the gravity theory corresponds to the regime of large t'Hoolf coupling $\lambda = N g_{\text{YM}}^2$ (strong coupling) in the planar limit, i.e. $N \to \infty$. In this setting, the gravitational constant is given by the Kaluza-Klein reduction along the S^5 from 10 dimensions to 5 dimensions

$$G_N^{(5)} = \frac{G_N^{(10)}}{R^5 \text{Vol} S^5} = \frac{G_N^{(10)}}{\pi^3 R^5} \tag{2.5.6}$$

where

$$G_N^{(10)} = 8\pi^6 \alpha'^4 g_s^2 \,, \qquad R = (4\pi g_s \alpha'^2 N)^{\frac{1}{4}} \,, \tag{2.5.7}$$

with g_s is the string coupling constant, α'^2 is the inverse of the string tension. Upon substituting these values in (2.5.4) the entanglement entropy in the strip for $\mathcal{N} = 4$ SU(N) SYM becomes

$$S_A = \frac{N^2 L^2}{2\pi a} - 2\sqrt{\pi} \left(\frac{\Gamma\left(\frac{2}{3}\right)}{\Gamma\left(\frac{1}{6}\right)} \right)^2 \frac{N^2 L^2}{\ell^2} \,. \tag{2.5.8}$$

Another two known instances of CFTs are the duals of $\text{AdS}_4 \times S^7$ and $\text{AdS}_7 \times S^4$ coming from an M-theory construction involving eleven dimensional supergravity. They come from the consideration of stacks of M2 and M5 branes or the strongly coupled limit of D2 and D4 branes in type IIA String Theory. Their dual theories are a 3D $\mathcal{N} = 8$ SCFT and a 6D $(2,0)$ SCFT respectively. Both theories are maximally symmetric. In eleven dimensional

supergravity the only parameter available is the Planck length, l_p. The 11D gravitational constant is given by

$$G_N^{(11)} = 2^4 \pi^7 l_p^9 \, . \tag{2.5.9}$$

In the case of the $\mathrm{AdS}_4 \times S^7$ we have that the radius of AdS_4 and of the S^7 are given by

$$2R_{\mathrm{AdS}_4} = R_{S^7} = l_p (32\pi^2 N)^{\frac{1}{6}} \, . \tag{2.5.10}$$

Upon Kaluza-Klein reduction of the gravitational constant along S^7 to four dimensions, the entanglement entropy results in

$$S_A = \frac{\sqrt{2}}{3} N^{\frac{3}{2}} \left[\frac{L}{a} - \frac{4\pi^3}{\Gamma\left(\frac{1}{4}\right)^4} \frac{L}{\ell} \right] \, . \tag{2.5.11}$$

In the other case of $\mathrm{AdS}_7 \times S^4$, we have that

$$R_{\mathrm{AdS}_7} = 2R_{S^4} = 2l_p (\pi N)^{\frac{1}{3}} \tag{2.5.12}$$

and one finds that

$$S_A = \frac{2}{3\pi^2} N^3 \left[\frac{L^4}{a^4} - 16\pi^{\frac{5}{2}} \left(\frac{\Gamma\left(\frac{3}{5}\right)}{\Gamma\left(\frac{1}{10}\right)} \right)^5 \frac{L^4}{\ell^4} \right] \, . \tag{2.5.13}$$

From these examples we see how a strong area law holds for the different theories with $N_{\text{eff}} \sim N^2$ for the large-N gauge theory, whereas $N_{\text{eff}} \sim N^{\frac{3}{2}}$ for the theory of N M2-branes and $N_{\text{eff}} \sim N^3$ for the theory of N M5-branes. The other remarkable fact is that the results are explicitly independent of the effective coupling constant.

In the case of taking another geometry for A different from the strip, we do not expect the results to change abruptly. The area law for the renormalized part of the entanglement entropy (entropic C-function) should hold the same. However the non-universal part is subject to receive additional UV divergent logarithmic corrections on top of the area law. This is the case for an odd number of spatial dimensions and compact surfaces with a non-zero extrinsic curvature[6] [18, 97, 105].

In the case we want to put the CFT at finite temperature we only have to consider the Schwarzschild AdS black hole with the same associated Hawking temperature. In that case applying the holographic ansatz one recovers for large temperatures an extensive renormalized entanglement entropy equal to the thermal entropy, as one would expect, $S_A(\ell) \sim N_{\text{eff}} R^{d-1} T^{d-1} L^{d-1} \ell$. The minimal surfaces tend to wrap the horizon around. However one still gets the UV divergent term satisfying the area law.

[6]There was some controversy regarding this topic raised by [104] but later independently analyzed in [105] and where validity of the holographic prescription was found.

So far we have only treated the conformal case finding a strong area law for the entanglement entropy (at zero temperature), mostly reviewing results available in the literature. These theories are local without any scale in them. Nonetheless we want to go beyond conformality and explore other theories. As found in [106, 107], entanglement entropy happens to be a good order parameter for confinement, indicating clearly a change in the effective number of degrees of freedom as well as the appearance of a mass scale below some energy scale. From this perspective our true motivation to study entanglement entropy is to see under what other circumstances the entanglement entropy arises as a good order parameter or indicator of other phenomena within the theory under consideration. In the next two chapters we will explore these topics using insights from the holographic constructions, presenting the findings of our original research [20, 21]. In particular in the following chapter we will analyze more carefully the validity of the area law and its relation to locality of the interactions. In chapter 4, we will go beyond conformality in local theories and study systematically its possible signatures in the renormalized entanglement entropy.

Chapter 3

Holographic entanglement entropy, area laws and locality

3.1 Introduction

In the previous chapter we have seen how the geometric entropy in the *vacuum* state of a weakly coupled quantum field theory satisfies the so-called *area law*, i.e. the entanglement entropy is proportional to the volume of the boundary of the region under consideration, measured in units of an appropriate ultraviolet (UV) cutoff [89]. In $d > 1$ spatial dimensions one finds[1]

$$S[A] \propto N_{\text{eff}} \frac{|\partial A|}{\varepsilon^{\,d-1}} + \dots \,, \tag{3.1.1}$$

where $|\partial A| \equiv \text{Vol}(\partial A)$ is the volume of the $(d-1)$-dimensional boundary of A and N_{eff} is the effective number of on-shell degrees of freedom (flavour, spin, color). The dots in (3.1.1) stand for subleading corrections in the short-distance expansion. Keeping the finite terms in the continuum limit one can define renormalized versions of the entanglement entropy, whose structure encodes properties related to physical energy thresholds like mass gaps [21], confinement scales [106, 107], etc, as we will discuss in detail in chapter 4.

One can associate the area law (3.1.1) with *local* QFTs defined in terms of UV fixed points. This is even the case at strong coupling, at least for those UV fixed points that can be studied via the AdS/CFT correspondence [108]. On the other hand, a *volume law* of the entanglement entropy can be associated to a violation of locality in the underlying theory. In order to argue this point at a heuristic level, we can consider a nonlocal version of the

[1] In $d = 1$ one encounters a logarithmic correction to the area law, $S_A = c/3 \ln \ell/a$.

Heisenberg's antiferromagnetic spin chain,

$$H = J \sum_{\langle i,j \rangle} \mathbf{S}_i \cdot \mathbf{S}_j \ , \tag{3.1.2}$$

where $J > 0$ and the sum runs over pairs of spins chosen uniformly at random, in such a way that each spin belongs to only one pair. The ground state is then the direct product of singlets

$$\frac{1}{\sqrt{2}} \left(|\uparrow_i \downarrow_j\rangle - |\downarrow_i \uparrow_j\rangle \right) \quad , \tag{3.1.3}$$

for each pair of sites. Each singlet contributes $\log 2$ to the entanglement entropy when the spins sit on opposite sides of the boundary, and zero in all other cases. Hence, the entropy is proportional to the number of singlets connecting the 'inside' and the 'outside'. For the model at hand, this is on average just the number of spins found inside A, i.e. $S[A] \sim |A|/\varepsilon$, a volume law.

In this chapter we provide further evidence linking the *extensivity* of the entanglement entropy with nonlocal behavior in the underlying theory. More specifically we study the examples of Little String Theory (LST) and noncommutative Yang–Mills Theory (NCYM) (see [109, 110] for reviews with a collection of early references on these subjects), using the AdS/CFT ansatz [111] for the entanglement entropy in the holographic description of these models. We find that the volume law

$$S[A] \propto \frac{|A|}{\varepsilon^{\,d}} \tag{3.1.4}$$

takes over the area law (3.1.1) when the characteristic size of A, defined as

$$\ell \equiv 2 \frac{|A|}{|\partial A|} \tag{3.1.5}$$

falls well below the critical nonlocality length, $\ell \ll \ell_c$. It is important to emphasize that we are referring here to extensivity of the leading short-distance term in the entanglement entropy, rather than the finite, cutoff-independent terms that can be identified as subleading corrections to (3.1.1). These UV-finite terms are quite interesting and the subject of some recent attention (cf. [111, 106, 21]) but will not be the main subject of this chapter.

This chapter is organized as follows. In section 3.2 we review the robustness of (3.1.1) for UV fixed points in the AdS/CFT representation and provide some insight on this fact by examining non-conformal examples of strongly coupled theories that can nevertheless be considered as local. In section 3.3 we study the entanglement of nonlocal theories. In subsection 3.3.1 we focus in the holographic description of LST and verify the emergence of a volume law at short distances. In subsection 3.3.2 we do the same for the holographic

description of NCYM. In section 3.4 we discuss how Lorentz symmetry at the boundary together with standard density of states are sufficient to guarantee the area law. We end with some conclusions in section 3.5.

3.2 Holographic entanglement entropy and locality

The holographic ansatz for the calculation of entanglement entropy in theories with UV fixed points [111] incorporates in a natural way the area law (3.1.1) (see also [112] for further developments). Any such holographic model is defined by a background of string or M-theory with asymptotic geometry $\mathrm{AdS}_{d+2} \times K_{d_K}$ near the boundary, where K_{d_K} is a compact Einstein manifold of dimension d_K. Away from the boundary the geometry can be more complex and background fields of various types may be excited, representing the breakdown of strict conformal symmetry by energy thresholds. We take the conformal boundary of the AdS_{d+2} at infinity to be given by a flat $(d+1)$-dimensional Minkowski space $\mathbb{R}^{d+1}$. Let A denote a purely spatial, d-dimensional domain in $\mathbb{R}^d$ with a smooth boundary ∂A and let $\overline{A}$ denote the minimal d-dimensional hypersurface in the bulk whose boundary on $\mathbb{R}^{d+1}$ precisely coincides with ∂A. Then, the holographic ansatz for the entanglement entropy is

$$S[A] = \frac{\mathrm{Vol}(\,\overline{A}\,)}{4G}\,, \tag{3.2.1}$$

where G is Newton's constant and the induced volume form of the bulk is defined in the Einstein frame. The hypersurface $\overline{A}$ is of codimension two on the complete bulk spacetime of dimension $d+2+d_K$, and furthermore completely wraps any compact internal cycle, such as the Einstein manifold K_{d_K} that is visible asymptotically. Hence, we can specify further (3.2.1) by working with the Kaluza–Klein reduction to $d+2$ dimensions and taking $G = G_{d+2}$ as the induced Newton's constant. Alternatively, in the particular examples of this chapter we will mostly deal with ten-dimensional backgrounds of type II string theory, and we may as well work in string-frame variables with an explicit dilaton background:

$$S[A] = \frac{1}{32\pi^6\alpha'^4}\int_{\bar{A}} d^8\sigma\, e^{-2\phi}\sqrt{G^{(8)}_{\mathrm{ind}}}\quad, \tag{3.2.2}$$

where $G^{(8)}_{\mathrm{ind}}$ denotes the determinant of the string-frame induced metric into $\bar{A}$ from the bulk, and the dilaton ϕ is normalized so that the local value of the ten-dimensional Newton's constant is $G_{10}(\phi) = 8\pi^6\alpha'^4 e^{2\phi}$.

We can now give a simple heuristic argument that explains the universality of (3.1.1) in any holographic background asymptotic to an AdS_{d+2} spacetime with metric

$$ds^2 \longrightarrow R^2\, u^2\left(-dt^2 + dx_d^2\right) + R^2\frac{du^2}{u^2}\,, \tag{3.2.3}$$

where R is the AdS radius of curvature. With this choice of coordinates, the holographic variable u has dimensions of energy and directly represents a fiducial energy scale parameter in the dual CFT. The conformal symmetry of the dual CFT is characterized by the scaling invariance of the bulk metric (3.2.3) under the combined transformation $(t, x_d, u) \to (\lambda\, t, \lambda\, x_d, \lambda^{-1} u)$. A minimal d-surface $\overline{A}$ in AdS_{d+2} with boundary ∂A penetrates into the bulk down to a 'turning point' $u \sim u_*$. Conformal symmetry implies that the minimization problem has no intrinsic length scale (the overall AdS radius R drops out of the variational problem). Therefore, using (3.1.5) as a measure of the size of A, we must have $u_* \sim 1/\ell$, provided u_* still remains well within the region where the AdS metric (3.2.3) is a good approximation. The minimal surface is locally a cylinder of the form $\partial A \times [u_\varepsilon, \infty]$ near the boundary, so that its volume gets a cutoff-dependent contribution of the form

$$\mathrm{Vol}(A)_{\mathrm{UV}} \sim R^d \,|\, \partial A \,|\, \int^{u_\varepsilon} \frac{du}{u}\, u^{d-1} \sim R^d \,|\, \partial A \,|\, \frac{u_\varepsilon^{d-1}}{d-1}\,, \tag{3.2.4}$$

which reproduces (3.1.1) with $u_\varepsilon \sim \varepsilon^{-1}$, since $N_{\mathrm{eff}} \sim R^d/G_{d+2}$ according to the standard AdS/CFT dictionary.

Heuristically we can associate the locality of the theory to the occurrence of a UV/IR relation of 'Heisenberg' type: $\ell(u_*) \sim 1/u_*$, since the radial coordinate u is interpreted as an energy scale of the CFT. We will regard this relation as the 'footprint' of a local theory, even in cases where the conformal symmetry is strongly violated.

An interesting example is provided by all the theories arising as holographic duals of Dp-brane backgrounds in type II string theory, i.e. super Yang–Mills models in $p+1$ dimensions, with gauge group $SU(N)$, and (dimensionful) 't Hooft coupling parameter $\lambda = g_{\mathrm{YM}}^2 N$ (cf. [113]). The relevant string-frame metric is scaled at the near-horizon region of the Dp-brane backgrounds:

$$ds^2/\lambda^{\frac{1}{5-p}} \propto u^{\frac{7-p}{5-p}} \left(-dt^2 + dx_p^2\right) + u^{\frac{p-3}{5-p}} \left(\frac{du^2}{u^2} + d\Omega_{8-p}^2\right)\,, \tag{3.2.5}$$

in units $\alpha' = 1$, and the dilaton profile

$$e^{-2\phi} \propto N^2\, \lambda^{\frac{p-7}{5-p}}\, u^{\frac{(7-p)(3-p)}{5-p}}\,, \tag{3.2.6}$$

generalizing the conformal $p = 3$ case. We use the radial energy variable u introduced in [114] and we neglect $O(1)$ numerical constants for the purposes of this discussion. Furthermore, it will be enough to estimate the entropy over trial cylinders capped at $u = u_*$, resulting in an expression

$$S[A] \sim N^2\, |A|\, \lambda^{\frac{p-3}{5-p}}\, u_*^{\frac{9-p}{5-p}} + \frac{5-p}{4}\, N^2\, \lambda^{\frac{p-3}{5-p}}\, |\partial A| \left(u_\varepsilon^{\frac{4}{5-p}} - u_*^{\frac{4}{5-p}}\right)\,, \tag{3.2.7}$$

which is extremal at the same Heisenberg-like UV/IR relation that featured in the conformal case:

$$u_* \sim \frac{|\partial A|}{2|A|} \equiv \frac{1}{\ell} \,. \tag{3.2.8}$$

For $p < 5$ this extremal surface is actually a local minimum of the entropy functional (3.2.5) and the resulting entanglement entropy scales as

$$S[\ell] \sim N_{\text{eff}}(\varepsilon)\frac{|\partial A|}{\varepsilon^{\,p-1}} - C_p\, N_{\text{eff}}(\ell)\frac{|\partial A|}{\ell^{\,p-1}} \,, \tag{3.2.9}$$

with C_p an $O(1)$ numerical constant. We find a local 'area law' with a renormalized effective number of degrees of freedom [2]

$$N_{\text{eff}}(\varepsilon) = N^2 \left(\frac{\lambda}{\varepsilon^{p-3}}\right)^{\frac{p-3}{5-p}} \,. \tag{3.2.10}$$

This growing number of degrees of freedom with energy is the same that becomes exposed when we excite the high-energy sector of the theory by thermal states. Here, a natural definition is to measure the effective number of degrees of freedom in terms of the thermal entropy density in units of the temperature of the system. In the bulk description, we estimate the thermal entropy density $s(T)$ by that of black holes in the background (3.2.5), according to the generalized AdS/CFT rules. The result is (cf. [113])

$$N_{\text{eff}}(T) \equiv \frac{s(T)}{T^p} \sim N^2 \left(\lambda T^{\,p-3}\right)^{\frac{p-3}{5-p}} \,. \tag{3.2.11}$$

Hence, the degrees of freedom that are being measured by the entanglement entropy in the UV are the same degrees of freedom that account for the entropy of a Yang–Mills plasma at strong coupling.

The discussion of Dp-brane systems must be restricted to the regime where the effective dimensionless 't Hooft coupling $\lambda_{\text{eff}} \sim \lambda T^{\,p-3}$ is very large, since this is the regime where the geometry is appropriately weakly curved. At the same time, N must be large enough so that the string loop expansion is under control. Beyond these thresholds one must use a variety of dualities to map out the phases of the system (cf. for example [113, 116]).

More fundamental is the restriction to $p < 5$. At $p = 5$ the previous formulas clearly break down, with N_{eff} becoming formally infinite, suggesting that the dual theory has a tower of field-theoretical excitations (a string theory). We will address this case in the next section, as our first example of a nonlocal theory. For $p > 5$ there are no working examples

[2] A similar result can be obtained for models with a logarithmic deviation from a fixed point, such as the gravity duals of 'cascading gauge theories' [115], where N_{eff} shows a logarithmic growth at high energies (cf. [106]).

of holography (for example, the density of states of black holes leads to negative specific heat). At the level of the previous formulas, the minimal hypersurface is pushed all the way to the cutoff scale $u_* = u_\varepsilon$, a first example of a *volume law*, albeit somewhat pathological (see section 4 for a thorough discussion of these cases).

3.3 Nonlocal Theories

In what follows, we turn to two examples of theories with an IR fixed point, i.e. a CFT limit at low energies, but with a built-in scale of nonlocality. In the dual geometrical description, we have backgrounds which approach AdS at *low* values of the energy variable, u, but differ very significantly at the UV boundary.

We start with the gravity dual of the worldvolume theory of NS5-branes [117]. This is related by an S-duality to the marginal case of D5-branes referred to in the previous section. Since the holographic formula for the entanglement entropy can be written in terms of the Einstein-frame metric, which is invariant under S-duality, the conclusions can be transported between Neveu–Schwarz and Dirichlet type five-branes.

Therefore, our first example arises naturally as the borderline case from the point of view of the arguments in the previous section. In particular, it corresponds to a formally infinite number of field-theoretical degrees of freedom $N_{\text{eff}} = \infty$. Not surprisingly, the dual system turns out to be a string theory, albeit of a very exotic variety.

The second example is of a different nature. We examine noncommutative Yang–Mills theories (NCYM) using their holographic description [118]. In this case, it is known that the nonlocality is of a milder nature, since it does not involve an infinite tower of field-theoretical degrees of freedom. Rather, it has to do with the violation of the microcausality rules enforced by Lorentz invariance. Accordingly, N_{eff} plays a less decisive role in this case, but nevertheless we will confirm that the entanglement entropy still probes the noncommutative nonlocality exposing a *volume law* at short distances.

3.3.1 Little String Theory

Little String Theory (LST) is defined as the decoupled world-volume theory on a stack of N NS5-branes, in the limit $g_s \to 0$ with fixed string slope α'. The effective length scale of the theory is the combination $R = \sqrt{N\alpha'}$. For large values of the rank, N, we have a dual geometrical description in terms of the near-horizon region of the NS5-branes background [119]:

$$ds^2 = -dt^2 + dx_5^2 + \frac{R^2}{r^2}dr^2 + R^2 d\Omega_3^2 \quad , \qquad e^\phi = \frac{g_s R}{r} \quad , \tag{3.3.1}$$

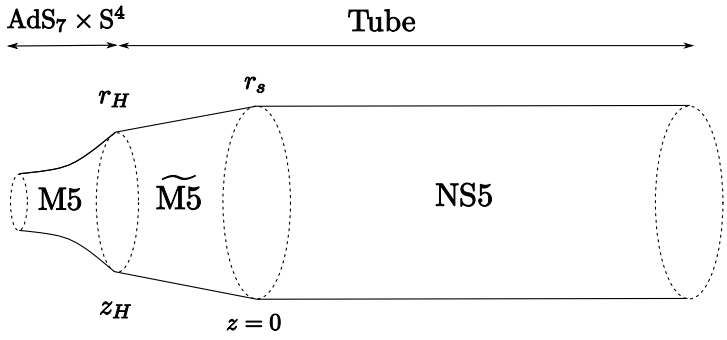

Figure 3.1: The different regions of the bulk type IIA background. The local string coupling grows towards smaller radii in the NS5 'tube', becoming of $O(1)$ at $r \sim r_s = g_s R$. At lower radii the system is well approximated by the uplifted solution to eleven dimensions, i.e. the smeared $\widetilde{\text{M5}}$-brane solution, which localizes below $r \sim r_H = g_s R/\sqrt{N}$ and flows to the $\text{AdS}_7 \times \mathbf{S}^4$ dual of the $(2,0)$ CFT in six dimensions. In the type IIB case, the $\widetilde{\text{M5}}$ phase is replaced by the near-horizon D5-brane background, and the matching at $r \sim r_H$ takes the system to a non-geometrical phase described by weakly-coupled Yang–Mills theory.

where $(t, x_5) \in \mathbb{R}^{1+5}$ parametrizes the NS5-branes world-volume, i.e. the spacetime of the LST. Changing variables to $r = g_s R \exp(z/R)$ yields

$$ds^2 = -dt^2 + dx_5^2 + dz^2 + R^2\, d\Omega_3^2\,, \qquad \phi(z) = -\frac{z}{R}\,, \tag{3.3.2}$$

confirming that R is the unique length scale of the problem, with a geometry $\mathbb{R}^{5+1} \times \mathbb{R} \times \text{S}^3$, the product of a fixed-radius sphere and a *flat* cylinder, and a linear dilaton of slope $1/R$ (cf. [117]). One can have type IIA and IIB NS5-branes giving rise to two different LSTs. We will focus on the type IIA case which has a clear holographic dual.

The interpretation of the dual theory as a string theory is borne out by the consideration of the density of states. According to the most basic of holography rules, we expect the high-energy spectrum to be well approximated by black holes in the background (3.3.2), which we will call 'the tube' in what follows. Black solutions with translational invariance on $\mathbb{R}^5$ can be written down by the substitution $dt^2 \to h(z, z_0)\, dt^2$ and $dz^2 \to dz^2/h(z, z_0)$, with the same dilaton profile and

$$h(z, z_0) = 1 - \exp\left(2(z_0 - z)/R\right)\,. \tag{3.3.3}$$

These black holes have a *constant* intrinsic temperature $T_H = (2\pi R)^{-1}$, independent of z_0, and moreover their Bekenstein–Hawking entropy yields a density of states of 'Hagedorn' type, betraying a stringy interpretation [120]:

$$\Omega(E)_{\text{BH}} = \exp(E/T_H)\,, \qquad E(z_0) = N E_H \exp(2z_0/R)\,. \tag{3.3.4}$$

In this expression $E(z_0)$ is the energy of the LST state that corresponds to a black hole with horizon at z_0. E_H is a threshold energy defined as

$$E_H = 2\pi\, N^3\, V_5\, T_H^6\ , \tag{3.3.5}$$

corresponding to the internal energy of a six-dimensional gas of $N_{\text{eff}} = N^3$ massless degrees of freedom at temperature T_H. Hence, E_H is the energy at which the LST matches to its low-energy limit, the $(2,0)$ six-dimensional CFT. In the holographic description, this matching occurs at $z = z_H = -R\log\sqrt{N}$, or $r = r_H = g_s R/\sqrt{N}$, and might be regarded as the 'infrared end' of the tube. For energies below E_H the density of states is well approximated by that of a six-dimensional CFT, with a holographic dual $\text{AdS}_7 \times \text{S}^4$ background of eleven-dimensional supergravity. To be more precise (see for example [113]), one finds the near-horizon limit of a stack of M5-branes localized in a circle, with metric

$$ds^2 = H^{-1/3}(-dt^2 + dx_5^2) + H^{2/3}\left(dx_{11}^2 + dr^2 + r^2 d\Omega_3^2\right)\ , \tag{3.3.6}$$

and profile function

$$H(r) = \sum_{n\in\mathbb{Z}} \frac{\pi N \ell_p^3}{\left[r^2 + (x_{11} - 2\pi R_{11} n)^2\right]^{3/2}}\ , \tag{3.3.7}$$

where the 11^{th} Planck length and circle radius are given by $\ell_p^3 = g_s \ell_s^3$, $R_{11} = g_s \ell_s$, with $\ell_s = \sqrt{\alpha'}$. Setting $\rho^2 = r^2 + x_{11}^2$, this geometry is well approximated at $\rho \ll R_{11}$ by

$$ds^2 \approx \frac{\rho}{(\pi N \ell_p^3)^{\frac{1}{3}}}\left(-dt^2 + dx_5^2\right) + \frac{(\pi N \ell_p^3)^{\frac{2}{3}}}{\rho^2}\left(d\rho^2 + \rho^2\, d\Omega_4^2\right) \tag{3.3.8}$$

which adopts the canonical $\text{AdS}_7 \times \text{S}^4$ form under the change of variables $\rho = 4\pi N \ell_p^3 u^2$, with $R_{\text{AdS}} = 2R_{\text{S}^4} = 2\ell_p(\pi N)^{1/3}$ and u the fiducial energy coordinate of the dual six-dimensional CFT.

On the other hand, for $r_H \ll r \ll r_s \sim g_s R$ the sum in (3.3.7) may be approximated by the first term alone, and we get the metric of N M5-branes smeared over the 11^{th} circle. In turn, this is nothing but the 11^{th} dimensional 'uplift' of the tube geometry:

$$ds_{11}^2 = e^{4\phi/3} dx_{11}^2 + e^{-2\phi/3} ds_{10}^2\ , \tag{3.3.9}$$

with ds_{10}^2 and ϕ given by (3.3.2). At $z = 0$ (or $r = r_s$) the 11^{th} circle acquires Planckian size, corresponding to the local string coupling of the type IIA description becoming of order one. The thermodynamic functions of black holes in these spaces are independent of the uplifting operation, when expressed in terms of physical energy, entropy and temperature parameters. In practice, we can compute using (3.3.2) and extend analytically the results down to $z = z_H$, where one matches to the computations done with the metric (3.3.8). For this reason, we shall refer to the whole $z \geq z_H$ region as 'the tube' in what follows.

Entanglement entropy in the LST regime

Let us compute the entanglement entropy of a region of size ℓ in $\mathbb{R}^5$, using (3.3.2) as bulk geometry. The precise formulas obtained can be readily extended to the eleven-dimensional intermediate regime in the region $z_H < z < 0$, using the metric (3.3.9), just as was the case for the thermodynamic functions. This results from the fact that the eleven-dimensional bulk hypersurface wraps the x_{11} direction and the volume form of (3.3.9) satisfies

$$d\mathrm{Vol}_{11} = e^{-2\phi} dx_{11} \wedge d\mathrm{Vol}_{10} \,, \tag{3.3.10}$$

so that both eleven-dimensional and ten-dimensional formulae give the same basic integral for the entropy as a function of the boundary data at large z.

For calculational convenience we will consider the particular case of the strip: $A = [-\ell/2, \ell/2] \times \mathbb{R}^4$. By translational symmetry on the $\mathbb{R}^4$ factor, we can work in terms on the entropy density $s[\ell]$ with the volume of $\mathbb{R}^4$ factored out. We have a functional

$$s[\ell] = \frac{|\mathrm{S}^3|}{32\pi^6 \alpha'^4 g_s^2 R^2} \int_{-\frac{\ell}{2}}^{\frac{\ell}{2}} dx\, r^2 \sqrt{1 + \frac{R^2}{r^2}\left(\frac{dr}{dx}\right)^2} \quad , \tag{3.3.11}$$

where $|\mathrm{S}^3| = R^3 \Omega_3$ is the volume of the 3-sphere. The bulk hypersurfaces are of the 'straight belt' form, $\overline{A} = \mathbb{R}^4 \times \gamma[r_*]$, where $\gamma[r_*]$ is a curve $r(x)$ subtending an asymptotic length ℓ on the boundary as $x \to \pm\ell/2$ and turning at $r_* = r(0)$, defined by $\partial_x r(0) = 0$. The smooth extremizing hypersurface verifies then

$$\ell(r_*) = 2R r_*^2 \int_{r_*}^{\infty} \frac{dr}{r\sqrt{r^4 - r_*^4}} = \frac{\pi}{2} R \,, \tag{3.3.12}$$

a very peculiar result that was already obtained in Ref. [111]. It shows that no smooth extremal surface exists if the opening at the boundary is different from $\ell = \ell_c \equiv \pi R/2$. Conversely, for $\ell = \ell_c$ there are an infinite number of them, parametrized by the turning point r_*. The entropy density at fixed r_* is

$$s[r_*] = \frac{\Omega_3 R^2}{16\pi^6 g_s^2 \alpha'^4} \int_{r_*}^{r_\varepsilon} \frac{r^3 dr}{\sqrt{r^4 - r_*^4}} = \frac{\Omega_3 R^2}{32\pi^6 g_s^2 \alpha'^4} \sqrt{r_\varepsilon^4 - r_*^4} \,, \tag{3.3.13}$$

where we have introduced r_ε as a regularization cutoff. This quantity is minimized for $r_* = r_\varepsilon$, suggesting that the minimal surface degenerates at the UV cutoff.

In order to further interpret this situation we shall consider the approximate minimization problem for a restricted set of hypersurfaces with the form of a cylinder of base ∂A and extending down to $z = z_*$, in the coordinates of (3.3.2). At $z = z_*$ we cap the cylinder with a copy of A. The contribution of the cylindrical part to the entropy is

$$S_{\mathrm{cyl}} = \frac{1}{32\pi^6 \alpha'^4} \int_{z_*}^{z_\varepsilon} dz\, e^{2z/R}\, |\partial A|\, |\mathrm{S}^3| = C\, N^4\, T_H^5\, |\partial A|\, R\, \left(e^{2z_\varepsilon/R} - e^{2z_*/R}\right) \,, \tag{3.3.14}$$

where we have used the Hagedorn temperature $T_H = (2\pi R)^{-1}$ and defined the constant $C = \Omega_3/2\pi$. The contribution of the endcap is

$$S_{\rm cap} = \frac{1}{32\pi^6\alpha'^4}\, e^{2z_*/R}\, |A|\, |\mathrm{S}^3| \ . \tag{3.3.15}$$

Combining the two, we have

$$S[A] \sim C\, N^4\, T_H^5\, R\, |\partial A|\, e^{2z_\varepsilon/R} + C\, N^4\, T_H^5\, e^{2z_*/R}\, (2|A| - R\, |\partial A|) \ . \tag{3.3.16}$$

With the standard definition of the size of A, $\ell = 2|A|/|\partial A|$ we see that the minimal hypersurface within this restricted class degenerates to $z_* = -\infty$ for $\ell > R$, or to $z_* = z_\varepsilon$ for $\ell < R$. In the marginal case $\ell = R$ there is a degeneracy with respect to z_*, corresponding to the continuous degeneracy found in (3.3.12), with a slightly renormalized value of the critical length, due to the non-smoothness of the class of hypersurfaces considered here.

Hence, we find that the entropy satisfies a volume law at short distances. We can interpret the cutoff factor $\exp(2z_\varepsilon/R)$ in terms of LST physical quantities using Eq. (3.3.4). Namely, if E_ε denotes the energy of the largest black hole that fits inside the cut-off tube, then we have $\exp(2z_\varepsilon/R) = E_\varepsilon/NE_H$, and we can finally write down the volume law in the form

$$S[A] \propto N_{\rm eff}(E_\varepsilon)\, \frac{|A|}{\ell_c^5} \ , \qquad \text{for} \quad |A| < \tfrac{1}{2}\ell_c\, |\partial A| \ . \tag{3.3.17}$$

with an effective cutoff length $\ell_c \sim 1/T_H \sim R$, and a running effective number of degrees of freedom given by

$$N_{\rm eff}(E_\varepsilon) = N^3\, \frac{E_\varepsilon}{E_H} \ , \tag{3.3.18}$$

Just as in the case of Dp-branes, this effective number of degrees of freedom corresponds exactly to the effective number of thermally excited states counted by a black hole of energy E_ε. A very interesting aspect of (3.3.17) is the treatment of the ultraviolet cutoff. The landmark of locality, i.e. Heisenberg-like UV/IR relation, breaks down and yet we must implement a cutoff procedure. The only way to enforce such a cutoff is in terms of the *total* energy of the system (see [121] for a thorough discussion of this phenomenon in the context of LST thermodynamics).

Infrared matching

The behavior for $\ell > \ell_c$ cannot be read off directly from (3.3.1), since we know that the 'tube' ends at $z_H = -R\log\sqrt{N}$ and we have to match the geometry to the near-horizon limit of a stack of M5-branes, the dual of a six-dimensional conformal field theory with $N_{\rm eff} = N^3$ degrees of freedom.

Hence for $\ell \gg \ell_c$ the minimal surface is determined by the AdS geometry of the infrared CFT and we expect an area law. In order to get a feeling of the transition from the volume law for $\ell \leq \ell_c$ to the area law for $\ell \gg \ell_c$, we can continue the analysis with the restricted hypersurface, the capped cylinder, but now with expression (3.3.16) appropriately matched to an AdS_7-like space. To perform this matching, we consider the entropy contribution of a 'cap' of boundary volume $|A|$ at height $u_H = T_H$ in the AdS space and demand that this equals (3.3.15) at $z_* = z_H$. The corresponding entropy associated to a surface capped at $u = u_*$ and extending up to the matching point $u = u_H = T_H$ is

$$S_{\rm AdS}(u_*) = 2CN^3\,|A|\,u_*^5 + 2CN^3\,|\partial A|\,\int_{u_*}^{u_H}\frac{du}{u}\,u^4\,. \tag{3.3.19}$$

and the total entropy results from adding (3.3.14) to this expression, evaluated at $z_* = z_H$. A local minimum occurs at $u_* = 2/5\ell$, provided $u_* \leq T_H$. In other words, the minimal hypersurface selects a standard local UV/IR correspondence for $\ell \geq \ell_H = 4\pi R/5$. In the remaining interval $\ell_c < \ell < \ell_H$ the minimum surface sits at the entrance of the tube, with $u_* = T_H$ and satisfying area law.[3]

We summarize the results of this section in Figs. 3.2 and 3.3. The strip entropy density $s[\ell] = S[A]/|\partial A|$ scales linearly with ℓ up to the critical length scale ℓ_c according to the volume law (3.3.17)

$$s[\ell] \sim \frac{N_{\rm eff}(E_\varepsilon)}{\ell_c^5}\,\ell\,, \qquad \ell < \ell_c\,. \tag{3.3.20}$$

A short area-law plateau follows

$$s[\ell] \sim \frac{N_{\rm eff}(E_\varepsilon)}{\ell_c^4}\,, \qquad \text{for } \ell_c < \ell < \ell_H\,, \tag{3.3.21}$$

and finally we get a very slow growth at large ℓ, corresponding to the infrared CFT:

$$s[\ell] \sim \frac{N_{\rm eff}(E_\varepsilon)}{\ell_c^4}\left(1 + b\left(1 - \ell_H^4/\ell^4\right)\right)\,, \qquad \text{for } \ell > \ell_H\,, \tag{3.3.22}$$

where b is a very small constant of $O(E_H/E_\varepsilon)$. Notice that there is no regime in which the cutoff-dependent terms adopt a field theoretical form. Instead, we find that ℓ_c takes the role of effective UV cutoff in the theory. However, the local regime, with a Heisenberg dispersion $u_* \sim 1/\ell$, is associated with an *area law*, while the nonlocal region is associated to a *volume law*. The sharp transition shown in Fig. 3.2 is expected to be an artifact of our usage of non-smooth hypersurfaces, and should be replaced by a rapid crossover in the exact treatment.

[3]The UV-finite contribution in this case satisfies a volume law. It is the short-distance contribution with explicit cutoff dependence that follows an area law. In keeping with our emphasis on the UV behavior in this chapter, we shall determine the area/volume scaling only in terms of the leading UV contribution to the entanglement entropy.

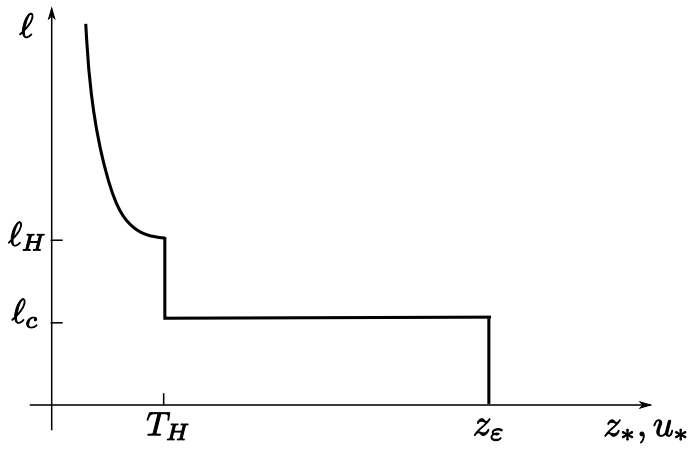

Figure 3.2: Schematic plot of the UV/IR relation, as determined by the toy minimal hypersurfaces of capped cylinders for a given value of ℓ, versus the location of the turning point in the bulk. For $\ell > \ell_H$ we have the standard 'Heisenberg-type' relation $\ell(u_*) \sim 1/u_*$, characteristic of local theories. In the interval $\ell_c < \ell < \ell_H$ the minimal surface is stuck at $u_* = u_H = T_H$ (the IR end of the tube). At $\ell = \ell_c$ there is a degenerate set of minimal surfaces with turning points anywhere in the tube, and finally for $\ell < \ell_c$ the only minimal surface is the one set at the cutoff scale $z = z_\varepsilon$.

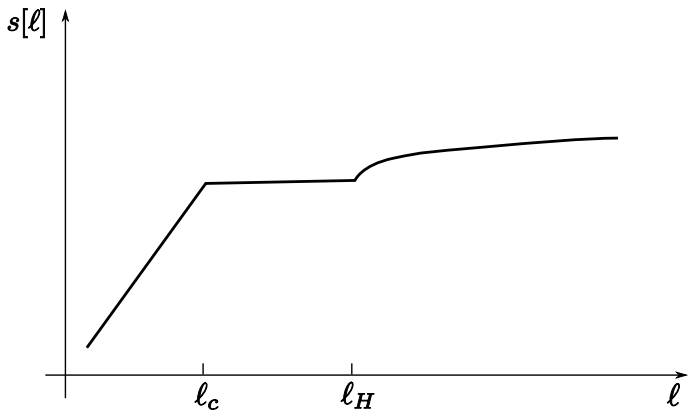

Figure 3.3: Schematic plot of the entropy density $s[\ell] = S[A]/|\partial A|$ for the toy minimal hypersurfaces of capped cylinders showing the local regime at $\ell \geq \ell_H$, the nonlocal volume law at $\ell < \ell_H$ and the intermediate transient.

Deconstructed LST

We have seen that the entanglement entropy for strips with small widths ($\ell \lesssim R$) is associated with surfaces lying at the UV cutoff of LST's dual geometry. We can ask what would happen if the LST model is given a more standard UV completion. For example, we may embed the LST theory into some UV fixed point admitting an AdS description in the gravity regime. In such models, the LST behavior is reduced to some transient in the energy variable or, in the geometric language, to some intermediate 'tube-like' geometry interpolating between and infrared (IR) AdS and some UV AdS corresponding to the asymptotic CFT at high energies. Embeddings of this type can be found in the literature, using ideas of 'deconstruction' [122, 123, 124].

One particularly simple model that admits an explicit bulk geometrical description was introduced in [124] and recently discussed at length in [121] (see this reference for more details). In this set up the UV fixed point is given by a $(2,0)$ CFT in six dimensions compactified on a circle. The merger with an intermediate LST-like background (3.3.2) is achieved via two intermediate transients described in Fig. 3.4.

To be more precise, the $\mathbb{R}^{5+1}$ world-volume of the NS5-brane is compactifed down to $\mathbb{R}^{4+1} \times \mathrm{S}^1$ on a circle of length L, with a differential warping between the $\mathbb{R}^{4+1}$ and S^1 factors in such a way that the metric is asymptotic to that of $\hat{N}$ D4-branes *smeared* over the circle of length L, where $\hat{N} \sim N^{3/2} L/g_s R$. The associated near-horizon metric

$$ds^2 \approx \frac{r}{R}\left(-dt^2 + dx_4^2\right) + \frac{R}{r}\left(dw^2 + dr^2 + r^2\, d\Omega_3^2\right) \ , \qquad e^{\phi} \approx g_s \tag{3.3.23}$$

matches the tube (3.3.2) at $r \sim r_\theta = R$. The w coordinate parametrizes the circle of size L. At even larger radii, of order $r \sim r_\Lambda = L$, the smeared D4-branes are revealed as an infrared approximation to the metric of $\hat{N}$ localized D4-branes, a system studied in the previous section of this chapter. To achieve the matching one proceeds as in the example around Eq. (3.3.7), defining now $\rho^2 = w^2 + r^2$ as the appropriate radial variable for the localized D4-branes throat.

Finally, the D4-branes develop strong coupling and match by an 11^{th} dimensional uplift to an $\mathrm{AdS}_7 \times \mathrm{S}^4$ background similar to the one appearing in the IR, but associated to a CFT with $\hat{N}^3$ degrees of freedom in the UV.

Let us consider a strip of the form $[-\ell/2, \ell/2] \times \mathrm{S}^1_L \times \mathbb{R}^3$ and define the entanglement entropy density $s[\ell]$ by factoring out the volume of the $\mathbb{R}^3$ factor. For turning points in the regime described by (3.3.23), corresponding to $r_\theta \ll r_* \ll r_\Lambda$, we have an entropy functional

$$s[\ell] = \frac{L\Omega_3}{16\pi^6 \alpha'^4 g_s^2} \int_{-\frac{\ell}{2}}^{\frac{\ell}{2}} dx\, r^3 \sqrt{1 + \frac{R^2}{r^2}\left(\frac{dr}{dx}\right)^2} \ . \tag{3.3.24}$$

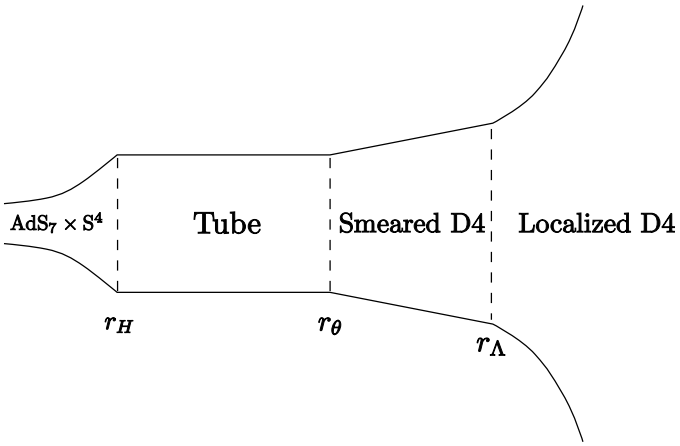

Figure 3.4: Schematic picture of the background profile in IIA deconstruction, showing the different regions of interest in the vicinity of the LST regime.

The smooth extremizing hypersurface then *fixes* the strip length to a constant value $\ell(r_*) = \ell_\theta$, independent of r_*,

$$\ell(r_*) = 2r_*^3 R \int_{r_*}^{\infty} \frac{dr}{r\sqrt{r^6 - r_*^6}} = \frac{\pi}{3} R \,, \tag{3.3.25}$$

just as in the case of the LST tube. The critical length ℓ_θ is somewhat smaller than $\ell_c = \pi R/2$, but with the same order of magnitude. In this situation, the volume of the bulk hypersurfaces at $\ell = \ell_\theta$ will be approximately minimized by the one with the largest possible value of r_*, i.e. $r_* \sim r_\Lambda$, the point where the metric is matched to that of localized D4-branes. For $\ell < \ell_\theta$ the turning point will occur inside the standard D4-brane metric, yielding standard Heisenberg dispersion $\ell \sim 1/u_*$, for an appropriate energy variable in the D4-brane throat. The resulting entropy will show the scaling (3.2.9) with the replacements $p \to 4$, $N \to \hat{N}$ and $\lambda \to g_s \hat{N}\sqrt{\alpha'}$. At even lower values of ℓ we enter the six-dimensional CFT scaling. The qualitative behavior of the dispersion relation is shown in Fig. 3.5.

At any rate, if the ultraviolet cutoff is taken all the way to the region dominated by the UV fixed point, the leading short-distance behavior of the entropy is guaranteed to be given by the six-dimensional area law

$$s[\ell] \sim \hat{N}^3 \frac{L}{\varepsilon^4} \,, \tag{3.3.26}$$

with finite-ℓ corrections that will be sensitive to the different thresholds visible in the UV/IR relation. The previous volume law is shifted to a volume law of just the UV-finite part of the entanglement entropy.

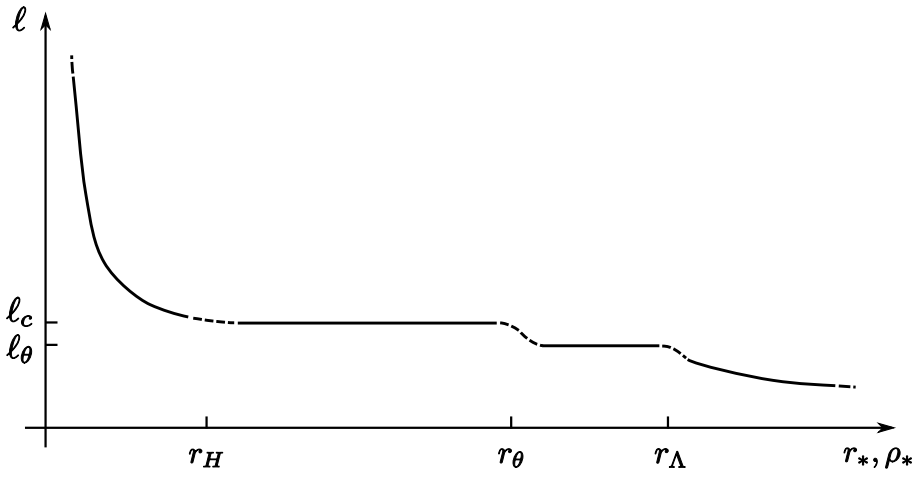

Figure 3.5: Schematic plot of ℓ as a function of r_*, ρ_* for the deconstructed LST background. In the tube region $r_H < r < r_\theta$ one has a constant behavior of ℓ as well as in $r_\theta < r < r_\Lambda$, whereas for the corresponding regions of $\ell > \ell_c$ and $\ell < \ell_\theta$ one has $\ell \sim \rho_*^{-\frac{1}{2}}$.

3.3.2 Noncommutative Yang–Mills

Compared to the example of LST, noncommutative theories epitomize a milder notion of nonlocality. Consider a maximally supersymmetric $SU(N)$ super Yang–Mills theory quantized on a spacetime $\mathbb{R}^2_\theta \times \mathbb{R}^{1+1}$, where $\mathbb{R}^2_\theta$ is the noncommutative plane defined by a Moyal algebra $[x, y] = i\theta$. Perturbative excitations behave as gluons with a rigid transversal length $L(p) = \theta p_\theta$, where p_θ is the projection of the momentum onto the noncommutative plane. The presence of these 'rigid rod' degrees of freedom introduces a basic nonlocality in the theory by the corresponding violation of Lorentz invariance, but it does not strictly affect the number of local degrees of freedom.

While propagation of such extended gluons is not affected by the noncommutative deformation, nontrivial θ dependence only arises in the interacting theory at the level of nonplanar corrections in the $1/N$ expansion. In particular, the density of states at large N is not sensitive to the noncommutative deformation.

The dual holographic description of these theories was introduced in Refs. [118], using the basic scaling of [108] in the string theory set up of Ref. [125]. The metric is

$$ds^2/R^2 = u^2\left(-dt^2 + dz^2 + f(u)(dx^2 + dy^2)\right) + \frac{du^2}{u^2} + d\Omega_5^2 \,, \tag{3.3.27}$$

with a dilaton and Neveu–Schwarz B-field:

$$e^{2\phi} = g_s^2 f(u) \,, \qquad B_{xy} = \frac{1}{\theta}(1 - f(u)) \,, \tag{3.3.28}$$

where g_s is the asymptotic string coupling in the infrared region $u \to 0$, related to the Yang–Mills coupling constant by $g^2_{\rm YM} = 2\pi g_s$. The curvature of the AdS region is controlled by the usual expression $R^4 = 4\pi g_s N \alpha'^2$, and the profile function

$$f(u) = \frac{1}{1+(a_\theta u)^4} \,, \qquad a_\theta = \sqrt{\theta}\,(4\pi g_s N)^{1/4} = (2\lambda)^{1/4}\sqrt{\theta}\,, \tag{3.3.29}$$

determines the θ-dependence through the effective length scale $a_\theta \propto \sqrt{\theta}$, renormalized by a fractional power of the 't Hooft coupling, a common occurrence in AdS holographic duals. In this form, the model is clearly asymptotic to the standard $\mathrm{AdS}_5 \times \mathrm{S}^5$ background at small values of u, which gives the energy coordinate of the infrared fixed point.

There is a further subtlety regarding the proper interpretation of this model which is of some relevance for our discussion below. The induced metric on the boundary, obtained as usual removing the u^2R^2 factor at fixed u, has in this case an anisotropy caused by the presence of the $f(u)$ factor in the noncommutative plane coordinated by (x, y). It is important however to realize that the physically relevant metric to which the energy-momentum tensor of the noncommutative theory couples is the so-called 'open-string metric', defined in Ref. [125] as

$$G_{ij} = g_{ij} - (\alpha'_{\rm eff})^2 \left(B\,\frac{1}{g}\,B \right)_{ij} \,, \tag{3.3.30}$$

where $\alpha'_{\rm eff}$ is the effective string slope parameter and g_{ij} is the metric entering the string sigma-model. In the case of the metric induced at fixed u by (3.3.27) we have (restricting to the noncommutative plane) $g_{ij} = f\delta_{ij}$, $B_{ij} = \theta^{-1}(1-f)\delta_{ij}$ and the effective string tension can be obtained by dropping a fundamental string at fixed u. Its mass per unit length is

$$\frac{1}{2\pi\alpha'_{\rm eff}} = \frac{R^2u^2}{2\pi\alpha'} \,,$$

which determines $\alpha'_{\rm eff}$. Using $a_\theta^8 = \theta^2 R^4/\alpha'^4$ from their definitions, we finally obtain $G_{ij} = \delta_{ij}$, i.e. the physical metric of the noncommutative theory is the standard Euclidean metric, despite the deformation induced by the holographic background [126] (for a recent example where this subtlety makes all the difference, see [127]). This means that, when considering the areas and volumes of a prescribed region, we will define $|A|$ and $|\partial A|$ as coordinate areas and volumes, using the standard Euclidean metric on $\mathbb{R}\times\mathbb{R}^2_\theta$, rather than the induced metric as it comes from (3.3.27). Conversely, the bulk volume that enters the holographic ansatz of the entanglement entropy will be computed in the bulk metric.

The computation

Let us consider the strip of *coordinate* width ℓ as entanglement region, and define $s[\ell]$ as the entropy density resulting from factorizing out the longitudinal volume of $\mathbb{R}^2$. The behavior

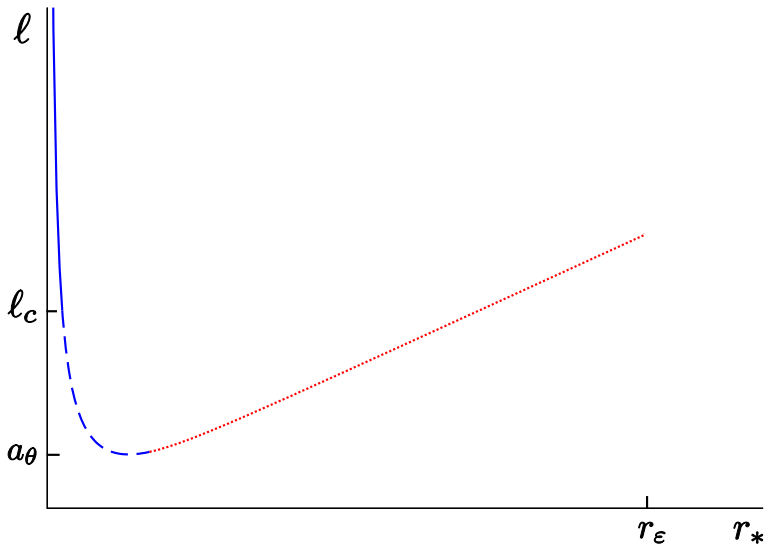

Figure 3.6: Numerical plot of the UV/IR relation in the noncommutative theory. Stable hypersurfaces (blue continuous line) disperse as $\ell \sim 1/u_*$ and unstable ones (red dotted line) disperse as $\ell \sim u_*$. The hypersurfaces with $\ell < \ell_c$ in the blue dashed line are metastable. Notice that there are no extremal smooth 3-surfaces with $\ell < \ell_{\rm min} \sim a_\theta$.

of the entanglement entropy is very sensitive to the orientation of this $\mathbb{R}^2$ plane of the strip, since the system has lost Lorentz invariance by the θ deformation. It is easy to see that the entropy functional is θ-independent when the strip plane is parallel to the noncommutative plane $\mathbb{R}^2_\theta$. Hence, the results coincide with those of the standard CFT in that case. In all other possible orientations, one finds a nontrivial result. We shall consider as representative the orthogonal orientation, in which the strip plane is orthogonal to $\mathbb{R}^2_\theta$. Without loss of generality we can align the strip along the y direction, so that ℓ is the coordinate extent of the strip in the x direction. Then, the entropy functional takes the form

$$s[\ell] = \frac{|\mathrm{S}^5| R^8}{32\pi^6 \alpha'^4 g_s^2} \int_{-\ell/2}^{\ell/2} dx\, u^3 \sqrt{1 + \frac{(du/dx)^2}{u^4 f(u)}}\ , \tag{3.3.31}$$

for a straight belt defined by a function $u(x)$ with turning point at $u_* = u(0)$, determined by the equation

$$\ell(u_*) = 2u_*^3 \int_{u_*}^{\infty} \frac{du}{u^2 \sqrt{f(u)(u^6 - u_*^6)}} = \frac{2}{u_*} \int_1^\infty \frac{ds \sqrt{1 + (a_\theta u_*)^4 s^4}}{s^2 \sqrt{s^6 - 1}}\ . \tag{3.3.32}$$

This function is shown in Fig. 3.6. It has a minimum at $\ell = \ell_{\rm min} \sim a_\theta$ and implies that there are no extremal, smooth hypersurfaces for $\ell < \ell_{\rm min}$. Conversely, for $\ell > \ell_{\rm min}$ there are two extremal hypersurfaces of which only the one with lower value of u_* is a local minimum

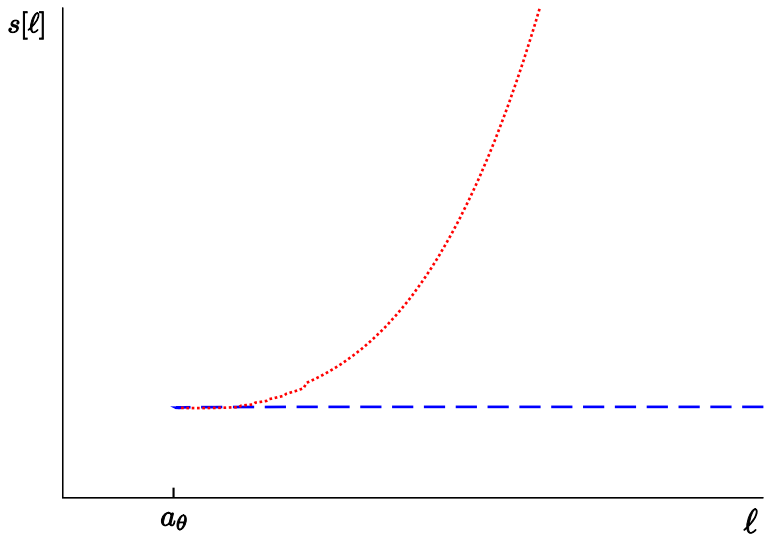

Figure 3.7: Numerical plot of the entanglement entropy for the smooth extremal hypersurfaces. The blue dashed line represents the metastable solutions whereas the red dashed line gives the entropy of the unstable solutions.

of the entropy functional. In the deep infrared $u_* a_\theta \ll 1$ we can approximate (3.3.32) by the usual local UV/IR relation,

$$\ell(u_*) \approx \frac{c_0}{u_*} , \qquad c_0 = 2\int_1^\infty \frac{ds}{s^2\sqrt{s^6-1}} = 2\sqrt{\pi}\frac{\Gamma\left(\frac{2}{3}\right)}{\Gamma\left(\frac{1}{6}\right)} . \tag{3.3.33}$$

On the other hand, in the deep noncommutative regime $u_* a_\theta \gg 1$ we have an exotic dispersion relation for the unstable extremal surfaces.

$$\ell(u_*) \approx c_\infty\, a_\theta^2\, u_* , \qquad c_\infty = 2\int_1^\infty \frac{ds}{\sqrt{s^6-1}} = \frac{\sqrt{\pi}}{3}\frac{\Gamma\left(\frac{1}{3}\right)}{\Gamma\left(\frac{5}{6}\right)} . \tag{3.3.34}$$

The entropy functional evaluated at the stable solution

$$s[\ell] = N^2\,\frac{\Omega_5}{\pi^4}\int_{u_*}^{u_\varepsilon} \frac{du\, u^4}{\sqrt{f(u)(u^6-u_*^6)}} \tag{3.3.35}$$

has a leading short-distance behavior

$$s[\ell] \sim N^2\, a_\theta^2\, u_\varepsilon^4 , \tag{3.3.36}$$

with the ℓ-dependent contribution being of order $-N^2/\ell^2$ and thus small in the limit of very large u_ε. We can compare this to the entropy of the degenerate surface sitting at the cutoff scale, $u = u_\varepsilon$, which scales extensively and is independent of $f(u)$,

$$s[\ell]_{\rm UV} \sim N^2 \ell\, u_\varepsilon^3 . \tag{3.3.37}$$

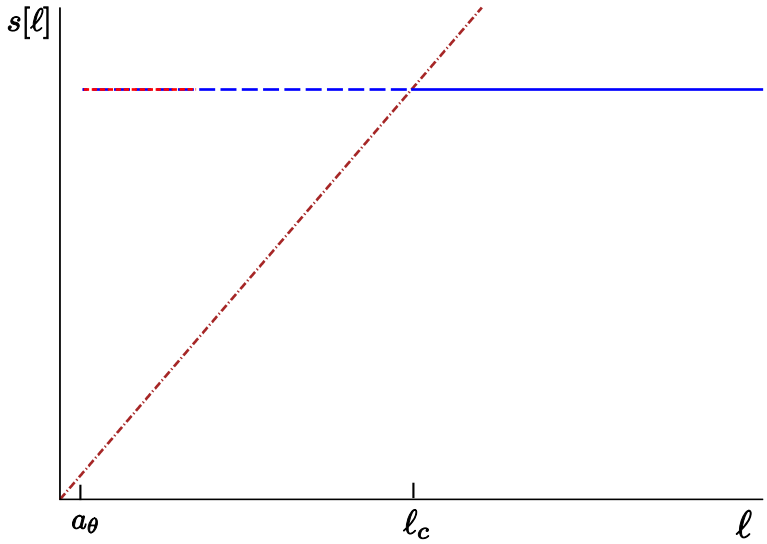

Figure 3.8: Numerical plot showing how the smooth stable 3-surface ceases to be the absolute minimum of induced volume at $\ell = \ell_c$. It is replaced by the extensive one at the cutoff scale for $\ell < \ell_c$ (brown dashed-dotted line).

We see that (3.3.37) is smaller than (3.3.36) provided $\ell < \ell_c$ with

$$\ell_c \sim u_\varepsilon a_\theta^2 \sim \frac{a_\theta^2}{\varepsilon} \sim \frac{\theta}{\varepsilon}\sqrt{\lambda}\,, \tag{3.3.38}$$

where $\lambda = g_{\rm YM}^2 N$ is the 't Hooft coupling of the IR fixed point and we have defined an effective cutoff length $\varepsilon \sim u_\varepsilon$ (see Fig. 4). That u_ε is the standard energy coordinate even for $u_\varepsilon a_\theta \gg 1$ is guaranteed by the known fact that the Hawking temperature of a black hole in the noncommutative bulk geometry (3.3.27) is independent of θ, as well as the Bekenstein–Hawking entropy. Hence, the u-coordinate of the horizon measures the temperature of the plasma phase of the NCYM theory, at least in the planar approximation.

Therefore, we can summarize the situation as follows. For large values of the strip's width, $\ell \gg \ell_c$, the short-distance contribution to the entanglement entropy shows an area law of the form

$$S[A] \propto N_{\rm eff}\frac{|\partial A|}{\varepsilon^2}\,, \qquad N_{\rm eff} = N^2\left(\frac{\ell_c}{a_\theta}\right)^2\,, \tag{3.3.39}$$

in particular, we see a renormalized value of the effective number of degrees of freedom. In this respect, the noncommutative theory differs markedly from its commutative counterpart. It should be stressed that only the cutoff-dependent contribution sees a deformed number of degrees of freedom as in (3.3.39), since the finite ℓ-dependent part has the standard scaling

$$C[\ell] \equiv \ell\frac{d}{d\ell}\,s[\ell] \sim \frac{N^2}{\ell^2}\,, \qquad \text{for} \quad \ell \gg \ell_c\,.$$

This behavior changes abruptly at $\ell \sim \ell_c$, and we switch to a *volume law*, characteristic of the nonlocal regime

$$S[A] \propto N^2 \frac{|A|}{\varepsilon^3} \,, \tag{3.3.40}$$

where this time N_{eff} is given by the standard IR value, N^2.

Finally, let us briefly point out that theories with noncommutative time can be formally defined, with $[t, z] = i\theta_e$. Even though these models are plagued with a variety of consistency problems [128] one can still carry out the analysis of the entanglement entropy at a formal level, along the preceding lines. The holographic dual has the same structure as (3.3.27) with the replacement of the 'magnetic' (x, y) plane by the 'electric' (t, z) plane in the metric, dilaton and B-field profiles. The (x, y) warping $f(u)$ is substituted by (t, z) warping $f_e(u)$, obtained by the replacement $\theta \to \theta_e$ and $a_\theta \to a_e$.

Repeating the previous analysis for this particular background we find that the local UV/IR relation $\ell u_* \sim 1$ holds in order of magnitude for the case that the strip length ℓ extends along the x or y directions, even for $\ell a_e \ll 1$. Accordingly, the area law holds for any $\ell > \varepsilon$. The short-distance scaling of the entanglement entropy still reveals an exotic number of degrees of freedom $N_{\text{eff}} \sim N^2(a_e/\varepsilon)^2$, just as in the case of 'magnetic' noncommutativity. For the case that the strip length ℓ extends along the z axis, one finds a critical length $\ell_c \sim a_e^2/\varepsilon$ for the transition to a volume law, just as the magnetic case. Now however the effective number of degrees of freedom jumps from $N_{\text{eff}} \sim N^2(\ell_c/a_e)^4$ at large ℓ to $N_{\text{eff}} \sim N^2(\ell_c/a_e)^2$ at $\ell < \ell_c$.

Interpretation of UV/IR mixing

A key consequence of our analysis is the occurrence of very strong UV/IR mixing effects in the noncommutative theory. The naive scale of nonlocality is $\sqrt{\theta}$, or rather its strong-coupling version a_θ. However, we see that the effects on the entanglement entropy, i.e. the onset of the volume law, take place at a length scale $\ell_c \sim a_\theta^2/\varepsilon$, larger than the naive one by a factor of a_θ/ε.

Continuing this result to the weakly coupled theory, it would mean that the effective scale of nonlocality is θ/ε rather than $\sqrt{\theta}$. In fact, this turns out to have a rather natural explanation. As reviewed in the introduction to this subsection, the elementary excitations of NCYM in perturbation theory are a sort of extended gluons, which behave as rigid rods of transverse size $L_{\text{eff}}(p) \sim \theta p_\theta$, with p_θ the projection of the momentum onto the noncommutative plane. Since the maximum momentum is $1/\varepsilon$, we find that the maximum size of a gluon is a rod of length θ/ε in the $\mathbb{R}^2_\theta$ plane. This reproduces the expected effective scale of nonlocality, and also explains why a strip which is cut parallel to the noncommutative plane

is insensitive to this 'growth' of the gluons.

3.4 Lorentz symmetry, entanglement entropy and the density of states

The two examples studied in this chapter might induce in the reader the impression that models with UV volume law are not that difficult to construct. In fact, we would like to argue that these two models, LST and NCYM, are quite special. We have already emphasized that the noncommutative model owes its volume law to the occurrence of rigid extended objects, particularly breaking Lorentz symmetry. In this section we point out that keeping Lorentz symmetry in the boundary theory severely restricts the possibilities.

More specifically, we will consider bulk systems with Einstein-frame metric of the form

$$ds^2/R^2 = \lambda(u)^2(-dt^2 + dx_d^2) + \frac{du^2}{\mu(u)^2} , \tag{3.4.1}$$

where the warp factors $\lambda(u), \mu(u)$ give the most general metric compatible with Lorentz symmetry on the $\mathbb{R}^{d+1}$ boundary theory. We can also assume that $\lambda(u) > 0, \mu(u) > 0$ and that $\lambda(u), \mu(u) \to u$ as $u \to 0$, i.e. we have an IR fixed point with $N_{\text{eff}} \sim R^d/G_{d+2}$ effective degrees of freedom.[4] This family of metrics includes LST, all near-horizon brane metrics and flat space as particular cases, but excludes noncommutative models with explicit violation of Lorentz symmetry.

We are interested in the behavior of minimal hypersurfaces at very large u. Using again the simple *ansatz* of a capped cylinder of base ∂A reaching down to $u = u_m$, we have

$$S(u_m) \sim N_{\text{eff}}|A|\,\lambda(u_m)^d + N_{\text{eff}}|\partial A| \int_{u_m}^{u_\varepsilon} \frac{du}{\mu(u)}\lambda(u)^{d-1} , \tag{3.4.2}$$

where the first term arises from the cap of geometry $|A|$ located at $u = u_m$ and the second term is the volume of the cylinder reaching out from u_m up to the cutoff u_ε. The turning point u_* is obtained by extremizing this expression with respect to u_m, leading to

$$\ell(u_*) \sim \frac{1}{\mu(u_*)\lambda'(u_*)} , \tag{3.4.3}$$

as the modified UV/IR relation, where $\lambda'(u)$ is the derivative of the warp factor with respect to u. Thus we recover the standard Heisenberg-like relation for the conformal case $\lambda(u) \sim \mu(u) \sim u$.

[4] In fact, we can relax this condition and keep some thresholds at low u related to nontrivial IR phenomena, such as mass gaps and confinement. Since we are emphasizing here the UV behavior, those details will not affect our analysis.

We can define a theory with *volume law* in the UV by requiring that the expression (3.4.2) is minimal at the UV cutoff, i.e. one does not decrease the total volume by lowering the position of the cap in the bulk spacetime. This condition is

$$\mu(u_\varepsilon)\lambda'(u_\varepsilon) < \frac{c}{\ell} \,, \tag{3.4.4}$$

where c is a constant of $O(1)$ and we evaluate the profile factors at the UV cutoff u_ε to indicate that we are interested in the deep UV behavior of the metric.

Now we can relate this behavior to the density of states of the theory, as defined by the Bekenstein–Hawking entropy of black holes with planar horizon. The corresponding black metrics take the form

$$ds^2/R^2 = \lambda(u)^2(-h(u)dt^2 + dx_d^2) + \frac{du^2}{\mu(u)^2 h(u)} \,, \tag{3.4.5}$$

with $h(u)$ a Schwarzschild-like factor with a first-order zero at the location of the horizon, $h(u_0) = 0$, with $h'(u_0) \sim 1/u_0$. Using standard methods we get for the Hawking temperature and Bekenstein–Hawking entropy density over $\mathbb{R}^d$:

$$T(u_0) = \frac{\lambda(u_0)\mu(u_0)}{b\, u_0} \,, \qquad s(u_0)_{\rm bh} \sim N_{\rm eff}\, \lambda(u_0)^d \,, \tag{3.4.6}$$

where b is a positive constant of $O(1)$. With the standard definition of the running effective number of degrees of freedom (species degeneracy) we have

$$N_{\rm eff}(u_0) \equiv \frac{s(u_0)}{T^d} \propto N_{\rm eff} \left(\frac{u_0}{\mu(u_0)}\right)^d \,. \tag{3.4.7}$$

We will say that a model is 'well behaved' when the running species degeneracy *does not decrease* as we access higher energies, i.e. $dN_{\rm eff}/du_0 \geq 0$. A further condition satisfied by a 'decent' holographic dual is that the specific heat should be positive, i.e. $dT/du_0 = T'(u_0) \geq 0$. Taking now the derivative of the temperature function we derive the expression

$$\mu(u_0)\lambda'(u_0) = u_0\, b\, T'(u_0) + b\, T(u_0) - \lambda(u_0)\mu'(u_0) \,,$$

and the last two terms can be related to the derivative of the running effective number of degrees of freedom, so that we can finally write

$$\mu(u_\varepsilon)\lambda'(u_\varepsilon) = b\, u_\varepsilon\, T'(u_\varepsilon) + b\, d\, T(u_\varepsilon)\, u_\varepsilon \left.\frac{d\log N_{\rm eff}}{du}\right|_{u=u_\varepsilon} \,. \tag{3.4.8}$$

Hence, we see that a positive specific heat $T'(u_\varepsilon) > 0$ in the UV, combined with a non-decreasing species degeneracy essentially guarantees that the inequality (3.4.4) will be violated and the entanglement entropy *will not* satisfy a volume law in the UV. In other words,

we will see an area law, because the UV asymptotics will be dominated by the cylinder rather than the cap.

Field-theoretical densities of states have a powerlike growth of $T(u_0)$, which is enough to ensure area law, even for an asymptotically constant $N_{\text{eff}}(u_0)$. The effect of N_{eff} in the argument is much milder, since any powerlike growth of $N_{\text{eff}}(u_0)$ only yields a constant $d\log N_{\text{eff}}/d\log u$ and a corresponding constant term on the right hand side of (3.4.8).

Conversely, models with Lorentz invariance on the boundary and volume law must have a 'pathological' density of states, either because the specific heat is negative, or because the species degeneracy decreases at high energies. For example, we may consider the case of flat space, with $\lambda(u) = \mu(u) = 1/R$, whose holographic dual, if formally defined, is expected to be a nonlocal theory [129]. Conforming to these expectations, when one calculates the entanglement entropy one finds it satisfies the volume law. And indeed, the density of states of black holes has an effective temperature $T(u_0) \sim (R^2 u_0)^{-1}$ with negative specific heat. The formal dimensional reduction of a higher-dimensional flat space behaves in a similar fashion, as well as the Dp-brane metrics with $p \geq 5$: they all present a volume law for the entanglement entropy and again both have negative specific heat and shrinking number of species (in verifying these examples, it is important to notice that (3.4.1) is written in Einstein-frame conventions after dimensional reduction to $d+2$ dimensions).

It is interesting to notice that the LST model is precisely a marginal case from the point of view of this analysis, since the effective temperature is constant $T = T_H$ in the 'LST plateau'. On the other hand, the NCYM model evades the discussion in this section, due to the violation of Lorentz symmetry, since the directional distortion of the bulk metric cancels out when computing both the Hawking temperature and the Bekenstein–Hawking entropy of black holes.

3.5 Conclusions

In this chapter we have strengthened the basic intuition that a certain degree of nonlocality tends to introduce a volume law in the scaling of the entanglement entropy, as opposed to the more standard area law, characteristic of local QFT. We have done this at very strong coupling, using the holographic definition of entanglement entropy, and testing these ideas in the case of two models with an available geometrical description, namely Little String Theory and noncommutative super Yang–Mills theory.

Our results are also interesting probes into the peculiar workings of holography in these nonlocal theories. Both models have standard IR fixed points with an AdS/CFT description and an intrinsic length of nonlocality. We find in both cases that the volume-law entangle-

ment entropy measures the effective number of degrees of freedom at high energies, weighed by the same number of degrees of freedom that get exposed by highly excited thermal states.

Both models pose interesting challenges beyond the leading classical approximation in the bulk description. In the case of LST, it has been emphasized recently that string loop corrections tend to destabilize the Hagedorn density of states, unless maximal energy cutoff is in place [121]. In the case of NCYM it is well known that non-planar corrections bring on the UV/IR effects into full strength [130]. Since one of the most important open problems in the holographic theory of entanglement entropy is the generalization beyond the classical approximation, these models will represent very stringent checks on any proposal in this direction.

Finally, we have seen that the two models studied in this chapter have a rather peculiar status. One can argue that the combination of Lorentz symmetry plus a more or less standard density of states at high energy is sufficient to guarantee an area law in the UV contribution to the entanglement entropy. The LST model arises as a marginal, exceptional case in this analysis, whereas the nocommutative model evades the argument by the violation of Lorentz symmetry. Not surprisingly, extending this treatment to the case of the holographic dual of strings in flat space, suspected to be a highly non-local theory, one finds a volume law of the entanglement entropy, thus endorsing the interpretation of volume-law scaling as a criterion of non-locality.

Chapter 4

Renormalized holographic entanglement entropy and extensivity

4.1 Introduction

After having explored the (UV divergent) non-universal part of the entanglement entropy and how its area-law behaviour can be related to the locality of the theory [20], let us now turn to the analysis of the universal contribution, i.e. the renormalized entanglement entropy or equivalently the entropy C-function [131], which are independent of any UV cutoff. The renormalized entanglement entropy is defined just as the universal part of the entanglement entropy, whereas the entropic C-function is given by (2.2.2),

$$C(\ell) = \ell \frac{dS_A(\ell)}{d\ell} \,, \tag{4.1.1}$$

where ℓ is the size scale of the A. It is obvious that both have the same functional behaviour, one just removes the leading UV term.

In chapter 2, we obtained the renormalized entanglement entropy for free massive theories and (strongly interacting) conformal ones without discussing it in detail. What we found was that the renormalized entanglement entropy also fulfills the area law, and what is more, the physical parameters of the theory were present in that area law. For conformal theories (with $d > 1$) the C-function for a strip of width ℓ was given by

$$C_{\rm A}^{\rm conformal}(\ell) \propto N_{\rm eff} \, \frac{|\mathbb{R}^{d-1}|}{\ell^{\,d-1}} \,, \tag{4.1.2}$$

whereas for the free massive theory with mass m, we had for $\ell \gg m^{-1}$ that

$$C_A^{\text{free massive}}(\ell) \propto N_{\rm eff} \, \frac{|\mathbb{R}^{d-1}|}{m^{\,1-d}} \,. \tag{4.1.3}$$

$|\mathbb{R}^{d-1}|$ refers to the (regularized) volume of $\mathbb{R}^{d-1}$. In the case of the conformal theory the only scale we have is the one introduced by the strip, ℓ, and that is the only parameter that can appear in the renormalized entanglement entropy. On the other hand in the massive theory we have an intrinsic scale in the theory, the mass, and it is that what shows up in the renormalized entanglement entropy when taking a region A much bigger than its associated length scale. When $\ell \ll m^{-1}$ one finds the conformal scaling, as one would expect since we are probing then the very high energy regime where it effectively becomes conformal.

These two examples naturally leads to the expectation that from the renormalized entanglement entropy one may read the different scales of the theory and effective degrees of freedom. In this chapter we set to study systematically the renormalized entanglement entropy browsing the different generic settings that can appear in the holographic constructions as given by different properties of the backgrounds and how they manifest in the renormalized entanglement entropy. We will always consider that the backgrounds are asymptotic to AdS but with different behaviours in the bulk. That means that all the theories we will consider will be local and hence obey the area law in the leading UV divergent term of the entanglement entropy. However this does not preclude the appearance of a volume law in the renormalized entanglement entropy as we will see later.

Renormalized Entanglement Entropy and Confinement

The first detailed study of the renormalized entanglement entropy as a tool to characterize the behaviour of the QFT was done in [106], where they explored this question for confining gauge theories (see also [107]).

The holographic dual of a confining gauge theory generically has the following structure. There is an internal manifold with some cycle. As one moves along the radial direction away from the boundary the internal cycle contracts till it smoothly vanishes at certain point. Near that point the geometry resembles a cigar. That the metric and dilaton remain smooth and finite at the tip of the cigar implies that the string tension is non-vanishing which is the manifestation that the dual gauge theory is confining. Examples of backgrounds in this class, that were considered in [106], are the geometries of coincident D3 and D4-branes on a circle with twisted boundary conditions [132], in which the shrinking cycle is a circle, and the KS geometry [133] in which it is a two-sphere. They are dual to a pure YM theory in 2+1, 3+1 dimensions and a cascading $SU(M(k+1) \times SU(Mk))$ supersymmetric theory respectively, all of them confining.

What the authors of [106] found is the following. There is a first order transition in the renormalized entanglement entropy as a function of the width of a strip, ℓ, with the point

where the transition takes places, very close to the glueball mass scale, $\ell_{\rm crit} \sim m^{-1}_{\rm glueball}$. More explicitly, the behaviour of the renormalized entanglement entropy becomes

$$S_A^{\rm renorm}(\ell) \simeq \begin{cases} -N_{\rm eff}\dfrac{|\mathbb{R}^{d-1}|}{\ell^{d-1}} & \text{for} \quad \ell < \ell_{\rm crit} \ , \\ \\ -N_{\rm eff}\dfrac{|\mathbb{R}^{d-1}|}{m_{\rm glueball}^{1-d}} & \text{for} \quad \ell > \ell_{\rm crit} \ . \end{cases} \tag{4.1.4}$$

$|\mathbb{R}^{d-1}|$ means the (regularized) volume of $\mathbb{R}^{d-1}$. We see that above the glueball scale, we have the entanglement entropy of a conformal theory whereas below the glueball scale we find the same one as a massive free theory, that is independent of ℓ. If we set as the reference entanglement entropy the one in the regime when $\ell > \ell_{\rm crit}$ (it is independent of ℓ), one finds that the change in the entropy at $\ell_{\rm crit}$ is given by

$$\Delta S_A(\ell_{\rm crit}) \simeq -N_{\rm eff}\frac{|\mathbb{R}^{d-1}|}{\ell_{\rm crit}^{d-1}} + \dots \tag{4.1.5}$$

giving us a change of order $N_{\rm eff}$ in the degrees of freedom at the transition.

For example in the case of the D3-branes we have that $N_{\rm eff} = N^2$ and this tells us that there is a change of order N^2 in the degrees of freedom of the theory. At the same time we read that the degrees of freedom below the glueball scale behave as free massive fields (with a mass equal to the glueball mass) and above it as a conformal theory. This type of behaviour is precisely what is expected for large N confining gauge theories. Their low energy effective description should reduce to a free field theory of glueballs (with a Hagedorn-like density of states), whereas at high energies it consists of an asymptotically free theory without any scale where the physical degrees of freedom are the quarks and no longer glueballs (which is the origin of going from order one to order N^2 in the number of degrees of freedom).

In the gauge theories dual to the gravitational backgrounds considered in [106], the glueball mass is separated from the Hagedorn temperature. The glueball mass is usually related to the inverse of the radius of the compact cycle that shrinks.[1] On the other hand the Hagedorn temperature is related to the scale of the massive string excitations living near the tip which is parametrically higher than the glueball scale. Thus the phase transition in the entanglement entropy happens long before the Hagedorn temperature, $\ell_{\rm crit} \gg \beta_H$. In real QCD we have only one scale $\Lambda_{\rm QCD}$ and everything happens around it. In fact when one tries to give an approximation to the entropic C-function by means of a set of massive fields with a Hagedorn spectrum, one finds that the transition would happen at the Hagedorn

[1] This is the case in the construction with stacks of D3 or D4-branes or else it is related to some units of flux as in the KS construction.

temperature scale [106]. Here the gravitational duals tells us however that the transition is linked to the glueball scale.

In the following we will explore more general scenarios than those of a confining gauge theory, analyzing the different types of qualitative behaviour that can be identified from the AdS/CFT side. We will focus on the property of *extensivity*, an admittedly non generic feature of geometric entropy in standard weak-coupling calculations at zero temperature.

In the next section we will argue that extensivity of the renormalized finite entropy is quite a generic feature of the holographic models with a gapped spectrum. We discuss in detail the conditions that ensure this behaviour, and comment on the relation to the confinement property, making contact with the results of [106] summarized above.

Finally, we focus on a particular model of especial interest, namely the case of conformal field theories in 2+1 dimensions with a magnetic field and/or electric charge condensates, holographically represented by zero-temperature extremal black holes with finite horizon area in AdS. The relevance of this system stems from the fact that the extensive law, characteristic of high-temperature states, does persists all the way down to zero temperature.

4.2 Extensivity and infrared walls

In order to fix the notation, let us consider $(d+2)$-dimensional spaces with Einstein-frame metric

$$ds^2 = R^2\,\alpha(u)^2\,\left(\frac{\beta(u)^2}{h(u)}\,du^2 + d\vec{x}^{\,2} + h(u)\,d\tau^2\right)\,, \tag{4.2.1}$$

which are assumed to asymptote AdS_{d+2} at $u\to\infty$ with radius R, i.e. the background profile functions, $\alpha(u)/u$, $\beta(u)\,u^2$ and $h(u)$ all approach unity at infinity. More general situations, where the model has no smooth UV fixed point, can be dealt with by defining a running number of degrees of freedom $N_{\rm eff}(u)$. We include the Lorentz-violating profile function $h(u)$ in order to extend the analysis to black-hole spacetimes.

One can further reduce the expression (2.3.6) for the particular situation of the strip: $\mathrm{A}(\ell) = [-\ell/2,\ell/2]\times\mathbb{R}^{d-1}$, leading to a bulk hypersurface $\overline{\mathrm{A}}$ called the 'straight belt' in [18]. The 'longitudinal' entropy density along the strip, $s_{\rm A} = S_{\rm A}/|\mathbb{R}^{d-1}|$, is given by

$$s_{\rm A} = \frac{R^d}{4G_{d+2}}\int_{-\frac{\ell}{2}}^{\frac{\ell}{2}} dx\,\gamma(u)\,\sqrt{1+\frac{(\beta(u)\partial_x u)^2}{h(u)}}\,, \tag{4.2.2}$$

with $\gamma(u)\equiv\alpha(u)^d$. This functional defines a variational problem for the profile $u(x)$, which is parametrized by the radial position u_* of the turning point $\partial_x u = 0$. The functional relation

between ℓ and u_* is given by

$$\ell(u_*) = 2\gamma(u_*) \int_{u_*}^{\infty} \frac{du\, \beta(u)}{\sqrt{h(u)\,(\gamma(u)^2 - \gamma(u_*)^2)}} \,. \tag{4.2.3}$$

Notice, however, that the minimizing hypersurface might not be a smooth one, in which case (4.2.3) ceases to apply.

The law $\ell(u_*) \sim 1/u_*$, characteristic of the conformal case, can be readily obtained by a heuristic argument. Let us model the surface $\overline{\mathrm{A}}$ as the union of two components. The first component is a cylinder extending from radial coordinate u_m up to u_ε, and subtending a strip of length ℓ in the boundary metric. The second component is the 'cap' at $u = u_m$. The entropy functional is obtained by adding the volumes of each component. Factoring out the longitudinal volume of the strip we find

$$s_A(u_m) \sim N_{\text{eff}}\, (u_\varepsilon^{d-1} - u_m^{d-1}\,) + N_{\text{eff}}\, u_m^d\, \ell \,,$$

with the first term coming from the cylinder and the second one from the cap at $u = u_m$. Minimizing with respect to u_m we find an optimal turning point satisfying $(d-1)\, u_*^{d-2} - \ell\, d\, u_*^{d-1} = 0$, which yields the desired relation $\ell u_* \sim 1$.

In a model that combines a UV fixed point and an intrinsic energy scale M, the holographic dual geometry will remain approximately AdS until we reach radial coordinates of order $u_0 \sim M$, and the form (4.1.2)

$$C_{\mathrm{A}}^{\text{conformal}}(\ell) \propto N_{\text{eff}}\, \frac{|\mathbb{R}^{d-1}|}{\ell^{\,d-1}} \,, \tag{4.2.4}$$

is a good approximation as long as $\ell M \ll 1$. A typical instance of nontrivial infrared (IR) behavior is that the radial coordinate 'terminates' at $u_0 = M$, either because of the existence of some sort of sharp wall, a 'repulsive' singularity, or perhaps a vanishing cycle along the rest of the dimensions. In this section we study the different types of qualitative behavior to be expected when the turning point u_* approaches the wall position u_0. By the conformal UV/IR relation, $\ell u_* \sim 1$, this will occur roughly around $\ell \sim 1/M$.

4.2.1 IR wall avatars

The precise functional dependence $\ell(u_*)$ is specified in Eq. (4.2.3), which we may rewrite as

$$\ell = \int_1^{\infty} \frac{dx\, \zeta(x)}{\sqrt{x^2 - 1}} \,, \tag{4.2.5}$$

where we have made a change of variables $x = \gamma(u)/\gamma(u_*)$ and we have defined the function $\zeta(x)$ by

$$\zeta(x) = 2\frac{\gamma(1)\, \beta(x)}{\gamma'(x)\sqrt{h(x)}} \,, \tag{4.2.6}$$

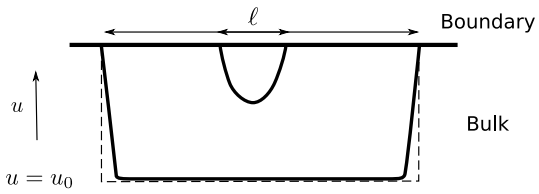

Figure 4.1: Schematic plot of the typical configuration of a smooth minimal surface that gives us the entanglement entropy in the presence of infrared walls. Close to the position of the infrared wall, the surface prefers to lean on it, giving an extensive contribution to the entropy. We also show the 'capped cylinder' in dashed lines, which becomes a better and better approximation to the minimal surface as $\ell \to \infty$.

where $\gamma' \equiv d\gamma/du$. The turning point $u = u_*$ lies at $x = 1$ in the new variables, so that $\gamma(1) = \gamma(u_*)$, and the wall sits at some $x = x_0 < 1$. In the following, we use the notation $\gamma(u_0) \equiv \gamma_0$ and $\gamma'(u_0) \equiv \gamma_0'$. There are three basic types of qualitative behavior as the turning point of *smooth* surfaces approaches the wall, $x_0 \to 1$, depending on whether ℓ diverges, approaches a constant value, or vanishes in this limit. These three alternatives can be translated into corresponding qualitative properties of the background, through the structure of the function $\zeta(x)$ in the vicinity of the wall $x \sim x_0$.

In our analysis, we shall adopt some technical assumptions derived from experience with concrete examples of holographic duals. First, we assume that $\beta(u)$ is smooth and positive for all $u \geq u_0$. The Schwarzschild-like factor $h(u)$ will be positive as well, except for a possible single zero at $u = u_0$. Finally, the warp factor $\gamma(u)$ is taken to be positive and monotonically increasing for all $u > u_0$, but we allow for the possibility that it may vanish right at the wall position. Within these technical assumptions, the only possible singularity structure of $\zeta(x)$ is either a pole at $x = x_0$, coming from a zero of the warp-factor derivative, $\gamma'(u_0) = 0$, or a square root singularity $\zeta(x) \sim (x - x_0)^{-1/2}$, coming from a regular black-hole horizon, $h(u_0) = 0$.

Since we are assuming that the model has an UV fixed point, we know that the contribution of large values of x to (4.2.5) is well approximated by the conformal law $\ell_{\text{high}} \sim 1/u_0 \sim 1/M$. Then, if $\zeta(x)$ is smooth in the vicinity of $x = 1$ we have a finite $\ell \propto 1/u_0$ as $u_* \to u_0$, perhaps decorated with some numerical factors involving dimensionless parameters of the background. A vanishing ℓ in the wall limit can only result from a vanishing warp factor $\gamma_0 = 0$.

Finally, when $\zeta(x)$ diverges as $(x - x_0)^{-1/2}$ or faster, we have $\ell \to \infty$ as $x_0 \to 1$. Then we say that the smooth surface *saturates* at the wall. In this case we have the situation depicted in Fig. 4.1, where a smooth surface asymptotically rests over the wall, forming a

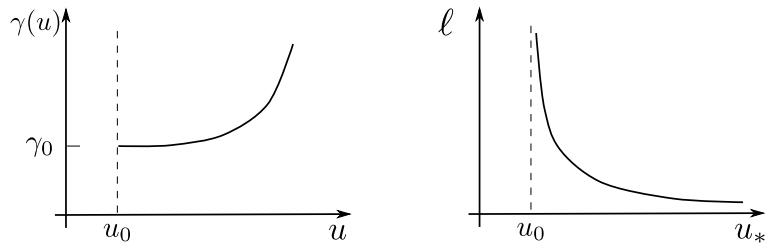

Figure 4.2: Qualitative behavior of the warp factor near a soft wall, with $\gamma_0' = 0$ and $\gamma_0 > 0$. On the right, the corresponding UV/IR relation with saturation, $\ell \to \infty$, at the wall.

cap that is smoothly joined by an almost cylindrical surface of section ∂A, reaching out to the boundary. In the limit of very large ℓ the resulting entropy is very well approximated by that of the 'capped cylinder', obtained by adjoining a 'cap' $u_0 \times$A to the cylinder $[u_0, \infty] \times \partial$A (in the case of the strip, the cylinder is just given by the two straight $[u_0, \infty] \times \mathbb{R}^{d-1}$ panels, suspended a distance ℓ apart).

We are now ready to detail the casuistics of different types of walls regarding their saturation properties.

Soft walls

These walls are characterized by a local minimum of the warp factor, $\gamma_0' = 0$, with $\gamma_0 > 0$ (we set $h(u) = 1$ for simplicity). Then $\zeta(x) \sim (x - x_0)^{-1}$ and the smooth surfaces saturate (cf. Fig. 4.2), $\ell \to \infty$ as $u_* \to u_0$. We call these walls 'soft' because the function $\gamma(x)$ usually extends for $x < x_0$, albeit with negative derivative. Static masses feel a repulsive gravitational force that prevents physical probes from reaching far into the $x < x_0$ region. Particular examples include the confinement models of [134] based on backgrounds with naked singularities. Hence, these models are usually regarded as formal qualitative tools at best.

Hard walls

These walls are defined by $\gamma_0, \gamma_0' > 0$, i.e. they behave formally as the 'sharp cutoff' regularization of a simple AdS background and are commonly used in phenomenological discussions of AdS/QCD, as in [135]. In a formal sense, they can be obtained as the 'stiff' limit of the soft walls in the previous subsection, that is to say the limit in which the minimum of $\gamma(u)$ at $u = u_0$ is made sharper and sharper.

Regarding the entanglement entropy, the most striking property of these walls is a UV/IR relation $\ell(u_*)$ with a maximal value of ℓ (cf. Fig. 4.3). Indeed, for $\ell > \ell_{\max}$ the minimizing

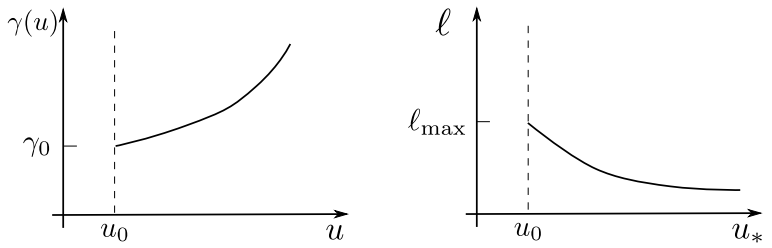

Figure 4.3: Qualitative behavior of the warp factor near a hard wall, with $\gamma_0' > 0$ and $\gamma_0 > 0$. On the right, the corresponding UV/IR relation with a maximal value of ℓ.

surface is not smooth. By explicit inspection, we can see that the cylinder $[u_0, \infty] \times \partial \mathrm{A}$, with a cap $u_0 \times \mathrm{A}$ right at the wall is a minimal surface (any perturbation takes an element of the surface to larger u, so that it increases the induced volume). Notice that this surface is not smooth because it has sharp edges at the juncture between the cap and the cylinder, but it is clearly connected and has the same topology as the smooth surfaces that extremize the problem for $\ell < \ell_{\max}$.

Resolved walls

These walls are characterized by a vanishing warp factor, $\gamma_0 = 0$, at the location of the wall. As a result, the function $\ell(u_*)$ vanishes as $u_* \to u_0$. As depicted in Fig. 4.4 there is again a maximal $\ell_{\max}$ but now there are two smooth extremal surfaces for any $\ell < \ell_{\max}$. This is the case studied at length in the examples of Ref. [106]. It corresponds to most well defined models of confinement, in which the vanishing induced metric $\gamma_0 = 0$ arises from a vanishing cycle in some extra dimension, in such a way that the higher-dimensional metric is completely smooth at $u = u_0$. For this reason we refer to these walls as 'resolved' by the higher-dimensional uplifting.

In addition to the mentioned examples studied in [106], there is a different type of model that belongs to this class, namely that of spherical distributions of D-branes in the Coulomb branch of $N = 4$ super Yang–Mills theory (cf. [136]). The dual supergravity configuration consists of a standard $\mathrm{AdS}_5 \times \mathrm{S}^5$ background for $u > M$, matched with a flat ten-dimensional metric inside the sphere at $u = M$, where M is the mass scale set by the Higgs mechanism in the Coulomb branch. The hypersurface entering the entropy ansatz wraps the S^5 spheres, which remain of constant volume for all $u > M$ but shrink to zero size as a standard angular sphere in polar coordinates for $u < M$. Since the five-dimensional warp factor $\gamma(u)$ is proportional to the volume of the internal manifold at fixed u, we find ourselves in the qualitative situation of Fig. 4.4.

Among the two solutions for each $\ell < \ell_{\rm max}$, the standard minimal embeddings correspond to the solution with the larger value of u, whereas the branch of solutions with $\ell \to 0$ as $u \to u_0$ corresponds to locally unstable surfaces. The absence of stable minimal surfaces for $\ell > \ell_{\rm max}$ makes this case similar to that of the hard wall, and the problem is resolved in the same fashion. Namely, the minimal surface at very large ℓ is not smooth, consisting of the capped cylinder lying right at the wall. [2] A crucial difference with respect to the hard wall case is that $\gamma_0 = 0$ and now the induced volume of the cap is not just minimal, but in fact it vanishes. Hence, the contribution of the minimal surface to the entropy is just given by the cylindrical portion, which was referred to in [106] as the 'disconnected surface', in the particular case of the strip.

It is important to stress, however, that the minimal surface with degenerate cap is just a member of a continuous set of surfaces with standard topology and with induced volume arbitrarily close to the minimal one. For this reason we do not think that the picture of a 'disconnected surface' is relevant or appropriate in general, despite the fact that it gives the same answer as the capped cylinder for the particular case of these walls (more on this in a subsequent section).

Thermal walls

Finally, the remaining case with a clear physical interpretation is that of a black hole horizon, $h(u_0) = 0$, corresponding to a plasma phase in the dual theory on the boundary. A regular (non-extremal) horizon will have $h'(u_0) \neq 0$ and the effective function diverges as $\zeta(x) \sim (x - x_0)^{-1/2}$ in the vicinity of the wall. This translates into a logarithmically divergent ℓ in the limit $u_* \to u_0$, as defined by (4.2.5). In other words, we have saturation by smooth surfaces and a behavior qualitatively similar to that of the soft walls.

The full Euclidean metric (4.2.1) of the black hole backgrounds is smooth at the wall, since the compact thermal cycle with the inverse temperature identification $\tau \equiv \tau + \beta$, attains vanishing size at $u = u_0$ in a smooth way. In this sense, this metric is similar to the higher-dimensional versions of the metric in the case of the resolved walls, discussed in the previous subsection. It is very important, however, to distinguish the two situations by recalling that the embedded surface $\overline{\rm A}$ is *always* localized in the τ direction, so that the vanishing thermal cycle does not translate in a vanishing induced metric at the wall, i.e. we still have $\gamma_0 > 0$ in this case. Conversely, the vanishing cycles in the examples of the previous subsection are being wrapped by the minimal surface, and do contribute to the vanishing of γ_0 there.

[2] As shown in [106] the capped cylinder remains the absolute minimum down to ℓ_c, a critical length of order $\ell_{\rm max}$, albeit somewhat smaller.

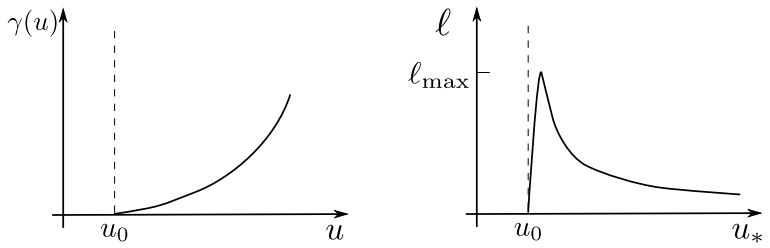

Figure 4.4: Qualitative behavior of the warp factor near a resolved wall, with $\gamma_0' > 0$ and $\gamma_0 > 0$. On the right, the corresponding UV/IR relation with a maximal value of ℓ and two smooth extremal surfaces for each $\ell < \ell_{\max}$.

4.2.2 Extensivity of the entropy

We conclude that in all cases the minimal surfaces effectively saturate at the wall. In some cases the saturating surface is smooth and well described by Eq. (4.2.5), whereas in some others the minimal surface is not smooth, given by the 'capped cylinder' at the wall. In either case, the entropy is well approximated by that of the capped cylinder, and in the cases of non-smooth minimal surfaces, it is exactly given (in the classical limit) by the volume of the capped cylinder. In fact, we may carry the complete discussion at a qualitative level in terms of a restricted family of surfaces, corresponding to cylinders of base ∂A with a cap at some $u = u_m \geq u_0$. The resulting entropy takes the form

$$S(u_m) = \frac{1}{4} N_{\text{eff}} \left[|\mathrm{A}|\, \alpha(u_m)^d + |\partial \mathrm{A}| \int_{u_m}^{u_\varepsilon} \frac{du}{\sqrt{h(u)}} \beta(u) \alpha(u)^d \right] , \tag{4.2.7}$$

where the first term is the contribution of the cap at $u = u_m$ and the second term corresponds to the cylinder extending from $u = u_m$ up to the cutoff scale $u = u_\varepsilon$. Recall that $|\mathrm{A}|$ and $|\partial \mathrm{A}|$ denote the volumes of A and its boundary in the field-theory metric. For the case of the strip $2|\mathrm{A}| = \ell |\partial \mathrm{A}|$. Taking the first derivative we find

$$\frac{dS}{du_m} = \frac{N_{\text{eff}}}{8} |\partial \mathrm{A}| \left[\ell\, d\, \gamma'(u_m) - 2 \frac{\beta(u_m)\gamma(u_m)}{\sqrt{h(u_m)}} \right] , \tag{4.2.8}$$

where we have made use of $\gamma(u) \equiv \alpha(u)^d$. Furthermore, equating it to zero fixes $u_m = u_*$ and we obtain the UV/IR relation in this approximation,

$$\ell(u_*) = \frac{2}{d} \frac{\beta(u_*)}{\sqrt{h(u_*)}} \frac{\gamma(u_*)}{\gamma'(u_*)} , \tag{4.2.9}$$

Eq. (4.2.9) shows all the qualitative features discussed previously on the basis of (4.2.5). In particular, we see that saturation, i.e. $\ell(u_* \to u_0) \to \infty$ occurs whenever $h(u_0) = 0$ or

$\gamma'(u_0) = 0$, whereas $\gamma(u_0) = 0$ ensures that there is a branch of solutions with $\ell \to 0$ in the wall limit. Eq. (4.2.8) also shows that for resolved walls and hard walls with $\gamma_0' > 0$, the entropy functional at fixed and large ℓ satisfies $dS/du_m > 0$ at $u_m = u_0$, so that the entropy is locally minimized by the capped cylinder at $u_m = u_* = u_0$ provided ℓ is large enough.

Hence, the entropy at very large ℓ is well approximated by the induced volume of the capped-cylinder in all cases. The contribution from the cylinder contains the cutoff dependence and it is proportional to $|\partial \mathrm{A}|$, i.e. it gives an area law. On the other hand, at large ℓ it is asymptotically independent of ℓ, so that it drops from the calculation of $C_{\mathrm{A}}(\ell)$. The remaining finite term is the volume of the cap at $u_* \approx u_0 = M$, appropriately redshifted to that radial position, i.e.

$$S_{\mathrm{cap}} \approx \frac{R^d \, \gamma_0 \, |\mathrm{A}|}{4 G_{d+2}} \, . \tag{4.2.10}$$

For a model asymptotic to AdS with curvature radius R, we can multiply and divide by $(u_0)^d$ to obtain the extensive law

$$C_{\mathrm{A}}(\ell) \approx S_{\mathrm{cap}} \propto \eta_M \, N_{\mathrm{eff}} \, M^d \, |\mathrm{A}| \, , \tag{4.2.11}$$

with N_{eff} the effective number of degrees of freedom at the UV fixed point CFT and $M = u_0$, the value of the capping coordinate, determining the scale of the mass gap. The new parameter

$$\eta_M = \frac{\gamma_0}{(u_0)^d} \tag{4.2.12}$$

keeps track of the 'flow' of relevant parameters from the UV fixed point at $u = \infty$ down to the IR mass scale $u_0 = M$. For example, for a model obtained by Kaluza–Klein reduction on some internal manifold K, we have

$$\eta_M = \frac{\mathrm{Vol}(K_0)}{\mathrm{Vol}(K_\infty)} \, , \tag{4.2.13}$$

where all volumes must be computed in Einstein-frame conventions, in the case of string backgrounds. In fact, we could define an effective 'infrared' number of degrees of freedom by the product $N_{\mathrm{eff},0} = \eta_M \, N_{\mathrm{eff}}$.

In many situations the flow parameter η_M is not qualitatively important. This is for example the case of black-hole backgrounds, with a dual interpretation in terms of thermal states of the QFT. In general $\gamma_0 \neq 0$ at such a black hole horizon, and we obtain an extensive component of the entropy, in accordance with general expectations (c.f. [18])

$$S_{\mathrm{A}}(T) \propto N_{\mathrm{eff}} \, T^d \, |\mathrm{A}| \, , \tag{4.2.14}$$

where $u_0 \sim T$ for a large-temperature black hole in AdS. In the next section we introduce a very interesting system in which magnetic fields or charge condensates are capable of

supporting a zero-temperature horizon with the formal properties of a thermal wall, namely supporting an nontrivial extensive law for the entanglement entropy.

Finally, the most notable exception to the extensive behavior is the case of resolved walls [106], with $\gamma_0 = 0$, which automatically yield $\eta_M = 0$ by the vanishing of $\mathrm{Vol}(K_0)$ in (4.2.13).

The role of disconnected surfaces

We have stressed that the 'disconnected surfaces' invoked in [106] are in fact standard connected surfaces in which the 'endcap' contributes zero volume due to the degenerate induced metric at the wall.[3] Indeed, there is a continuous family of surfaces of standard topology that approximate arbitrarily well the volume of the so-called disconnected surface. Exactly the same situation occurs in the two-point function of Polyakov loops, using in that case the vanishing circle Euclidean black hole backgrounds (cf. for example the discussion in [137]).[4]

Invoking disconnected surfaces has the additional problem that they would naturally minimize the large ℓ entropy in the presence of thermal walls, a situation in which we would lose the understanding of the extensivity of thermal entanglement entropy. We believe it more likely that disconnected surfaces are related to a different observable, namely the so-called *mutual information* (cf. for example [138] for a discussion of its properties and uses in quantum information). Mutual information between a bipartite partition of a system is defined as

$$I[\mathrm{A},\mathrm{B}] \equiv S_{\mathrm{A}} + S_{\mathrm{B}} - S_{\mathrm{A}\cup\mathrm{B}} \ , \tag{4.2.15}$$

where the last term is the total von Neumann entropy of the whole system, and it vanishes for a pure state. On the other hand, for a thermal state the extensive terms cancel out of (4.2.15) and one is left with the area-law terms sensitive to the UV cutoff. Applying this prescription to the holographic ansatz in a black hole background one finds that the 'caps' in the saturation surfaces are subtracted out by the standard Bekenstein–Hawking entropy and what remains is twice the volume of the uncapped cylinder, scaling with an area law. This prediction is in agreement with the work of Ref. [139] where they demonstrate for lattice systems that the mutual information follows an area law. In this respect we propose to reinterpret the work in [140] as a calculation of the mutual information rather than the strict entanglement entropy at finite temperature.

[3] The term 'disconnected surface' strictly refers to the case of the strip, in which $\partial\mathrm{A}$ is the union of two $\mathbb{R}^{d-1}$ planes. More generally, the 'disconnected surface' is regarded as the cylinder $[u_0,\infty]\times\partial\mathrm{A}$.

[4] We stress once more that the surfaces computing entanglement entropy are always orthogonal to thermal circles, somewhat like *spatial* Wilson lines and strictly *unlike* timelike Wilson lines, also known as Polyakov lines.

Phase transitions

In the previous subsections we have discussed the different qualitative possibilities corresponding to different types of walls. With little more effort one can extend the analysis further and consider combined situations, where for instance a soft wall, with $\gamma_0' = 0$, develops a degenerate metric at the wall position, $\gamma_0 \to 0$. In this case, one must study the relative rates at work, and concludes that the behavior of the prefactor $\gamma(1)$ dominates, producing a situation akin to that of resolved walls.

Another interesting complication is the consideration of systems with IR walls *and* finite temperature. In this case one must compare the competing effects of the warp factor $\gamma(u)$ *versus* the Schwarzschild factor $h(u)$. One must also consider phase transitions of the background, or Hawking–Page type. Roughly speaking the dominating background at a given temperature is the one with the largest value of the wall coordinate (up to transient effects that depend on the precise value of the free energies). For $T \ll M$ the system is characterized by a zero-temperature wall and $h(u) = 1$ (the 'confined phase'), whereas for $T \gg M$ the system is always in the plasma phase, and the relevant wall is the thermal one, determined by the zero of $h(u_0) = 0$.

We may then consider the behavior of the function $s_{\rm A}(\ell, T, M)$. For $\ell^{-1} \gg T, M$ the entanglement entropy shows conformal behavior. On the other hand, for $\ell^{-1} < \max(T, M)$ the minimal surface will be well-approximated by the capped cylinder, and the finite part of the entanglement entropy will scale 'extensively' with the law (4.2.14) for $T \gg M$ or the law (4.2.11) for $T \ll M$. In the cold phase the actual behavior will depend on whether η_M vanishes or not. If $\eta_M = 0$, such as the case of resolved walls, the entanglement entropy at very large ℓ makes a $\mathcal{O}(N_{\rm eff})$ jump across the thermal phase transition. On the other hand, for soft or hard walls with $\eta_M \sim 1$ the large-ℓ entropy is extensive at *both* low and high temperatures and only the numerical coefficient, proportional to η_M, may jump discontinuously across the deconfining phase transition.

4.3 A cold case example

The characteristic example of an extensive renormalized geometric entropy is that of a highly thermalized state, which is modeled by a large AdS black hole in the holographic map. In this picture, the condition for extensivity is the occurrence of an effective wall at $u = u_0$ which saturates the growth of the minimal hypersurface as $\ell \to \infty$. In the zero-temperature limit, $u_0 \sim T \to 0$ and the extensive term vanishes. In this section we present an example of a system that maintains the extensivity down to zero temperature, provided we have a

magnetic field and/or electric charge densities on the vacuum, supported by a large number of degrees of freedom.

As an explicit example with specific interest we can focus on the extremal dyonic black hole in AdS_4, studied recently in [17]. This black hole has a zero-temperature horizon with finite entropy density, supported by magnetic and electric fluxes. The holographic dual corresponds to a maximally supersymmetric conformal field theory in $2+1$ dimensions, the worldvolume theory of a stack of N M2-branes, in the presence of an external magnetic field and an electric charge chemical potential, both of them associated to a gauged $U(1)$ subgroup of the $SO(8)$ R-symmetry. The dyonic black hole is a solution of the Einstein–Maxwell theory on AdS_4 emerging as a consistent truncation of eleven dimensional supergravity on $AdS_4 \times S^7$ [16].

The geometry is given by

$$ds^2 = R^2\, u^2 \left(h(u) d\tau^2 + dx_1^2 + dx_2^2\right) + \frac{R^2\, du^2}{u^2\, h(u)} \,, \tag{4.3.1}$$

with

$$h(u) = 1 + (h^2+q^2)\frac{u_0^4}{u^4} - (1+h^2+q^2)\frac{u_0^3}{u^3} \,, \tag{4.3.2}$$

and electromagnetic field

$$F = B\, dx_1 \wedge dx_2 + \mu\, u_0\, dt \wedge du^{-1} \,, \tag{4.3.3}$$

where the dimensionless electric and magnetic parameters h, q are related to the magnetic field B and the charge chemical potential μ in the dual CFT by the relations

$$B = h\, u_0^2 \,, \qquad \mu = -q\, u_0 \,. \tag{4.3.4}$$

The Hawking temperature of this black hole is given by

$$T = \frac{u_0}{4\pi}\left(3 - h^2 - q^2\right) \,. \tag{4.3.5}$$

The crucial property for our purposes is that these black holes admit a zero-temperature limit at finite u_0, provided $h^2 + q^2 \to 3$. Note that the restriction $h^2 + q^2 = 3$ is perfectly compatible with general independent values of μ and B. In this limit, the horizon position becomes a function of the magnetic field and the chemical potential through

$$u_0^2 \equiv M_{\rm eff}^2 = \frac{1}{6}\left[\mu^2 + \sqrt{\mu^4 + 12B^2}\right] \,. \tag{4.3.6}$$

The resulting model satisfies the conditions laid down in the previous section. There is an effective mass scale determined by the charge and magnetic condensate, $M_{\rm eff}$, which marks the threshold separating the conformal behavior of the entropy,

$$s_{\rm A} \sim N_{\rm eff}\left(\frac{1}{\varepsilon} - \frac{1}{\ell}\right) \tag{4.3.7}$$

from the extensive behavior

$$s_{\rm A} \sim N_{\rm eff}\left(\frac{1}{\varepsilon} + M_{\rm eff}^2\,\ell\right) \ . \tag{4.3.8}$$

One can check the preceding statements by calculating numerically the entanglement entropy per unit length in the direction parallel to the strip. More precisely we find [5]

$$s_{\rm A} = \frac{\sqrt{2}}{3} N^{\frac{3}{2}} \left\{\frac{1}{\varepsilon} + f(\ell)\right\} \ , \tag{4.3.9}$$

where $f(\ell)$ is cutoff independent and interpolates between the two extreme limits (4.3.7) and (4.3.8), as shown in Fig. 4.5. The explicit form of $f(\ell)$ is given parametrically by

$$f(u_*) = u_* \left\{-1 + \int_0^1 dv \left(\frac{1}{v^2\sqrt{h(v)}\sqrt{1-v^4}} - \frac{1}{v^2}\right)\right\} \ , \quad \ell(u_*) = \frac{2}{u_*}\int_0^1 \frac{v^2 dv}{\sqrt{h(v)}\sqrt{1-v^4}} \tag{4.3.10}$$

where

$$h(v) = 1 + 3\frac{u_0^4}{u_*^4}v^4 - 4\frac{u_0^3}{u_*^3}v^3 \ .$$

These results can be generalized to arbitrary CFTs in dimension $d+1$, with 'cold' charge condensates dual to extremal charged black holes in AdS_{d+2} (magnetic fields appear together with the charge only for $d+2=4$). The corresponding supergravity solutions are studied in Ref. [141]. In these cases, the large volume asymptotics of the geometric entropy is controlled by the chemical potential:

$$S_{\rm A} \sim N_{\rm eff}\, M_{\rm eff}^d\, |{\rm A}| \ , \tag{4.3.11}$$

with $M_{\rm eff} = \mu$.

In the preceding discussion we saw how the radius of the black hole vanishes as B and μ are taken to zero, Eq. (4.3.6). Therefore, the entanglement entropy $s_{\rm A}(\ell,\mu)$ at fixed ℓ also interpolates smoothly between the two asymptotic laws (4.3.7) and (4.3.8) as μ is turned on. One may wonder whether this smooth transition is maintained in other situations, in particular in the case where the CFT lives on a sphere S^d of radius R_S, dual to asymptotic AdS geometries in global coordinates [141]. The main effect of the finite radius is to set a minimal value of chemical potential, $\mu_c \sim 1/R_S$, below which no extremal black holes are found. This transition is smooth in the sense that the black hole, present for $\mu > \mu_c$, still grows from *zero size*, according to the formula

$$u_0(\mu) = M_{\rm eff} = \frac{\sqrt{d^2-1}}{(d+1)R_S}\sqrt{\frac{\mu^2}{\mu_c^2} - 1} \ ,$$

[5] The absolute normalization follows from the relation $G_4 = 3R^2/\sqrt{8N^3}$ which gives us in this case $N_{\rm eff} = \sqrt{2N^3}/3$.

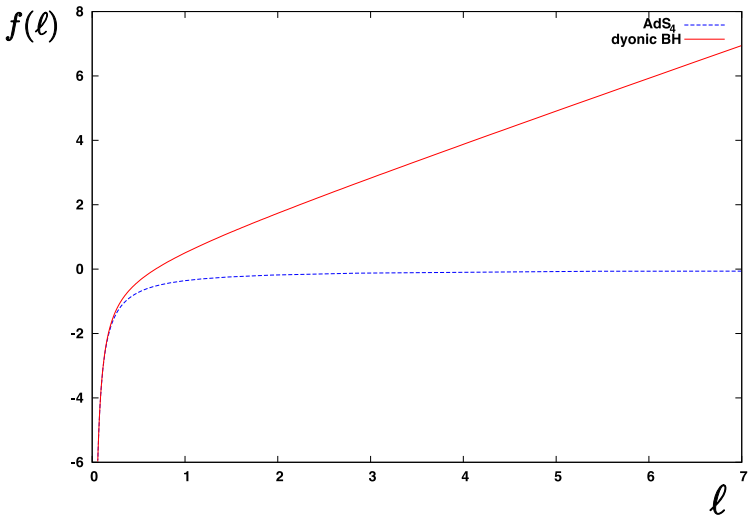

Figure 4.5: Numerical plot of the function $f(\ell)$, as defined in Eq. (4.3.9), in units where $u_0 = M_{\rm eff} = 1$. The red continuous line corresponds to the case of a CFT in $2+1$ dimensions in the presence of an external magnetic field and/or charge condensate, with a bulk dual given by the dyonic black hole background. The blue dashed line corresponds to the same CFT without any magnetic field or charge condensate, as given by the AdS_4 dual background. We see how extensive behavior, linear in ℓ, sets it at $M_{\rm eff}\ell \gg 1$ in the presence of magnetic field and/or charge condensate.

where $\mu_c^2 = d/(d-1)R_S^2$. The phase transition between pure AdS and charged black holes becomes more severe as soon as we depart from zero temperature. Switching on the temperature parameter we generate a critical line in the (T,μ) plane,

$$\left(\frac{T}{T_c}\right)^2 + \left(\frac{\mu}{\mu_c}\right)^2 = 1\ , \tag{4.3.12}$$

interpolating between our smooth $\mu = \mu_c$ critical point at $T = 0$ and the standard $\mu = 0$ Hawking–Page transition [142] at $T = T_c = d/2\pi R_S$. All $T > 0$ phase transitions on the critical line (4.3.12) are of first order, i.e. as we increase μ at fixed T, the black hole nucleates with a *finite* size $u_0(T) = 2\pi T/d$. Hence, a discontinuous behavior of s_A as a function of μ will only occur at $T > 0$, at least within the classical approximation, to order $\mathcal{O}(N_{\rm eff})$.

4.4 Concluding remarks

Our main observation in this chapter is the recognition of the extensivity as a generic property of renormalized entanglement entropy at zero temperature, when calculated using the AdS/CFT ansatz of Ref. [18]. Whenever the holographic geometry shows an infrared 'wall'

that effectively puts an end to the spacetime, the very large volume asymptotics of the geometric entropy shows extensive behavior *in principle*. In practice, many IR walls in concrete holographic models are associated to vanishing cycles in extra dimensions. In all these cases, as explicitly pointed out in [106], the extensive term in the entropy vanishes to leading order in the $1/N_{\text{eff}}$ expansion (this was characterized in the text as $\eta_M = 0$). It was suggested in [106] that the vanishing of the renormalized entanglement entropy can be regarded as an order parameter for confinement, as all of these models hold that property. Confinement, or finite string tension, arises in a rather similar fashion from the geometrical point of view, namely the saturation of Wilson loops at an IR wall is very similar to the saturation of minimal hypersurfaces of [18]. There are subtle differences though, since Wilson loops are orthogonal to vanishing cycles in extra dimensions, directly responsible for $\eta_M = 0$. On the other hand, in high-temperature plasma phases the extensive behavior of the minimal hypersurfaces resembles that of *spatial* Wilson loops.

In the case of the thermal wall models, one can say that the extensivity is associated to the breaking of conformal symmetry without the generation of a mass gap, since the plasma has $\mathcal{O}(N_{\text{eff}})$ massless degrees of freedom. In contrast, the resolved walls have a mass gap and the extensive term in the entropy vanishes. The case of the soft and hard wall models is different: they still present extensivity on the renormalized entanglement entropy. One can really say that this behaviour is really at odds with the expected properties of a system with mass gap, eq. (4.1.4). We then interpret it as an unphysical feature of this class of models.

Hence, we see that the entanglement entropy can distinguish between different models of confinement and mass gap, separating well-defined models from phenomenological ones with unphysical features.

It is worth stressing that these comments only apply to leading order in the large N_{eff} expansion. There are many examples of confinement models *without* strict mass gap, having Goldstone bosons in the spectrum from some spontaneously broken global symmetry (cf. for example [143]). However, in all these cases, the number of massless modes is $\mathcal{O}(1)$ in the large N_{eff} limit, and thus their effects are invisible in the classical approximation to the geometric entropy that is being used here.

The typical example of extensive renormalized entanglement entropy is that of highly thermalized states. We have shown in this chapter that one can find systems where the extensivity holds down to zero temperature, supported by magnetic field and/or charge condensates. This is an interesting prediction of the AdS/CFT ansatz for entanglement entropy, although the microscopic interpretation of this property in weak coupling remains an open problem. Indeed, it would be very interesting to check the conditions for this extensivity using purely QFT methods. Finally, the identification of systems with peculiar

entropy behavior at zero temperature opens up possible applications to new quantum phase transitions [9].

Part II: Non-relativistic Systems

Chapter 5

Non-relativistic Conformal Theories and their Holographic Duals

In the context of High Energy Physics one is used to think only about relativistic theories and fixed points of QFT which are conformal invariant. In these relativistic theories time and space are in equal footing and, when present, the dilation symmetry acts with the same weight on both space and time, i.e. $t \to \lambda t$, $\vec{x} \to \lambda \vec{x}$. However in Nature we have many other systems[1] that can be described by non-relativistic theories. The critical points of these non-relativistic theories poses the dilation symmetry but now it acts in general as $t \to \lambda^z t$, $\vec{x} \to \lambda \vec{x}$. That is, they have an anisotropic scale invariance, z is the *dynamical exponent*. Generically the dispersion relation will be of the form $\omega \sim k^z$.

In addition to the dilatation symmetry, D, with dynamical exponent z, the generic symmetry group will consist of time translations H, spatial translations P_i and spatial rotations M_{ij}. This symmetry algebra closes on itself and is called the *Lifshitz* algebra. One example of a theory exhibiting a fixed point with this symmetry (with $z = 2$) is the Lifshitz field theory

$$\mathcal{L} = (\partial_t \phi)^2 - \kappa \left(\nabla^2 \phi\right)^2 \ . \tag{5.0.1}$$

It describes the critical point of Rokhsar-Kivelson dimer model (see for example [144] and references therein).

One can consider the addition of Galilean boosts K_i to the algebra. When we do this we have a fully Galilean invariant theory. In this case one usually includes a central extension of the algebra,[2] a mass operator N. The resulting symmetry algebra involving

[1] For example, optimally doped cuprates, non-Fermi liquid metals near heavy electron critical points, gases of ultracold atoms, anyons, ...

[2] It is also interpreted as a number operator. It is conserved in the theory (Bargmann superselection rule). Not all non-relativistic theories admit a particle number and thus particle number is not conserved.

$\{P_i, M_{ij}, H, D, K_i, N\}$ with dynamical scaling exponent z forms the symmetry group for Galilean and scale invariant field theories. In the particular case of $z = 2$ one can further extend the symmetry algebra with the introduction of an extra 'special conformal' generator C. The resulting algebra is known as the *Schrödinger* algebra [145, 146]. It can be viewed as the non-relativistic version of conformal symmetry.

In the following we will be interested in the study of field theories symmetric under the Schrödinger group and in particular in the construction of their holographic duals. Although we will restrict our discussion to them, there has been other studies dealing with the holographic duals of Lifshitz theories and with Galilean theories with arbitrary z. For the sake of concreteness in our presentation we refer to the literature for their study, cf. for example [144, 147].

In this chapter we will review the Schrödinger invariant theories and the construction of their holographic duals, that we will study in later chapters. In section 5.1 we present in detail the Schrödinger invariant theories. In section 5.2 we discuss the paramount example of Schrödinger invariant theory that is studied in the laboratory, fermions at unitarity. Then in section 5.3 we switch to the discussion of the holographic construction of Schrödinger invariant theories. We present the general constructions that we have so far as well as their embedding in String Theory and its finite temperature and chemical potential versions.

5.1 Non-relativistic Conformal Field Theories

5.1.1 The Schrödinger group

In d spatial dimensions the geometry of the Galilei group is described as follows. The group acts on the spatial coordinates $\vec{x}$ and time t as:

$$(t, \vec{x}) \to g(t, \vec{x}) = (t + \beta, \mathscr{R}\vec{x} + \vec{v}t + \vec{a}) \quad , \tag{5.1.1}$$

where $\beta \in \mathbb{R}$; $\vec{v}, \vec{a} \in \mathbb{R}$ and $\mathscr{R}$ is a rotation matrix in d spatial dimensions. In quantum mechanics the Galilei group acts on the Hilbert space by projective representations. For example, for a scalar complex field ϕ of mass M

$$\phi(t, \vec{x}) \to \exp\left[-\frac{iM}{2}(\vec{v}^2 t + 2\vec{v}\cdot\vec{x})\right]\phi(g^{-1}(t, \vec{x})) \quad . \tag{5.1.2}$$

The presence of the mass-dependent phase factor in the transformation law tells us of a superselection rule forbidding the superposition of states of different masses. By enlarging the Galilei group through a central extension, the introduction of a mass operator or particle number, we can make the representations unitary [148].

The centrally extended Galilean algebra consists of the following generators: one particle number N, one time translation H, d spatial translations P_i, $\frac{d(d-1)}{2}$ spatial rotations M_{ij} and d Galilean boosts K_i. The non-trivial commutators are

$$\begin{aligned}
&[M_{ij}, M_{kl}] = i(\delta_{ik}M_{jl} - \delta_{jk}M_{il} + \delta_{il}M_{kj} - \delta_{jl}M_{ki}) \quad , \\
&[M_{ij}, K_k] = i(\delta_{ik}K_j - \delta_{jk} \quad , K_i) \quad , \qquad [M_{ij}, P_k] = i(\delta_{ik}P_j - \delta_{jk}P_i) \quad , \\
&[P_i, K_j] = -i\delta_{ij}N \quad , \qquad [H, K_j] = -iP_j \quad .
\end{aligned} \tag{5.1.3}$$

Galilei invariance requires the Bargmann superselection rule for masses to hold [145]. This rule states that every term in the Lagrangian of the non-relativistic Galilei-invariant theory must conserve the total mass, as given by the particle number. Hence, for the scattering process of the incoming particles $a, b, \ldots$ into the final particles $a', b', \ldots$

$$a + b + \cdots \to a' + b' + \ldots \tag{5.1.4}$$

the total mass must be conserved

$$M_a + M_b + \cdots = M_{a'} + M_{b'} + \ldots \tag{5.1.5}$$

In the non-relativistic theories the mass plays the role of the conserved charge.

It is remarkable that the group of spacetime symmetries of the non-interacting Schrödinger/ diffusion equation is larger than the Galilei group and forms the Schrödinger group [145, 146]. This is the non-relativistic counterpart of the conformal group. For the dynamical exponent[3] $z = 2$, which determines the relative scaling of time and space coordinates $[t] = [\vec{x}]^z$, there are two additional generators: the scaling generator D and the special conformal generator C. The dilatation symmetry scales the time and spatial coordinates differently in non-relativistic physics:

$$(t, \vec{x}) \to (\alpha^2 t, \alpha\vec{x}) \qquad \alpha \in \mathbb{R}. \tag{5.1.6}$$

The action of the special conformal transformation on time and spatial coordinates is given by [145]:

$$(t, \vec{x}) \to (\frac{t}{1-\gamma t}, \frac{\vec{x}}{1-\gamma t}) \qquad \gamma \in \mathbb{R}. \tag{5.1.7}$$

The additional non-trivial commutators of the Schrödinger algebra are

$$\begin{aligned}
&[P_i, D] = -iP_i \quad , \quad [P_i, C] = -iK_i \quad , \quad [K_i, D] = iK_i \quad , \\
&[D, C] = -2iC \quad , \quad [D, H] = 2iH \quad , \quad [C, H] = iD \quad .
\end{aligned} \tag{5.1.8}$$

The Hamiltonian H, scale generator D and conformal generator C close a subalgebra $sl(2, R)$ of the full Schrödinger algebra.

[3] which is consistent with the Galilei symmetry

5.1.2 Non-relativistic Conformal Field Theories

The important point is that besides the free Schrödinger theory there are known examples of interacting theories which respect the Schrödinger symmetry at the quantum level. These theories are called non-relativistic conformal field theories (NRCFT) [149]. One of them is believed to be two-component cold fermions at unitarity [149], which is one the main physical motivations behind this study and that we will describe in more detail later in sections 5.2, 7.4.

In close analogy with relativistic conformal field theories it is possible to introduce primary operators[4] in NRCFT [149]. A local primary operator $\mathscr{O}(t,\mathbf{x})$,

$$\mathscr{O}(t,\mathbf{x}) = e^{iHt-iP_ix_i}\mathscr{O}(0)e^{-iHt+iP_ix_i}\ , \tag{5.1.9}$$

has a well defined scaling dimension $\Delta_{\mathscr{O}}$ and a particle number $N_{\mathscr{O}}$:

$$[D,\mathscr{O}(0)] = i\Delta_{\mathscr{O}}\mathscr{O}(0), \qquad [N,\mathscr{O}(0)] = N_{\mathscr{O}}\mathscr{O}(0), \tag{5.1.10}$$

where $\mathscr{O}(0)\equiv\mathscr{O}(t=0,\mathbf{x}=0)$. At the same time the primary operator $\mathscr{O}$ also commutes with K_i and C:

$$[K_i,\mathscr{O}] = 0 \qquad [C,\mathscr{O}] = 0. \tag{5.1.11}$$

The primary operator $\mathscr{O}$ with the scaling dimension $\Delta_{\mathscr{O}}$ and the particle number $N_{\mathscr{O}}$ defines an irreducible representation of the full Schrödinger group. Once we have a primary operator $\mathscr{O}$, one can build up a tower of operators taking commutators with P_i and H,

$$[H,\mathscr{O}] = -i\partial_t\mathscr{O}\ , \qquad [P_i,\mathscr{O}] = i\partial_i\mathscr{O}\ . \tag{5.1.12}$$

This is due to the fact that if $\mathscr{O}$ has dimension $\Delta_{\mathscr{O}}$ then $[P_i,\mathscr{O}]$ has dimension $\Delta_{\mathscr{O}}+1$ and $[H,\mathscr{O}]$ has dimension $\Delta_{\mathscr{O}}+2$ as can be seen from (5.1.8). Thus the different representations are obtain by taking spatial and time derivatives of primary operators.

The action of the other commutators on a primary operator $\mathscr{O}$ at an arbitrary spacetime point is

$$[D,\mathscr{O}] = i(2t\partial_t + x_i\partial_i + \Delta_{\mathscr{O}})\mathscr{O} \tag{5.1.13}$$

$$[K_i,\mathscr{O}] = (-it\partial_i + N_{\mathscr{O}}x_i)\mathscr{O} \tag{5.1.14}$$

$$[C,\mathscr{O}] = -i(t^2\partial_t + tx_i\partial_i + t\Delta_{\mathscr{O}})\mathscr{O} + \frac{x^2}{x}N_{\mathscr{O}}\mathscr{O} \tag{5.1.15}$$

From (5.1.8) we also have that $[K_i,\mathscr{U}]$ would have dimension $\Delta_{\mathscr{U}}-1$ and $[C,\mathscr{U}]$ would correspond to dimension $\Delta_{\mathscr{U}}-2$.

[4] quasiprimary in the language of [150, 151]

The Schrödinger symmetry and causality condition put powerful constraints on the functional form of the correlation functions of the primary operators. In the case of the two-point correlation function of two scalar primary operators,

$$G_2(\bar{x}_1, \bar{x}_2) = \langle 0|\varphi_1(\bar{x}_1)\varphi_2^*(\bar{x}_2)|0\rangle \ , \tag{5.1.16}$$

using that $\langle 0|[K_i, \varphi_1(\bar{x}_1)\varphi_2^*(\bar{x}_2)]|0\rangle = 0$ with (5.1.14) and together with scale invariance one can obtain a set of differential equations fixing the form of the two-point correlation function up to an overall constant. The resulting form of the 2-point scalar correlation function (after Wick rotation) [150, 151] is[5]

$$G_2(\bar{x}_1, \bar{x}_2) = \langle \varphi_1(\bar{x}_1)\varphi_2^*(\bar{x}_2)\rangle = \delta_{\Delta_1,\Delta_2}\delta_{M_1,M_2}\mathscr{C}_\varphi \frac{\theta(t_1-t_2)}{(t_1-t_2)^{\Delta_1}} \exp\left[-\frac{M_1}{2}\frac{(\vec{x}_1-\vec{x}_2)^2}{t_1-t_2}\right], \tag{5.1.17}$$

where $\bar{x}_i = (t_i, \vec{x}_i)$, M_i and Δ_i denote the non-relativistic mass and the scaling dimension corresponding to the operator φ_i. $\mathscr{C}_\phi$ denotes a normalization constant.

It is possible to construct a kinematic Schrödinger invariant

$$y = \frac{[(\vec{x}_1-\vec{x}_3)(t_2-t_3) - (\vec{x}_2-\vec{x}_3)(t_1-t_3)]^2}{(t_1-t_2)(t_1-t_3)(t_2-t_3)} \tag{5.1.18}$$

from three spacetime points $\bar{x}_1$, $\bar{x}_2$ and $\bar{x}_3$. For this reason, the functional form of the 3-point function of scalar operators $G_3(\bar{x}_1, \bar{x}_2, \bar{x}_3) = \langle \varphi_1(\bar{x}_1)\varphi_2(\bar{x}_2)\varphi_3^*(\bar{x}_3)\rangle$ is fixed up to a scaling function $\Psi(y)$ [150]

$$\begin{aligned} G_3(\bar{x}_1, \bar{x}_2, \bar{x}_3) &= \delta_{M_1+M_2,M_3}\theta(t_1-t_3)\theta(t_2-t_3)(t_1-t_3)^{-\Delta_{13,2}/2}(t_2-t_3)^{-\Delta_{23,1}/2}(t_1-t_2)^{-\Delta_{12,3}/2}\times \\ &\times \exp\left[-\frac{M_1}{2}\frac{(\vec{x}_1-\vec{x}_3)^2}{t_1-t_3} - \frac{M_2}{2}\frac{(\vec{x}_2-\vec{x}_3)^2}{t_2-t_3}\right]\Psi\left(\frac{[(\vec{x}_1-\vec{x}_3)(t_2-t_3) - (\vec{x}_2-\vec{x}_3)(t_1-t_3)]^2}{(t_1-t_2)(t_1-t_3)(t_2-t_3)}\right), \end{aligned} \tag{5.1.19}$$

where we introduced $\Delta_{ij,k} = \Delta_i + \Delta_j - \Delta_k$. The scaling function $\Psi(y)$ is an arbitrary differentiable function which may have a parametric dependence on the non-relativistic masses M_1 and M_2. Here we see that the Schrödinger group is less powerful than the relativistic one, since in the relativistic case the three-point function is completely fixed by the symmetry.

As in the case of the relativistic conformal field theories (CFT), one has a state-operator correspondence for non-relativistic conformal field theories (NRCFT). When putting a CFT on a spatial sphere of constant curvature, the Euclidean Hamiltonian is proportional to the dilaton operator in flat Minkowski space, and hence one can equate energies on the sphere to conformal dimensions of local operators in the hyperplane [152]. In the case of NRCFT,

[5] in a flat infinite space

the correspondence is between primary operators and the energy eigenstates of the system in a harmonic potential [149]. Setting the frequency of the harmonic potential to Ω, the Hamiltonian of the system in the harmonic potential corresponds to

$$H_{\rm osc} = H + \Omega^2 C \ . \tag{5.1.20}$$

If $\mathscr{O}$ is a primary operator at $t = 0, \mathbf{x} = 0$, constructed from annihilation operators, such that $\mathscr{O}^\dagger$ acts non-trivially on the vacuum $|0\rangle$, then the state formed by

$$|\Psi_{\mathscr{O}}\rangle = e^{-H}\mathscr{O}^\dagger|0\rangle \tag{5.1.21}$$

satisfies that

$$H_{\rm osc}|\Psi_{\mathscr{O}}\rangle = \Delta_{\mathscr{O}}\Omega|\Psi_{\mathscr{O}}\rangle \tag{5.1.22}$$

as can be checked from the Schrödinger algebra (5.1.8) and the properties of a primary operator, (5.1.10) and (5.1.11). Actually the Hamiltonian $H_{\rm osc}$ can be solved in terms of the raising and lowering operators

$$L_+ = H - C + iD \ , \qquad L_- = H - C - iD \ . \tag{5.1.23}$$

The eigenstates are organized into ladders with spacing between steps equal to 2 [153].

One way to see that the addition of C to H is equivalent to placing the system in a harmonic potential is given by the following representation of the Schrödinger algebra. Consider a non-relativistic theory described by a second-quantized field $\psi_\alpha(\mathbf{x})$ (where α represents some spin index) and such that they satisfy the usual commutation or anti-commutation relation

$$[\psi_\alpha(\mathbf{x}), \psi^\dagger_\beta(\mathbf{y})]_\pm = \delta(\mathbf{x}-\mathbf{y})\delta_{\alpha\beta} \ . \tag{5.1.24}$$

Define a number density and momentum density,

$$n(\mathbf{x}) = \psi^\dagger(\mathbf{x})\psi(\mathbf{x}) \ , \qquad j_i(\mathbf{x}) = -\frac{i}{2}\left(\psi^\dagger(\mathbf{x})\partial_i\psi(\mathbf{x}) - \partial_i\psi^\dagger(\mathbf{x})\psi(\mathbf{x})\right) \ . \tag{5.1.25}$$

Then a representation of the Schrödinger algebra is given by

$$\begin{aligned} &N = \int d\mathbf{x}\, n(x) \ , \qquad P_i = \int d\mathbf{x}\, j_i(x) \ , \qquad M_{ij} = \int d\mathbf{x}\ (x_i j_j(\mathbf{x}) - x_j j_i(\mathbf{x})) \ , \\ &K_i = \int d\mathbf{x}\, x_i n(\mathbf{x}) \ , \qquad C = \int d\mathbf{x}\, \frac{x^2}{2} n(\mathbf{x}) \ , \qquad D = \int d\mathbf{x}\, x_i j_i(\mathbf{x}) \ . \end{aligned} \tag{5.1.26}$$

One clearly recognizes how adding C is equivalent to placing the system in a harmonic trap (of frequency unity).

5.2 An example of NRCFT: Fermions at Unitarity

Next we will present a brief contextualization and overview of fermions at unitarity, a system that can be seen as a prototype of non-relativistic system at strong coupling [154, 155]. Nonetheless this is not the only scenario where NRCFT appear. Other examples where a NRCFT makes its appearance, are in Nuclear Physics in dilute neutron matter [156] and at quantum critical points in condensed matter systems [9].

The physics of ultracold atoms in the previous decade was reshaped by the achievement of Bose-Einstein condensation (BEC) and of Fermi degeneracy in ultracold, dilute gases. These phenomena are entirely due to the particle statistics whereas the interactions are very weak. Nonetheless in the past few years, there have been two new major developments that have enlarged considerably the range of physics accessible with ultracold gases: the possibility to tune the interaction strength in cold gases by Feshbach resonances and the possibility to change the spatial dimensionality with optical potentials as well as to generate strong periodic potentials for cold atoms. Now we are able to enter the regime characteristic of strongly correlated systems. In fact the perfect control and tunability of the interactions in these systems provide a completely novel approach to study basic problems in many-body physics and, in particular, to enter regimes that have never accessible in condensed matter or nuclear physics. It allows to design, test and manipulate important toy models used in condensed matter. Apart from BEC with these ultracold gases, one can realize in the laboratory BCS-pairing, the (1-d) Luttinger liquid, quantum Hall physics in fast rotating gases, an ideal and tunable version of the Hubbard model, ... [154]

In particular people have been able to explore experimentally for fermions the crossover from a molecular BEC, of tightly bound pairs in real space, to a BCS-superfluid of weakly bound Cooper pairs and where pairing only shows up in momentum space. Bosons are much difficult to realize since the BCS-pairing of bosons is unstable to the creation of deeply bound molecules due 3-body collisions (Efimov effect) that in the case of fermions are suppressed due the Pauli exclusion principle. It is precisely at this crossover that the scattering length of the atoms becomes infinite and the system becomes effectively conformal while remaining non-relativistic.

The effective interaction of ultracold, dilute gases is fixed by the s-wave scattering length. At the same time one can control the scattering length through a Feshbach resonance. Alkali atoms such as ^{6}Li and ^{40}K have a single valence electron. When a dilute gas of atoms is cooled to very low temperatures, we can view the atoms as pointlike particles interacting via interatomic potentials which depend on the hyperfine quantum numbers. A Feshbach resonance arises if a molecular bound state, a so called “closed” channel, crosses near the

threshold of an energetically lower "open" channel, i.e. not forming bound states. One can think of a zero-energy bound state. Because the magnetic moments of the open and closed states are in general different, Feshbach resonances can be tuned using an applied magnetic field. At resonance the two-body scattering length in the open channel diverges, and the cross section σ is limited only by unitarity, $\sigma(k) = 4\pi/k^2$ for low momenta k. In the unitarity limit, details about the microscopic interaction are irrelevant, and the system displays universal properties.

Near a Feshbach resonance the scattering length, a, behaves as

$$a = a_0 \left(1 + \frac{\Delta B}{B - B_0}\right) , \tag{5.2.1}$$

where a_0 is the non-resonant scattering length, B is the magnetic field, B_0 is the position of the resonance,[6] and ΔB is the width. A small negative scattering length corresponds to the a weak attractive interaction between the atoms, that is the BCS limit. On the other side of the resonance the scattering length is positive. This is the BEC limit, the interaction is strongly attractive and the fermions form deeply bound molecules that eventually condense. The BEC/BCS crossover corresponds to the limit $a \to \pm\infty$ and one refers to it as *fermions at unitarity*. It corresponds to an isolated quantum critical point at zero temperature.

One natural starting point to describe fermions at unitarity is by means of the fermionic fields, ψ_α, $\alpha = 1, 2$, in an open channel, that couple resonantly to the closed channel bound state, ϕ, a scalar "dimer" or "diatom" [155]. The Lagrangian is

$$\mathcal{L} = i\psi_i^\dagger \partial_t \psi_i - \frac{|\nabla\psi|^2}{2m} + i\phi^*\partial_t\phi - \frac{|\nabla\phi|^2}{4m} + \phi^*\psi_1\psi_2 + \phi\psi_1^\dagger\psi_2^\dagger , \tag{5.2.2}$$

where m is the mass of the fermions.[7] Depending on the regularizaton scheme, one may need to add a counterterm $c_0^{-1}\phi^*\phi$. A chemical potential for each spin component is added by means of $\mu_i\psi_i^\dagger\psi_i$. In a completely equivalent way one can consider the theory

$$\mathcal{L} = i\psi_i^\dagger \partial_t \psi_i - \frac{|\nabla\psi|^2}{2m} + c_0\psi_1^\dagger\psi_2^\dagger\psi_1\psi_2 . \tag{5.2.3}$$

The connection to (5.2.2) is given by a Hubbard-Stratonovich transformation and where the kinetic term for ϕ is generated by fermion-loops.

The theory (5.2.2) becomes weakly coupled as $d \to 4$ (a non-interacting BEC) and as $d \to 2$ (a perfect non-interacting gas) [157, 158]. This allows to treat the theory in an ε-expansion around $2 + \varepsilon$, $4 - \varepsilon$. One finds the existence of a non-trivial fixed point at $2 + \varepsilon$,

[6] For ^{6}Li one has $B_0 = 835$G, while for ^{40}K it is $B_0 = 202$G.

[7] By dimensional analysis, if we set that $[t] = -2$, $[x] = -1$, that is the dimensions at the non-relativistic conformal point, we obtain that $[\psi] = d/2$, $[\phi] = 2$ and $[m] = 0$. We see then that m does not set any scale, it is just a dimensionless parameter of the theory.

supporting that this theory is describing a NRCFT for the physically relevant case of $d = 3$. The only known analytic results for $d = 3$ that have been obtained are through a combination of both ε-expansions with Borel-Padé resummations [157], finding rough agreement with Monte-Carlo simulations and experiments [154].

One can also devise a large N version of (5.2.2) with N fermions flavors. The theory is then invariant under $U(1) \times Sp(2N)$ and have been studied in a 1/N expansion [158, 159], again finding a non-trivial fixed point for $d = 3$.

All in all one can say that the direct treatment of (5.2.2) for $d = 3$ by field theoretical methods is not still under perfect control.

To have an idea of the challenges in which a theoretical description like (5.2.2) must succeed to fully account for fermions at unitary, we will just mention three characteristics that are so far not fully understood from first principles [155, 154].

- At zero temperature, the ground state properties of the unitary gas are determined by a single universal number, the Bertsch parameter[8] ξ. It appears for example in the question of what is the energy of the ground state with a given density n. By dimensional analysis, we only have the density and the mass, m, of each particle, and thus it must be proportional to the energy of the free gas

$$\epsilon = \frac{E}{V} = \xi\, \epsilon_{\text{free}}(n) = \xi \frac{n^{\frac{5}{3}}}{m} \,. \tag{5.2.4}$$

  The experimental data give $\xi \simeq 0.32$, whereas Monte Carlo simulations give 0.43-0.41 and the ε-expansions of [157] give 0.36-0.39. We can see the Bertsch parameter as the analog of the famous 3/4 in the context of $\mathcal{N} = 4$ SYM in AdS/CFT.

- Fermions at unitarity show interesting transport coefficients like a very small shear viscosity, typical of nearly perfect fluids. The experimental data indicate that the shear viscosity to entropy ratio is ~ 0.5, that is slightly above the holographic bound of $1/4\pi \simeq 0.08$. Experimentally one also observes large elliptic flows and very small damping rate for collective excitations. Understanding it is still an open challenge.

- The Fermi gas at unitarity is in a superfluid phase below some critical temperature T_c. There is an attractive interaction in the spin singlet channel which leads to s-wave superconductivity below some critical temperature T_c. In the unitary limit the only energy scale in the problem is the Fermi energy E_F, and we must have $k_B T_c = \alpha E_F$ with some numerical constant α. Experimental results (and quantum Monte Carlo simulations) indicate $\alpha \simeq 0.15$, which by the way is much larger that ordinary electronic superconductors.

[8] George Bertsch offered a money price to whoever gave the best theoretical value of this parameter. Since then it is called the Bertsch parameter.

In short, fermions at unitarity have become a prototype of conformal non-relativistic system at strong coupling. Its experimental realization triggered a revival of the study of NRCFTs. But nonetheless the theoretical understanding of the system is by no means straight neither complete and much is left to be learned.

5.3 Holographic duals of Non-relativistic conformal theories

Inspired by the relative success of the application of the AdS/CFT correspondence to the conceptual and quantitative understanding of the (relativistic strongly coupled) quark/gluon plasma, particularly in its hydrodynamic regime, real-time dynamics, transport coefficients, one can hope to use once again the tools of AdS/CFT to gain some intuition into NRCFTs and along the way the particular case of fermions at unitary.

Although nobody claims to have the exact holographic dual of fermions at unitary, here we will develop and study some holographic proposals that realize the Schrödinger group as the underlying symmetry of the system. The hope then is that these constructions be in the same universality class as fermions at unitary. This would eventually allow us to identify universal properties or put bounds on observables, like the ratio of viscosity to entropy, or understand semi-quantitatively the general properties of the system.

5.3.1 The holographic background

The original approach [160, 161] to construct the holographic dual of a non-relativistic Schrödinger invariant field theory is based on the realization of the symmetry group as the group of isometries of a geometry rather than a pure String Theory construction. Here the crucial ingredient, already known long time ago, is the embedding of the Schrödinger algebra as a subalgebra of the (relativistic) conformal algebra in one higher dimension. In particular, one can characterize the Schrödinger algebra as the subalgebra of the conformal group that commutes with the light-cone momentum (cf. for example [160, 151, 162, 163]).

More explicitly, the conformal algebra is given by

$$
\begin{aligned}
&[\tilde{M}^{\mu\nu}, \tilde{M}^{\alpha\beta}] = i(\eta^{\mu\alpha}\tilde{M}^{\nu\beta} + \eta^{\nu\beta}\tilde{M}^{\nu\alpha} - \eta^{\mu\beta}\tilde{M}^{\nu\alpha} - \eta^{\nu\alpha}\tilde{M}^{\mu\beta}) \quad , \\
&[\tilde{M}^{\mu\nu}, \tilde{P}^{\alpha}] = i(\eta^{\mu\alpha}\tilde{P}^{\nu} - \eta^{\nu\alpha}\tilde{P}^{\mu}) \quad , \\
&[\tilde{D}, \tilde{P}^{\mu}] = -i\tilde{P}^{\mu} \quad , \qquad [\tilde{D}, \tilde{K}^{\mu}] = i\tilde{K}^{\mu} \quad , \\
&[\tilde{P}^{\mu}, \tilde{K}^{\nu}] = -2i(\eta^{\mu\nu}\tilde{D} + \tilde{M}^{\mu\nu}) \quad , \qquad [\tilde{K}^{\rho}, \tilde{M}^{\mu\nu}] = -i(\eta^{\rho\mu}\tilde{K}^{\nu} - \eta^{\rho\nu}\tilde{K}^{\mu}) \quad ,
\end{aligned}
\tag{5.3.1}
$$

where the Greek indices run from 0 to $d+1$. If we introduce light cone coordinates $x^{\pm} = (x^0 \pm x^{d+1})/\sqrt{2}$, the subalgebra that commutes with the light-cone momentum $\tilde{P}^+ = (\tilde{P}^0 + \tilde{P}^{d+1})/\sqrt{2}$ is given by

$$\begin{aligned} &H = \tilde{P}^- \quad , \qquad P^i = \tilde{P}^i \quad , \qquad M^{ij} = \tilde{M}^{ij} \quad , \\ &K^i = \tilde{M}^{i+} \quad , \qquad D = \tilde{D} + \tilde{M}^{+-} \quad , \qquad C = \frac{\tilde{K}^+}{2} \quad , \end{aligned} \tag{5.3.2}$$

where the latin indices run from 1 to d. One can verify that this fulfills the Schrödinger algebra, (5.1.3) (5.1.8), with $N = \tilde{P}^+$. In this construction we realize the mass operator at the level of the QFT as the introduction of an additional dimension. The momentum of the fields along that direction gives us the corresponding non-relativistic mass (see [151] for a related discussion).

As a trivial example of this construction one can think of how the free Klein-Gordon equation can be recast into the free Schrödinger equation. Taking the Klein-Gordon equation in light-cone coordinates

$$\left(2\frac{\partial^2}{\partial x^+ \partial x^-} + \frac{\partial^2}{\partial \vec{x}^2}\right)\psi(x^+, x^-, \vec{x}) = 0 \ , \tag{5.3.3}$$

if one reinterprets x^+ as the time coordinate and considers the momentum $p^+ = -i\partial_{x^-}$ to be fixed, one obtains

$$i\frac{\partial}{\partial t}\psi = -\frac{1}{2p^+}\frac{\partial^2}{\partial \vec{x}^2}\psi \ . \tag{5.3.4}$$

And this is nothing else that the free Schrödinger equation when identifying p^+ with the non-relativistic mass $M \equiv p^+$.

Following this approach one starts with the AdS metric, the holographic dual of the conformal group, in light-cone coordinates. Then one further deforms it so that only the isometries fulfilling the Schrödinger algebra with $z = 2$ survive. The resulting metric is[9] [160, 161]

$$ds^2 = -\beta^2\frac{dt^2}{u^4} + \frac{-2dtd\xi + dx^i dx^i + du^2}{u^2} \tag{5.3.5}$$

with $i = 1, \ldots, d$. We will denote the space given by this geometry as Sch_{d+3} and according to the standard AdS/CFT dictionary is believed to be dual to a NRCFT. The parameter β is a measure of the deformation from pure AdS in the light-cone frame, that corresponds to

[9] The metric for an arbitrary dynamical exponent z is given by

$$ds^2 = -\beta^2\frac{dt^2}{u^{2z}} + \frac{-2dtd\xi + dx^i dx^i + du^2}{u^2} \ .$$

$\beta = 0$. As we will see later, at tree level β has no real physical meaning and only amounts to a shift in the mass of the non-relativistic particles. This metric is regular everywhere[10] and can be realized as a solution of the Einstein equations with a negative cosmological constant supported by an Abelian Higgs model in the broken symmetry phase [161] or equivalently a massive vector field [160]. The action is the last case is

$$S = \int d^{d+2}xdu\sqrt{-g}\left(R - 2\Lambda - \frac{1}{4}F_{\mu\nu}^2 - \frac{1}{2}m^2A_\mu^2\right) \tag{5.3.6}$$

with $F_{\mu\nu} = 2\nabla_{[\mu}A_{\nu]}$. The metric (5.3.5) with $A^\xi = 1$ is a solution to the above action provided

$$\Lambda = -\frac{1}{2}(d+1)(d+2)\ , \qquad m^2 = 2(d+2)\ . \tag{5.3.7}$$

An important reason to work as a full-fledged theory with the deformed metric and not AdS in the light-cone frame is that, remarkably, the causal structure of the Schrödinger metric is the one of a non-relativistic theory, i.e. sections of the spacetime with u fixed share the same future and past causal sets. The spacetime is said to be non-distinguishing [164]. However, as we will clarify in later chapters, at tree level both constructions are equivalent.

The isometries of this metric are given by

$$\begin{aligned}
&N = i\partial_\xi \quad , \qquad H = i\partial_t \quad , \qquad M^{ij} = -i(x^i\partial_j - x^j\partial_i) \quad , \\
&K^i = i(x^i\partial_\xi + t\partial_i) \quad , \qquad D = i(2\partial_t + x^j\partial_j + u\partial_u) \quad , \\
&C = i(t^2\partial_t + \frac{x^{j\,2} + u^2}{2}\partial_\xi + tx^j\partial_j + tu\partial_u) \quad .
\end{aligned} \tag{5.3.8}$$

They obey the Schrödinger algebra with the given identifications. It is worth stressing that the isometry of (5.3.5) associated with the light-cone momentum, $N \equiv \tilde{P}^+$, the central charge of the Schrödinger algebra, is identified with ∂_ξ. From the quantum field theory point of view, $\tilde{P}^+$ is the mass operator, so that the momentum along ∂_ξ at the boundary can be identified with the non-relativistic mass. Applying the usual holographic dictionary the value of a field at the boundary of the spacetime acts as source of the QFT operator. Since we want to consider operators with a well defined non-relativistic mass, we have to further impose that the fields in the Schrödinger metric have a well defined momentum along the ∂_ξ direction at the boundary.

The other issue is that the non-relativistic mass can be interpreted as number operator. As such its values should be discretized. This forces upon us the compactification along the ∂_ξ direction. However this direction is null, we would be dealing with a discrete light cone

[10] Although not geodesically complete, these coordinates only cover a patch of the full spacetime. See later discussion in section 6.2.3.

quantization (DLCQ). This implies that we have to be extremely careful with the divergences arising from the zero modes there (at the loop level) [165]. As we will see introducing a finite chemical potential or temperature (both breaking conformal invariance) will make the ∂_ξ-direction spatial like and hence this problem ceases. Strictly speaking then the Sch_{d+3} metric (5.3.5) can only be trusted at tree level or else needs to be regularize at the loop-level (see chapter 7).

As a first check that the metric given by Sch_{d+3} is really describing a NRCFT, apart from its isometry algebra, comes from the computation of the 2-point function for some primary scalar operators, with definite scaling weights and non-relativistic masses. Using the standard AdS/CFT dictionary, a scalar field in the bulk, ϕ, will source a scalar operator at the boundary theory, $\mathscr{O}$. In this sense one can consider a massive field with mass m_0 that couples minimally to gravity,

$$S = -\int d^{d+3}x\sqrt{-g}\left(\partial_\mu\phi^*\partial^\mu\phi + m_0^2\phi^*\phi\right) \tag{5.3.9}$$

together with the requirement that is has a definite momentum along the ∂_ξ-direction, i.e

$$\phi(\xi, x) = e^{-iM\xi}\phi(x)\ , \tag{5.3.10}$$

and hence imposing that the dual operator $\mathscr{O}$ has a definite mass M.

By solving the equations of motion for this scalar one can find the scaling dimension as well as the 2-point function. The solutions to the equations of motion are exactly the same as in pure AdS_{d+3}, but in light-cone coordinates with a fixed momentum along a light-like direction, and provided one shifts the mass to $m^2 = m_0^2 + \beta^2 M^2$. That is, one finds two different solutions [160, 161]

$$\phi(x)_\pm = z^{\frac{d}{2}+1}K_\pm(pz)\ , \qquad p = (\vec{k} - 2M\omega)^{\frac{1}{2}}\ , \qquad \nu = \sqrt{m^2 + \frac{(d+2)^2}{4}} \tag{5.3.11}$$

where $\vec{k}$ and ω denote the spatial momentum and frequency of the field.

In the case when $\nu \geq 1$, ϕ_+ is non-normalizable and ϕ_- is normalizable. This tells us that ϕ_+ is the source for $\mathscr{O}$, with a scaling dimension

$$\Delta = \frac{d+2}{2} + \nu\ , \tag{5.3.12}$$

whereas ϕ_- corresponds to a condensate for $\mathscr{O}$. Only when $0 < \nu < 1$ both solutions are normalizable. In this case there is an ambiguity in the choice of source and condensate. Each choice corresponds to a possible quantization of the theory where the scaling dimension for the operator $\mathscr{O}$ is then $\Delta_\pm = (d+2)/2 \pm \nu$. This ambiguity is in fact welcome, since it can

be seen as the analogous sign of what happens for fermions described by (5.2.2) where the same theory can be in its free fixed point or at the unitary point. In fact in this case the diatom operator $\psi_\uparrow\psi_\downarrow$ has a dimension $\Delta^{(\uparrow\downarrow)}$ which is symmetric with respect to $(d+2)/2$, it is given by

$$\Delta^{(\uparrow\downarrow)}_{\text{free fermions}} = \frac{d+2}{2} + \frac{d+2}{2} = d\,, \qquad \Delta^{(\uparrow\downarrow)}_{\text{unitary fermions}} = \frac{d+2}{2} + \frac{d-2}{2} = 2\,. \tag{5.3.13}$$

From the expressions for the scaling dimension one can see that there is a lower bound

$$\Delta > \frac{d}{2} \tag{5.3.14}$$

that precisely corresponds to the Breitenlohner–Freedman bound in AdS [166]. This bound is expected for a NRCFT since the operator dimensions correspond to energy eigenvalues of the fields in a harmonic potential, where a lower bound clearly exists. Later we will find that the bound actually agrees with it (cf. chapter 6).

From the explicit solutions (5.3.11) one can obtain the 2-point function. It given by [161]

$$\langle \mathscr{O}_1(\vec{x},t)\mathscr{O}_2(\vec{x},t)\rangle = \delta_{\Delta_1,\Delta_2}\delta_{M_1,M_2}\mathscr{C}_\varphi \frac{\theta(t_1-t_2)}{(t_1-t_2)^{\Delta_1}} \exp\left[-\frac{M_1}{2}\frac{(\vec{x}_1-\vec{x}_2)^2}{t_1-t_2}\right], \tag{5.3.15}$$

that perfectly agrees with the requirements of Schrödinger invariance, Eq. (5.1.17). This is a reassuring sign in favor of this construction making sense as a dual of a NRCFT. Later in chapter 7 we will study the higher order correlation functions.

5.3.2 Embedding in String Theory: TsT transformation

Before proceeding to present the finite temperature and finite chemical case, that basically amounts to finding a black hole solution that asymptotes to Sch_{d+3}, we will detour by giving first a String Theory embedding of Sch_5. As a byproduct we will obtain a straight procedure to find finite temperature and chemical potential solutions.

Instead of constructing directly Sch_{d+3} as the near horizon metric of some stack of branes, that gives a direct identification of the dual QFT theory as the worldvolume theory of the branes, we will use instead the TsT transformation [167] (or equivalently the Melvin twist [168]) on a given familiar String Theory construction. The TsT transformation is a solution generating technique in the context of type II supergravity. By applying a TsT transformation to $\text{AdS}_{d+3}\times Y$ (with Y a Sasaki-Einstein manifold) one can obtain $\text{Sch}_{d+3}\times Y'$ [169, 164, 170]. By following the action of the TsT transformation on the dual QFT to $\text{AdS}_{d+3}\times Y$, one can then obtain the dual QFT of $\text{Sch}_{d+3}\times Y'$. What is more, one can find consistent truncations of $\text{Sch}_{d+3}\times Y'$ to Sch_{d+3} accompanied by some extra matter [169]

validating from a String Theory point of view the original constructions of [160, 161]. All this has been worked in detail for $d = 2$ in [169, 164, 170].

All we need to perform a TsT transformation is to start from a background with two isometries along some coordinates φ_1 and φ_2. Then one performs three easy steps: firstly, one performs a T-duality along φ_1 and introduce the dualised direction $\tilde{\varphi}_1$. Secondly, one makes the coordinate shift $\varphi_2 \to \varphi_2 + \beta\tilde{\varphi}_1$. Thirdly, one performs another T-duality along $\tilde{\varphi}_1$. The first and third steps are dualities and do not change the physics. The second step might change the periodicities of $\tilde{\varphi}_1$ and φ_2, but it is guaranteed to give a new supergravity solution. See appendix A for the general transformation on a general metric.

This way we start from $\mathrm{AdS}_5 \times S^5$ in lightcone coordinates,

$$\frac{ds^2}{R^2} = \frac{-2dtd\xi + dx_1^2 + dx_2^2 + du^2}{u^2} + (d\varphi + \mathcal{A})^2 + ds^2(\mathbb{CP}^2) \ , \tag{5.3.16}$$

where we wrote the S^5 sphere as a fibration over a $\mathbb{CP}^2$ base. φ is the local coordinate of the Hoft fiber and $\mathcal{A}$ is the is the 1-form potential for the Kähler form on $\mathbb{CP}^2$. We also assume we have the RR 5-form giving N units of flux on the S^5. Then we perform the TsT transformation: first a T-duality along φ into $\tilde{\varphi}$, a shift $\xi \to \xi + \beta\tilde{\varphi}$, and T-dualize $\tilde{\varphi}$ to φ back again. The end result does not modify the RR 5-form but yields

$$\begin{aligned} \frac{ds^2}{R^2} &= -\beta^2\frac{dt^2}{u^4} + \frac{-2dtd\xi + dx_1^2 + dx_2^2 + du^2}{u^2} + (d\varphi + \mathcal{A})^2 + ds^2(\mathbb{CP}^2) \ , \\ B^{\mathrm{NS}} &= \frac{\beta}{u^2} dt \wedge (d\varphi + \mathcal{A}) \ , \end{aligned} \tag{5.3.17}$$

that is we obtain the $\mathrm{Sch}_5 \times S^5$ and at the same time introduce a NS-NS 2-form.

From a QFT point of view what the TsT transformation does on $\mathcal{N} = 4$ SYM is to select a $U(1)$ from the $SU(4)$ R-symmetry and twist[11] the theory by the R-charge associated with

[11] If one considers ξ to be periodic, with period L_ξ, then one imposes the fields to be also periodic in ∂_ξ-direction, i.e.

$$e^{L_\xi \partial_\xi}\phi(x) = \phi(x) \ .$$

Upon the TsT transformation we change to a new $\tilde{\xi} = \xi + \beta\tilde{\varphi}$. This implies that now one has to require the periodic identification to be along $\partial_{\tilde{\xi}} = \partial_\xi + \beta\partial_{\tilde{\varphi}}$, i.e.

$$e^{L_{\tilde{\xi}}\partial_{\tilde{\xi}}}\phi(x) = e^{L_{\tilde{\xi}}(\partial_\xi - i\beta q_R)}\phi(x) = \phi(x) \ ,$$

where q_R is the R-charge of the field $\phi(x)$ along the $U(1)$ given by ∂_φ. Hence the quantization of the momentum along the original ∂_ξ-direction is changed from $p_\xi = 2\pi n/L_\xi$ with $n \in \mathbb{Z}$ to

$$p_\xi = \frac{2\pi n}{L_{\tilde{\xi}}} - \beta q_R \ .$$

The original momentum along ∂_ξ is shifted by the $U(1)$ R-charge.

that $U(1)$ (breaking the R-symmetry to $SU(3) \times U(1)$) [164, 170]. An implementation of this twist [169] is a deformation of the original theory by replacing the ordinary products by a non-commutative $*$-product, depending on the parameter β, and given by

$$f * g = e^{i2\pi\beta(P_\xi^f Q^g - P_\xi^g Q^f)} fg \quad . \tag{5.3.18}$$

P_ξ is the light-like momentum charge associated to the ∂_ξ-direction and Q is the charge associated with the selected $U(1)$ R-symmetry. This type of theories are called dipole theories [171, 172, 173, 174]. Their holographic duals were studied in [171, 172] and precisely correspond to the type of (5.3.17). The appearance of a sort of non-commutativity in the dual QFT should not be a real surprise. In String Theory the presence of background B-fields is usually linked to the introduction of non-commutative of spacetime in the dual QFT [125] and here it is no exception. Hence we can say that the holographic dual of $\text{Sch}_5 \times S^5$ is a dipole theory deformation of $\mathcal{N} = 4$ SYM (or as it is called in [170] a DLCQ_β).

A consistent dimensional reduction of type IIB on a five-dimensional Sasaki-Einstein manifold, Y, that includes Sch_5 as solution (and the finite temperature solution of next section), is possible as shown in [169]. The effective action is composed of gravity coupled to a massive $U(1)$ vector field and one scalar, which is actually a truncation of one with two more scalars. In fact it results in the effective action (5.3.6) that was introduced as a guess in the original proposal of [160, 161].

Here we were just able to embed the case of $d = 2$ in a String Theory construction. To deal with the physical relevant case of $d = 3$ we should start with AdS_6 but precisely a String Theory construction of AdS_6 is absent. Nonetheless in the literature, the TsT transformation of all other standard available brane constructions (like stack of M-branes) of AdS has been studied (cf. ex. [175]).

5.3.3 Schrödinger Black Holes and Thermodynamics

Now that we have at our disposal the TsT transformation, that served to give a String Theory embedding to Sch_5 starting from AdS_5, we can try to use it to obtain the finite temperature case. The metric describing the dual theory at finite temperature must have a black hole with equal Hawking temperature and asymptote to Sch_5. The obvious candidate is to apply the TsT transformation to an Schwarzschild-AdS black hole. When one does it, a three parameter family of planar black holes asymptoting to Sch_5 is found [164, 170, 169].

Let us start with the planar Schwarzschild-AdS_5 black hole

$$\frac{ds^2}{R^2} = u^{-2}\left(-f d\tilde{t}^2 + dy^2 + d\vec{x}^2 + \frac{du^2}{f}\right) + d\Omega_5^2 \,, \qquad f = 1 - \frac{u^4}{u_+^4} \,. \tag{5.3.19}$$

The position of the horizon is at u_+. First we take a set of boosted light-cone coordinates with a parameter λ,

$$t = \lambda\left(\tilde{t} + y\right) \ , \qquad \xi = \frac{\tilde{t} - y}{2\lambda} \ , \tag{5.3.20}$$

such that the planar Schwarzschild-AdS$_5$ black hole becomes

$$\frac{ds^2}{R^2} = u^{-2}\left(-(1+f)dtd\xi + \frac{(1-f)}{4\lambda^2}dt^2 + (1-f)\lambda^2 d\xi^2 + d\vec{x}^2 + \frac{du^2}{f}\right) + d\Omega_5^2 \ . \tag{5.3.21}$$

Then we perform the TsT transformation. The resulting geometry (in the String Frame) is

$$\begin{aligned}\frac{ds^2}{R^2} =& \frac{1}{u^2}\left(-(1+f)dtd\xi + \frac{(1-f)}{4\lambda^2}dt^2 + \lambda^2(1-f)d\xi^2 + d\vec{x}^2 + \frac{du^2}{f}\right) + \\ &- \frac{\beta^2}{u^4 K}\left(\lambda^2(1-f)d\xi - \frac{(1+f)}{2}dt\right)^2 + ds^2(\mathbb{CP}^2) + \frac{1}{K}\left(d\varphi + \mathcal{A}\right)^2 \ ,\end{aligned} \tag{5.3.22}$$

where

$$K = 1 + \frac{\beta^2\lambda^2 u^2}{u_+^4} \ . \tag{5.3.23}$$

One also gets a dilaton

$$\Phi = -\frac{1}{2}\ln K \ , \tag{5.3.24}$$

and a NS-NS 2-form

$$B^{\rm NS} = \frac{\beta}{u^2 K}\left(\lambda^2(1-f)d\xi - \frac{(1+f)}{2}dt\right) \wedge \left(d\varphi + \mathcal{A}\right) \ . \tag{5.3.25}$$

We still have the NS-NS 2-form, now the S^5 is squashed and a non-trivial dilaton field appears. More importantly in this case ∂_ξ becomes spacelike in the bulk and hence we can really trust the computations on this background without the need to worry about compact light-light directions. Furthermore the metric is stationary but not static, it has a non-zero $g_{t\xi}$. One interprets this fact as a rotating black brane in the ∂_ξ-direction.

Once we have the solution one can make a dimensional reduction to five dimensions and compute with the associated five-dimensional action the thermodynamics using the standard procedure. The effective action becomes gravity coupled to a massive 1-form and a scalar field[12] [169, 164]

$$S = \frac{1}{16\pi G_5}\int d^5x\sqrt{-g}\left(R - \frac{4}{3}(\partial_\mu\phi)^2 - \frac{1}{4}e^{-\frac{8}{3}\phi}F_{\mu\nu}^2 - 4A_\mu^2 - V(\phi)\right) \tag{5.3.26}$$

with a scalar potential

$$V(\phi) = 4e^{\frac{2}{3}\phi}(e^{2\phi} - 4) \ . \tag{5.3.27}$$

[12]The 5-dimensional action of eq. (4.10) in [169] is the same as the 5d action of eq. (3.13) in [164] under the identifications $u = -2/5\phi$, $v = -1/15\phi$, $\Phi = \phi$.

The dimensionally reduced solution is

$$\begin{aligned}\frac{ds^2}{R^2} =& \frac{K^{\frac{1}{3}}}{u^2}\left(-(1+f)dtd\xi + \frac{(1-f)}{4\lambda^2}dt^2 + \lambda^2(1-f)d\xi^2 + d\vec{x}^2 + \frac{du^2}{f}\right) + \\ & - \frac{\beta^2 K^{-\frac{2}{3}}}{u^4}\left(\lambda^2(1-f)d\xi - \frac{(1+f)}{2}dt\right)^2\end{aligned} \tag{5.3.28}$$

$$\begin{aligned} A &= \frac{\beta}{u^2 K}\left(\lambda^2(1-f)d\xi - \frac{(1+f)}{2}dt\right) \\ e^{\phi} &= K^{-\frac{1}{2}}\end{aligned} \tag{5.3.29}$$

One can compute the generalized free energy through the action (5.3.26). One invokes that the saddle point approximation of a Euclidean path integral over the geometry with the action (5.3.26) is the same as the saddle point approximation of the grand canonical partition function and obtains the generalized free energy, F, as

$$e^{-\frac{F}{T}} = \mathrm{Tr}\exp\left(-\frac{H}{T} + \frac{\mu N}{T}\right) \simeq e^{-I} \qquad \Rightarrow \qquad F = T\,I \tag{5.3.30}$$

where T denotes the temperature and I is the (renormalized) on-shell action. One can evaluate the on-shell action by just computing differences of actions between Sch_5 and the resulting geometry (5.3.28) [176] or equivalently by the introduction of counterterms. Since the asymptotics of the metric are different from AdS, the last procedure is delicate but can be done [164]. However as pointed out in [169], the TsT transformation[13] does not affect the horizon geometry and leaves the entropy, temperature and chemical potential unchanged (when measured in the very same conjugate coordinates associated to them) [177]. This implies that the free energy does not change and hence the resulting gravitational action when evaluated on the solutions, remains the same after the TsT transformation. According to this, the resulting on-shell action is [164, 176]

$$I = -\frac{1}{16\pi G_5}\int d^4x\, r_+^4 \tag{5.3.31}$$

which is the same as the planar Schwarzschild-AdS_5 black hole (5.3.19), where $r_+ = u_+^{-1}$. The integral is over the boundary coordinates.

Nonetheless in these constructions we are using light-cone coordinates with respect the usual Poincaré coordinates. Although the TsT transformation leaves the thermodynamics invariant, the thermodynamics of the light-cone frame is completely different to the

[13] One can view these solutions as eight-dimensional solutions after Kaluza-Klein reduction along ξ and φ from type IIB supergravity. Then you have an $SL(2,\mathbb{R})$ symmetry group, that corresponds to the TsT transformation.

thermodynamics in the usual coordinates because the notion of time (or what is the same temperature) changes.[14] The Killing vector, χ^a, that generates the horizon, is given by

$$\chi = \frac{1}{\lambda}\frac{\partial}{\partial \tilde{t}} = \frac{\partial}{\partial t} + \frac{1}{2\lambda^2}\frac{\partial}{\partial \xi} \ . \tag{5.3.32}$$

The Hawking temperature is then $T = \kappa/2\pi$ with κ the horizon surface gravity,

$$\kappa^2 = -\frac{1}{2}(\nabla^a \chi^b)(\nabla_a \chi_b) \ , \tag{5.3.33}$$

that results in

$$T = \frac{r_+}{\pi\lambda} \ . \tag{5.3.34}$$

The expression of the Killing vector χ, (5.3.32), implies that we have a chemical potential,[15]

$$\mu = \frac{1}{2\lambda^2} \ , \tag{5.3.35}$$

associated to the direction ∂_ξ. Since the momentum along ∂_ξ is associated to the number density, we interpret this chemical potential as giving a chemical potential to the number operator of the dual QFT. Hence we see that the dual theory of (5.3.28) is at a non-zero temperature and with a number chemical potential.

From the renormalized on-shell action, (5.3.31), and the temperature and chemical potential, (5.3.35), we can obtain the thermodynamic quantities written in QFT physical variables. The grand canonical free energy per unit volume becomes

$$F = -cN^2 V M T^2 \left(\frac{T}{\mu}\right)^2 \tag{5.3.36}$$

with c a constant, V is the volume and M is the non-relativistic mass of a particle.[16] It gives you an entropy,[17]

$$S = 4cN^2 V M T \left(\frac{T}{\mu}\right)^2 \ , \tag{5.3.37}$$

[14] Remember t, ξ are the boosted light coordinates of the usual Poincaré coordinates $\tilde{t}, y$,

$$t = \lambda(\tilde{t} + y) \ , \qquad \xi = \frac{\tilde{t} - y}{2\lambda} \ .$$

[15] It is the angular velocity of the horizon.

[16] As we will see in detail in chapter 6, the non-relativistic mass is given by the inverse of the length of the ∂_ξ-direction.

[17] We have the following relations

$$F = E - TS - \mu N = -PV \ ,$$
$$S = -\frac{\partial F}{\partial T} \ , \qquad N = -\frac{\partial F}{\partial \mu} \ .$$

that precisely coincides with the Bekenstein-Hawking entropy, that can be seen as a consistency of the computation. Furthermore it leads to an equation of state given by

$$PV = E \, . \tag{5.3.38}$$

All this is in perfect agreement with non-relativistic conformal invariance: imposing Schrödinger invariance one can arrive to the fact that the free energy and equation of state will be of the form [178, 158]

$$F = VM^{\frac{d}{2}}T^{\frac{d+2}{2}}\mathcal{F}\left(\frac{T}{\mu}\right) \, , \qquad dPV = 2E \, ,$$

where $\mathcal{F}$ is an arbitrary function.

Last but not least, the free energy is always negative. That means that the black hole configuration is always preferred to the Sch_{d+3} at finite temperature. Thus the system does not have any Hawking-Page-like phase transition. Nonetheless, in chapter 6 we will comment on Sch-black holes in global coordinates (equivalent to putting the NRCFT in an external harmonic potential) that do present a Hawking-Page phase transition.

One can find generalizations of the action (5.3.26) and the planar Sch-black hole solutions (5.3.28) to arbitrary dimensions [178]. These generalizations are a pure guess and are not backed by any String Theory construction or dimensional reduction from supergravity. For these constructions the grand canonical free energy per unit volume still retains the form

$$F = -cN_{\text{eff}}VM^{\frac{d}{2}}T^{\frac{d+2}{2}}\left(\frac{T}{\mu}\right)^{\frac{d+2}{2}} \tag{5.3.39}$$

and the equation of state are

$$dPV = 2E \, , \tag{5.3.40}$$

in perfect agreement with Schrödinger invariance. We also have that the energy per particle becomes

$$\frac{E}{N} = \frac{d}{d+2}|\mu| \tag{5.3.41}$$

which formally coincides with that of a low-temperature non-interacting Fermi gas. This immediately implies that the Bertsch parameter is one.[18]

However there is something troublesome about the thermodynamics in (5.3.39) when compared with fermions at unitarity. The limit of zero chemical potential at fixed temperature is singular. Certainly this is not a feature that one finds when dealing with fermions at unitarity (cf. ex. [158]). In this sense we can say that these thermodynamics are unrealistic. Furthermore, we would expect the appearance of a superfluidity phase at small T/μ that is

[18] For fermions at unitarity the experimental value for the Bertsch parameter is $\simeq 0.32$ [154].

what happens for fermions at unitary. This model cannot correspond to a superfluid phase since the signature of superfluidy is the spontaneous breaking of the $U(1)$ associated to particle number and here that symmetry is unbroken. It corresponds to the $U(1)$ isometry along ∂_ξ. We will comment on these issues and how to interpret them in chapter 8.

On the other hand from (5.3.39) one can compute transport coefficients. People calculated the ratio of shear viscosity to entropy [164, 170, 178]. The result is the saturation of the KSS bound [2]

$$\frac{\eta}{s} = \frac{1}{4\pi} \ . \tag{5.3.42}$$

This result gives evidence that the system is indeed in a strongly coupled regime behaving as a perfect fluid. It is in accord qualitatively to the what is measured for fermions at unitary for which we have that the ratio is ~ 0.5.

In this respect, in [179] they considered higher curvature corrections, R^2, in (5.3.26) to (5.3.28) and found a renormalization of z at order $\mathcal{O}(N^{-1})$ as well as a weak violation of the KSS bound again at $\mathcal{O}(N^{-1})$. In this case the dual QFT seems to correspondence to a DLCQ$_\beta$ of $\mathcal{N} = 2$ $Sp(N)$ SYM.

Also in [180] the fluid-gravity correspondence [181] has been extended to the Sch spacetimes, where they managed to construct inhomogeneous black holes solutions with Sch$_5$ asymptotics, by means of TsT transformations. All these solutions still have ∂_ξ as a Killing vector.

As a summary, we can say that we have at our disposal a family of backgrounds at finite temperature and chemical potential. The transport coefficients agree at a qualitatively level to fermions at unitary but nonetheless the thermodynamics are different.

In the following chapters we will further study and clarify some aspects of the holographic duals that we presented. In chapter 6 we will study the Hamiltonian picture of the duality and will introduce the holographic dual corresponding to global coordinates or what is the same when one places the NRCFT in an external harmonic potential. In chapter 7 we will study the correlation functions at zero temperature and chemical temperature of the Sch$_{d+3}$ backgrounds. Among other things, we will explicitly compare the 3-point function at tree level with the result coming from fermions at unitarity, finding perfect agreement. This gives room to the expectation that at least the duality works at tree level and zero temperature and chemical potential. Finally in chapter 8 we will present a (free) statistical model that matches the thermodynamics of the Schrödinger black holes, confirming that the universality class of the holographic duals at finite temperature shown above does not lie in the one of fermions at unitarity. Nonetheless this will suggest the modifications that are needed to find the desired class of backgrounds.

Chapter 6

The spectrum of non-relativistic AdS/CFT and harmonic trapping

In this chapter we develop the Hamiltonian picture of the holographic duals given by Sch_{d+3}. In section 6.1 we begin by briefly going again through the construction of Refs. [3, 4] but pointing out some interesting modifications of detail. In section 6.2 we find the single-particle bulk Hamiltonian of a bulk bosonic field and encounter the De Alfaro, Fubini, Furlan system [182]. In the process we find that all physical results can be obtained from an exact AdS bulk metric, with no extra matter required. We also show how to describe the harmonic trapping in this system and point out a fully geometrical interpretation of the procedure. We end in section 6.3 with some speculations regarding applications which are naturally suggested by the Hamiltonian methods developed in this chapter. In particular we consider a matching to harmonically trapped fermions at unitarity, as well as hypothetical patterns of quasiparticle spectra in models with dynamical mass gap generation. Finally, we end with our conclusions and open questions raised by this analysis.

6.1 Introduction

Following [3], the Schrödinger algebra in d spatial dimensions can be conveniently seen as a projection of the full relativistic conformal algebra in $d+2$ spacetime dimensions, down to a subgroup that leaves fixed a light-cone momentum p^+. In fact it is not possible to embed the Schrödinger group into the conformal group with the same number of spatial dimensions [183, 184]. See also [185]. This suggests that the appropriate metrics can be obtained as a projection of an AdS_{d+3} space. Starting from the Poincaré patch of AdS_{d+3} spacetime with

curvature radius R

$$ds^2 = \frac{r^2}{R^2}(-2dx^+dx^- + d\vec{x}^2) + \frac{R^2}{r^2}dr^2 \tag{6.1.1}$$

in an appropriate light-cone frame, the idea is to project the dynamics onto the sector with fixed eigenvalue of the light-cone momentum $p^+ = \partial/\partial x^-$. Interpreting now $x^+ = t$ as a time coordinate, we rewrite the previous metric as

$$ds^2 = \frac{r^2}{R^2}(-2dt\, d\xi + d\vec{x}^2) + \frac{R^2}{r^2}dr^2 \ , \tag{6.1.2}$$

where we have renamed $x^- = \xi$. The generator or time translations $p^- = i\partial_t = H$ is a Hamiltonian, and one realizes the full Schrödinger group in terms of those isometries of (6.1.2) that leave the ξ-momentum $p^+ = -i\partial_\xi = M$ fixed and interpreted as a mass parameter. A quantization of the mass parameter is realized by a compactification of the $x^- = \xi$ direction on a light-like circle. The resulting isometry group includes the full Galilean group in d spatial dimensions as a subgroup, together with an $SL(2,\mathbb{R})$ subgroup generated by the Hamiltonian, H, a dilation generator D, and a special conformal transformation C.

We will find it convenient to follow the parametrization in [4] and consider the more general set of deformations of (6.1.2), labeled by the dynamical exponent z:

$$ds^2 = -\beta^2\frac{r^{2z}}{R^{2z}}dt^2 + \frac{r^2}{R^2}(-2dt\, d\xi + d\vec{x}^2) + \frac{R^2}{r^2}dr^2 \ , \tag{6.1.3}$$

where β^2 is a positive real number. The isometries of these deformed metrics include the Galilean group in d dimensions, as well as a dilation symmetry

$$(t, \vec{x}, r, \xi) \longrightarrow (\lambda^z\, t, \lambda\, \vec{x}, \lambda^{-1}\, r, \lambda^{2-z}\, \xi) \ . \tag{6.1.4}$$

The Schrödinger group arises in the particular case $z = 2$, and includes an additional generator of special conformal transformations. *A priori*, any model with a fixed quantized mass spectrum, $M = -i\partial_\xi$, breaks explicitly all $z \neq 2$ dilations, suggesting that only $z = 2$ metrics are physically relevant. However, one of our results is the recognition that the metric (6.1.3) with $z = 1$ is a valid background supporting the full Schrödinger group at the quantum level, at least in the free approximation of the bulk degrees of freedom or tree level, which is where our analysis is valid (see also chapter 7). This special background will have peculiar geometrical properties: it is nothing but pure AdS and a suitable generalization of it will be seen to provide the dual of the system placed in a harmonic potential, while remaining pure AdS. One can also give for $z = 2$ the analog of the system in the harmonic potential. That the $z = 1$ metric is pure AdS can be seen by starting from the AdS metric in Poincaré coordinates

$$ds^2 = \frac{r^2}{R^2}(-d\tau^2 + d\chi^2) + \frac{R^2}{r^2}dr^2 + \frac{r^2}{R^2}d\vec{x}^2 \tag{6.1.5}$$

and making the change of coordinates

$$t = \frac{\chi - \tau}{5^{\frac{1}{4}}} \quad , \qquad \xi = \frac{-\lambda_+ \chi + \lambda_- \tau}{5^{\frac{1}{4}}} \tag{6.1.6}$$

with $\lambda_\pm = \frac{1}{2}\left(1 \pm \sqrt{5}\right)$. Then the metric becomes

$$ds^2 = \frac{r^2}{R^2}(-dt^2 - 2dtd\xi) + \frac{R^2}{r^2}dr^2 + \frac{r^2}{R^2}d\vec{x}^2 \qquad . \tag{6.1.7}$$

6.2 Energy spectrum

We shall model bulk degrees of freedom in terms of a complex, minimally coupled scalar field of mass m, in the free approximation, with action

$$S_\phi = -\tfrac{1}{2}\int d^{d+3}x\,\sqrt{-g}\,\left(g^{\mu\nu}\partial_\mu\phi^*\partial_\nu\phi + m^2\phi^*\phi\right) . \tag{6.2.1}$$

Our reduction procedure will be imposed by compactifying the ξ direction on a circle of radius $1/M$, and subsequently projecting all degrees of freedom onto the sector with fixed ξ momentum $-i\partial_\xi = M$. Alternatively, we may compactify on a circle of radius $1/\lambda$ and project onto the sector with ξ-momentum $M = N\lambda$, with a positive integer number, N, acquiring the interpretation of a conserved particle number. In either case, working with (6.2.1) the procedure boils down to imposing a restriction to field configurations of the form[1]

$$\phi(t, \xi, r, \vec{x}\,) = e^{iM\xi}\,\gamma(r)\,\varphi(t, r, \vec{x}\,) , \tag{6.2.2}$$

where $\gamma(r)$ is an appropriate rescaling function that we include for convenience. For a metric as general as

$$ds^2 = -2A(r, \vec{x}\,)dt^2 - 2B(r)d\xi dt + G(r)dr^2 + F(r)\,d\vec{x}^{\,2} , \tag{6.2.3}$$

with *arbitrary* $\vec{x}$ dependence on the time-time component, insertion of the *ansatz* (6.2.2) in the action with

$$\gamma(r) = \left(4\pi^2 B(r)F(r)^d\right)^{-1/4} \tag{6.2.4}$$

yields the action of a non-relativistic quantum mechanical system

$$S_M = -\int dt\,d^dx\,d\rho\,\left[\frac{1}{2}\,(-i\varphi^*\partial_t\varphi + i\partial_t\varphi^*\varphi) + \frac{1}{2M}\left(|\vec{\partial}\varphi|^2 + |\partial_\rho\varphi|^2\right) + U(\rho, \vec{x}\,)\,|\varphi|^2\right] , \tag{6.2.5}$$

where we have defined a new radial coordinate ρ that solves

$$d\rho = dr\sqrt{\frac{G(r)}{B(r)}} , \tag{6.2.6}$$

[1] Dynamical reductions of this type were studied in [186].

and an effective nonrelativistic effective potential U given by

$$U(\rho,\vec{x}\,)=\frac{m^2}{2M}B(\rho)+M\frac{A(\rho,\vec{x}\,)}{B(\rho)}+\frac{1}{8M}\partial_\rho^2\,\log\left(B(\rho)F(\rho)^d\right)+\frac{1}{32M}\left[\partial_\rho\,\log\left(B(\rho)F(\rho)^d\right)\right]^2\,. \tag{6.2.7}$$

6.2.1 Conformal Quantum Mechanics

We may now turn to the particular case of the family of metrics with Galilean invariance (6.1.3) and we find an associated Hamiltonian

$$H=\frac{\vec{p}^{\,2}}{2M}-\frac{1}{2M}\frac{d^2}{d\rho^2}+\frac{(d+1)(d+3)+4(mR)^2}{8M\rho^2}+\beta^2\frac{M}{2}\left(\frac{R}{\rho}\right)^{2z-2}\,, \tag{6.2.8}$$

where $\vec{p}=-i\vec{\partial}$ is the momentum in the spatial coordinates $\vec{x}$ and $r=R^2/\rho$. For the Schrödinger invariant case, $z=2$, we see that the total Hamiltonian consists on a separated free part, for a particle of mass M, and an extra term coming from the holographic coordinate and featuring a well-known system, i.e. the conformal quantum mechanics studied in Ref. [182]:

$$H_{z=2}=H_{\vec{x}}+H_\rho(b_2)\,, \tag{6.2.9}$$

with $H_{\vec{x}}=\vec{p}^{\,2}/2M$ and $H_\rho(b)$ given by

$$H_\rho(b)=-\frac{1}{2M}\frac{d^2}{d\rho^2}+\frac{b}{2M\rho^2}\,, \tag{6.2.10}$$

parametrized by a dimensionless coupling constant, b.[2] For $z=2$ we have

$$b_2=\frac{(d+1)(d+3)}{4}+(m^2+\beta^2M^2)R^2\,. \tag{6.2.11}$$

We see explicitly that the effect of β^2 reduces to a renormalization of the scalar field mass from m^2 to $\bar{m}^2=m^2+\beta^2M^2$.

At this stage, we meet a surprise, since the case $z=1$, *a priori* not enjoying a manifest Schrödinger symmetry, does split in the same manner as the $z=2$ case, up to an additive redefinition of the Hamiltonian. We find

$$H_{z=1}-\beta^2\frac{M}{2}=H_{\vec{x}}+H_\rho(b_1)\,, \tag{6.2.12}$$

with

$$b_1=\frac{(d+1)(d+3)}{4}+(mR)^2\,. \tag{6.2.13}$$

[2]Notice that the value of the mass in H_ρ is immaterial, since we can rescale it by a rescaling of ρ, a consequence of the conformal character of this system.

Incidentally, it is interesting that the required additive shift of the Hamiltonian is just the rest mass for the particular case $\beta^2 = 2$. The crucial property of the conformal Hamiltonian $H_\rho = p_\rho^2/2M + b/2M\rho^2$ is that it generates an $SL(2,\mathbb{R})$ group when combined with the generator of dilations, $D_\rho = \frac{1}{2}(\rho\, p_\rho + p_\rho \rho)$, and special conformal transformations $C_\rho = \frac{1}{2}M\rho^2$.

Since the free Hamiltonian $H_{\vec{x}}$, together with $D_{\vec{x}} = \frac{1}{2}(\vec{x}\cdot\vec{p} + \vec{p}\cdot\vec{x})$ and $C_{\vec{x}} = \frac{1}{2}M|\vec{x}|^2$, generates a commuting $SL(2,\mathbb{R})$ group, we find that the full spectrum is acted on by the $SL(2,\mathbb{R})$ generated by

$$H - \gamma^2 M\delta_{z,1} = H_{\vec{x}} + H_\rho\ , \qquad D = D_{\vec{x}} + D_\rho\ , \qquad C = C_{\vec{x}} + C_\rho\ ,$$

and both the $z = 2$ and the $z = 1$ systems exhibit full Schrödinger symmetry at the quantum level. The action of the dilation of the quantum $SL(2,\mathbb{R})$ group on the coordinates corresponds to (6.1.4) with $z = 2$. However this dilation transformation *is not* an isometry of the $z = 1$ metric, so that we cannot expect it to survive local interactions in the bulk. We will return to this issue at the end of section 6.2.3.

In both situations the dynamics of the holographic direction contribute a continuous spectrum of excitations which are well-contained in the UV regime ($r \to \infty$ or $\rho \to 0$) since the potential diverges there, and accumulate at the IR end, as the conformal potential vanishes in the $r \to 0$ limit. This situation is analogous to the behavior of a relativistic conformal field theory in infinite volume, as obtained from the study of bulk dynamics on the Poincaré patch of AdS.

The form of the radial potential suggests that the appropriate UV/IR correspondence in this model is $\omega \sim 1/M\rho^2$, where ρ is the radial variable appearing in (6.2.10) and ω is a physical quantum of energy. If we formally impose an infrared cutoff in the system, say at $\rho \sim L_\rho$, the spectrum at high energies will discretize in momentum modes $p_\rho \sim 2\pi n_\rho/L_\rho$. This means that the high-energy density of states gets a contribution from the holographic direction as an extra dimension of length L_ρ. We will dwell on the significance of this fact at the end of this chapter.

For $z < 1$, the non-conformal term in the effective potential of (6.2.8) grows at large ρ and sets a mass gap in the system, in analogy with similar deformations in the so-called AdS/QCD models.

6.2.2 Trapping the system

A standard strategy at discretizing the spectrum in standard AdS/CFT models is to put the system on a finite volume. If the procedure is carefully chosen, the resulting Hamiltonian may still enjoy useful constraints from the conformal symmetry. In standard AdS/CFT

models, this happens when putting the CFT on a spatial sphere of constant curvature, whose Hamiltonian is proportional to the dilation operator in flat Minkowski space, hence one can equate energies on the sphere to conformal dimensions of local operators on the hyperplane [152].

There is an analogous construction in systems with non-relativistic conformal symmetry [19]. Confining the system to a harmonic trap of frequency Ω corresponds to adding the potential

$$V_{\rm trap} = \frac{1}{2}\, M\Omega^2 |\vec{x}|^2 \ .$$

Hence, from the explicit form of the generator of special conformal transformations for a Schrödinger invariant system we learn that

$$H_{\rm trapped} = H_{\rm untrapped} + \Omega^2\, C \ . \tag{6.2.14}$$

The $SL(2,\mathbb{R})$ group can then be used to obtain exact properties of the spectrum such as its discrete gap and a number of virial theorems for certain expectation values (cf. Ref. [153]). Furthermore, it can be shown that the spectrum of $H_{\rm trapped}$ sets the spectrum of conformal weights of local operators in the untrapped system, i.e. for each local conformal operator in the untrapped system we have an energy eigenstate of the harmonically trapped system, $|\mathcal{O}\rangle$, whose energy satisfies

$$E_{\mathcal{O}} = \Omega \Delta_{\mathcal{O}} \ , \tag{6.2.15}$$

with $\Delta_{\mathcal{O}}$ the conformal weight (eigenvalue of the dilation operator) of the scaling operator $\mathcal{O}$ (see [19]). For the model induced by the non-relativistic AdS/CFT correspondence studied here, the full generator of special conformal transformations can be written as

$$C = C_{\vec{x}} + C_\rho = \frac{1}{2}\, M|\vec{x}\,|^{\,2} + \frac{1}{2}\, M\rho^2 \ , \tag{6.2.16}$$

so that

$$H_{\rm trapped} = \frac{\vec{p}^{\,2}}{2M} + \frac{1}{2}\, M\Omega^2|\vec{x}|^2 + H_\rho(b) + \frac{1}{2}\, M\Omega^2\rho^2 \ , \tag{6.2.17}$$

and we see that the prescription (6.2.14) induces naturally the corresponding 'trapping' in the holographic coordinate ρ, with the same characteristic frequency. Notice however that a rescaling of the radial coordinate $\rho \to \lambda\rho$ induces an effectively rescaled mass $M_\lambda^2 = \lambda^2 M$ and consequently the trapping in the holographic variable corresponds to a potential $\frac{1}{2}M_\lambda^2\Omega^2\rho^2$. Hence, we can still change the effective mass of the radial Hamiltonian without changing the trapping frequency.

It remains to show how to induce the harmonic trapping at the level of the geometrical description. Going back to (6.2.7) and setting $B(r) = F(r) = 1/G(r) = r^2/R^2 = R^2/\rho^2$, we

may now use the fact that all the $\vec{x}$ dependence in the effective potential $U(\vec{x},\rho)$ is controlled by the value of the time-time component of the metric $A(\vec{x},\rho)$. In the absence of an explicit 'external' potential we have $A(r) = \beta^2(r/R)^{2z}/2$ and, adding the perturbation

$$\delta A(\vec{x},r) = \frac{r^2}{R^2}\,\frac{1}{M}\delta U(\vec{x},\rho)\ , \tag{6.2.18}$$

generates a potential term on the effective Hamiltonian $\delta U(\vec{x},\rho)$. The dynamics of the 'radial problem' remains decoupled from the standard spacetime degrees of freedom for all potential deformations of the form

$$\delta U(\vec{x},\rho) = V(\vec{x}\,) + v(\rho)\ , \tag{6.2.19}$$

with otherwise arbitrary functions V and v. The $SL(2,\mathbb{R})$ covariant harmonic trap is induced by quadratic deformations with the same coefficient: $V(\vec{x}\,) = \frac{1}{2}M\Omega^2|\vec{x}\,|^2$ and $v(\rho) = \frac{1}{2}M\Omega^2\rho^2$.

Harmonic trapping is a rather realistic situation in actual experiments involving cold atoms [187, 188]. From the theoretical point of view it has the additional interest of being exactly solvable. Indeed, the Hamiltonian

$$H_{\text{conformal trapped}} = -\frac{1}{2M}\frac{d^2}{d\rho^2} + \frac{b}{2M\rho^2} + \frac{1}{2}\,M\Omega^2\rho^2 \tag{6.2.20}$$

is diagonalized by eigenfunctions

$$f_n(\rho) = \rho^{\nu+\frac{1}{2}}\,L_n^\nu(\sqrt{2}M\Omega\rho^2)\,e^{-M\Omega\rho^2/\sqrt{2}}\ , \tag{6.2.21}$$

where ν is the real positive solution of

$$\nu^2 = b + \frac{1}{4} \tag{6.2.22}$$

and L_n^ν is a generalized Laguerre polynomial. The corresponding spectrum of eigenvalues is

$$\varepsilon_q = \Omega(\nu + 1 + 2q)\ , \qquad q \in \mathbb{Z}_+\ . \tag{6.2.23}$$

These formulae assume that $\nu^2 > 1$. For $0 < \nu^2 \leq 1$, corresponding to $-1/4 < b \leq 3/4$ and including some cases of attractive potentials for negative b, there are two possible normalizable solutions at $\rho = 0$. One is the function in (6.2.21), and the other is the same function with $\nu \to -\nu$. The spectrum constructed on top of this second branch of solutions is given by (6.2.23) with the same redefinition $\nu \to -\nu$. [3]

[3]The solutions with asymptotics $\rho^{\frac{1}{2}-\nu}$ are sometimes referred to as 'resonant'. Even if they are normalizable on $\rho \in [0,+\infty)$ for $0 < \nu^2 < 1$, their first derivative is not. Hence, the kinetic energy has divergent expectation value in this branch of solutions, as has the potential energy, the two divergences cancelling out to give a finite total energy.

These two possible quantizations of the system are the nonrelativistic incarnation of a well known instance in the standard AdS/CFT correspondence [189, 190]. Going back to the bulk parameters, the two inequivalent quantizations correspond to the range in effective masses

$$-\left(\frac{d+2}{2}\right)^2 < (\overline{m}R)^2 \leq 1-\left(\frac{d+2}{2}\right)^2 , \tag{6.2.24}$$

where $\overline{m}^2 = m^2 + \beta^2 M^2 \delta_{z,2}$. The lower limit on $\overline{m}^2$ allows for tachyonic bulk fields in a finite range of masses. This tachyonic bound coincides exactly with the Breitenlohner–Freedman bound of AdS_{d+3} (cf. [166]). Since we define the nonrelativistic AdS/CFT correspondence as a reduction of the higher-dimensional AdS/CFT map, we find this result rather satisfying. Violating the Breitenlohner–Freedman bound in this context, i.e. continuing to $b < -1/4$, makes the conformal potential too strongly attractive and the Hamiltonian problem is not selfadjoint (cf. [191]).

The full spectrum of H_{trapped} is given by

$$E^{\pm}_{\vec{n},q} = \Omega\left(\frac{d}{2} + \sum_{i=1}^{d} n_i + 2q + 1 \pm \nu\right) , \qquad n_i, q \in \mathbb{Z}_+ \tag{6.2.25}$$

where the term $d/2$ comes from the zero-point energy of the d-dimensional oscillator in the $\vec{x}$ coordinates and the $(-)$ sign only applies for $0 < \nu^2 < 1$. Using now the general rule (6.2.15) we have a spectrum of operator dimensions

$$\Delta^{\pm}_{\vec{n},q} = \sum_{i=1}^{d} n_i + 2q + \frac{d+2}{2} \pm \nu , \qquad n_i, q \in \mathbb{Z}_+ , \tag{6.2.26}$$

with the $\vec{n} = q = 0$ cases corresponding to the conformal primaries studied in [3, 4] in terms of the two-point functions. In particular, the two branches of quantum states in the Hamiltonian formalism, given by the analytic continuation $\nu \to -\nu$ for $0 < \nu^2 < 1$ correspond to the two branches of boundary conditions studied in [3], with the associated conformal weights $\Delta^{\pm} = \Delta(\pm\nu)$.

6.2.3 A purely geometrical interpretation of the harmonic trapping

In this section we provide a geometrical interpretation of the special case $z = 1$, which shows full Schrödinger symmetry at the quantum level, as well as the $z = 2$ case.

It turns out that the $z = 1, 2$ metric, deformed with harmonic trapping, $V(\vec{x}) = \frac{1}{2}M\Omega^2|\vec{x}\,|^2$, $v(\rho) = \frac{1}{2}M\Omega^2\rho^2$, can be written as

$$ds^2 = \left(-\beta^2\frac{r^{2z}}{R^{2z}} + \frac{1}{2}\Omega^2\frac{r^2}{R^2}|\vec{x}|^2\right)dt^2 + \frac{r^2}{R^2}(-2dt\,d\xi + d\vec{x}^{\,2}) + \frac{R^2}{r^2}dr^2 - \frac{1}{2}\Omega^2R^2dt^2 , \tag{6.2.27}$$

since this metric reproduces the trapped Hamiltonian (6.2.17).

What makes the above metric relevant is that for the particular case of $z = 1$ it is nothing but pure AdS again. As a mere curious fact, one can under the change of variables $\Omega^2 = 2a^2/R^4$, $r^2 = r'^2 - a^2$, write it in the form

$$ds^2 = -\left(\frac{r'^2}{R^2} + \frac{a^2(r'^2 - a^2)}{R^6}|\vec{x}\,|^2\right) dt^2 - 2\frac{r'^2 - a^2}{R^2} d\xi dt + \frac{R^2 r'^2 dr'^2}{(r'^2 - a^2)^2} + \frac{r'^2 - a^2}{R^2} d\vec{x}^{\,2}\,, \quad (6.2.28)$$

and after a further double Wick rotation, $\xi \to it_B$ and $t \to i\theta_B$, the resulting metric is *locally* equivalent to that of a rotating, extremal, topological AdS black hole, studied in Ref. [192]. Of course, the same applies to the non-rotating solution $a = 0$, corresponding to the untrapped $z = 1$ background. Since these black holes are topological, the metric is locally pure AdS spacetime, and thus solves Einstein's equations with a simple cosmological constant term.

On the other hand, the metric (6.2.27) for $z = 2$ can be seen to be supported by exactly the same extra matter as Sch_{d+3} in the original constructions by [3, 4]. This, together with the fact that for the relativistic case the CFT on the sphere is given by AdS in global coordinates, hints that the above metric may represent Sch_{d+3} in global coordinates. Remember that Sch_{d+3} as given by (6.1.3) is not geodesically complete and hence indicates that the coordinates are just covering a local patch. Remarkably this happens to be precisely the case. As it has been shown in [193] there exits a change of coordinates that takes Sch_{d+3} in (6.1.3) to (6.2.27) with $z = 2$, and moreover (6.2.27) is geodesically complete, meaning the coordinates are global. This way we have a perfect analog to the usual AdS/CFT, but in which a global coordinate description of the Sch correspond to put the NRCFT in a harmonic trap.

As also later pointed out in [169], the metric (6.2.27) with $\beta = 0$ for $z = 1$ can alternatively be seen as a Penrose limit of AdS in global coordinates. Furthermore if one performs a TsT transformation (provided we add a sphere) on the resulting geometry, the effect is to add the $\beta^2 dt^2/r^4$ term. This way the $z = 2$ harmonic trapping can be obtained as the TsT transformation of the Penrose limit of (global) AdS. This construction via Penrose limits is interesting since it allows us to also generate the finite temperature version, i.e. find a black-hole metric that is asymptotic to (6.2.27). Here the starting point is to take the Kerr-AdS black hole. Upon taking the Penrose limit one arrives at a black hole that is asymptotic to the $z = 1$ case of (6.2.27). This metric was studied in [169] for $d = 2$ and in [194] for arbitrary dimensions. Moreover if one performs a TsT transformation on this metric (times a sphere) one obtains black hole solutions that are asymptotic to (6.2.27) with $z = 2$. These metrics still have a $U(1)$ isometry related to ∂_ξ, the number operator is conserved so that they cannot be interpreted as a superfluid phase. Since the TsT transformation respects the

(renormalized) action of the solutions, all the thermodynamics and phase diagram of the $z = 2$ black holes are the same as the $z = 1$ case studied in [194], for example the entropy is given by[4]

$$S = cN_{\text{eff}} \left(\frac{T}{\Omega}\right)^d \left(\frac{T}{|\mu|}\right) \ . \tag{6.2.29}$$

where μ denotes the chemical potential and c is some constant. In particular one obtains a Hawking-Page-like phase transition for the nucleation of black holes in global Sch at a certain critical temperature $T_c \sim \Omega$.

One of the advantages of the holographic descriptions lies in their specification of an *ansatz* for the interactions that respect the relevant conformal symmetry. In particular, in the context of a bulk scalar degree of freedom we can consider interaction terms of the form

$$S_{\text{int}} \sim g_k \int d^{d+3}x \ \sqrt{-g} \ \ |\,\phi\,|^{2k} \ , \tag{6.2.30}$$

or straightforward local generalizations with covariant derivatives. These interaction terms can be used to compute connected n-point functions of those operators $\mathcal{O}_\phi$ dual to the scalar field ϕ. Any such interaction term, written as a perturbation around the AdS_{d+3} background metric, respects the conformal symmetry provided this symmetry is realized as an isometry of the bulk metric. In this respect, we find a distinction between the $z = 2$ and $z = 1$ cases discussed so far. The quantum $SL(2, \mathbb{R})$ algebra of the $z = 1$ system is not realized as an isometry of the $z = 1$ deformed metric [5] so that generic bulk interactions of the type (6.2.30) will break the Schrödinger group of the pure AdS construction.

The appropriate interpretation of the pure AdS constructions with $z = 1$ is then that of *approximate* nonrelativistic fixed points, i.e. to the extent that the interactions (6.2.30) are 'small' the Schrödinger symmetry will classify two point functions (the spectrum of scaling dimensions) but will be weakly broken at the level of three-point functions. A typical system with such a behavior is a microscopic model with a vectorlike large N_f limit. In such class of models, the effective couplings satisfy a scaling law $g_k \sim 1/N_f^k$ and one can envisage situations with a fixed point at $N_f = \infty$, broken by $1/N_f$ corrections. Conversely, any fixed point that is exact to all orders of the $1/N_f$ expansion will require use of a background metric of type $z = 2$. We will make precise these comments in next chapter, chapter 7, where we will demonstrate that the equivalence of $z = 1$ and $z = 2$ only holds at tree level in the dual NRCFT.

[4] up to subleading corrections

[5] This metric, being locally AdS, does have a large isometry group, at least locally, the point being that the *particular* $SL(2, \mathbb{R})$ group that is generated quantum mechanically is not part of it.

6.3 Towards applied non-relativistic AdS/CFT

In this final section we speculate on two possible applications of the previous formalism. We comment on broad conceptual lines rather than the precise implementation of the program, that is left for future work.

6.3.1 Matching to fermions at unitarity

Fermions at unitarity [195] are widely regarded as one of the main arenas of potential applications of these constructions. In this section we show that a rather precise correspondence may be achieved between the bound state problem of unitarity fermions on a harmonic trap, and the effective quantum mechanical system described in the preceding sections.

Following Ref. [153], the bound state problem of N particles of mass λ on a harmonic trap of frequency Ω and satisfying the unitarity boundary conditions,

$$\lim_{\vec{x}_i \to \vec{x}_j} \psi(\vec{x}_1, \cdots, \vec{x}_N) = \frac{c_{ij}}{|\vec{x}_i - \vec{x}_j|^{d-2}} + O(\vec{x}_i - \vec{x}_j) \tag{6.3.1}$$

can be separated into a center of mass degree of freedom with coordinate $\vec{x} = N^{-1} \sum_i \vec{x}_i$, mass $M = N\lambda$, and free dynamics

$$H_{\rm CM} = -\frac{\vec{\partial}^2}{2M} + \frac{1}{2} M\Omega^2 |\vec{x}\,|^2 \,, \tag{6.3.2}$$

plus an 'internal' Hamiltonian problem

$$H_{\rm int} = \frac{1}{2\lambda} \left(-\frac{d^2}{d\rho^2} + \frac{dN - d - 1}{\rho} \frac{d}{d\rho} + \frac{\Lambda_{(N,d)}}{\rho^2} \right) + \frac{1}{2} \lambda\, \Omega^2 \rho^2 \,, \tag{6.3.3}$$

in terms of a collective radial coordinate measuring the effective size of the trapped droplet:

$$\rho = \left(\sum_{i=1}^{N} (\vec{x}_i - \vec{x}\,)^2 \right)^{1/2} . \tag{6.3.4}$$

In (6.3.3), the quantities $\Lambda_{(N,d)}$ are the eigenvalues of the Laplacian on a proper submanifold of the sphere, $\mathbf{S}^{dN-d-1}$, related to the relative angular variables, and with complicated boundary conditions. The eigenvalues $\Lambda_{(N,d)}$ encode all the information on the contact constraints (6.3.1) and therefore characterize those dynamical details of the system which do not follow simply from the symmetries.

By a simple wave function rescaling, this system can be rewritten as the sum of a harmonically trapped free Hamiltonian of mass M plus a harmonically trapped conformal quantum mechanics of mass λ and coupling parameter

$$b = \nu^2 - \frac{1}{4} \,, \tag{6.3.5}$$

with

$$\nu^2 = \Lambda_{(N,d)} + \left(\frac{dN-d-2}{2}\right)^2 . \tag{6.3.6}$$

The resulting spectrum is known and takes the form

$$\varepsilon_q = \Omega(\nu + 1 + 2q) , \qquad q \in \mathbb{Z}_+ \tag{6.3.7}$$

on the internal degrees of freedom. We can match this spectrum by a nonrelativistic AdS construction with radius of curvature $R = 1/M$ and a scalar field of bulk mass m determined by

$$\nu^2 = \left(\frac{d+2}{2}\right)^2 + (\bar{m}R)^2 = \Lambda_{(N,d)} + \left(\frac{dN-d-2}{2}\right)^2 , \tag{6.3.8}$$

where $\bar{m}^2 = m^2$ for the $z = 1$ model, or $\bar{m}^2 = m^2 + \beta^2 M^2$ for the standard $z = 2$ background metrics. Of course, in the case $z = 1$ we must discard the additive constant $\beta^2 M/2$ to the Hamiltonian.

We see that the crucially unknown parameter of the problem, the spectrum $\Lambda_{(N,d)}$, gets mapped under the NRAdS/CFT correspondence to the local data of the bulk degrees of freedom, in this case the mass spectrum of bulk fields, according to the precise correspondence (6.3.8). In this respect, it is of great interest that the AdS prescription imposes a lower bound on $\Lambda_{(N,d)}$ following from the Breitenlohner–Freedman bound:

$$\Lambda_{(N,d)} > -\left(\frac{dN-d-2}{2}\right)^2 . \tag{6.3.9}$$

Finally, in this construction we obtain a rather direct physical interpretation of the holographic radial coordinate ρ, as a mean-square radius of the droplet of cold atoms, according to (6.3.4). The holographic direction accounts for the collective excitations of the droplet.

6.3.2 Quasiparticles

We have described the spectral properties of non-relativistic AdS/CFT systems either in free space or trapped by appropriate harmonic potentials. In this section we comment on the more general structures that can be expected when the conformal symmetry is broken dynamically by infrared effects. More specifically, we consider metric deformations which respect the Schrödinger group asymptotically as $\rho \to 0$ (the UV regime) but induce a mass gap at some low scale. The situation is analogous to that of harmonic trapping, but restricted to the radial holographic dynamics, i.e. we keep the system untrapped in the $\vec{x}$ coordinates.

A natural candidate for such a dynamical mass generation is that of $d = 2$ systems with attractive contact interactions, i.e. systems with delta-function interactions. In this case the

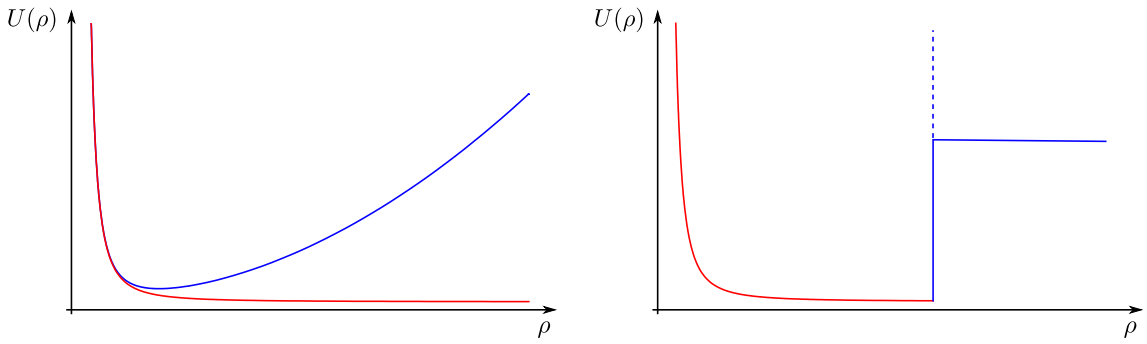

Figure 6.1: Plots of the potential $U(\rho) = \frac{b}{2M\rho^2} + v(\rho)$ that one can induce on the holographic radial coordinate ρ to model the generation of a mass gap. The red line presents the conformal potential, with vanishing $v(\rho)$, while the blue line represents the potential with non-zero $v(\rho)$. On the left plot we have the harmonic deformation, $v(\rho) = \frac{1}{2}M\Omega_\rho^2\rho^2$, while on the right we add a sharp wall of finite or infinite height.

quantum-field theory description of bound states involves a classically scale invariant four-fermion interaction $\psi^\dagger\psi^\dagger\psi\psi$, which undergoes logarithmic running at one loop. Energies of bound states are formally similar to $\Lambda_{\rm QCD}$ in the sense that they are non-perturbative in the bare coupling of the delta-function potential. Thus, this is a natural arena to investigate the geometrical realization of the mass gap.

While waiting for other realistic well formulated models to come, there are two simple phenomenological models for such mass-gap generation: a hard wall at some $\rho = L_\rho$, imposing a vanishing Dirichlet condition on wave functions at the hard wall, or a harmonic wall

$$v(\rho) = \frac{1}{2}\, M\Omega_\rho^2\, \rho^2 \tag{6.3.10}$$

for which all of our previous results apply, except that the $\vec{x}$ system is not trapped and $SL(2,\mathbb{R})$ covariance is broken at the level of the full spectrum (for instance, one loses the theorem (6.2.15), but maintains the exact results on the ρ-sector).

Expanding the dynamical field

$$\varphi(t,\vec{x},\rho) = \sum_\alpha f_\alpha(\rho)\Psi_\alpha(t,\vec{x}\,)$$

in a complete basis of normalized eigenfunctions of the radial Hamiltonian

$$H_\rho f_\alpha(\rho) = \varepsilon_\alpha\, f_\alpha(\rho)\ , \tag{6.3.11}$$

we can now quantize the system regarding the bulk field as a local operator, leading to the

second-quantized non-relativistic Hamiltonian

$$\mathcal{H}_{\text{free}} = \int d^d x \sum_\alpha \Psi^\dagger_\alpha(\vec{x}\,) \left(-\frac{\vec{\partial}^{\,2}}{2M} + \varepsilon_\alpha \right) \Psi_\alpha(\vec{x}\,) \ . \tag{6.3.12}$$

When the eigenvalue problem (6.3.11) has a discrete spectrum, the index α can be interpreted as a species index for a tower of 'quasiparticle types' in (6.3.12), with ε_α acquiring the interpretation of 'internal energies' for each particle type. This means that these quasiparticle types are to be interpreted as bound states, *molecules*, in complete analogy with well-known relativistic constructions in which, for instance, the eigenvalues of the bulk radial problem transmute into a tower of glueball masses, as viewed from the boundary (cf. [196]).

The spectrum of internal energies is determined by the gap potential. In the case (6.3.10) the spectrum of internal energies is evenly spaced, with step $2\Omega_\rho$, as in (6.2.23) and (6.3.7). For a hard wall, the spectrum of internal energies has a high-energy asymptotics of the form $\varepsilon_\alpha \sim 4\pi^2\alpha^2/2ML_\rho^2$, with α a positive integer.

Other situations can be contemplated. For instance, if the gap potential $v(\rho)$ has a minimun at $\rho = 0$ but asymptotes to a positive constant v_∞ as $\rho \to \infty$, we have a discrete spectrum of a finite number of quasiparticles with internal energies $0 < \varepsilon_\alpha < v_\infty$ followed at higher energies by a continuum spectrum, as in the Schrödinger invariant model (see Fig. 6.1).

One interesting piece of information that can be obtained from the knowledge of the internal energies ε_α is the high-energy density of states. Assume for example that $\Psi^\dagger_\alpha$ in (6.3.12) create bosons of internal energy ε_α, then the free energy of such a gas is given by

$$\frac{F(T)}{T} = V \sum_\alpha \int \frac{d^d p}{(2\pi)^d} \log \left[1 - e^{-\frac{1}{T}\left(\frac{\vec{p}^{\,2}}{2M} + \varepsilon_\alpha\right)} \right] \ . \tag{6.3.13}$$

If we simulate the mass gap by a sharp wall at $\rho = L_\rho$, the internal energy spectrum is given asymptotically by $\varepsilon_\alpha = (2\pi\alpha)^2/2ML_\rho^2$, with α a large integer number. Then, the entropy will scale at high temperatures as

$$S(\beta) \sim V L_\rho (MT)^{\frac{d+1}{2}} \ , \tag{6.3.14}$$

that is, the tower of quasiparticles contributes like an effective extra spatial dimension of size L_ρ. On the other hand, if we use a harmonic trap of frequency Ω_ρ, the contribution of the quasiparticles sum in (6.3.13) amounts to a factor of T/Ω_ρ, or equivalently to *two* extra dimensions of effective length $L_{\text{eff}} = (M\Omega_\rho)^{-1/2}$.

Local interaction terms of type (6.2.30) induce corresponding local interactions between the quasiparticles. In particular, inserting the basic ansatz (6.2.2) into (6.2.30) and performing the ξ and ρ integrations we find effective interaction terms in the effective many body

Hamiltonian of the 'molecules':

$$\mathcal{H}^{(k)}_{\rm int} \sim \frac{g_k}{M} \sum_{\alpha,\cdots,\beta,\cdots} V_{\alpha_1,\cdots,\alpha_k,\beta_1,\ldots\beta_k} \int d^dx\ \Psi^\dagger_{\alpha_1}(\vec{x}\,)\cdots\Psi^\dagger_{\alpha_k}(\vec{x}\,)\Psi_{\beta_1}(\vec{x}\,)\cdots\Psi_{\beta_k}(\vec{x}\,)\ , \qquad (6.3.15)$$

where the contact interactions are determined by overlapping integrals

$$V_{\alpha_1,\cdots\alpha_k,\beta_1,\cdots\beta_k} = \frac{1}{2\pi}\int d\rho \left(\frac{\rho}{R}\right)^{d-1} f^*_{\alpha_1}(\rho)\cdots f^*_{\alpha_k}(\rho) f_{\beta_1}(\rho)\cdots f_{\beta_k}(\rho)\ . \qquad (6.3.16)$$

It would be interesting to delve further into the possible applications of this formalism.

6.4 Concluding remarks

In this work we have implemented the elements of the Hamiltonian picture for the proposed non-relativistic AdS/CFT correspondence in Refs. [3, 4]. At the level of free bulk dynamics, we find that the conformal symmetry is realized by a decoupled system in the radial holographic coordinate, given by the conformal quantum mechanics of De Alfaro, Fubini and Furlan.

This analysis throws two important lessons. The first is the existence of background metrics that realize the Schrödinger group at the quantum level, even in the absence of the corresponding isometries. The second is that the deformations away from pure AdS metrics have rather mild effects in the free bulk approximation, such as a simple mass renormalization of scalar fields. It would be interesting to study in a systematic way whether the mild effects of the β^2 parameter in (6.1.3) stay so 'mild' at the level of interactions, or when the bulk system includes other types of matter, such higher spin modes. For example, contact interactions of type (6.2.30) are independent of β^2, since this parameter drops from the expression of the volume density $\sqrt{-g}$. However, more complicated interactions with derivatives will certainly be sensitive to β^2 and the question is whether the $\beta^2 \to 0$ limit is smooth, so that we can use pure AdS backgrounds to describe exact fixed points. Working with a light-like compactification certainly calls for caution, regarding possibly singular quantum effects associated to zero modes. The fact that one explicitly projects the theory onto a sector of *non vanishing* momentum is perhaps enough to ensure that no such problems will arise. We will deal with these questions in next chapter, 7.

The Hamiltonian analysis also led us to finding a family of metrics implementing the harmonic trapping. According to Schrödinger invariance, the spectrum of excitations in these harmonic traps is one to one correspondence to the scaling dimensions of the dual NRCFT operators. We obtained agreement with those found in [3, 4]. We found the $z = 1$ metric to be related to pure AdS. Moreover, the harmonic trap metric for $z = 2$ happens

to be the global version of Sch_{d+3} [193]. Also via a TsT transformation starting from the Penrose limit of Kerr-AdS black holes one can construct the finite temperature and chemical potential version in a harmonic trap.

Having a Hamiltonian formalism allowed us to make contact with detailed Hamiltonian results for the problem of fermions at unitarity in harmonic traps. We have seen that the conformal quantum mechanics in the holographic coordinate is hidden in the standard many-body bound state problem in terms of the effective Hamiltonian for the mean-square size of the trapped droplet, thus giving a direct interpretation of the holographic coordinate in the physical system of interest. On the other hand, the main computational challenge, i.e. the determination of the $\Lambda_{(N,d)}$ spectrum, is simply reformulated in terms of the mass spectrum of bulk fields. In the absence of the particular holographic dual to fermions at unitary, the holographic picture does not yet help in determining the $\Lambda_{(N,d)}$ coefficients. Unfortunately the QFT dual of Sch_{d+3}, a dipole theory, [170, 164, 169] is by no means a good approximation to fermions at unitary at this level.

Chapter 7

Correlation functions in the non-relativistic AdS/CFT correspondence

7.1 Introduction

In what follows we will proceed to the study of the correlation functions in the Schrödinger background proposed in [160, 161] with dynamical exponent $z = 2$, which we will take as the definition of our dual non-relativistic CFT at zero temperature and zero chemical potential via the usual AdS/CFT dictionary. Analogously to the case of a (relativistic) conformal invariant theory, the form of the correlation functions is constrained. In the case of the Schrödinger symmetry the constrains are milder and already in the 3-point function an overall function is left undetermined. For example [150, 151], the 2-point function (after Wick rotation) is fixed to

$$G_2(\bar{x}_1, \bar{x}_2) = \langle \varphi_1(\bar{x}_1)\varphi_2^*(\bar{x}_2)\rangle = \delta_{\Delta_1,\Delta_2}\delta_{M_1,M_2}\mathscr{C}_\varphi \frac{\theta(t_1-t_2)}{(t_1-t_2)^{\Delta_1}} \exp\left[-\frac{M_1}{2}\frac{(\vec{x}_1-\vec{x}_2)^2}{t_1-t_2}\right], \quad (7.1.1)$$

while the 3-point function is resctricted to

$$\begin{aligned} &G_3(\bar{x}_1, \bar{x}_2, \bar{x}_3) = \langle \varphi_1(\bar{x}_1)\varphi_2(\bar{x}_2)\varphi_3^*(\bar{x}_3)\rangle = \\ &= \delta_{M_1+M_2,M_3}\theta(t_1-t_3)\theta(t_2-t_3)(t_1-t_3)^{-\Delta_{13,2}/2}(t_2-t_3)^{-\Delta_{23,1}/2}(t_1-t_2)^{-\Delta_{12,3}/2}\times \\ &\times \exp\left[-\frac{M_1}{2}\frac{(\vec{x}_1-\vec{x}_3)^2}{t_1-t_3} - \frac{M_2}{2}\frac{(\vec{x}_2-\vec{x}_3)^2}{t_2-t_3}\right] \Psi\left(\frac{[(\vec{x}_1-\vec{x}_3)(t_2-t_3)-(\vec{x}_2-\vec{x}_3)(t_1-t_3)]^2}{(t_1-t_2)(t_1-t_3)(t_2-t_3)}\right), \end{aligned} \quad (7.1.2)$$

where $\bar{x}_i = (t_i, \vec{x}_i)$, M_i and Δ_i denote the non-relativistic mass and the scaling dimension corresponding to the operator φ_i, $\Delta_{ij,k} = \Delta_i + \Delta_j - \Delta_k$ and $\mathscr{C}_\phi$ denotes a normalization

constant. The scaling function $\Psi(y)$ is an arbitrary differentiable function which may have a parametric dependence on the non-relativistic masses M_1 and M_2. Here we see that the Schrödinger group is less powerful than the relativistic one, since in the relativistic case the three-point function is completely fixed by the symmetry.

One interesting question is to compare whether the physics that one gets from the holographic correlation functions match our expectations from the non-relativistic theory describing cold atoms. This study will be our primary concern in this chapter.

First, we will study in general the n-point scalar correlation functions in position space. We will not derive the full bulk-to-boundary and bulk-to-bulk propagators in position space for the Schrödinger spacetime. Nonetheless, we will exploit the following fact to get the computations done at tree level: fields must have a definite non-relativistic mass momentum at the boundary. The holographic construction is based on the embedding of the Schrödinger group into the conformal group in one higher dimension, where the one extra dimension is the geometrical realization of the central extension of the Galilean group by the mass operator as momentum. In this sense fields must have a definite momentum along this extra coordinate at the boundary so as to correspond to an operator with a well-defined non-relativistic mass. This will allow us to map the computation of the n-point correlation functions at tree level to momentum projections of AdS correlation functions in light-cone coordinates. Then we will employ this trick to compute the 2- and 3-point functions. From a QFT point of view, this mapping at tree level is analogous to the equivalence of planar graphs in a non-commutative and a commutative QFT. At least for $d = 2$ one can argue [169] that the dual QFT of the Schrödinger spacetime is related to a non-commutative theory that arises from $\mathcal{N} = 4$ SYM, the dual of AdS, giving ground for this equivalence. The results of the computation of the 2- and 3-point functions will back our belief that the holographic theory given by the Schrödinger background and the theory of cold fermions at unitarity are closely related at tree level. The function not fixed by the Schrödinger symmetry in the 3-point function will be exactly the same as the function obtained in a computation in the theory of cold atoms. We will also discuss in detail the physical meaning of this function.

The chapter is organized as follows: In Section 7.2 we describe a general recipe for calculation of the scalar n-point functions at tree level and discuss the problems coming from the loops in the associated Witten diagrams. In Section 7.3 we perform the simplest test of our prescription by computing the 2-point function. Section 7.4 is devoted to the calculation of the 3-point function in the holographic theory. We also compute the 3-point function in the theory of cold atoms. We compare both results and analyze the information contained in the correlation function. Finally, in Section 7.5 we conclude and present some outlook.

7.2 Scalar n-point functions in the Schrödinger background

In this section we will set up for the computation of the n-point function of scalar operators from the Schrödinger holographic dual in position space. First, we will analyze the case of the contribution from tree-level Witten diagrams, whose evaluation we will map to Fourier transformations of tree-level AdS correlation functions in the light-cone frame. Afterward, the case of loops in the Witten diagrams will be considered.

Since only in Euclidean space the computation of the correlation functions is well defined, we will implicitly work in the Euclidean, upon the usual Wick rotation $t \to it$. The Wick rotated version of the Schrödinger equation corresponds to the diffusion equation if we further flip the sign of the non-relativistic mass. The Lorentzian result is then easily obtained after the inverse Wick rotation from the Euclidean answer since we are at zero temperature. In our case the Euclidean Schrödinger metric, Sch^E_{d+3}, corresponds to

$$ds^2_E = \beta^2 \frac{dt^2}{u^4} + \frac{-2idtd\xi + dx^i dx^i + du^2}{u^2} \quad . \tag{7.2.1}$$

It is a complex metric. However, as long as the associated action remains real, as it is the case here, this should cause no trouble [164, 197]. In the Lorentzian we have to ask the fields to behave at the boundary as $\phi(X) = e^{-iM\xi}\phi(\bar{x})$, whereas in the Euclidean they have to behave as $\phi(X) = e^{iM\xi}\phi(\bar{x})$. This way one recovers a Schrödinger equation or a diffusion equation respectively for the fields at the boundary when we start from a relativistic action in the light-cone frame.

We want to compute the n-point functions of field theory operators dual to scalar fields living in Sch^E_{d+3}. The action of a complex scalar field will be generically of the form

$$S = \int d^d x \sqrt{g} \left[\partial_\mu \phi \partial^\mu \phi^* + m_0^2 |\phi|^2 + \mathcal{L}_I\right] \quad . \tag{7.2.2}$$

From this action, according to the usual holographic dictionary, the building blocks that we need to compute in order to obtain the n-point functions are the bulk-to-boundary and the bulk-to-bulk propagator. For example, the 3-point amplitude at tree level corresponding to interaction vertices of the form $\mathcal{L}_I = (\phi_1\phi_2\phi_3 + c.c.)$ will be

$$G_3(X,Y,Z) = \int \frac{da}{u^{d+3}} K_1(a;X) K_2(a;Y) K_3(a;Z) \quad , \tag{7.2.3}$$

where $K_i(a;X_i)$ is the bulk-to-boundary propagator.[1]

[1]Notation: $a = (t_a, \vec{a}, \xi_a, u_a)$, $\bar{a} = (t_a, \vec{a})$, $A = (t_a, \vec{a}, \xi_a)$.

However, there is something very particular to Sch^E_{d+3} that we can exploit: the fields have a definite momentum along ∂_ξ at the boundary, that is

$$\lim_{u\to 0}\phi(x) = e^{iM\xi}\phi(\bar{x}) \quad . \tag{7.2.4}$$

7.2.1 Tree level

Let us consider what this means for the computation of the correlators at tree level. At tree level, by definition, we have no loops and thus all momenta flowing in each propagator is fixed in terms of the momenta of the external insertions. Our boundary conditions for the fields are such that they have a definite momentum along the ∂_ξ direction. This implies that all propagators in the tree-level diagrams must have a definite momentum along ∂_ξ. Thus we can use, instead of the full propagators in position space, the propagators that are projected to have a definite momentum along ∂_ξ. Remarkably, one can show that these projected propagators in the Schrödinger spacetime are the same as the projected propagators coming from AdS in the light-cone frame, after a shift of the relativistic mass $m^2 = m_0^2 + \beta^2 M^2$. This way we can construct the tree-level amplitudes from the AdS propagators after a momentum projection along ∂_ξ. In general we can further state that all we need to do is to have the corresponding AdS amplitude at tree level in light-cone coordinates and project each operator insertion to have a momentum along ∂_ξ corresponding to the non-relativistic mass, M_i, i.e.

$$\langle\phi_1(\bar{x}_1)\dots\phi_n(\bar{x}_n)\rangle^{(\text{tree level})}_{\text{Sch}} = \int\prod_{k=1}^{n} d\xi_k\, e^{-i\sum_{j=1}^{n}(M_j\xi_j)}\langle\phi_1(\bar{x}_1,\xi_1)\dots\phi_n(\bar{x}_n,\xi_n)\rangle^{(\text{tree level})}_{\text{AdS}} \tag{7.2.5}$$

The expression is valid for both a compact or non-compact ∂_ξ-direction with the evident modifications.[2]

For clarity, let us expound the preceding comments with an example, the 3-point function with contact interactions at tree level. In this case, cf. Fig. 7.1, we will have that the amplitude is obtained from the functional derivative with respect to $\phi_i(\bar{x}_i)$ of the following

[2]When ξ is compact, the integration domain is restricted to the period and one also has to impose that the relativistic n-point function be periodic in ξ_k.

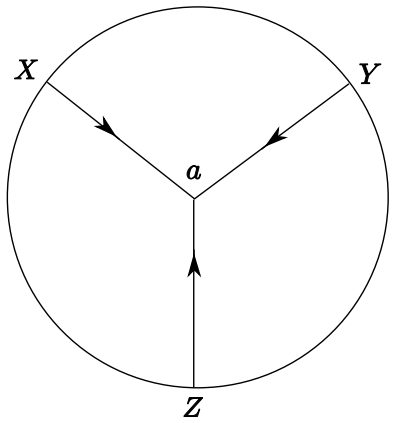

Figure 7.1: Witten diagram that gives the tree level contribution to the 3-point function.

integral

$$\begin{aligned}
&\int dX\, dY\, dZ \int \sqrt{g}\, da\, K_1(a;X)K_2(a;Y)K_3(a;Z)\phi(X)\phi(Y)\phi(Z) = \\
&= \int d\bar{x}\, d\bar{y}\, d\bar{z}\, d\xi_x\, d\xi_y\, d\xi_z \int \sqrt{g}\, d\bar{a}\, d\xi_a\, du_a\, K_1(\bar{a}-\bar{x},\xi_a-\xi_x,u_a)K_2(\bar{a}-\bar{y},\xi_a-\xi_y,u_a)\times \\
&\qquad \times K_3(\bar{a}-\bar{z},\xi_a-\xi_z,u_a)e^{iM_1\xi_x}e^{iM_2\xi_y}e^{iM_3\xi_z}\phi(\bar{x})\phi(\bar{y})\phi(\bar{z})
\end{aligned} \tag{7.2.6}$$

After the functional derivative with respect to $\phi_i(\bar{x}_i)$, a simple change of variables in ξ_i and integration over ξ_a, we obtain that the amplitude is given by

$$\begin{aligned}
G_3(\bar{x},\bar{y},\bar{z}) = 2\pi\delta(\sum_{k=1}^{3} M_k) \int d\tilde{\xi}_x\, d\tilde{\xi}_y\, d\tilde{\xi}_z \int \sqrt{g}\, d\bar{a}\, du_a\, K_1(\bar{a}-\bar{x},\tilde{\xi}_x,u_a)\times \\
\times K_2(\bar{a}-\bar{y},\tilde{\xi}_y,u_a)K_3(\bar{a}-\bar{z},\tilde{\xi}_z,u_a)e^{-iM_1\tilde{\xi}_x}e^{-iM_2\tilde{\xi}_y}e^{-iM_3\tilde{\xi}_z}
\end{aligned} \tag{7.2.7}$$

For definiteness we assumed the ∂_ξ-direction to be non-compact as we will do in the rest of the expressions in this section when integrating over ξ. The same results hold for a compact ξ changing the Dirac deltas by Kronecker deltas as well as the overall factor of 2π by the period along ∂_ξ. Also the masses then become discrete, $M_i = 2\pi j/L_\xi$ with $j \in \mathbb{Z}^*$ and L_ξ the period along ∂_ξ.

From this example, we see that the Bargmann superselection rule is automatically implemented as the conservation of the ∂_ξ-component of the momentum. One can associate an arrow with each propagator, such that the ingoing mass in a vertex should equal the outgoing mass. ϕ contributes with $+M$, whereas ϕ^* contributes with $-M$. We also see that

the bulk-to-boundary propagator is always going to enter in through the combination

$$\begin{aligned}\phi(\bar{x},\xi,u_x) &= \int d\bar{y}d\xi' K(\bar{x}-\bar{y},\xi-\xi',u_x)\phi(\bar{y},\xi') \\ &= e^{iM\xi}\int d\bar{y}d\tilde{\xi}\, K(\bar{x}-\bar{y},\tilde{\xi},u_x)\, e^{-iM\tilde{\xi}}\,\phi(\bar{y})\end{aligned} \tag{7.2.8}$$

Hence we can introduce what we will call the *projected* bulk-to-boundary propagator

$$K_M(\bar{x}-\bar{y},\xi-\xi',u_x) = e^{iM(\xi-\xi')}\int d\tilde{\xi}\, K(\bar{x}-\bar{y},\tilde{\xi},u_x)\, e^{-iM\tilde{\xi}} \tag{7.2.9}$$

and use it to construct directly the amplitudes in Sch^E_{d+3} from the corresponding Witten diagrams.

Now we can ask, what is the differential equation that the projected bulk-to-boundary propagator satisfies? The bulk-to-boundary propagator satisfies that

$$\left(\nabla_x^2 - m_0^2\right) K(x-y) = 0 \quad , \qquad \lim_{u\to 0} K(x-y) \sim u^{d+2-\Delta}\delta(\bar{x}-\bar{y}) \quad . \tag{7.2.10}$$

In Sch^E_{d+3} the operator $(\nabla_x^2 - m_0^2)$ is given by

$$\nabla_x^2 - m_0^2 = u^2\partial_u^2 - (d+1)u\partial_u + 2iu^2\partial_t\partial_\xi + u^2\partial_i^2 + \beta^2\partial_\xi^2 - m_0^2 \tag{7.2.11}$$

If we consider the projected bulk-to-boundary propagator, we see that it will satisfy

$$\left[\partial_u^2 - \frac{d+1}{u}\partial_u - 2M\partial_t + \partial_i^2 - \frac{1}{u^2}\left(\beta^2M^2 + m_0^2\right)\right] K_M(\bar{x}-\bar{y},\xi-\xi',u) = 0 \tag{7.2.12}$$

Remarkably, one can compare it to the action of $(\nabla_x^2 - m^2)$ on the projected propagator but in a pure AdS_{p+2} background in light-cone coordinates (basically eq. (7.2.1) but with $\beta = 0$),

$$\left[\partial_u^2 - \frac{p}{u}\partial_u - 2M\partial_t + \partial_i^2 - \frac{m^2}{u^2}\right] K_M(\bar{x}-\bar{y},\xi-\xi',u) = 0 \tag{7.2.13}$$

We see both equations (7.2.12) and (7.2.13) are the same provided we identify $p = d+1$ and take the mass in AdS to be $m^2 = m_0^2 + \beta^2M^2$. Hence we see that the projected propagator in Sch_{d+3} is the same as the projection of the propagator in AdS_{d+3} in light-cone coordinates with a suitable shift of the mass,

$$K_M(\bar{x}-\bar{y},\xi-\xi',u_x) = e^{iM(\xi-\xi')}\int d\tilde{\xi}\, K_\Delta^{(\text{AdS})}(\bar{x}-\bar{y},\tilde{\xi},u_x)\, e^{-iM\tilde{\xi}} \tag{7.2.14}$$

such that

$$\Delta(\Delta-d-2) = m^2 = m_0^2 + \beta^2M^2 \quad . \tag{7.2.15}$$

This is nothing but a reflection of the fact that the equations of motion of a free scalar with a definite momentum along ∂_ξ in Sch_{d+3} are the same as another free scalar in AdS_{d+3} in light-cone coordinates with a shifted mass and the same momentum along ∂_ξ.

Now that we have an integral expression (see Appendix B for the explicit form) of the projected bulk-to-boundary propagator in terms of known functions, we can revisit the expression for the 3-point function (7.2.7) in terms of the projected bulk-to-boundary propagators, corresponding to the diagram in Fig. 7.1,

$$\begin{aligned}
\langle\phi_1(\bar{x})\phi_2(\bar{y})\phi_3(\bar{z})\rangle_{\mathrm{Sch}}^{(\text{tree level})} &= \\
&= 2\pi\delta(\sum_{k=1}^{3} M_k)\int \sqrt{g}\, d\bar{a}\, du_a\, K_{M_1}(\bar{a}-\bar{x},u_a)K_{M_2}(\bar{a}-\bar{y},u_a)K_{M_3}(\bar{a}-\bar{z},u_a) \\
&= 2\pi\delta(\sum_{k=1}^{3} M_k)\int d\tilde{\xi_x}\, d\tilde{\xi_y}\, d\tilde{\xi_z}\int \sqrt{g}\, d\bar{a}\, du_a\, K^{(\mathrm{AdS})}_{\Delta_1}(\bar{a}-\bar{x},\tilde{\xi_x},u_a)\times \\
&\qquad\qquad \times K^{(\mathrm{AdS})}_{\Delta_2}(\bar{a}-\bar{y},\tilde{\xi_x},u_a)K^{(\mathrm{AdS})}_{\Delta_3}(\bar{a}-\bar{z},\tilde{\xi_z},u_a)\, e^{-iM\tilde{\xi_x}}e^{-iM\tilde{\xi_y}}e^{-iM\tilde{\xi_z}} \\
&= \int d\xi_x\, d\xi_y\, d\xi_z\, e^{-iM_1\xi_x}e^{-iM_2\xi_y}e^{-iM_3\xi_z}\langle\phi_1(\bar{x},\xi_x)\phi_2(\bar{y},\xi_y)\phi_3(\bar{z},\xi_z)\rangle_{\mathrm{AdS}}^{(\text{tree level})}
\end{aligned} \tag{7.2.16}$$

The end result is that we can read off the tree level 3-point function in Sch from the corresponding 3-point function in AdS space in light-cone coordinates projecting to definite momenta, the non-relativistic masses, along a light-light direction, as advertised at the beginning.

It is immediate that we can generalize this result to all n-point functions that are built from bulk-to-boundary propagators, i.e. only one vertex in the bulk, and to the case of the 2-point function at tree level. The 2-point function is going to be given as

$$\langle\phi_1(\bar{x})\phi_2(\bar{y})\rangle_{\mathrm{Sch}}^{(\text{tree level})} = \int d\xi_x\, d\xi_y\, e^{-iM\xi_x}e^{-iM\xi_y}\langle\phi_1(\bar{x},\xi_x)\phi_2(\bar{y},\xi_y)\rangle_{\mathrm{AdS}}^{(\text{tree level})} \tag{7.2.17}$$

When the tree-level diagram contains bulk-to-bulk propagators the argument holds the same way. For example, let us consider the leading contribution to the 4-point function at tree level from 3-point contact interactions $\mathcal{L}_I = \phi_1\phi_2\phi_3 + c.c.$, corresponding to the diagram in Fig. 7.2. Denoting by $G(a-b)$ the bulk-to-bulk propagator and again taking into account that $\phi_j(\bar{x}_j,\xi_j) = e^{iM_j\xi_j}\phi(\bar{x}_j)$ and a simple change of coordinates in ξ_j, we have that the amplitude is

$$\begin{aligned}
G_4(\bar{x},\bar{y},\bar{z},\bar{v}) = -2\pi\delta(\sum_{j=1}^{4} M_j)\int g\, d\bar{a}d\bar{b}du_a du_b\, d\tilde{\xi}K_{M_1}(\bar{a}-\bar{x},\tilde{\xi_x},u_a)K_{M_2}(\bar{a}-\bar{y},\tilde{\xi_y},u_a)\times \\
\times G(\bar{a}-\bar{b},\tilde{\xi},u_a-u_b)K_{M_3}(\bar{b}-\bar{z},\tilde{\xi_z},u_b)K_{M_4}(\bar{b}-\bar{v},\tilde{\xi_v},u_b)e^{-i(M_3+M_4)\tilde{\xi}}
\end{aligned} \tag{7.2.18}$$

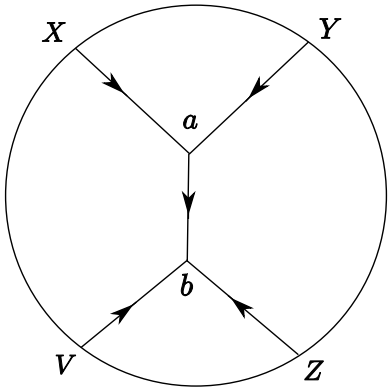

Figure 7.2: Witten diagram that gives the tree level contribution to the 4-point function with 3-point contact interactions.

We can see that the bulk-to-bulk propagator is projected along ∂_ξ with a mass equal to the mass entering the vertex that it connects, a reflection that the mass is conserved in the bulk vertices.

In general in the Witten diagrams where there are no loops, the bulk-to-bulk propagator is going to appear always projected by a mass such that the mass is conserved at each vertex. Again one can associate an arrow with each propagator, such that the ingoing mass in a vertex should equal the outgoing mass. ϕ contributes with $+M$, whereas ϕ^* contributes with $-M$.

Hence it makes sense to introduce the *projected* bulk-to-bulk propagator as

$$G_M(\bar{x}-\bar{y},\xi-\xi',u_x-u_y) = e^{iM(\xi-\xi')}\int d\tilde{\xi}\, G(\bar{x}-\bar{y},\tilde{\xi},u_x-u_y)\, e^{-iM\tilde{\xi}} \tag{7.2.19}$$

Analogously to the case of the projected bulk-to-boundary propagator it can be shown that the projected bulk-to-bulk propagator in Sch_{d+3} can be related to a projection of the bulk-to-bulk propagator in AdS_{d+3} written in light-cone coordinates as

$$G_M(\bar{x}-\bar{y},\xi-\xi',u_x-u_y) = e^{iM(\xi-\xi')}\int d\tilde{\xi}\, G_\Delta^{(\mathrm{AdS})}(\bar{x}-\bar{y},\tilde{\xi},u_x-u_y)\, e^{-iM\tilde{\xi}} \tag{7.2.20}$$

with

$$\Delta(\Delta-d-2) = m^2 = m_0^2+\beta^2M^2 \quad . \tag{7.2.21}$$

This way, as another example, the 6-point function at tree level, see Fig. 7.3, is going to

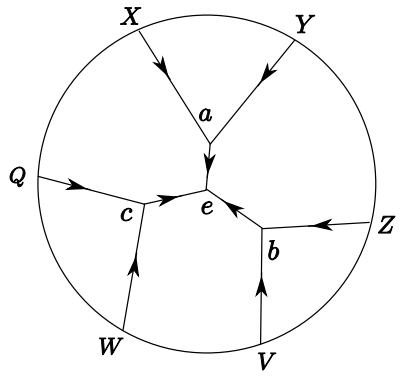

Figure 7.3: Witten diagram that gives the tree level contribution to the 6-point function with 3-point contact interactions.

be given by

$$\begin{aligned}
&\langle\phi_1(\bar{x})\phi_2(\bar{y})\phi_3(\bar{z})\phi_4(\bar{v})\phi_5(\bar{w})\phi_6(\bar{q})\rangle = \\
&\quad = -2\pi\delta(\sum_{j=1}^{6} M_j)\int g^2\, d\bar{a}\, d\bar{b}\, d\bar{c}\, d\bar{e}\, du_a du_b du_c du_e K_{M_1}(\bar{a}-\bar{x},u_a)K_{M_2}(\bar{a}-\bar{y},u_a) \\
&\qquad \times K_{M_3}(\bar{b}-\bar{z},u_b)K_{M_4}(\bar{b}-\bar{v},u_b)K_{M_5}(\bar{c}-\bar{w},u_c)K_{M_6}(\bar{c}-\bar{q},u_c)\times \\
&\qquad \times G_{M_1+M_2}(\bar{e}-\bar{a},u_e-u_a)G_{M_3+M_4}(\bar{e}-\bar{b},u_e-u_b)G_{M_5+M_6}(\bar{e}-\bar{c},u_e-u_c)
\end{aligned} \tag{7.2.22}$$

where now all functions are known quantities.

Finally we arrive to the observation that in any tree-level diagram we will have that

$$\langle\phi_1(\bar{x}_1)\dots\phi_n(\bar{x}_n)\rangle_{\text{Sch}}^{(\text{tree level})} = \int\prod_{k=1}^{n} d\xi_k\, e^{-i\sum_{j=1}^{n}(M_j\xi_j)}\langle\phi_1(\bar{x}_1,\xi_1)\dots\phi_n(\bar{x}_n,\xi_n)\rangle_{\text{AdS}}^{(\text{tree level})} \tag{7.2.23}$$

One can easily understand that this must be the case. We take the pure AdS amplitude, built from AdS propagators, but then we perform non-relativistic mass projections at the boundary that forces all the rest of mass projections in the internals of the tree level diagram that we see through the projected propagators corresponding to the Sch amplitude. This way one can understand the pure AdS amplitude as a neat one-higher dimensional representation of the Sch correlation functions at tree level, which we can read off after appropriate non-relativistic mass projections at the operator insertions.

What is the QFT viewpoint of relation (7.2.23)? As explained in [169], the holographic dual of the Sch_{d+3} for $d = 2$ can be seen as a dipole theory [171, 172, 173, 174] constructed from $\mathcal{N} = 4$ SYM. These dipole theories are a certain type of non-commutative theory that we can construct from an ordinary theory through the introduction of the non-commutative

$*$ product, depending on the parameter β, given by

$$f * g = e^{i2\pi\beta(\tilde{P}_-^f Q^g - \tilde{P}_-^g Q^f)} fg \quad . \tag{7.2.24}$$

$\tilde{P}_-$ is the light-like momentum charge and Q is another charge associated with some global symmetries. In the case of $\mathcal{N} = 4$ SYM one takes $\tilde{P}_-$ as the charge associated with the momentum along the light-cone direction ∂_ξ and Q as the charge associated to a $U(1)$ of the $SO(6)$ R-symmetry. The introduction of this product precisely reduces the spacetime symmetries of the initial SYM theory to the Schrödinger subgroup. The bulk equivalent of the introduction of the non-commutative product consists on the TsT transformation of the original AdS background that gives the Sch metric along a non-trivial profile for the dilaton and B-field [169, 172]. In non-commutative theories the planar-diagrams are simple. They are equal to the planar-diagrams of the ordinary theory except for some overall phase depending only on the external particles [198, 199]. Thus we can understand that the tree-level contributions (corresponding to the planar diagrams in the QFT) to the correlation functions are basically the same as computed from Sch or AdS as given by (7.2.23).

To summarize we have seen that at tree level, when there are no loops in the associated Witten diagrams, the correlation function of scalars can be computed in terms of projected propagators coming from pure AdS written in light-cone coordinates. Furthermore, the amplitude is exactly the mass projection of the equivalent pure AdS amplitude. Hence, at tree level we can expect no difference in the scalar amplitudes and all derived observables between the results coming from Sch and light-cone pure AdS provided we shift the mass of the scalar and the fields have a definite momentum along ∂_ξ.

7.2.2 Loops

In the case when there appears loops in the associated Witten diagrams for the amplitudes, we cannot rewrite them in terms of projected propagators, i.e. there are undetermined masses over which we must integrate. Hence we cannot compute loop-amplitudes in the Schrödinger spacetime from projections of equivalent full AdS amplitudes. The $1/N$ corrections of each theory are different. This is in agreement to the non-commutative interpretation of the QFT theory for $d = 2$ [169], where only at the planar level one has equivalence between the non-commutative and commutative theories. Furthermore, what becomes evident is that when we choose the ∂_ξ direction to be compact,[3] there appears divergence associated with the zero-modes of the KK tower on the null S^1_ξ, as is common in any DLCQ theory [165].

[3]This choice is motivated by the interpretation of the mass operator as a number operator, whose eigenvalues are quantized.

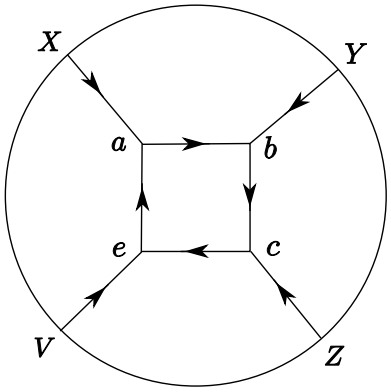

Figure 7.4: Witten diagram which gives a 1-loop contribution to the 4-point function

In order to give sense to the theory we must abandon the idea of making the ∂_ξ-direction compact or regularize it by making the ∂_ξ-circle spacelike. One natural way to make the S^1_ξ spacelike is with the introduction of a non-zero chemical potential still at zero temperature through the proposed metric[4] [170]

$$ds^2 = -\beta^2 \frac{dt^2}{u^4} + \gamma^2 u^2 d\xi^2 + \frac{-2dtd\xi + dx^i dx^i + du^2}{u^2} \tag{7.2.25}$$

and at the end try to arrange things such that we can safely take the zero chemical potential limit $\mu \propto \gamma^2 \to 0$.

As an example let us consider a one loop contribution to the 4-point function. See Fig. 7.4. The amplitude is given in terms of

$$\begin{aligned} G_4(\bar{x},\bar{y},\bar{z},\bar{v}) = \int g^2\, d\bar{a}\, d\bar{b}\, d\bar{c}\, d\bar{e}\, d\xi_a d\xi_b d\xi_c d\xi_e\, du_a du_b du_c du_e K_{M_1}(\bar{a}-\bar{x},u_a) K_{M_2}(\bar{b}-\bar{y},u_b)\times \\ \times K_{M_3}(\bar{c}-\bar{z},u_c) K_{M_4}(\bar{e}-\bar{v},u_e) \mathcal{A}(\bar{a},\bar{b},\bar{c},\bar{e},u_a,u_b,u_c,u_e) \end{aligned} \tag{7.2.26}$$

with

$$\begin{aligned} \mathcal{A}(\bar{a},\bar{b},\bar{c},\bar{e},u_a,u_b,u_c,u_e) &= \int d\xi_a d\xi_b d\xi_c d\xi_e\, G(\bar{a}-\bar{b},\xi_a-\xi_b,u_a-u_b) G(\bar{b}-\bar{c},\xi_b-\xi_c,u_b-u_c)\times \\ &\times G(\bar{c}-\bar{e},\xi_c-\xi_e,u_c-u_e) G(\bar{e}-\bar{a},\xi_e-\xi_a,u_e-u_a) e^{-iM_1\xi_a} e^{-iM_2\xi_b} e^{-iM_3\xi_c} e^{-iM_4\xi_e} \\ &= 2\pi\delta(\sum_{j=1}^{4} M_j) \int d\tilde{\xi}_a d\tilde{\xi}_b d\tilde{\xi}_c\, G(\bar{a}-\bar{b},\tilde{\xi}_a,u_a-u_b) G(\bar{b}-\bar{c},\tilde{\xi}_b,u_b-u_c)\times \\ &\times G(\bar{c}-\bar{e},\tilde{\xi}_c,u_c-u_e) G(\bar{e}-\bar{a},-\tilde{\xi}_a-\tilde{\xi}_b-\tilde{\xi}_c,u_e-u_a) e^{-iM_1\tilde{\xi}_a} e^{-i(M_1+M_2)\tilde{\xi}_b} e^{-i(M_1+M_2+M_3)\tilde{\xi}_c} \end{aligned} \tag{7.2.27}$$

[4]This metric comes from a suitable scaling of the Schrödinger black hole metrics (5.3.28).

We see that in this case there are bulk-to-bulk propagators that are not projected bulk-to-bulk propagators. This result can be generalized to any Witten diagram that contains loops.

If we go to Fourier space we can see clearly how, when the ∂_ξ-direction is compact with length L_ξ, we are going to face the usual divergence from the zero modes in the circle, following the same argument as in [165]. In momentum-space the bulk-to-boundary and bulk-to-bulk propagators are given by

$$K^\epsilon(u,k) = \left(\frac{u}{\epsilon}\right)^{\frac{d+2}{2}} \frac{\mathcal{K}_\nu(ku)}{\mathcal{K}_\nu(k\epsilon)} \tag{7.2.28}$$

$$G(u_a,u_b,k) = \begin{cases} -(u_a u_b)^{\frac{d+2}{2}} \mathcal{I}_\nu(ku_a)\mathcal{K}_\nu(ku_b) & \text{for} \quad u_a < u_b \\ -(u_a u_b)^{\frac{d+2}{2}} \mathcal{K}_\nu(ku_a)\mathcal{I}_\nu(ku_b) & \text{for} \quad u_a > u_b \end{cases} \tag{7.2.29}$$

such that

$$\nu = \left(\frac{(d+2)^2}{4} + m_0^2 + \beta^2 \frac{n^2}{L_\xi^2}\right)^{\frac{1}{2}} \quad , \qquad k = \sqrt{-2i\frac{n\omega}{L_\xi} + \vec{p}^2} \quad . \tag{7.2.30}$$

ϵ denotes an infinitesimal cutoff at the boundary in the radial coordinate. $n \in \mathbb{Z}$ such that $M = n/L_\xi$ is the mass momentum. $\mathcal{I}_\nu$, $\mathcal{K}_\nu$ are the modified Bessel functions. The position space propagators are recovered from

$$\begin{aligned} K(\bar{a},\bar{x},u_a) &= (2\pi L_\xi)^{-1} \sum_{n=-\infty}^{\infty} \int \frac{d^d\vec{p}}{(2\pi)^d}\frac{d\omega}{2\pi} e^{-i\vec{p}\cdot(\vec{a}-\vec{x})} e^{-i\omega(t_a-t_x)} e^{-i\frac{n}{L_\xi}(\xi_a-\xi_x)} K^\epsilon(u_a,k) \\ G(\bar{a},\bar{b},u_a,u_b) &= (2\pi L_\xi)^{-1} \sum_{n=-\infty}^{\infty} \int \frac{d^d\vec{p}}{(2\pi)^d}\frac{d\omega}{2\pi} e^{-i\vec{p}\cdot(\vec{a}-\vec{b})} e^{-i\omega(t_a-t_b)} e^{-i\frac{n}{L_\xi}(\xi_a-\xi_b)} G(u_a,u_b,k) \end{aligned} \tag{7.2.31}$$

Note that the only difference with respect to the AdS propagators in momentum space [200] is the dependence of ν on the mass momentum $M = n/L_\xi$, as is evident from eq. (7.2.12).

The position propagators can be seen as a sum of propagators with a definite momentum over S^1_ξ. For the zero-modes, the propagator is going to be proportional to $\delta(t)$, as is immediate from (7.2.30), (7.2.31), or even directly from (7.2.12). Then a closed loop with two zero-momentum modes will involve $\delta(t)^2 \propto \delta(0)$, resulting in the typical DLCQ divergence. To solve it we have to regularize by making the null circle to be space-like. We can do it by turning on a non-zero chemical potential still at zero temperature by means of the metric (7.2.25) introduced in [170]. The other option is to discard altogether the possibility of a compact ∂_ξ-direction. The last option poses the conceptual problem of throwing away a genuine number operator interpretation for the mass operator of the theory.

7.3 Scalar 2-point function

In order to illustrate the general method, introduced in Sec. 7.2, we compute first a scalar 2-point function. According to Eq. (7.2.17) the 2-point scalar correlator $G_2 = \langle\phi_1(t_1,\vec{x}_1)\phi_2(t_2,\vec{x}_2)\rangle_{\rm Sch}^{(\text{tree level})}$ in the non-relativistic holography is given by

$$G_2 = \int d\xi_1\, d\xi_2\, e^{-i(M_1\xi_1+M_2\xi_2)}\langle\phi_1(X_1)\phi_2(X_2)\rangle_{\rm AdS}^{(\text{tree level})}. \tag{7.3.1}$$

The relativistic 2-point function in Euclidean space is well-known from the relativistic AdS/CFT [201]

$$\langle\phi_1(X_1)\phi_2(X_2)\rangle_{\rm AdS}^{(\text{tree level})} = \frac{C_{12}\delta_{\Delta_1,\Delta_2}}{|X_1-X_2|^{2\Delta_1}}, \tag{7.3.2}$$

where $X=(t,\vec{x},\xi)$ and $|X|^2 = \vec{x}^2 - 2it\xi$. C_{12} is a position-independent constant which is taken to one under canonical normalization.

After introducing a center of mass coordinate $\eta = \xi_1+\xi_2$ and a relative coordinate $\xi = \xi_1-\xi_2$ we end up with

$$G_2 = \frac{1}{2}\int d\eta\, d\xi\, e^{-i\frac{M_1+M_2}{2}\eta}e^{-i\frac{M_1-M_2}{2}\xi}\langle\phi_1(X_1)\phi_2(X_2)\rangle_{\rm AdS}^{(\text{tree level})}. \tag{7.3.3}$$

The integration over η produces a Bargmann superselection delta function $\delta(M_1+M_2)$. The remaining ξ integral was evaluated in [151] and can be found in Appendix B

$$\begin{aligned} G_2 &= 2\pi\delta(M_1+M_2)\int d\xi e^{-iM_1\xi}\langle\phi_1(X_1)\phi_2(X_2)\rangle_{\rm AdS}^{(\text{tree level})} = \\ &= \frac{2\pi C_{12}\delta_{\Delta_1,\Delta_2}\delta(M_1+M_2)}{(2i(t_1-t_2))^{\Delta_1}}\int d\xi e^{-iM_1\xi}\frac{1}{\left(\xi+\frac{i(\vec{x}_1-\vec{x}_2)^2}{2(t_1-t_2)}\right)^{\Delta_1}} = \\ &= \mathscr{C}_\phi\delta_{\Delta_1,\Delta_2}\delta(M_1+M_2)\frac{\theta(t_1-t_2)}{(t_1-t_2)^{\Delta_1}}\exp\left(-\frac{M_1}{2}\frac{(\vec{x}_1-\vec{x}_2)^2}{(t_1-t_2)}\right), \end{aligned} \tag{7.3.4}$$

where $\mathscr{C}_\phi = \frac{2\pi C_{12}\alpha M_1^{\Delta_1-1}}{(2i)^\Delta}$. In the case of a compact ∂_ξ-direction, one arrives at a same expression with the same functional dependence, see Appendix D. It is reassuring that the final result coincides with Eq. (7.1.1) which follows from the Schrödinger symmetry.

7.4 Scalar 3-point function

In this Section we tackle a more difficult aim: computation of the 3-point correlator. First, a specific 3-point function is calculated using QFT methods for cold atoms at unitarity. Then we employ the general method of Sec. 7.2 to obtain the scalar 3-point function from non-relativistic holography. We compare the non-universal scaling functions $\Psi(y)$ (7.1.2) for cold atoms and holographic theory. Finally, we provide a few remarks on physical information stored in the scaling function $\Psi(y)$.

7.4.1 3-point function for cold atoms at unitarity

In this subsection we compute the 3-point function in a non-relativistic QFT of cold atoms with contact interaction. The two-component fermions near a broad Feshbach resonance at $T = 0$ are described by a microscopic action[5] [202]

$$S_E[\psi] = \int dt \int d^d x \sum_{i=1}^{2} \psi_i^*(\partial_t - \frac{\Delta}{2m} - \mu)\psi_i - c_0 \psi_1^* \psi_2^* \psi_2 \psi_1, \tag{7.4.1}$$

where two species of the fermionic atoms of mass m are denoted by ψ_1 and ψ_2, μ stands for a chemical potential and c_0 characterizes the microscopic interaction strength. The action has an internal $SU(2) \times U(1)$ symmetry. The QFT defined by Eq. (7.4.1) must be equipped with a UV cutoff Λ due to the contact nature of the interaction term. In this analysis we are interested in a vacuum state, i.e. the state of zero temperature and density. In vacuum the bare parameters μ and c_0 are the functions of the cut-off Λ and the low-energy s-wave scattering length a only. In order to simplify the analysis, it is useful to rewrite Eq. (7.4.1) by means of the Hubbard-Stratonovich transformation:

$$S_E[\psi, \phi] = \int dt \int d^d x \sum_{i=1}^{2} \psi_i^*(\partial_t - \frac{\Delta}{2m})\psi_i + \frac{1}{c_0}\phi^*\phi - (\phi^* \psi_1 \psi_2 + \phi \psi_2^* \psi_1^*), \tag{7.4.2}$$

where ϕ denotes a composite bosonic diatom of mass $2m$. The theory (7.4.2) becomes strongly interacting in the unitary regime $|a| \to \infty$ in $d = 3$. In the vacuum state in the unitary limit $\mu = 0$ and $c_0 = c_0(\Lambda)$, where the concrete functional form depends on the regularization procedure. For example, for sharp momentum regularization in $d = 3$

$$-\frac{1}{c_0} = \frac{m}{4\pi a} - \int^{\Lambda} \frac{d^3 q}{(2\pi)^3} \frac{m}{\vec{q}^2}. \tag{7.4.3}$$

At unitarity the only scale defined by the scattering length a drops out and the theory becomes classically scale invariant. The QFT defined by Eq. (7.4.2) is believed to be an example of the non-relativistic CFT which respects the Schrödinger spacetime symmetry [149].

The exact Euclidean propagators $G_\psi(\omega, \vec{q})$ and $G_\phi(\omega, \vec{q})$ can be obtained from (7.4.2) using the non-perturbative Lippmann-Schwinger integral equations. In non-relativistic vacuum there is no particle-antiparticle production and hence the atom propagator $G_\psi(\omega, \vec{q})$ is not renormalized. In the momentum space it looks [202]

$$G_\psi(\omega, \vec{q}) = \frac{1}{i\omega + \epsilon_{\vec{q}}} \qquad \epsilon_{\vec{q}} = \frac{\vec{q}^2}{2m}, \tag{7.4.4}$$

[5] In order to do a direct comparison with [150, 151] we work in Euclidean time

Quantum effects make the diatom field ϕ fully dynamical with the propagator in the scale-free unitary regime given by [202]

$$G_\phi(\omega,\vec{q}) = \frac{(\frac{4\pi}{m})^{\frac{d}{2}}}{\Gamma(1-\frac{d}{2})}\frac{1}{(i\omega+\frac{\epsilon_{\vec{q}}}{2})^{\frac{d}{2}-1}}. \tag{7.4.5}$$

The diatom propagator is strongly renormalized. The form of $G_\psi(\omega,\vec{q})$ and $G_\phi(\omega,\vec{q})$ is consistent with the Schrödinger symmetry leading to the scaling dimensions of the atom field ψ and the diatom field ϕ

$$\Delta_\psi = \frac{d}{2} \qquad \Delta_\phi = 2. \tag{7.4.6}$$

This is in contrast to free fermions where one has that $\Delta_\psi = \frac{d}{2}$, $\Delta_\phi = d$.

In a very similar fashion one can describe the non-relativistic bosons near a broad Feshbach resonance. The microscopic $U(1)$ symmetric action in vacuum is

$$S[\psi,\phi] = \int dt \int d^dx \psi^*(\partial_t - \frac{\Delta}{2m})\psi + \frac{1}{c_0}\phi^*\phi + \frac{1}{2}(\phi^*\psi\psi + \phi\psi^*\psi^*), \tag{7.4.7}$$

where ψ represents a complex bosonic atom, while ϕ stands for a composite bosonic diatom. The full Euclidean propagators at unitarity can be calculated exactly in vacuum and are given by

$$\begin{aligned} G_\psi(\omega,\vec{q}) &= \frac{1}{i\omega+\epsilon_{\vec{q}}} \qquad \epsilon_{\vec{q}} = \frac{\vec{q}^2}{2m} \\ G_\phi(\omega,\vec{q}) &= \frac{(\frac{4\pi}{m})^{\frac{d}{2}}}{\Gamma(1-\frac{d}{2})}\frac{2}{(i\omega+\frac{\epsilon_{\vec{q}}}{2})^{\frac{d}{2}-1}}. \end{aligned} \tag{7.4.8}$$

While the microscopic actions (7.4.2) and (7.4.7) look very similar, the QFTs defined by them are rather different. This is due to the different statistics of atoms in Eqs. (7.4.2) and (7.4.7). Nevertheless, the one- and two-body sectors[6] of the bosonic theory (7.4.7) have the same form (up to a simple multiplicative factors) as the one- and two-body sectors of the fermionic theory [203, 204] and respect the non-relativistic Schrödinger spacetime symmetry. In the three-body sector the bosonic theory (7.4.7) exhibits the Efimov effect [205], i.e. the non-relativistic conformal anomaly, while there is no Efimov effect for the two-component fermions.

In this subsection we will calculate the specific 3-point function[7] $\langle\psi(\bar{x}_1)\psi(\bar{x}_2)\phi^*(\bar{x}_3)\rangle$

[6] We define a n-body sector as a set of 2n-point Greens' functions written in terms of elementary atoms. In this sense $\langle\phi^*\phi\rangle$ belongs to the two-body sector because $\phi\sim\psi\psi$ is composed of two atoms.

[7] $\bar{x}_i = (t_i,\vec{x}_i)$ in accordance with our notation.

for bosons at unitarity[8] defined by Eq. (7.4.7), demonstrating the consistency with the non-relativistic conformal form (7.1.2) and determining the scaling function $\Psi(y)$. The calculation of the 3-point function can be conveniently done in the position space, hence first we rewrite the propagators (7.4.8) in the position representation (for details see Appendix C)

$$\begin{aligned} G_\psi(t,\vec{x}) &= \int \frac{d\omega}{2\pi}\frac{d^dq}{(2\pi)^d}\frac{1}{i\omega+\epsilon_{\vec{q}}}e^{i(\omega t-\vec{q}\cdot\vec{x})} = C_\psi\theta(t)t^{-\frac{d}{2}}\exp\left(-\frac{m}{2}\frac{\vec{x}^2}{t}\right), \\ G_\phi(t,\vec{x}) &= \frac{(\frac{4\pi}{m})^{\frac{d}{2}}}{\Gamma(1-\frac{d}{2})}\int\frac{d\omega}{2\pi}\frac{d^dq}{(2\pi)^d}\frac{2}{(i\omega+\frac{\epsilon_{\vec{q}}}{2})^{\frac{d}{2}-1}}e^{i(\omega t-\vec{q}\cdot\vec{x})} = C_\phi\theta(t)t^{-2}\exp\left(-m\frac{\vec{x}^2}{t}\right) \end{aligned} \tag{7.4.9}$$

where $C_\psi = \left(\frac{m}{2\pi}\right)^{\frac{d}{2}}$ and $C_\phi = (4)^{\frac{d}{2}}\frac{(d-2)\sin\left(\frac{\pi}{2}d\right)}{\pi}$. The last equation is in agreement with Eq. (7.1.1) after the identification $M_\psi = m$ and $M_\phi = 2m$. The unitarity scaling dimensions of ψ and ϕ can be easily read off from Eq. (7.4.9): $\Delta_\psi = \frac{d}{2}$ and $\Delta_\phi = 2$.

Now we are ready to calculate the 3-point function $\langle\psi(\bar{x}_1)\psi(\bar{x}_2)\phi^*(\bar{x}_3)\rangle$ which corresponds to scattering of two atoms ψ into a diatom ϕ. The non-relativistic Bargmann superselection rule for masses is satisfied $m+m-2m=0$ and hence the 3-point function is non-trivial. There are two important observations which allow us to calculate the full 3-point function

- There is no condensate in vacuum $\langle\psi\rangle = 0$, $\langle\phi\rangle = 0$. This implies that the full 3-point function is given by the connected part only.

- The Yukawa vertex is not renormalized in the non-relativistic vacuum [203, 204]. Hence only one Feynman diagram contributes to the full 3-point function (Fig. 7.5). The specific 3-point correlator is completely determined by the full Euclidean propagators (7.4.8) of atoms and diatoms, i.e. by the scaling dimensions of the fields.

From translation invariance the 3-point function depends only on the distances $\bar{x}_1-\bar{x}_3$, $\bar{x}_2-\bar{x}_3$ and $\bar{x}_2-\bar{x}_1$. Setting $\bar{x}_3 = (t_3,\vec{x}_3) = 0$ we obtain

$$\begin{aligned} G_3(\bar{x}_1,\bar{x}_2) &= \int d\bar{x}G_\phi(\bar{x})G_\psi(\bar{x}_1-\bar{x})G_\psi(\bar{x}_2-\bar{x}) = \\ &= C_\psi^2C_\phi\int d^dx\int dt\theta(t)\theta(t_1-t)\theta(t_2-t)t^{-2}(t_1-t)^{-\frac{d}{2}}(t_2-t)^{-\frac{d}{2}}\times \\ &\quad\times\exp\left[-\frac{m}{2}\left(\frac{2\vec{x}^2}{t}+\frac{(\vec{x}_1-\vec{x})^2}{(t_1-t)}+\frac{(\vec{x}_2-\vec{x})^2}{(t_2-t)}\right)\right]. \end{aligned} \tag{7.4.10}$$

[8]This specific 3-point correlator belongs to the two-body sector because it "consists" of four elementary fields and hence must be consistent with the non-relativistic conformal form (7.1.2). The 3-point correlator $\langle\psi_1(\bar{x}_1)\psi_2(\bar{x}_2)\phi^*(\bar{x}_3)\rangle$ for the fermionic theory (7.4.2) can be calculated along the same lines as the bosonic 3-point correlator [203, 204].

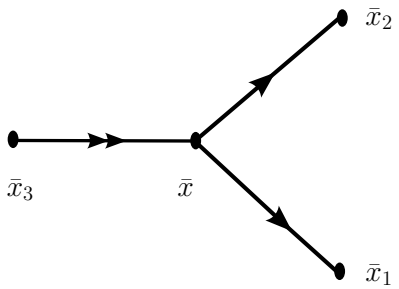

Figure 7.5: A Feynman diagram which gives the 3-point function for atoms at unitarity. The lines with a single arrow denote the exact atom propagator G_ψ, while the line with two arrows represents the fully renormalized diatom propagator G_ϕ.

The product of three θ functions in Eq. (7.4.10) is non-vanishing only if $t_1 > 0$ and $t_2 > 0$. This is in agreement with the causal factor $\theta(t_1 - t_3)\theta(t_2 - t_3)$ in Eq. (7.1.2). The product $\theta(t)\theta(t_1-t)\theta(t_2-t)$ in Eq. (7.4.10) restricts the time integration domain to $t \in (0, \min(t_1, t_2))$. Without loss of generality we take $t_1 > t_2$ yielding $t \in (0, t_2)$ in Eq. (7.4.10).

We first perform the Gaussian spatial integration in d dimensions

$$G_3(\bar{x}_1, \bar{x}_2) = \left(\frac{2\pi}{m}\right)^{\frac{d}{2}} C_\psi^2 C_\phi \theta(t_1)\theta(t_2) \int_0^{t_2} dt \tau^{\frac{d}{2}} t^{-2} (t_1 - t)^{-\frac{d}{2}} (t_2 - t)^{-\frac{d}{2}} \times \\ \times \exp\left[\frac{m}{2}\left(\tau\left[\frac{\vec{x}_1}{t_1 - t} + \frac{\vec{x}_2}{t_2 - t}\right]^2 - \frac{\vec{x}_1^2}{t_1 - t} - \frac{\vec{x}_2^2}{t_2 - t}\right)\right], \tag{7.4.11}$$

where we introduced $\tau = \left(\frac{2}{t} + \frac{1}{t_1 - t} + \frac{1}{t_2 - t}\right)^{-1} = \frac{t(t_1-t)(t_2-t)}{2t_1 t_2 - t(t_1+t_2)}$.

At this point it is convenient to perform a substitution $t \to z = \frac{t(t_2-t_1)}{t(t_1+t_2)-2t_1t_2}$. The new dimensionless variable z ranges in the interval $z \in (0, 1)$. The argument of the exponential in (7.4.11) can now be conveniently rewritten as

$$-\frac{m}{2}\frac{\vec{x}_1^2}{t_1} - \frac{m}{2}\frac{\vec{x}_2^2}{t_2} - \underbrace{\frac{m}{2}\frac{(\vec{x}_1 t_2 - \vec{x}_2 t_1)^2}{t_1 t_2 (t_1 - t_2)}}_{y} z. \tag{7.4.12}$$

Due to our assumption $t_1 > t_2$, a new variable y is non-negative $y \geq 0$.

The final integration can now be done straightforwardly with the result

$$G_3(\bar{x}_1, \bar{x}_2) = \frac{\theta(t_1)\theta(t_2)}{t_1 t_2 (t_1 - t_2)^{\frac{d}{2}-1}} \exp\left(-\frac{m}{2}\frac{\vec{x}_1^2}{t_1} - \frac{m}{2}\frac{\vec{x}_2^2}{t_2}\right) \underbrace{\left(\frac{2\pi}{m}\right)^{\frac{d}{2}} \frac{C_\psi^2 C_\phi}{2} \int_0^1 dz z^{\frac{d}{2}-2} \exp(-yz)}_{\Psi(y)}. \tag{7.4.13}$$

After recalling that in our case $\Delta_{12,3} = d - 2$ and $\Delta_{13,2} = \Delta_{23,1} = 2$, we observe that the final formula agrees with the Henkel's prediction (7.1.2) after recovering $\bar{x}_3$ coordinates: $\bar{x}_1 \to \bar{x}_1 - \bar{x}_3$ and $\bar{x}_2 \to \bar{x}_2 - \bar{x}_3$.

We are now in position to determine the non-universal scaling function $\Psi(y)$ for $y \geq 0$

$$\begin{aligned}\Psi(y) &= \left(\frac{2\pi}{m}\right)^{\frac{d}{2}} \frac{C_\psi^2 C_\phi}{2} \int_0^1 dz z^{\frac{d}{2}-2} \exp(-yz) = \\ &= \left(\frac{2\pi}{m}\right)^{\frac{d}{2}} \frac{C_\psi^2 C_\phi}{2} y^{-\frac{d}{2}+1} \gamma(\frac{d}{2}-1, y) \quad ,\end{aligned} \tag{7.4.14}$$

where the second line is valid for $d > 2$ and a lower incomplete gamma function $\gamma(n, y)$ is defined by

$$\gamma(n, y) = \int_0^y t^{n-1} e^{-t} dt \quad . \tag{7.4.15}$$

We remark that it is possible to generalize the theory (7.4.1) to a model with N fermion flavors [203, 206]:

$$S_E^N[\psi] = \int dt \int d^d x \sum_{\alpha=1}^{N} \sum_{i=1}^{2} \psi_{i\alpha}^*(\partial_t - \frac{\Delta}{2m} - \mu)\psi_{i\alpha} - \frac{c_0}{N} \sum_{\alpha,\beta=1}^{N} \psi_{1\alpha}^* \psi_{2\alpha}^* \psi_{2\beta} \psi_{1\beta}. \tag{7.4.16}$$

For $N = 1$ one recovers the original (7.4.1) theory. The theory is invariant under $U(1) \times Sp(2N)$ internal group and admits a sensible $1/N$ expansion. The calculation of the 3-point function $G_3^N = \langle \psi_{1\alpha}(\bar{x}_1)\psi_{2\alpha}(\bar{x}_2)\phi^*(\bar{x}_3)\rangle$ can be done straightforwardly with the result $G_3^N = N G_3^{N=1}$.

7.4.2 3-point function from non-relativistic holography

According to Eq. (7.2.16) the 3-point correlator $G_3 = \langle \phi_1(t_1, \vec{x}_1)\phi_2(t_2, \vec{x}_2)\phi_3(t_3, \vec{x}_3)\rangle_{\text{Sch}}^{(\text{tree level})}$ in the non-relativistic holography is given by

$$G_3 = \int d\xi_1\, d\xi_2\, d\xi_3\, e^{-i(M_1\xi_1 + M_2\xi_2 + M_3\xi_3)} \langle \phi_1(X_1)\phi_2(X_2)\phi_3(X_3)\rangle_{\text{AdS}}^{(\text{tree level})}. \tag{7.4.17}$$

When ∂_ξ is not compact, the conformal 3-point function in Euclidean space is well-known from the relativistic AdS/CFT [201, 200, 207]

$$\langle \phi_1(X_1)\phi_2(X_2)\phi_3(X_3)\rangle_{\text{AdS}}^{(\text{tree level})} = \frac{C_{123}}{|X_1 - X_2|^{\Delta_{12,3}} |X_2 - X_3|^{\Delta_{23,1}} |X_3 - X_1|^{\Delta_{31,2}}}, \tag{7.4.18}$$

here $X = (t, \vec{x}, \xi)$, $|X|^2 = \vec{x}^2 - 2it\xi$ and $\Delta_{ij,k} = \Delta_i + \Delta_j - \Delta_k$. C_{123} is a position-independent coefficient which is a function of the scaling dimensions Δ_i, given under canonical normalization by

$$C_{123} = -\frac{\Gamma(\frac{\Delta_{12,3}}{2})\Gamma(\frac{\Delta_{13,2}}{2})\Gamma(\frac{\Delta_{23,1}}{2})\Gamma(\frac{\Delta_1+\Delta_2+\Delta_3-4}{2})}{2\pi^4 \Gamma(\Delta_1 - 2)\Gamma(\Delta_2 - 2)\Gamma(\Delta_3 - 2)} \quad . \tag{7.4.19}$$

It is convenient to introduce a center-of-mass and relative coordinates

$$\eta = \xi_1 + \xi_2 + \xi_3 \qquad \xi = \xi_1 - \xi_3 \qquad \xi' = \xi_2 - \xi_3. \tag{7.4.20}$$

The integration over the center-of-mass coordinate η produces a $\delta(M_1+M_2+M_3)$ which is a Bargmann superselection rule:

$$G_3 = 2\pi\delta(M_1+M_2+M_3)\int d\xi\, d\xi'\, e^{-i(M_1\xi+M_2\xi')}\langle\phi_1(X_1)\phi_2(X_2)\phi_3(X_3)\rangle_{\rm AdS}^{(\text{tree level})}. \quad (7.4.21)$$

Now Eq. (7.4.18) can be substituted into Eq. (7.4.21) and remaining integrals in Eq. (7.4.21) were evaluated in the Appendix of [151]

$$G_3 = \delta(M_1+M_2+M_3)\theta(t_1-t_3)\theta(t_2-t_3)(t_1-t_3)^{-\Delta_{13,2}/2}(t_2-t_3)^{-\Delta_{23,1}/2}(t_1-t_2)^{-\Delta_{12,3}/2}\times$$
$$\times\exp\left[-\frac{M_1}{2}\frac{(\vec{x}_1-\vec{x}_3)^2}{t_1-t_3}-\frac{M_2}{2}\frac{(\vec{x}_2-\vec{x}_3)^2}{t_2-t_3}\right]\Psi\left(\frac{[(\vec{x}_1-\vec{x}_3)(t_2-t_3)-(\vec{x}_2-\vec{x}_3)(t_1-t_3)]^2}{(t_1-t_2)(t_1-t_3)(t_2-t_3)}\right) \quad (7.4.22)$$

The scaling function $\Psi(y)$, which is not directly fixed by the Schrödinger symmetry, has the integral representation [151]:

$$\Psi(y) = \tilde{C}_{123}\int_{\mathbb{R}+i\epsilon} dv \int_{\mathbb{R}+i\epsilon'} dv'\, e^{-iM_1v-iM_2v'}(v-v'+iy)^{-\Delta_{12,3}/2}(v')^{-\Delta_{23,1}/2}v^{-\Delta_{13,2}/2}, \quad (7.4.23)$$

where $\tilde{C}_{123} = 2\pi C_{123}(-2i)^{-\frac{1}{2}(\Delta_1+\Delta_2+\Delta_3)}$ and the last expression is valid for $y\in\mathbb{R}$. See appendix D for the case of a compact ∂_ξ-direction.

7.4.3 Comparison of the scaling functions

Now we can compare the non-universal scaling functions $\Psi(y)$ of cold atoms and non-relativistic holography. To do so we first introduce a related function $\Phi(y)$

$$G_3 = \delta(M_1+M_2+M_3)\theta(t_1-t_3)\theta(t_2-t_3)(t_1-t_3)^{-\Delta_{13,2}/2}(t_2-t_3)^{-\Delta_{23,1}/2}|t_1-t_2|^{-\Delta_{12,3}/2}\times$$
$$\times\exp\left[-\frac{M_1}{2}\frac{(\vec{x}_1-\vec{x}_3)^2}{t_1-t_3}-\frac{M_2}{2}\frac{(\vec{x}_2-\vec{x}_3)^2}{t_2-t_3}\right]\Phi\left(\frac{[(\vec{x}_1-\vec{x}_3)(t_2-t_3)-(\vec{x}_2-\vec{x}_3)(t_1-t_3)]^2}{(t_1-t_2)(t_1-t_3)(t_2-t_3)}\right) \quad (7.4.24)$$

In comparison with (7.1.2) we changed $(t_1-t_2)\to|t_1-t_2|$. This implies $\Phi(y)=\Psi(y)$ for $y\geq 0$ and $\Phi(y)=\Phi(-y)$ because the full 3-point function is symmetric under $t_1\leftrightarrow t_2$. In Euclidean QFT the scaling function $\Phi(y)$ must be real for $y\in\mathbb{R}$.

For cold atoms the analytic expression for the scaling function was found in Eq. (7.4.14). To achieve a simple comparison with the holographic calculation we normalize $\Phi(y)$ such that $\Phi(y=0)=1$. We plot the normalized scaling function for spatial dimensions $d=3,4,5$ taking $m=1$ in Fig. 7.6.

In the holographic case the scaling function has the integral representation (7.4.23). To perform a direct comparison with cold atoms we evaluate Eq. (7.4.23) for $\Delta_1=\Delta_2=\frac{d}{2}$,

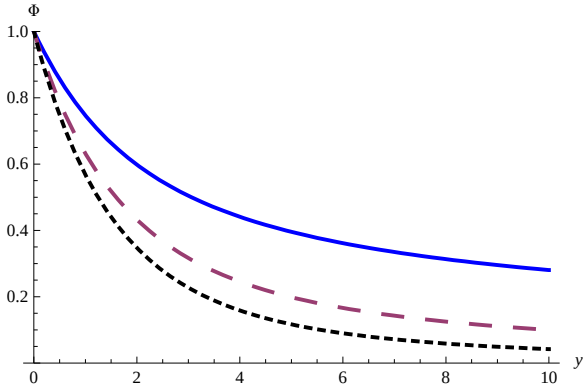

Figure 7.6: The normalized scaling function $\Phi(y)$ for various dimensions $d = 3$ (solid), $d = 4$ (dashed) and $d = 5$ (dotted).

$\Delta_3 = 2$ and $M_1 = M_2 = 1$. For general even dimension $d = 2n$ the two integrals in Eq. (7.4.23) can be done analytically using the residue theorem. Employing a useful relation

$$\gamma(n, y) = (n-1)! + \frac{\partial^{n-1}}{\partial^{n-1} s}\left(\frac{e^{ys}}{s}\right)\Big|_{s=-1} \qquad n \in \mathbb{N}, \tag{7.4.25}$$

which directly follows from the definition (7.4.15) we arrive at

$$\Phi(y) = N_d y^{-\frac{d}{2}+1}\gamma(\frac{d}{2} - 1, y), \tag{7.4.26}$$

where N_d is a $y-$independent numerical factor. This agrees with the cold atoms expression (7.4.14) up to normalization. In the case of odd dimensions $d = 2n + 1$ the integral (7.4.23) has a branch cut and one has to use the integral representation of the incomplete gamma function [208]

$$\gamma(\alpha, x) = \Gamma(x) - \frac{e^{-x}x^{\alpha}}{\Gamma(1-\alpha)}\int_0^{\infty}\frac{e^{-t}t^{-\alpha}}{x+t}dt \quad , \tag{7.4.27}$$

arriving at the same result (7.4.26). Thus for even and odd dimensions the scaling function $\Phi(y)$, calculated from non-relativistic holography, agrees with $\Phi(y)$ for cold atoms. In the case of a compact ∂_ξ one also finds agreement, see Appendix D.

At this point it is important to stress that, although the original motivation for the non-relativistic holography were fermions at unitarity, there are various thermodynamic evidence by now [178, 209] that the holography, which defines some Schrödinger invariant field theory, is not exactly dual to the theory of unitary fermions. It is interesting that our vacuum calculation of the 3-point scaling function $\Phi(y)$, which is not fixed by the Schrödinger symmetry and is thus non-universal, gives the same result for cold atoms and holography. In this respect it would be interesting to study and compare the higher point functions in both theories.

7.4.4 Physical meaning of the scaling function

The general form of the non-relativistic 3-point function (7.4.24) is quite complex and in order to gain some understanding of the physical information stored in it (and especially in the scaling function $\Phi(y)$) we must take a specific kinematic configuration of $\bar{x}_1$, $\bar{x}_2$ and $\bar{x}_3$. First, by translational invariance we can take $\bar{x}_3 = (t_3, \vec{x}_3) = 0$ and the general form (7.4.24) simplifies to

$$G_3(\bar{x}_1, \bar{x}_2, \bar{x}_3 = 0) = \delta(M_1 + M_2 + M_3)\theta(t_1)\theta(t_2)(t_1)^{-\Delta_{13,2}/2}(t_2)^{-\Delta_{23,1}/2}|t_1 - t_2|^{-\Delta_{12,3}/2}\times \\ \times \exp\left[-\frac{M_1}{2}\frac{\vec{x}_1^2}{t_1} - \frac{M_2}{2}\frac{\vec{x}_2^2}{t_2}\right]\Phi(y) \quad , \tag{7.4.28}$$

where the scaling argument y is given by

$$y = \frac{[\vec{x}_1 t_2 - \vec{x}_2 t_1]^2}{t_1 t_2 (t_1 - t_2)} = \frac{1}{2}\left(\frac{(\vec{x}_1 - \vec{x}_2)^2}{t_1 - t_2} + \frac{\vec{x}_2^2}{t_2} - \frac{\vec{x}_1^2}{t_1}\right) \quad . \tag{7.4.29}$$

In order to simplify things even further we assume that $\vec{x}_1$ and $\vec{x}_2$ lay on the same ray, which starts at the origin[9], and that $\bar{x}_2$ scales non-relativistically, i.e. $\bar{x}_2 = (l^2, \vec{l})$, where l is some length scale assume to be $O(1)$.

In general, the non-relativistic scaling of time and space separation is substantial in the analysis of the structure of the non-relativistic Greens' functions. For example, the generic fall-off of the 2-point function (7.3.4) as $\bar{x}_1 - \bar{x}_2 \to \infty$ is exponential. However, if one takes $(\vec{x}_1 - \vec{x}_2)^2 \sim (t_1 - t_2)$, i.e. applies the non-relativistic scaling, the propagator (7.3.4) decays by a power-law.

We choose the point $\bar{x}_1$ to be close to the point $\bar{x}_2$, i.e. $\bar{x}_1 = (l^2(1+\epsilon_t), \vec{l}(1+\epsilon_x))$, where $\epsilon_t, \epsilon_x > 0$ and $\epsilon_t, \epsilon_x \ll 1$. Both (7.4.28) and (7.4.29) can be expanded in the small quantities ϵ_t, ϵ_x

$$\begin{aligned} G_3(l, \epsilon_t, \epsilon_x) &\sim l^{-\sum \Delta_i}\epsilon_t^{-\frac{\Delta_{12,3}}{2}}\Phi(y)[1 + O(\epsilon_x, \epsilon_t)] \\ y &= \frac{1}{2}\frac{\epsilon_x^2}{\epsilon_t} + O(\epsilon_x, \epsilon_t). \end{aligned} \tag{7.4.30}$$

From the last expression it is clear that the scaling function $\Phi(y)$ determines the singular behavior of the 3-point function G_3 as $\bar{x}_1 \to \bar{x}_2$.

In order to illustrate this fact consider our special case with $\Phi(y)$ given by (7.4.26), $M_1 = M_2 = 1$ and $\Delta_{12,3} = d - 2$

$$G_3(l, \epsilon_t, \epsilon_x) \sim l^{-d-2}\epsilon_x^{-d+2}\gamma(\frac{d}{2} - 1, \frac{1}{2}\frac{\epsilon_x^2}{\epsilon_t}). \tag{7.4.31}$$

We can distinguish two limits:

[9] This choice makes the problem essentially one-dimensional.

- $\epsilon_t \gg \epsilon_x$, i.e. $\bar{x}_1$ approaches $\bar{x}_2$ much faster in the spatial than in the temporal direction. Using the limit

$$\lim_{y\to 0} \gamma(a,y) = a^{-1} y^a \tag{7.4.32}$$

we arrive at

$$G_3(l,\epsilon_t,\epsilon_x) \sim l^{-d-2} \epsilon_t^{1-\frac{d}{2}}. \tag{7.4.33}$$

- $\epsilon_t \ll \epsilon_x$, i.e. $\bar{x}_1$ approaches $\bar{x}_2$ much faster in the temporal than in the spatial direction. In this case

$$\lim_{y\to \infty} \gamma(a,y) = \Gamma(a) \tag{7.4.34}$$

and we end up with

$$G_3(l,\epsilon_t,\epsilon_x) \sim l^{-d-2} \epsilon_x^{2-d}. \tag{7.4.35}$$

In both limiting cases the 3-point function diverges for $d > 2$ as $\bar{x}_1 \to \bar{x}_2$ and the limits of the scaling function $\Phi(y)$ determine the concrete singularity behavior.

The last expression, (7.4.35), is actually in agreement with the usual requirement for a wave function to describe fermions at unitarity [149]: the wave-function of N spin-up and M spin-down fermions $\Psi(\vec{x}_1,\ldots,\vec{x}_N;\vec{y}_1,\ldots,\vec{y}_M)$ behaves like $|\vec{x}_i - \vec{y}_j|^{2-d}$ when $|\vec{x}_i - \vec{y}_j| \to 0$ for any pair of fermions with opposite spins i, j. This simply follows from the scaling dimension of the operators at unitarity. So that we can take these results as reassuring of being at the unitary regime with which the holographic computation agrees.

7.5 Conclusions

In this chapter we have explored the computation of the n-point scalar correlation functions in the framework of non-relativistic holography in the vacuum state, i.e. at zero temperature and density, of the theory defined as the holographic dual of the Schrödinger metric with $z = 2$ [160, 161]. Following the standard holographic dictionary the correlators can be expressed in terms of Witten diagrams. At tree level we have demonstrated how the computation in Sch_{d+3} can be done equivalently from the correlation functions of pure AdS after a projection of the non-relativistic mass momentum in every insertion at the boundary in the light-cone frame.

$$\langle \phi_1(\bar{x}_1)\ldots\phi_n(\bar{x}_n)\rangle_{\mathrm{Sch}}^{(\text{tree level})} = \int \prod_{k=1}^{n} d\xi_k \, e^{-i\sum_{j=1}^{n}(M_j\xi_j)} \langle \phi_1(\bar{x}_1,\xi_1)\ldots\phi_n(\bar{x}_n,\xi_n)\rangle_{\mathrm{AdS}}^{(\text{tree level})} \tag{7.5.1}$$

This is a useful trick since AdS amplitudes have already been well studied in the literature. The mapping works irrespectively of whether we have a compact or non-compact ∂_ξ-direction.

It shows that all observables at tree level are going to agree in the Sch_{d+3} construction and the pure AdS construction in light-cone coordinates with definite ∂_ξ-momentum, as was loosely noted in [210, 22]. This tree-level mapping can be understood from the QFT side to be in the same footing as the agreement of the correlation functions at the planar level between a non-commutative and commutative QFT, since, at least for $d = 2$, one can argue [169] that the Schrödinger background is dual to a non-commutative version of $\mathcal{N} = 4$ SYM, the dual of AdS. At the loop level, or what is the same $1/N$ corrections, we do not have this mapping anymore. In this case we have no option but to perform all the computations directly in the Schrödinger background, which is the only one that has the correct non-relativistic causal structure [164]. At the loop level we also see explicitly the need for regularization of the theory when the ∂_ξ-direction is compact. In this case, we have a null-compact direction and the zero modes along that direction cause the typical divergences one finds in DLCQ theories [165]. One way to regularize it is by the introduction of a non-zero chemical potential that makes the circle to be space-like. When the ∂_ξ-direction is non-compact this problem is not present.

We have tested the tree-level mapping to AdS by the computation of the 2-point scalar function finding agreement with the expected result completely fixed by symmetry considerations, for both compact and non-compact ∂_ξ-direction.

We have also computed the holographic 3-point scalar function for both compact and non-compact ∂_ξ-direction. The result respects the form dictated by the Schrödinger symmetry although it is not completely fixed by it. There is freedom for an unknown scaling function. Remarkably, the form of this function coincides with the result coming from the theory of cold atom at unitarity, that we have also computed. Upon closer examination, this function governs the singular behaviour when two operators approach. And it reproduces, since it is the same as the theory of cold atoms at unitarity, the expected singular behaviour in the unitary regime. We see this as a non-trivial check that the holographic theory really contains a conformal non-relativistic theory in the unitary regime.

Our computations at tree level worked well in both cases where ξ is periodic or not. This is understandable: the compactification procedure does not break any spacetime symmetry and the Bargmann superselection rule, which is characteristic for the non-relativistic systems, is valid in both cases. On the one hand, the compactification of ξ leads naturally to the discreteness of the mass spectrum of a simple one-species system. On the other hand, working with the non-compact ξ allows to describe the systems with more than one species of particles, that is evidently of great interest in the cold atoms physics. This last scenario should not be rejected. At tree level with a non-compact ξ, one can consistently restrict by hand the different values of the masses out of the possible continuum and obtain physical

sound answers by virtue of the Bargmann superselection rule.

Our work here has just scratched the surface of many more interesting questions awaiting to be addressed. Among them we can consider:

- It would be interesting to study the higher-point (especially 4-point) correlation functions in the framework of the non-relativistic AdS/CFT. Although the general functional constraints, implied by the Schrödinger symmetry, are not known for the higher-point function so far, it seems straightforward to apply our prescription to the 4-point scalar correlator already known in AdS. In fact, later in [211] the functional dependence of 4-point functions was deduced and seen to match the holographic non-relativistic construction, but the part not fixed by the symmetry was not computed.

- Recently the non-relativistic AdS/CFT was extended to fermionic fields [212]. Since the original motivation of the non-relativistic holography were two-component fermions at unitarity, it is tempting to study general n-point functions for holographic fermions. Our expectations are that one should be able to demonstrate the mapping of the computations of the fermionic correlation functions in Sch to AdS at tree level. Actually the case of 2-point functions was explicitly shown to work this way in [212].

- Another interesting question would be the computation of the correlation functions at finite chemical potential in the background (7.2.25).

- One should also try to address the working of the regularization at the loop-level in the compact ξ case.

We leave these questions for future study.

Chapter 8

Ideal gas matching for thermal Galilean holography

8.1 Introduction

In this chapter we exhibit a nonrelativistic ideal gas with a Kaluza–Klein tower of species, featuring a singular behavior of thermodynamic functions at zero chemical potential. In this way, we provide a qualitative match to the thermodynamics of recently found black holes in backgrounds with asymptotic nonrelativistic conformal symmetry.

As we have seen a generalization of the AdS/CFT program [1] to the case of nonrelativistic conformal field theories [156] was proposed in [3, 4]. The basic idea is the embedding of the Schrödinger group [213] in d spatial dimensions, $\mathrm{Sch}(d)$, into the relativistic conformal group in $d+2$ spacetime dimensions $\mathrm{SO}(2, d+2)$. Under this embedding, the Schrödinger group arises from a fixed light-like momentum projection $P^+ = NM$, where N is a positive integer interpreted as particle number, and M is the nonrelativistic mass.

Geometrically, this projection can be achieved by a formal compactification of the $d+2$ dimensional conformal field theory on a light-like circle of radius $1/M$, and a similar light-like compactification of the AdS_{d+3} dual of the parent CFT, plus a deformation, yields the required nonrelativistic bulk description. This results in the following family of metrics

$$ds^2 = -2\gamma^2 \frac{r^{2z}}{R^{2z}} dt^2 + \frac{r^2}{R^2}(-2dt\, d\xi + d\vec{x}^{\,2}) + \frac{R^2}{r^2} dr^2 \,, \tag{8.1.1}$$

where z is a real parameter controlling the relative scaling dimensions of time and spatial coordinates. The strict case of Schrödinger symmetry is $z = 2$, although other values of z also yield interesting systems with Galilean scale invariance. The light-like coordinate ξ is

compactified on a circle of size $1/M$ and the real parameter γ^2 is related to the chemical potential of the $U(1)$ isometry along the light-like circle once the system is put at finite temperature. In particular, black hole solutions with asymptotic metric given by the $z = 2$ case of (8.1.1) have been constructed and shown to have a peculiar thermodynamical scaling (cf. [214, 215, 216, 176]).[1] The entropy reads

$$S(T,\mu) \propto N_{\text{eff}}\,(MT)^{\,d/2}\,\left(\frac{T}{|\mu|}\right)^{\frac{d+2}{2}}\,, \tag{8.1.2}$$

with a distinct singularity in the limit of vanishing ratio $|\mu|/T$. In writing (8.1.2) we have restored the dimensional mass parameter M and the effective number of degrees of freedom $N_{\text{eff}} \sim R^{d+1}/G_{d+3}$, coming from the overall power of the inverse Newton's constant in the effective Euclidean action. Other black hole metrics corresponding to hot spacetimes with $z = 1$ asymptotics in (8.1.1) have been constructed as Penrose limits of AdS–Kerr black holes [215, 194], yielding a high-temperature limit with the form

$$S(T,\mu) \propto N_{\text{eff}}\,\left(\frac{T}{\Omega}\right)^{d}\,\left(\frac{T}{|\mu|}\right)\,, \tag{8.1.3}$$

where again we have restored the harmonic trapping frequency Ω, implicit in the Penrose limits of ref. [215, 194]. The singular behavior of (8.1.2) and (8.1.3) at small chemical potential is quite puzzling and certainly begs for an explanation.

In this chapter we find an ideal gas model which precisely matches the laws (8.1.2) and (8.1.3), by simply considering a nonrelativistic Kaluza–Klein tower of charged 'species'. These species arise naturally from a light-like compactification of a *relativistic* theory with N_{eff} degrees of freedom in $d + 2$ dimensions. Furthermore, we consider thermal ensembles on the metrics (8.1.1), which can be considered as Hawking radiation corrections to the thermodynamics of black holes, and find consistent scaling laws once the appropriate UV/IR rules are taken into account.

8.2 The nonrelativistic Kaluza–Klein gas

Let us consider an ideal gas of nonrelativistic particles with N_{eff} degenerate internal degrees of freedom, and a conserved charge

$$N = \sum_{n>0} n\,N_n\,, \tag{8.2.1}$$

[1] See also [217] for more on Schrödinger black holes.

where n is a further species index and N_n is the particle number of type n. Single particles of type n contribute n units to the conserved charge N, and have mass $M_n = nM$.

This system can be obtained from a light-like compactification (DLCQ) of a $d+2$ dimensional system of free massless relativistic particles with N_{eff} degrees of freedom (cf. for example [218]), i.e. we consider these fields on the metric

$$ds^2 = -2\,dt\,d\xi + d\vec{x}^{\,2}\ , \tag{8.2.2}$$

with $\xi \equiv \xi + 2\pi/M$. The conserved charge N is defined as the quantized momentum in the ξ direction, and n appears as the Fourier index in the decomposition

$$\phi^a(\xi, t, \vec{x}\,) \propto \sum_{n>0} \phi^a_n(t, \vec{x}\,)\, e^{-in\xi/M} + \text{h.c.}\ ,$$

where a is the internal index running over N_{eff} values. Notice that we have removed the zero mode $n = 0$, which produces notorious problems in DLCQ. In the following, we will refer to each ϕ^a_n field labeled by the index n as the n-th KK (Kaluza–Klein) species.

We are interested in the grand canonical free energy, $F(\beta, \mu)$, or rather its dimensionless version $I(\beta, \mu) = \beta F(\beta, \mu)$, with $\beta = 1/T$ the inverse temperature and μ the chemical potential coupling to the total conserved charge $N = \sum_n nN_n$,

$$I(\beta, \mu) = \beta F(\beta, \mu) = -\log \text{Tr}\, \exp\left(-\beta H + \beta\mu N\right)\ . \tag{8.2.3}$$

8.2.1 Ideal gas in a box

In a reflecting box of volume $V_d = L^d$, each KK species has a single-particle energy spectrum $E_n(\vec{p}\,) = \vec{p}^{\,2}/2M_n$, with $\vec{p} \in \frac{2\pi}{L}\mathbb{Z}^d$. The grand canonical free energy takes the form

$$I(\beta, \mu) = \beta F(\beta, \mu) = N_{\text{eff}} \sum_{n>0} \sum_{\vec{p}} (-1)^F \log\left[1 - (-1)^F e^{-\beta E_n(\vec{p}\,) + \beta\mu n}\right]\ , \tag{8.2.4}$$

where we have allowed for the case of a fermionic tower with $(-1)^F = -1$.

The density $\langle N\rangle / V_d = \rho$ is then given by

$$\rho = \sum_{n>0} n\,\rho_n = \sum_{n>0} n\,\frac{\langle N_n\rangle}{V_d} = -\frac{1}{\beta}\frac{\partial I}{\partial \mu}\ , \tag{8.2.5}$$

where the density per KK species is

$$\rho_n = \frac{N_{\text{eff}}}{V_d} \sum_{\vec{p}} \frac{1}{\exp\left[\beta(E_n(\vec{p}\,) - \mu n)\right] - (-1)^F}\ . \tag{8.2.6}$$

The partial thermodynamical functions at fixed n are defined for $\mu \leq 0$ in the bosonic case. In the fermionic case, the fixed-n functions are defined for any real μ, but the complete thermodynamical functions, such as the overall density ρ in (8.2.5) will diverge for $\mu > 0$ upon summation in n. For this reason, we shall restrict attention to the $\mu \leq 0$ region in both Fermi and Bose cases.

In the large volume limit at *fixed* $\beta\mu < 0$ we can replace the momentum sums by integrals through the standard prescription

$$\sum_{\vec{p}} \to V_d \int \frac{d^d p}{(2\pi)^d} \,, \tag{8.2.7}$$

to obtain the well known result for the partial free energy density, $f_n(\beta, \mu)$:

$$\beta\, f_n(\beta,\mu) = (-1)^F\, N_{\text{eff}} \left(\frac{M_n T}{2\pi}\right)^{d/2} \int \frac{d^d\vec{\ell}}{(2\pi)^{d/2}} \log\left[1 - (-1)^F \exp(-\tfrac{1}{2}\vec{\ell}^{\,2} + \beta\mu n)\right] \,. \tag{8.2.8}$$

On evaluating the sum over the KK species, we can distinguish two regimes. At $\beta\mu \ll -1$ we have the classical dilute gas limit, a Boltzmann gas with the KK tower dominated by the $n = 1$ term with exponential accuracy:

$$\beta f(\beta,\mu) \approx -N_{\text{eff}} \left(\frac{MT}{2\pi}\right)^{d/2} e^{-|\mu|/T} \,. \tag{8.2.9}$$

In the opposite regime, $\beta|\mu| \ll 1$, we may approximate the sum over n by an integral, obtaining

$$\beta f(\beta,\mu) \approx N_{\text{eff}}\,(-1)^F \left(\frac{MT}{2\pi}\right)^{d/2} \left(\frac{T}{|\mu|}\right)^{\frac{d+2}{2}} \int \frac{d^d\vec{\ell}}{(2\pi)^{d/2}} \int_0^\infty dx\, x^{\frac{d}{2}} \log\left[1 - (-1)^F e^{-x-\vec{\ell}^{\,2}/2}\right] \,. \tag{8.2.10}$$

We can further evaluate the integral by expanding the logarithm and integrating term by term to obtain the final result at $\beta|\mu| \ll 1$, in complete agreement with (8.1.2), up to numerical coefficients:

$$\beta f(\beta,\mu)_\pm \approx -N_{\text{eff}}\, C_\pm \left(\frac{MT}{2\pi}\right)^{\frac{d}{2}} \left(\frac{T}{|\mu|}\right)^{\frac{d+2}{2}} \,, \tag{8.2.11}$$

where $\pm = (-1)^F$ indicates the Bose or Fermi statistics and

$$C_\pm = \pm G_{\frac{d}{2}+2}(\pm 1) \,, \tag{8.2.12}$$

in terms of the function

$$G_\alpha(z) \equiv \sum_{k=1}^{\infty} \frac{z^k}{k^\alpha} \,, \tag{8.2.13}$$

with special values at $z = \pm 1$ given by Riemann's zeta function: $G_\alpha(1) = \zeta(\alpha)$, and $G_\alpha(-1) = \zeta(\alpha)(2^{1-\alpha} - 1)$. Thus, we find essentially the same result for Bose and Fermi KK towers, up to the global factor $(1 - 2^{-1-d/2})$.

These results are obtained under the assumption that the infinite volume limit is taken *before* the $\beta\mu \to 0$ limit. In the particular case of Bose gases, the phenomenon of Bose condensation takes place when the $V_d \to \infty$ limit is taken in conjunction with the $\beta\mu \to 0$ limit, in such a way that the particle density on the ground state is kept fixed.

Applying (8.2.7) to the partial densities we obtain

$$\rho_n = N_{\text{eff}} \left(\frac{M_n T}{2\pi} \right)^{d/2} G_{d/2}\left(z^n\right) \ , \tag{8.2.14}$$

where we have introduced the fugacity $z = \exp(\beta\mu)$. This expression has a finite limit as $z \to 1$, so that the temperature cannot be lowered below a critical value if the density is kept fixed. For temperatures below the critical one

$$T_c^{(n)} = \frac{2\pi}{M_n} \left(\frac{\rho_n}{\zeta(d/2)} \right)^{\frac{2}{d}} \ , \tag{8.2.15}$$

formula (8.2.14) applies only to the density in *excited* states, $\rho_n^{(e)}$, where $\rho_n = \rho_n^{(0)} + \rho_n^{(e)}$, with $\rho_n^{(0)}$ representing the ground state particle density of the n-th species. Hence, we have

$$\rho_n^{(e)} = \rho_n - \rho_n^{(0)} = \rho_n \left(\frac{T}{T_c^{(n)}} \right)^{\frac{d}{2}}$$

in the condensation regime, $T < T_c^{(n)}$, provided we can keep each partial density, ρ_n, fixed as an independent control parameter. Coming back to the grand-canonical formalism, this would entail introducing independent chemical potentials for each KK species.

Keeping a single chemical potential, dual to the total charge $N = \sum_n n N_n$, one finds for the analog of (8.2.14)

$$\rho = N_{\text{eff}} \left(\frac{MT}{2\pi} \right)^{d/2} \sum_{n=1}^{\infty} n^{d/2} \, G_{d/2}\left(z^n\right) \ . \tag{8.2.16}$$

Since the right hand side of this expression diverges as $z \to 1$, there is no lower bound on the temperature as we eliminate $\beta\mu$ in favor of ρ, and correspondingly there is no critical temperature analog to (8.2.15). A more explicit understanding is obtained if we regularize the KK tower to be finite, $n \leq n_\Lambda$. Denoting $\Sigma(n_\Lambda) = \sum_{n=1}^{n_\Lambda} n^{d/2}$, we have now Bose condensation below the critical temperature

$$T_c^{(\Lambda)} = \frac{2\pi}{M} \left(\frac{\rho}{\Sigma(n_\Lambda)\zeta(d/2)} \right)^{\frac{2}{d}} \ . \tag{8.2.17}$$

Since $\Sigma(n_\Lambda) \sim (n_\Lambda)^{1+d/2}$ at large n_Λ, the critical temperature approaches zero as the KK tower regulator is removed, $n_\Lambda \to \infty$. In hindsight, we can now understand the absence of a finite critical temperature for Bose condensation as a consequence of the spectrum having no gap at finite volume, since the nonrelativistic mass of the KK species grows without limit as $n \to \infty$.

8.2.2 Ideal gas in a harmonic trap

The ideal gas made of KK species can also be analyzed on a harmonic trap, rather than a sharp containment box. In this case, we have a single-particle Hamiltonian

$$H_n = -\frac{1}{2M_n}\vec{\partial}^{\,2} + \frac{1}{2}\, M_n \Omega^2 |\vec{x}|^{\,2} \tag{8.2.18}$$

for the n-th species. The single-particle spectrum is controlled by the trapping frequency, independently of the value of n:

$$E_n(\vec{n}\,) = \Omega \sum_{i=1}^{d} n_i \ , \tag{8.2.19}$$

where we have conventionally redefined the origin of energies to zero, by subtracting the ground state energy $E_{\rm vac} = (-1)^F \Omega d/2$. The resulting grand-canonical free energy reads

$$\beta F(\beta,\mu) = N_{\rm eff}\,(-1)^F \sum_{n=1}^{\infty} \sum_{\vec{n}\in\mathbb{Z}^d} \log\left[1-(-1)^F e^{-\beta\Omega\sum_i n_i - \beta|\mu|n}\right] \ . \tag{8.2.20}$$

From this expression it is already clear that $|\mu|$ plays the role of an effective trapping frequency in a extra dimension. We can thus distinguish a number of regimes depending on the relative value of the ratios $\beta\Omega$, $\beta|\mu|$, and $\Omega/|\mu|$.

For $\beta\mu \ll -1$ we have the dilute classical gas, dominated by a single species $n = 1$, up to corrections of relative order $\exp(-|\mu|/T)$. Hence, in this regime we obtain the standard results for an ideal gas in a harmonic trap.

For $\beta|\mu| \ll 1$ the whole tower contributes evenly, and we can approximate the sum over n by an integral. In the very high-temperature limit, $T \gg \Omega, |\mu|$, we can approximate the $\vec{n}$ sum by an integral as well, and we obtain

$$I(\beta,\mu) \approx -N_{\rm eff}\, D_\pm \left(\frac{T}{\Omega}\right)^d \left(\frac{T}{|\mu|}\right) \ , \tag{8.2.21}$$

where $\pm \sim (-1)^F$ refers again to the statistics and

$$D_\pm = \pm G_{d+2}(\pm 1) \ . \tag{8.2.22}$$

More explicitly, $G_{d+2} = \zeta(d+2)$, and $-G_{d+2}(-1) = \zeta(d+2)(1-1/2^{d+1})$. We see that the result (8.1.3) is also reproduced in all detail, up to the value of the numerical coefficients $D_\pm$.

In the case that the temperature is below the gap, $T \ll \Omega$, but still $T \gg |\mu|$, we have effectively a one-dimensional system, with

$$I(\beta,\mu) \approx -N_{\rm eff}\, 2^{-F}\zeta(2)\left(\frac{T}{|\mu|}\right)\exp(-\Omega/T)\ , \tag{8.2.23}$$

where $F = 0$ for Bose statistics and $F = 1$ for Fermi statistics, as usual.

8.3 Hawking radiation corrections

In this section we consider the thermal ensemble of radiation with $O(1)$ degrees of freedom, propagating on the metrics (8.1.1). By analogy with the similar situation in relativistic AdS/CFT examples, this would represent a piece of the $1/N_{\rm eff}$ corrections to the thermodynamic functions of the CFT (cf. [219]).

Following the analysis of ref. [22] (see also [210]), such radiation degrees of freedom have a single-particle Hamiltonian with a factorized 'center of mass' dynamics with effective mass $M_n = nM$, and an 'internal' holographic dynamics given by a particular case of conformal quantum mechanics [182]. For the $z = 1$ metric,

$$H_n^{(z=1)} = -\frac{1}{2Mn}\vec{\partial}^{\,2} + \gamma^2 Mn + \frac{1}{2Mn}\left(-\frac{d}{d\rho^2} + \frac{b}{\rho^2}\right)\ . \tag{8.3.1}$$

where $b = (d+1)(d+3)/4$ when the bulk relativistic mass of the radiation is taken to vanish. The additive shift $\gamma^2 Mn$ amounts to a corresponding shift of the chemical potential $\mu \to \mu + \gamma^2 M$. This suggests that turning on the deformation proportional to γ^2 in (8.1.1) is equivalent to switching on a chemical potential, a point already made in the analysis of black hole metrics in [214, 215]. Hence, we shall define the chemical potential after this shift is effectively subtracted, and consider a radiation free energy

$$\beta F(\beta,\mu)^{\rm rad} = I(\beta,\mu)^{\rm rad} \sim \sum_{n\geq 1}\sum_{\vec{p}} \log\left[1 - \exp\left(-\beta(E'_n + |\mu|n)\right)\right]\ , \tag{8.3.2}$$

where $E'_n = E_n - \gamma^2 Mn$. The sharpest statement can be made for the case of a harmonically trapped gas, for which we add a potential

$$V_{\rm trap} = \frac{1}{2}\, Mn\Omega^2|\vec{x}\,|^2 + \frac{1}{2}\, Mn\Omega^2\rho^2\ ,$$

leading to the single-particle spectrum

$$E'_n = \Omega \left(\frac{d}{2} + \sum_{i=1}^{d} n_i + 2q + 1 + \nu \right) , \tag{8.3.3}$$

with $\nu^2 = b + 1/4$. We see that the radial quantum number, $q \in \mathbb{Z}^+$, amounts to an extra dimension in the large temperature limit, $T \gg \Omega$. Hence, we would find a high-T asymptotics

$$I(\beta, \mu)^{\text{rad}} \sim - \left(\frac{T}{\Omega} \right)^{d+1} \left(\frac{T}{|\mu|} \right) . \tag{8.3.4}$$

This result is analogous to a well-known situation in relativistic AdS/CFT [1], where one finds that the entropy of gravitons in AdS_{d+1} in global coordinates scales like T^d at high temperature, thus revealing the full dimensionality of the bulk [220]. This free energy, as well as (8.3.4), is subleading to the black-hole free energy, proportional to N_{eff}, in the limit that N_{eff} is taken to infinity faster than any other dimensionless quantities. There is a Hawking–Page transition (cf. [221]) whenever the black-hole free energy changes sign as a function of T. Careful examination of the thermodynamical functions in [215, 194] reveals that this happens at temperatures of order $T_c \sim \Omega$. Hence, for $T < T_c$ we expect the thermodynamics to be dominated by radiation of $O(1)$ degrees of freedom.

Analogous phenomena take place in the $z = 2$ case, with single-particle Hamiltonian

$$H_n^{(z=2)} = -\frac{1}{2Mn} \vec{\partial}^{\,2} + \frac{1}{2Mn} \left(-\frac{d}{d\rho^2} + \frac{b_n}{\rho^2} \right) . \tag{8.3.5}$$

In this case, there is no γ^2-dependent shift, but b_n depends on n. In particular, the single-particle spectrum on a trap is just like (8.3.3) except for the fact that ν_n has now n-dependence:

$$\nu_n^2 = \nu_{n=0}^2 + 2\gamma^2 (MR)^2 n^2 .$$

Hence, there is an asymptotic term at large n which scales like a shifted chemical potential. Performing an analogous subtraction as in the $z = 1$ case ensures that the singularity is a pole at $\mu = 0$ as before. The results are then similar to the $z = 1$ case.

For untrapped metrics, such as (8.1.1), the radiation entropy suffers from an infrared problem as a consequence of the continuous spectrum in the radial direction. For heuristic purposes, we can deal with this situation by imposing a hard cutoff in the holographic variable dictated by the UV/IR relation. If we impose a radial cutoff $\rho \leq \rho_L$ in a system with $1/\rho^2$ potential, the spectrum will present a gap

$$E_{\text{gap}} \sim \frac{1}{M_n \rho_L^2} .$$

If we want to associate this gap to the presence of a box of size L, we must set $\rho_L \sim L$, so that the ρ variable directly represents a length scale in the boundary theory. Now, the presence of the black hole is associated to an energy scale of the order of the temperature T, and this corresponds to a radial cutoff (horizon location in ρ coordinates)

$$\rho_T \sim (M_n T)^{-1/2} \ .$$

Therefore, the effect of this cutoff on the high-energy spectrum enters in the partition function through terms like

$$\exp\left(-\beta \frac{4\pi^2 n_\rho^2}{2M_n \rho_T^2}\right) \sim \exp\left(-2\pi^2 n_\rho^2\right) \ ,$$

a small T-independent contribution, and thus negligible in the large-T limit. Hence, these considerations show that the entropy of the Hawking radiation sitting far from the horizon of a Schrödinger black hole scales just like (8.1.2), with the replacement of N_{eff} by some $O(1)$ numerical coefficient. By the same token, this entropy in Hawking radiation may be interpreted as part of the $1/N_{\text{eff}}$ corrections to the thermodynamics of the nonrelativistic CFT.

8.4 Conclusions

The thermodynamic functions of black holes with asymptotic Galilean isometries, (8.1.2), (8.1.3), were found to diverge in the limit of large ratio $T/|\mu|$. This behavior is somewhat puzzling, especially when compared to what is expected for cold atoms at unitarity [195, 222], the putative physical systems to which these holographic fluids should apply (cf. [216] for a discussion).

In this note we propose a simple explanation of the singular behavior of (8.1.2) and (8.1.3), in terms of an ideal gas with a nonrelativistic Kaluza–Klein tower of species. For the cases with a concrete string theory dual, our results can be interpreted as the small λ limit of the thermodynamic functions, with λ the 't Hooft coupling of the higher-dimensional Yang–Mills theory and $N_{\text{eff}} = N^2$, the gluon degrees of freedom. Furthermore, the situation is similar to that of relativistic AdS/CFT examples, in that only numerical coefficients would distinguish the ideal gas regime, $\lambda \ll 1$, from the black hole regime, $\lambda \gg 1$.

Our findings show that the nonrelativistic black hole spacetimes considered so far, actually count degrees of freedom in full $d+2$ spacetime dimensions. The technical device of light-like compactification was used as a formal tool to achieve Galilean invariance, with local physics in the extra light-like direction to be treated as an 'artifact' of the regularization.

Instead, we have seen that high-temperature black hole metrics fully excite local degrees of freedom in the extra dimension. It is likely that any black hole spacetime whose horizon is 'smeared' in the extra light-like direction will show this problem. Hence, the true superfluid phase of nonrelativistic systems in d spatial dimensions is likely to be related to black holes that localize in the extra dimension.

In the application to systems of atoms in the unitarity limit, the conserved charge N should measure the number of atoms. Hence, one expects the n-th KK species field to be related to the n-th power of the microscopic atomic field, $\phi_n \sim (\psi)^n$. This means that bound states with an arbitrary number of atoms would survive in the 'classical limit' implicit in the leading gravity approximation of the bulk. This is akin to large-N limits of gauge theories, where arbitrarily large 'string operators' are kept in the leading $N \to \infty$ limit (a fact mirrored in the bulk AdS description by the infinite towers of string and Kaluza–Klein excitations kept in the leading approximation at zero string coupling $g_s \sim 1/N \sim 0$). According to this logic, thermodynamical divergences associated to the large 'length' of composite atomic operators, $(\psi)^n$, would be analogous to the divergences associated to infinitely long gauge strings, i.e. the Hagedorn critical behavior.

We therefore conclude that more work is needed in order to evaluate the applicability of current nonrelativistic AdS/CFT constructions to explicit nonrelativistic critical points found in Nature.

General Conclusions

Chapter 9

Summary and general conclusions

In this thesis we have studied entanglement entropy and Schrödinger invariant non-relativistic systems from the AdS/CFT correspondence. This study takes place within the much broader program of application of the AdS/CFT correspondence to Condensed Matter. Our study is directly connected to the application of AdS/CFT to the investigation of systems near quantum phase transitions. By means of the entanglement entropy one can gain information of the quantum structure of the ground states at the quantum critical points, as we have shown in the first part of this thesis. In the second part, we have contributed to the study of the holographic duals to Schrödinger invariant quantum critical points with $z = 2$.

Entanglement Entropy

Entanglement entropy allows to study the structure of the non-degenerate ground state of systems near quantum phase transitions or generically described by QFTs. From the scaling of the entanglement entropy as a function of the length scale of a region under consideration, one can read many properties of the theory. In particular, in chapter 3 we saw how the locality of the interactions is encoded in the area law of the non-universal contribution (or UV cutoff dependent). On the other hand, in chapter 4, we saw how the renormalized entanglement entropy, or what is the same the universal contribution independent of any UV cutoff, encodes the information related to the presence of mass gaps and the effective number of degrees of freedom of the theory. All these analyses were done in the large N_{eff} limit for strongly coupled $z = 1$ systems by means of the holographic ansatz of [18].

As a result of the analysis of chapter 3, we argued that the combination of Lorentz symmetry plus a more or less standard density of states at high energy is sufficient to guarantee an area law in the UV contribution to the entanglement entropy. We found and

analyzed two non-local families of theories outside this category: non-commutative super Yang-Mills and Little String Theory. Both present a volume law below its spatial non-locality scale. The first one evaded the area law due to the effective violation of Lorentz symmetry below the non-commutative scale. LST is also outside due to its unusual density of states corresponding to a Hagedorn-like behaviour with a limiting temperature above the energy scale of non-locality.

The main conclusion of chapter 3 is that entanglement entropy gives a very easy criterion of locality in the theory, i.e. area law in the non-universal contribution, and that can be traced back to combination of Lorentz symmetry plus a standard density of states at high energy. As a consequence, any non-local theory will violate any of these. In particular our analysis endorses the interpretation of the dual of flat spacetime as a non-local theory due to its volume law.

In chapter 4, we learned that from the renormalized entanglement entropy one may read the different scales of the theory and effective degrees of freedom. We studied systematically the renormalized entanglement entropy for the different generic settings that can appear in the holographic constructions asymptotic to AdS. We found that in phenomenological models (soft and hard walls) of confinement, the renormalized entanglement entropy presents a volume law. This is in contrast to String Theory well-defined models (resolved walls) where the renormalized entanglement entropy vanishes, or equivalently saturates. Only the last one is in agreement with a weak coupling analysis. Hence we interpret the volume law as an unphysical feature of the pure phenomenological models.

We also obtained that generically, and as expected, that black hole geometries give rise to an extensive contribution to the renormalized entanglement entropy at finite temperature. We found, nonetheless, a case where this extensivity holds down to zero temperature: that of dyonic black holes (backed by a String Theory construction). It correspond to systems with a charge condensate and/or external magnetic field at zero temperature. This behaviour is new and hints for new types of quantum critical points not identified by weak coupling QFT analysis.

Last but not least we also speculated about a possible modification of the holographic prescription of [18] in the presence of black hole geometries at finite temperature. By incorporating the possibility that the minimal hypersurfaces cross the horizon, we think the same holographic quantity is now measuring the mutual information. This is in agreement with an area law on both sides of the duality.

Let us close by commenting on some open questions regarding entanglement entropy. One of the most pressing issues in all our analysis and the available holographic prescription

itself is that it only captures leading $\mathcal{O}(N_{\text{eff}})$ contributions to the entanglement entropy. Subleading $1/N_{\text{eff}}$ corrections are simply not available. One should try to extend the ansatz in this direction.

It would be also be interesting to extend the analysis to other $z \neq 1$ critical systems, in particular to the Schrödinger invariant $z = 2$ models and to Lifshitz-type of theories. A quick application of the holographic ansatz in these models suggests that the area law continues to hold. But a more complete systematic treatment would be desirable. See [223] for a recent work in this direction. We also consider the extension of the holographic prescription to encompass the topological entanglement entropy. Although there was an attempt to address it in [224] we feel a much careful analysis is needed.

Non-relativistic AdS/CFT

In the second part of this thesis, we have studied the holographic duals of Schrödinger invariant field theories, first put forward in [3, 4]. The main physical motivation after it, is the rendering of the quantum critical point of fermions at unitarity that shows precisely invariance under the Schrödinger group.

In chapter 6 we analyzed the Hamiltonian picture of the Sch_{d+3} background. We found that at the level of free bulk dynamics, the conformal symmetry is realized in a conformal quantum mechanics for the holographic radial coordinate. More remarkably the same conformal quantum mechanics was found by means of pure AdS constructions. The Hamiltonian approach also led us to the right ansatz for a metric incorporating the effect of external harmonic trapping onto the system. We found perfect agreement of the state-operator correspondence in the Schrödinger invariant theory, as realized between the energy eigenstates in the harmonic trapping and the scaling dimensions of fields. The very same structure of energy eigenstates was found to agree with computations in cold atom gases in harmonic traps. This comparison motivated us to give a physical interpretation of the radial holographic direction as accounting for the collective excitations of the gas. Building of the Hamiltonian formalism we also gave some heuristic models for other scenarios where molecules may be formed.

In chapter 7, we deepened in our analysis of the Sch_{d+3} background but from the point of view of the n-point functions, at zero temperature and zero chemical potential. We gave an explicit formula relating the scalar n-point function at tree level in Sch_{d+3} to the same n-point function in AdS, as a projection of the operator insertions along the light-like direction

implementing the number operator,

$$\langle\phi_1(\bar{x}_1)\dots\phi_n(\bar{x}_n)\rangle_{\rm Sch}^{(\text{tree level})} = \int\prod_{k=1}^{n} d\xi_k\, e^{-i\sum_{j=1}^{n}(M_j\xi_j)}\langle\phi_1(\bar{x}_1,\xi_1)\dots\phi_n(\bar{x}_n,\xi_n)\rangle_{\rm AdS}^{(\text{tree level})} \ .$$

This formula demonstrates the complete equivalence at tree level of the light-cone construction in pure AdS_{d+3} and Sch_{d+3}. This equivalence is supported by the String Theory implementations of Sch_5, that is dual to certain type of non-commutative deformation of $\mathcal{N}=4$ SYM theory. At tree level, the correlation functions of a non-commutative theory and its commutative version coincide, up to some overall phases. At the loop level we no longer have this relation between the n-point functions and we have to use the Sch_{d+3} background. We found that at the loop level with a compact number direction, we have the typical problem of DLCQs and one needs to regulate the theory. One possibility is by means of a finite chemical potential.

From the tree level relation between AdS and Sch correlation functions, we were able to compute the scalar 2- and 3-point functions at tree level. We compared it with the results of the QFT of bosons at unitarity. Although the 3-point function is not fully constrained by symmetry, we found agreement except for the expected overall normalization. This sets the hope that at least the correspondence can be put to work at tree level.

Finally in chapter 8 we addressed the finite temperature and finite chemical potential version of Sch_{d+3} available in the literature, the Schwarzschild-Sch_{d+3} black hole [170, 169, 164]. In particular we investigated the reason after the pathological behaviour of the thermodynamic functions, found to diverge as a power of $T/|\mu|$. This is specially puzzling when compared to what is expected for cold atoms at unitarity, where one does not find this divergent behaviour but rather a crossover to a superfluid phase. We gave a simple explanation in terms of an ideal gas with a non-relativistic Kaluza-Klein tower of species, that reproduces all the thermodynamics observables of the dual Schwarzschild-Sch black hole. This ideal gas can be seen as the analog of the weak coupling description of the underlying system to the Schwarzschild-Sch black hole. Our analysis shows that the non-relativistic black hole is actually counting degrees of freedom in full the $d+2$ spacetime dimensions and fully exciting the extra dimension. We concluded that the true superfluid phase of non-relativistic systems in d dimensions is likely to be related to black holes that localize in the extra dimension.

From all this work we reach the conclusion that the Sch_{d+3} can only be seen as a promising candidate to describe the quantum critical point of conformal non-relativistic theories at tree level and zero temperature and chemical potential. Right now much more work is needed in order to evaluate the applicability of current non-relativistic AdS/CFT constructions to the case of finite temperature and chemical potential, which is where the real applications

to Condensed Matter lie. We place the quest of suitable backgrounds at finite temperature and chemical potential as the most urgent open problem to be addressed in the future.

As closing words, let me just comment that the application of the AdS/CFT correspondence and holographic methods to Condensed Matter is still an unfolding story in its infancy. The phenomena and models that have been addressed include cold atom gases at unitarity [3, 4], superconductivity [5], superfluidity [6], quantum liquids [7, 8]. The AdS/CFT correspondence shines in those regimes where the notion of quasiparticles or order parameters are completely lost. However at the same time we can only apply it with some control in situations where high amounts of supersymmetry and gauge theories in the large N limit are present, which are not readily found in the laboratory. As soon as we want to leave these scenarios we either lose complete computational power since we would end up with highly curved spacetimes, or else, we simply lose any control on the dual quantum field theory by just taking some phenomenological ad hoc background. In the current situation it seems very difficult to be able to make direct experimental predictions from the holographic duals. Nonetheless, we can regard all these constructions as giving a fresh and new intuition, and even quantitative benchmarks, to some old and very difficult problems that people so far could only partially handle by complicated expansions and techniques, from what you may extract some number but certainly no physical picture or intuition at all. Let us then hope that this new holographic avenue really opens new ways of thinking and brings the kind of original insight necessary to make new progress.

Appendices

Appendix A

TsT transformation

The TsT transformation is a generating solution transformation for type II supergravity. One starts from a background with two isometries along some coordinates φ_1 and φ_2. Upon dimensional reduction along them, the eight dimensional gravity has an $SL(2,\mathbb{R})$ symmetry. This symmetry corresponds to the TsT transformation. As a first step, one performs a T-duality along φ_1 and introduce the dualised direction $\tilde{\varphi}_1$. Secondly, one makes the coordinate shift $\varphi_2 \to \varphi_2 + \beta\tilde{\varphi}_1$. Thirdly, one performs another T-duality along $\tilde{\varphi}_1$.

Let us give the TsT transformation for a general solution formed by $M_5 \times Y_5$,

$$\begin{aligned} ds^2 &= g_{ab}dx^a dx^b + ds^2(\tilde{B}) + h^2(d\varphi + \tilde{P})^2 \ , \\ F_5 &= 4\left(\text{vol}(M_5) + \text{vol}(\tilde{B}) \wedge h(d\varphi + \tilde{P})\right) \ . \end{aligned} \tag{A.0.1}$$

Here g_{ab} is the metric for M_5. Y_5 is a Sasaki-Einstein manifold that we write as a fibration: φ is a Killing direction in Y_5, $ds^2(\tilde{B})$ is the metric of the four-dimensional spate transverse to ∂_φ, h^2 is the norm of ∂_φ, and $\tilde{P}$ is a connection one-form on $\tilde{B}$. We assume all other fields are zero.

If we make the TsT transformation along φ and x^-, T-dualizing first φ to $\tilde{\varphi}$, then shifting $x^- \to x^- + \beta\tilde{\varphi}$ and T-dualising back $\tilde{\varphi}$ to φ, the result is

$$\begin{aligned} ds^2 &= \left[g_{ab}dx^a dx^b - \beta^2 e^{2(\Phi-\Phi_0)}h^2 g_{a-}g_{b-}dx^a dx^b + ds^2(\tilde{B}) + e^{2(\Phi-\Phi_0)}h^2(d\varphi + \tilde{P})^2\right] \ , \\ F_5 &= 4\left(\text{vol}(M_5) + \text{vol}(\tilde{B}) \wedge h(d\varphi + \tilde{P})\right) \ , \\ B &= \beta e^{2(\Phi-\Phi_0)}h^2 g_{a-}dx^a \wedge (d\varphi + \tilde{P}) \ , \\ e^{-2(\Phi-\Phi_0)} &= 1 + \beta^2 h^2 g_{--} \ , \end{aligned} \tag{A.0.2}$$

where Φ_0 is the value of the dilaton before the duality.

We see that M is transformed, in particular if $M_5 = AdS_5$ it goes to Sch_5. Y_5 gets generically squashed. The F_5 remains the same. And we add a non-trivial profile for the dilaton and a NS 2-form.

Appendix B

Projected bulk-to-boundary propagator in position space

In the relativistic AdS/CFT the bulk-to-boundary propagator in position space can be computed employing the discrete inversion symmetry of AdS space [1]. The Schrödinger spacetime (5.3.5) does not posses this symmetry. Nonetheless, we can compute the projected propagator as introduced in Sec. 7.2, Eq. (7.2.9). Here we will present a derivation of the explicit expression for it,

$$K_M(\bar{x}-\bar{y},\xi-\xi',u_x) = e^{iM(\xi-\xi')}\int d\tilde{\xi}\, K_\Delta^{(\mathrm{AdS})}(\bar{x}-\bar{y},\tilde{\xi},u_x)\, e^{-iM\tilde{\xi}} \quad . \tag{B.0.1}$$

In order to get the non-relativistic bulk-to-boundary propagator we must Fourier transform the well-known AdS bulk-to-boundary propagator [1] to a fixed ξ-momentum, M, in the Euclidean light-cone frame

$$\mathscr{K}_M(u,\bar{x}) = C_\Delta \int_{-\infty}^{\infty} d\xi \exp[-iM\xi]\left(\frac{u}{u^2+\vec{x}^2-2it\xi}\right)^\Delta \quad , \tag{B.0.2}$$

with $C_\Delta = \frac{\Gamma(\Delta)}{\pi^{\frac{d+2}{2}}\Gamma[\Delta-\frac{d+2}{2}]}$ and $\Delta(\Delta-d-2) = m_0^2+\beta^2M^2$.

The integral in Eq. (B.0.2) was done in Appendix B [151] and we follow these calculations

closely

$$\begin{aligned}\mathscr{K}_M(u,\bar{x}) &= C_\Delta\left(\frac{u}{2it}\right)^\Delta\int_{-\infty}^{\infty}d\xi\exp[-iM\xi]\frac{1}{(\xi+\frac{i(u^2+\vec{x}^2)}{2t})^\Delta}= \\ &= C_\Delta\left(\frac{u}{2it}\right)^\Delta(M)^{\Delta-1}\int_{-\infty}^{\infty}d\xi\exp[-i\xi]\frac{1}{(\xi+\frac{iM(u^2+\vec{x}^2)}{2t})^\Delta}= \\ &= C_\Delta\left(\frac{u}{2it}\right)^\Delta(M)^{\Delta-1}\exp[-\frac{M}{2}\frac{u^2+\vec{x}^2}{t}]\underbrace{\int_{\mathbf{R}+\frac{iM}{2}\frac{u^2+\vec{x}^2}{t}}d\xi e^{-i\xi}\xi^{-\Delta}}_{\alpha\theta(t)}= \\ &= \gamma\left(\frac{u}{t}\right)^\Delta\theta(t)\exp[-\frac{M}{2}\frac{u^2+\vec{x}^2}{t}],\end{aligned} \tag{B.0.3}$$

where we introduced a constant $\gamma = C_\Delta\alpha(2i)^\Delta M^{\Delta-1}$. It is simple to check that Eq. (B.0.3)[1] indeed solves the scalar field equation (7.2.12) provided that the condition (7.2.15) holds.

It is instructive to investigate the behavior of the propagator near the "boundary" ($u\to 0$). The function $\mathscr{K}_M(u,\bar{x})$ has two important properties

- $\mathscr{K}_M(u,\bar{x})$ has its support at the origin of the "boundary space", i.e. at $t=0$ and $\vec{x}=0$, in the limit $u\to 0$.

- The integral of $\mathscr{K}_M(u,\bar{x})$ over the boundary coordinates t and $\vec{x}$ has the form

$$\int d\bar{x}\mathscr{K}_M(u,\bar{x}) = u^{d+2-\Delta}I, \tag{B.0.4}$$

  where I is independent of the radial coordinate u

$$I = \gamma\int d\bar{x}\exp[-\frac{M}{2}\frac{1+\vec{x}^2}{t}]. \tag{B.0.5}$$

These two properties imply that near the "boundary" ($u\to 0$) the function

$$\mathscr{K}_M(u,\bar{x})\to u^{d+2-\Delta}\delta(\vec{x})\delta(t) \tag{B.0.6}$$

which is a correct behavior of the bulk-to-boundary propagator in the position space.

The explicit expression of the projected bulk-to-boundary propagator is then

$$\begin{aligned}K_M(\bar{x}-\bar{y},\xi-\xi',u) &= e^{iM(\xi-\xi')}\mathscr{K}_M(u,\bar{x}-\bar{y})= \\ &= \gamma e^{iM(\xi-\xi')}\left(\frac{u}{\Delta t}\right)^\Delta\theta(\Delta t)\exp[-\frac{M}{2}\frac{u^2+\Delta\vec{x}^2}{\Delta t}]\end{aligned} \tag{B.0.7}$$

where $\Delta t = t_x - t_y$ and $\Delta\vec{x} = \vec{x}-\vec{y}$.

[1] without the causal factor $\theta(t)$

Appendix C

Inverse Fourier transformation

In this Appendix we present a calculation of the inverse Fourier transformation of a general non-relativistic scale-invariant propagator in d spatial dimensions

$$G(t,\vec{x}) = \int \frac{d\omega}{2\pi}\frac{d^dq}{(2\pi)^d}(i\omega+\epsilon_{\vec{q}})^\alpha e^{i(\omega t-\vec{q}\cdot\vec{x})}, \tag{C.0.1}$$

where $\epsilon_{\vec{q}} = \frac{\vec{q}^2}{2M}$ with the non-relativistic mass M. We assume that α is real and negative.

First, the $d-1$ dimensional angular integration can be performed employing a general formula

$$\int \frac{d^dq}{(2\pi)^d} f(q)e^{-i\vec{q}\cdot\vec{x}} = \left(\frac{1}{2\pi}\right)^{\frac{d}{2}}\int_0^\infty dq f(q) q\left(\frac{q}{x}\right)^{\frac{d}{2}-1} J_{\frac{d}{2}-1}(qx), \tag{C.0.2}$$

which is valid for an arbitrary radial function $f(q)$. In our case $f(q) = (i\omega+\epsilon_{\vec{q}})^\alpha$ and we arrive at

$$G(t,x) = \left(\frac{1}{2\pi}\right)^{\frac{d}{2}}\int_0^\infty dqq\left(\frac{q}{x}\right)^{\frac{d}{2}-1} J_{\frac{d}{2}-1}(qx)\int\frac{d\omega}{2\pi}e^{i\omega t}(i\omega+\epsilon_{\vec{q}})^\alpha, \tag{C.0.3}$$

where $x^2 = \vec{x}\cdot\vec{x}$.

The frequency integration in Eq. (C.0.3) can be done by performing a substitution $i\omega \to i\omega + \epsilon_{\vec{q}}$

$$G(t,x) = (i)^\alpha\left(\frac{1}{2\pi}\right)^{\frac{d}{2}}\int_0^\infty dqq\left(\frac{q}{x}\right)^{\frac{d}{2}-1} J_{\frac{d}{2}-1}(qx)e^{-\frac{q^2t}{2M}}\int_{\mathbb{R}-i\frac{q^2}{2M}}\frac{d\omega}{2\pi}e^{i\omega t}\omega^\alpha. \tag{C.0.4}$$

The integrand has a branch point at $\omega = 0$. The branch cut goes from zero to infinity and we choose it to be along the positive imaginary axis. This choice corresponds to the retarded causal structure of the propagator. Due to this singularity structure of the integrand, the integration contour in Eq. (C.0.4) can be shifted to the real axis.

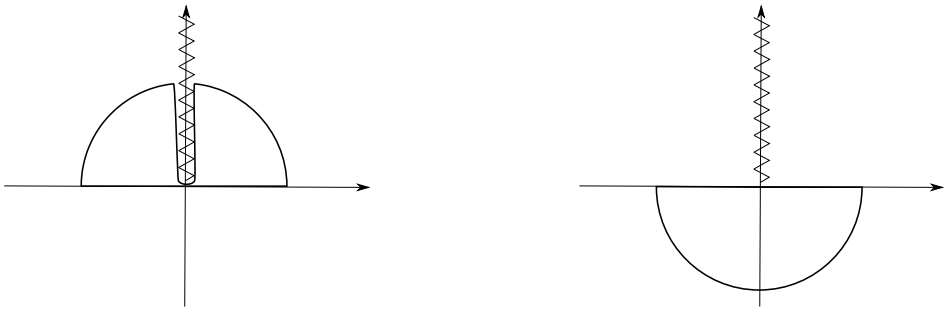

(a) $t > 0$ (b) $t < 0$

Figure C.1: Contour of integration for $t > 0$ and $t < 0$. The branch cut of ω^α was chosen to be along the positive imaginary axis.

If $t > 0$, we can consider a contour like the one in Fig. C.1 (a). Applying the residue theorem we obtain that the integral along the real axis is related to an integral along the positive imaginary axis by

$$\begin{aligned}\int_{-\infty}^{\infty} \frac{d\omega}{2\pi}\omega^\alpha e^{i\omega t} &= -i^{\alpha+1}\int_0^\infty \frac{d\chi}{2\pi}\chi^\alpha e^{-\chi t} - i^{\alpha+1}e^{2\pi i\alpha}\int_\infty^0 \frac{d\chi}{2\pi}\chi^\alpha e^{-\chi t} \\ &= i^{\alpha+1}(e^{2\pi i\alpha}-1)\int_0^\infty \frac{d\chi}{2\pi}\chi^\alpha e^{-\chi t},\end{aligned} \tag{C.0.5}$$

where we took $\chi = i\omega$. Now applying that

$$\int_0^\infty \frac{d\chi}{2\pi}\chi^\alpha e^{-\chi t} = \frac{\Gamma(\alpha+1)t^{-\alpha-1}}{2\pi} = -\frac{t^{-\alpha-1}}{2\Gamma(-\alpha)\sin(\pi\alpha)} \tag{C.0.6}$$

we obtain

$$\int_{-\infty}^{\infty} \frac{d\omega}{2\pi}\omega^\alpha e^{i\omega t} = i^\alpha e^{i\pi\alpha}\frac{t^{-\alpha-1}}{\Gamma(-\alpha)}. \tag{C.0.7}$$

If $t < 0$, we have to consider the contour in Fig. C.1 (b). It is clear that the integral is then zero. Hence

$$\int_{-\infty}^{\infty} \frac{d\omega}{2\pi}\omega^\alpha e^{i\omega t} = i^\alpha e^{i\pi\alpha}\frac{t^{-\alpha-1}}{\Gamma(-\alpha)}\theta(t). \tag{C.0.8}$$

Putting this into Eq. (C.0.4) we obtain

$$G(t,x) = \frac{1}{\Gamma(-\alpha)(2\pi)^{\frac{d}{2}}}t^{-\alpha-1}\theta(t)\underbrace{\int_0^\infty dqq\left(\frac{q}{x}\right)^{\frac{d}{2}-1}J_{\frac{d}{2}-1}(qx)e^{-\frac{q^2t}{2M}}}_{F(t,x)}. \tag{C.0.9}$$

Under the assumptions $t > 0$ and $x > 0$, the momentum integral in Eq. (C.0.9) can be done analytically

$$F(t,x) = \left(\frac{t}{M}\right)^{-\frac{d}{2}} e^{-\frac{Mx^2}{2t}}. \tag{C.0.10}$$

Hence, we obtain the final result

$$G(t,x) = \left(\frac{M}{2\pi}\right)^{\frac{d}{2}} \frac{\theta(t)}{\Gamma(-\alpha)} t^{-\Delta} e^{-\frac{Mx^2}{2t}}, \tag{C.0.11}$$

where we defined the scaling dimension $\Delta = 1 + \frac{d}{2} + \alpha$.

Appendix D

2- and 3-point functions on Sch_{d+3} for compact ∂_ξ-direction

In this Appendix we will give the computation of the 2 and 3-point function on Sch_{d+3} for a compact ∂_ξ-direction using the general relation (7.2.5) discussed in the main text. According to (7.2.5) we have to perform the Fourier transform of the corresponding (relativistic) point function. For the computation to be consistent we need to start from the relativistic n-point function that is fully periodic in ξ_k.

D.1 2-point function

Let us consider the 2-point function when one takes ξ to be compact, $\xi \in [0, L]$. One needs to have a periodic relativistic 2-point function in ξ. The usual one is clearly not

$$\langle \phi_1(0)\phi_2(\bar{x},\xi)\rangle = \frac{C_{12}}{(-2i\xi t + x^2)^\Delta} \ . \tag{D.1.1}$$

But one can construct easily one that is indeed periodic in ξ, just take

$$\langle \phi_1(0)\phi_2(\bar{x},\xi)\rangle = \sum_{n\in\mathbb{Z}} \frac{C_{12}}{(-2it(\xi+nL) + x^2)^\Delta} \ . \tag{D.1.2}$$

This is a simple linear combination of 2-point functions and, hence, it is going to fulfill the differential equations for the propagator that are linear.

This way the 2-point function when we have the periodically identified ξ is (this is the

exact equivalent of equation (52))

$$\begin{aligned} G_2 &= L\delta_{M_1+M_2,0}\int_{-\frac{L}{2}}^{\frac{L}{2}}\langle\phi_1(X_1)\phi_2(X_2)\rangle_{\text{AdS}}^{(\text{tree level})} \\ &= \frac{LC_{12}\delta_{\Delta_1,\Delta_2}\delta_{M_1+M_2,0}}{2i(t_1-t_2)^{\Delta_1}}\int_{-\frac{L}{2}}^{\frac{L}{2}}d\xi e^{-iM_1\xi}\sum_{n\in\mathbb{Z}}\left(\xi+nL+\frac{i(\vec{x}_1-\vec{x}_2)^2}{2(t_1-t_2)}\right)^{-\Delta_1} \end{aligned} \tag{D.1.3}$$

Here the masses are quantized as $M_i = 2\pi j/L$ with $j \in \mathbb{Z}$.

Now if we do the simple change of variables

$$\tilde{\xi} = \xi + \frac{i(\vec{x}_1-\vec{x}_2)^2}{2(t_1-t_2)} \tag{D.1.4}$$

one finds

$$G_2 = \frac{LC_{12}\delta_{\Delta_1,\Delta_2}\delta_{M_1+M_2,0}}{2i(t_1-t_2)^{\Delta_1}}e^{\frac{-M_1(\vec{x}_1-\vec{x}_2)^2}{2(t_1-t_2)}}\int_{-\frac{L}{2}+\frac{i(\vec{x}_1-\vec{x}_2)^2}{2(t_1-t_2)}}^{\frac{L}{2}+\frac{i(\vec{x}_1-\vec{x}_2)^2}{2(t_1-t_2)}}d\tilde{\xi}e^{-iM_1\tilde{\xi}}\sum_{n\in\mathbb{Z}}\left(\tilde{\xi}+nL\right)^{-\Delta_1} \tag{D.1.5}$$

The last integral is proportional to $\theta(t_1-t_2)$ and independent of $\vec{x}$ and t. Hence we see that the final result agrees with Schrödinger symmetry, Eq. (7.1.1).

D.2 3-point function

The 3-point function, G_3, in a (relativistic) conformal field theory is completely fixed (up to an overall constant) by the symmetries of the theory. That is, it is completely fixed by a set of linear partial differential equations that come from imposing invariance under the generators of the conformal group. As such, applying an identical procedure as in the 2-point function, in order to find the 3-point function that is periodic in the different ξ_j all we have to do is to substitute $G_3(\xi_j)$ by $\sum_{n_j} G_3(\xi_j + Ln_j)$.

Starting then from (7.4.17) and following the same manipulations as in the non-compact ξ case, it is immediate that the spacetime dependence will be exactly the same as in the non-periodic ξ case. On the other hand the expression for the scaling function that one has to evaluate, reduces to

$$\Phi(y) = \int_{-\frac{L}{2}+i\varepsilon}^{\frac{L}{2}+i\varepsilon}dv\int_{-\frac{L}{2}+i\varepsilon'}^{\frac{L}{2}+i\varepsilon'}dv'e^{-iM_1v-iM_2v'}\sum_{n,n'\in\mathbb{Z}}(v-v'+Ln-Ln'+iy)^{-\frac{\Delta_{12,3}}{2}}(v+Ln)^{-\frac{\Delta_{13,2}}{2}}(v'+Ln')^{-\frac{\Delta_{23,1}}{2}} \tag{D.2.1}$$

with $\varepsilon, \varepsilon' > 0$.

For the case, $\Delta_1 = \Delta_2 = d/2$, $\Delta_3 = 2$, $M_1 = M_2 = 1$, the integral becomes

$$\Phi(y) = \int_{-\frac{L}{2}+i\varepsilon}^{\frac{L}{2}+i\varepsilon}dv\int_{-\frac{L}{2}+i\varepsilon'}^{\frac{L}{2}+i\varepsilon'}dv'e^{-iv-iv'}\sum_{n,n'\in\mathbb{Z}}(v-v'+Ln-Ln'+iy)^{-\frac{d-2}{2}}(v+Ln)^{-1}(v'+Ln')^{-1} \tag{D.2.2}$$

In order to evaluate (D.2.2), we apply the residue theorem together with a contour of integration that consists on a rectangle with base $[-L/2, L/2]$ and height extending towards minus the imaginary infinity for both integrals. We first do the integral in v'. Assuming $y > 0$, there is only one pole that lies within the contour of integration, the one at $v' = 0$. The residue at $v' = 0$ is

$$\lim_{v'\to 0} \sum_{n,n'\in\mathbb{Z}} \frac{v' e^{-iv-iv'}}{(v - v' + Ln - Ln' + iy)^{\frac{d-2}{2}}(v + Ln)(v' + Ln')} = \sum_{n\in\mathbb{Z}} \frac{e^{-iv}}{(v + Ln + iy)^{\frac{d-2}{2}}(v + Ln)} \tag{D.2.3}$$

Thus

$$\Phi(y) = -2\pi i \int_{-\frac{L}{2}+i\varepsilon}^{\frac{L}{2}+i\varepsilon} \sum_{n\in\mathbb{Z}} \frac{e^{-iv}}{(v + Ln + iy)^{\frac{d-2}{2}}(v + Ln)} \, . \tag{D.2.4}$$

Applying again the residue theorem with the same contour of integration and the relations (7.4.25) or (7.4.27) depending on whether is d is even or odd respectively, one arrives to

$$\Phi(y) = N_d \, y^{-\frac{d}{2}+1} \gamma(\frac{d}{2} - 1, y) \, . \tag{D.2.5}$$

We see that the only difference with respect to the non-compact ξ case is that L appears as a multiplicative factor of the 3-point function instead of 2π. The scaling function is exactly the same as in the non-compact case, Eq.(7.4.26),

Appendix E

Introducción

[1] Durante la pasada década hemos sido testigos de una revolución en el campo de Teoría de Cuerdas con el advenimiento de la correspondencia AdS/CFT o conjectura de Maldacena [1]. La Teoría de Cuerdas en sus principios nació como un modelo de mesones, para luego ser descartado en favor de Cromodinámica Cuántica (QCD), y finalmente reconocido como una teoría consistente de Gravedad Cuántica. Como tal, antes de la conjetura de Maldacena, Teoría de Cuerdas era vista como un posible candidato de una teoría cuántica unificada de todas las fuerzas incluida gravedad. Sin embargo después del trabajo de Juan Maldacena en 1997 [1], fue aparente que Teoría de Cuerdas podía ser vista independientemente como una teoría dual de alguna Teoría Cuántica de Campos. Ésta es una dualidad fuerte-débil. Más precisamente, la aproximación semiclásica a Teoría de Cuerdas, supergravedad, en espacio-tiempos asintóticos a Anti de Sitter (AdS) es dual al régimen de fuerte acoplo de teorías de Yang-Mills maximalmente supersimétricas. Y viceversa, el regimen débilmente acoplado de estas teorías gauge es dual al régimen fuertemente acoplado de Teorías de Cuerdas. La correspondencia AdS/CFT nos permite un tratamiento del regimen no-perturbativo de Teoría Cuántica de Campos por medio de un límite semiclásico, de débil acoplo, de una teoría de gravedad y al mismo tiempo nos da una definición de Teoría de Cuerdas a través de una Teoría Cuántica de Campos débilmente acoplada. La dualidad gauge/gravedad se ha convertido en una herramienta útil para investigar teorías de campos fuertemente acopladas. Este enfoque ha visto ya muchos éxitos dando una nueva comprensión de varios fenómenos teóricos de campos en teorías gauge como la transición de confinamiento-deconfinamiento, rotura de simetría quiral, cálculo de coeficientes de transporte en la fase de plasma, etc. Entre los descubrientos más sobresalientes se encuentra el nexo inesperado entre la universalidad de la física de agujeros negros y predicciones de cotas universales en el lado de la teoría de

[1] Traducción al español del capítulo 1 / Spanish translation of chapter 1.

campos. Un ejemplo es el cociente de la viscosidad cortante y la densidad de entropía [2]. El acuerdo cualitativo entre el valor predicho de $1/4\pi$ y el medido para los plasmas creados en el Colisionador de Iones Relativistas Pesados (RHIC) indica que la dualidad gauge/gravedad es útil para estudios de QCD.

No obstante dada la generalidad de los principios subyacentes a la correspondencia gauge/gravedad, parece natural buscar nuevos sistemas y fenómenos que sean descritos por medio de dicha dualidad. Éste es un vasto territorio inexplorado puesto que la mayoría de los esfuerzos se han enfocado sobre QCD y en sus primos supersimétricos. Sin embargo durante los dos últimos años nuevas conexiones y estudios teóricos han sido establecidos señalando la utilidad de la dualidad gauge/gravedad en otros sistemas fuertemente correlacionados, particularmente aquellos que vienen de Física del Estado Sólido. Estos nuevos fenómenos incluyen modelos de gases de átomos fríos en el regimen de unitariedad [3, 4], superconductividad [5], superfluided [6], líquidos cuánticos [7, 8]. La mayoría de ellos están relacionados con problemas difíciles largo tiempo sin solución en Matería Condensada y como tal cualquier nuevo progreso implicaría desarrollos significativos.

Criticalidad Cuántica

La aplicación de la dualidad gauge/gravedad a Matería Condensada está intimamente conectada con la existencia de *transiciones de fase cuánticas* y sus puntos críticos asociados [9]. Éstas consisten en transiciones de fase a temperatura cero asociadas a un cambio no-analítico en las propiedades físicas del sistema bajo variaciones suaves de algún parámetro del sistema, como campos magnéticos aplicados o presión.

Como cualquier transición, las transiciones de fase cuánticas pueden ser de diferentes tipos. Nuestro interés estará en aquellas de segundo orden. Para ellas el espectro de excitaciones energéticas en criticalidad es continuo. De hecho el salto de energía Δ se anula como

$$\Delta \sim J|g - g_c|^{z\nu} \,, \tag{E.0.1}$$

donde g es el parámetro que variamos y g_c es us valor crítico. Al mismo tiempo la escala de longitud de correlación ξ diverge como

$$\xi^{-1} \sim \Lambda|g - g_c|^{\nu} \,. \tag{E.0.2}$$

El cociente de exponentes críticos en (E.0.1) y (E.0.2) da un exponente crítico dinámico z: la escala característica de energía desaparece como la potencia a la z de la escala característica inversa de longitud

$$\Delta \sim \xi^{-z} \,. \tag{E.0.3}$$

La divergencia de la longitud de correlación del sistema en el punto cuántico crítico, indica que el sistema se convierte en invariante bajo escala. Lo que es más, el sistema puede ser descrito de forma efectiva por un punto crítico de una teoría cuántica de campos, con exponente dinámico z.

Hay dos posibilidades para el diagrama de fase a $T > 0$ cerca de un punto crítico cuántico. El punto crítico cuántico puede ser aislado o ser el punto final de una línea de transiciones de fase a $T > 0$. En el caso de un punto crítico cuántico aislado, en la vecindad inmediata de la línea uno puede describir el sistema en términos de una teoría clásica para algún parámetro de orden cuya validez conforme nos acercamos al punto crítico cuántico va disminuyendo.

En cualquiera de los dos casos, la relevancia de estos puntos críticos cuánticos viene del hecho que paradójicamente dominan el diagrama de fase para $T > 0$. En regiones donde la deformación fuera de criticalidad debido a una escala de energía Δ es menos importante que la deformación debida a temperatura finita, i.e. $\Delta < T$, el sistema puede ser descrito por el punto crítico cuántico a temperatura finita. Esta observación nos conduce al hecho contraintuitivo de que la huella del punto crítico a temperatura cero crece a medida que la temperatura aumenta.

Un ejemplo se encuentra en la transición de superfluido-aislante en dos dimensiones espaciales [10]. Un modelo simple para esto es el modelo de Bose Hubbard en llenado entero. Está descrito por el Hamiltoniano en la red

$$H = -t \sum_{\langle ij \rangle} \left(b_i^\dagger b_j + b_j^\dagger b_i \right) + U \sum_i n_i (n_i - 1) \, , \tag{E.0.4}$$

donde b_i son los operadores de aniquilación para los diferentes bosones. U es la repulsión entre bosones, y t es el elemento de matriz de interacción entre bosones. En función del cociente U/t, el sistema está en uno de los posibles regímenes, un aislante o un superfluido, ambos de los cuales tienen un descripción clásica efectiva de su dinámica y transporte con un concepto claro de cuasipartícula. Para pequeño U/t, estamos en la región superfluida y a través de una transición de tipo Kosterlitz-Thouless, podemos usar la ecuación de Gross-Pitaevski para describir las fluctuaciones de ondas de espines y vórtices. Para gran U/t el sistema se comporta como un aislante y podemos considerar las excitaciones de partícula y agujero en el aislante. Éstas son lo suficientemente diluidas a bajas T para permitir un descripción de gas clásico via la ecuación de Boltzmann. En la región intermedia tenemos una transición de fase cuántica y en su vecindad ninguna de las descripciones clásicas es posibles. La teoría describiendo el punto crítico cuántico resulta ser un teoría conforme de campos en $2 + 1$ dimensiones asociada a un punto fijo de Wilson-Fisher, que puede implementarse con la teoría familiar de $\lambda \, \phi^4$. De hecho uno puede usar esta teoría para describir un sistema

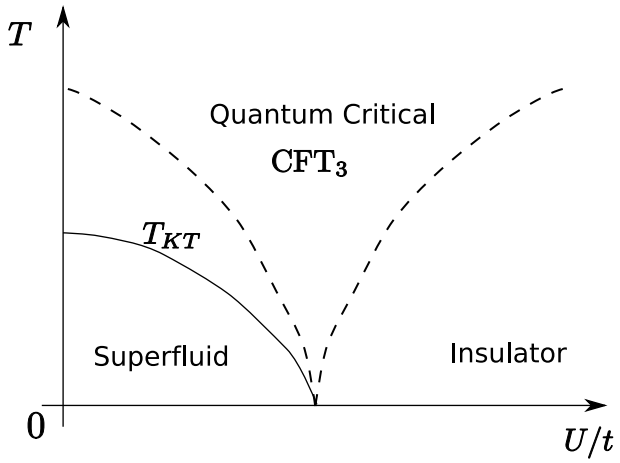

Figure E.1: Diagrama de fase de un model de Bose Hubbard en llenado entero. Las líneas de rallas son cruces, mientras que las línea continua es la transición de Kosterlitz-Thouless a T_{KT}.

cerca del punto crítico a temperatura finita con un cruce suave a los otros regímenes. Véase figura E.1.

La teoría de la región crítica cuántica muestra que los coeficientes de transporte, y los tiempos de relajación al equilibrio local, no son proporcionales a un tiempo de dispersión libre entre excitaciones, como en el caso de una teoría de Boltzmann de cuasipartículas [11]. Sino, el sistema se comporta como un fluido perfecto en el que el tiempo de relajación es tan corto como sea posible, y está determinado por la temperatura absoluta. Los coeficientes de transporte de esta fluido perfecto crítico cuántico también no dependen de la fuerza de interacción, y pueden ser conectados a constantes fundamentales de la naturaleza. Tales son los ejemplos de la conductividad eléctrica σ o el transporte de momento relacionado con la viscosidad de corte η (más precisamente con el cociente de la viscosidad y la densidad de entropía s), i.e.

$$\sigma = \frac{e_*^2}{h}\Phi_\sigma \ , \qquad \frac{\eta}{s} = \frac{\hbar}{k_B}\Phi_\eta \ , \tag{E.0.5}$$

donde Φ_σ y Φ_η son algunos números de orden unidad. e_* es la carga de los portadores.

Debido a la ausencia de una imagen a base de cuasipartículas en el regimen de acoplo fuertes, un cálculo directo de los observables desde la acción de la QFT es difícil. El único enfoque conocido para extraer algunas predicciones analíticas viene de expansiones en gran N y $(d'-\varepsilon)$. Sin embargo, ambas expansiones no son ni directas ni rigurosas, y requieren una resumación motivada físicamente de la expansión perturbartiva desnuda a todo orden. Uno querría tener soluciones exactas a los puntos críticos cuánticos donde uno pueda comprobar los resultados anteriores, así como nuevas herramientas que nos provean con intuición sobre la posible fenomenología.

La correspondencia AdS/CFT

Aquí es donde la correspondencia AdS/CFT hace su aparición como una herramienta útil para explorar los alrededores de estos puntos críticos cuánticos.

Hemos visto que cerca de los puntos críticos cuánticos, los sistemas pueden ser descritos por medio de teorías conformes de campos (a temperatura cero o finita). Lo que la correspondencia AdS/CFT vindica es para ciertos tipos de CFTs en $d+1$ dimensiones, uno puede dar una descripción débilmente acoplada en términos de una teoría clásica gravitatoria en AdS_{d+2}. Más genéricamente tenemos que una teoría en un espacio-tiempo en $d+2$ dimensiones asintótico a AdS_{d+2} va a ser dual a alguna QFT en $d+1$ dimensiones en su regimen de fuerte acoplo y límite de gran N, donde N es un número de grados de libertad, y que tiene un punto fijo conforme en el UV. Por medio de esta dualidad fuerte-débil uno puede esperar explorar y ganar intuición del lado de la QFT, que de otra manera es de muy difícil estudio por medio de métodos convencionales.

La correspondencia AdS/CFT es todavía una conjetura, ninguna demostración rigurosa se conoce hasta hoy día.[2] No obstante evidencia aplastante en su favor se ha ido reuniendo. Nosotros no vamos a intentar motivarla una vez más[3] sino que resaltaremos su estructura y la relación de los diferentes elementos que la componen. De hecho tomaremos la correspondencia en su versión más radical y nos atrevermos a proponer la definición de una teoría cuántica de campos directamente por medio de una teoría dual gravitatoria siguiendo el diccionario holográfico.

La correspondencia AdS/CFT puede ser entendida como una realización de la propuesta del 'campo maestro' [14] al límite de gran N de teorías gauge. En el límite de gran N uno espera que la integral de caminos esté dominada por puntos de silla cuya contribución puede ser reasignada a puntos de silla de una acción clásica efectiva para un campo maestro que, en principio, no está relacionado con los grados de libertad en el UV de la teoría gauge. Lo que la conjetura de Maldacena nos dice es que los puntos de silla clásicos pertenecen a una teoría gravitatoria en una dimensión extra. La dimensión exra se convierte en un geometrización de la escala de energía de la teoría de campos y nos permite conceptualizar fenómenos dependientes de escala, tales como confinamiento y temperatura, de forma novedosa.

Para construir ejemplos controlados de la dualidad y el diccionario preciso, uno empieza con una construcción de Teoría de Cuerdas. Normalmente conlleva una pila de branas. La teoría del worldvolume a energías bajas es una teoría gauge. Por otro lado un número

[2] a pesar de progresos excepcionales en esta dirección bajo el paraguas de integrabilidad en el caso particular de la dualidad $\mathcal{N}=4$ SYM - $\mathrm{AdS}_5 \times S^5$, véase para más información [12] y referencias ahí.

[3] véase por ejemplo [13].

suficiente de branas reaccionarán de vuelta en la geometría y un límite de horizonte cercano de desacoplo da un espacio-tiempo que se conjetura codifica la misma información física que la teoría del worldvolume a bajas energías, la teoría gauge. El ejemplo por antonomasia es la dualidad entre $\mathcal{N} = 4$ SU(N) SYM en cuatro dimensiones y supercuerdas tipo IIB en $\mathrm{AdS}_5 \times S^5$.

Como consecuencia de este tipo de construcciones uno termina con un espacio-tiempo cuyas isometrías corresponden a las simetrías globales de la QFT dual. Simetrías tipo R se mapean a las isometrías de variedades compactas. En el caso de $\mathcal{N} = 4$ SU(N) SYM, es una CFT y por lo tanto la necesidad de tener AdS. La R-simetría $SU(4)$ corresponde a la S^5.

Uno también obtiene que los acoplos y los parámetros de ambos QFT y teoría gravitatoria están completamente fijados como función unos de otros. En la teoría gauge uno tiene básicamente el acoplo de Yang-Mills g_{YM} y el rango del grupo gauge N. En el límite de gran N éstos aparecen en la combinación del parámetro de t´Hoof $\lambda = g^2_{\mathrm{YM}} N$. Por otro lado, la teoría gravitatoria tiene tres parámetros: el radio de AdS R, la constante gravitatoria $G_N^{(d+2)}$ y la longitud de la cuerda ℓ_s. Para el caso particular de $\mathcal{N} = 4$ SU(N) SYM uno obtiene

$$\frac{R^4}{l_s^4} = \lambda \,, \qquad \frac{R^8}{G_N^{(10)}} \sim N^2 \,. \tag{E.0.6}$$

De esto vemos que cuando la teoría de YM es débilmente acoplada ($\lambda \ll 1$), el espacio-tiempo está altamente curvado y viceversa. Cuando el espacio-tiempo está débilmente curvado podemos usar la aproximación de supergravedad a la Teoría de Cuerdas pero la QFT dual está fuertemente acoplada. Desde esta relación también aprendemos que en general tendremos que

$$N_{\mathrm{eff}} \sim \frac{R^d}{G_N^{(d+2)}} \tag{E.0.7}$$

donde N_{eff} es el número de effectivo de grados de libertad gauge y $G_N^{(d+2)}$ se refiere a la constante de Newton bajo dimensión reduccional a lo largo de la variedad compacta.

La dualidad también nos enseña una relación muy detallada entre campos en el lado gravitatorio y operadores en la QFT dual. Normalmente pueden ser identificados gracias a la regla de que los modos no-normalizables de los campos en la frontera del espacio-tiempo actúan como fuentes de sus respectivos operadores duales. En particular tenemos la igualdad de la función de partición de la teoría gravitatoria y la teoría gauge, tal que

$$Z_{\mathrm{string}}[\phi(x)|_{\mathrm{boundary}} = \phi_0(\vec{x})] = \langle e^{\int d^{d+1}\phi_0(\vec{x})\mathcal{O}(\vec{x}))} \rangle_{\mathrm{QFT}} \,. \tag{E.0.8}$$

Además corrientes conservadas globales en la QFT son duales a campos gauge. De la misma manera, la conservación del tensor de energía-momento en la QFT (dual al campo de la

métrica) requiere que la teoría dual contenga gravedad. Las funciones de correlación pueden ser calculadas tomando derivadas funcionales de (E.0.8). Éstas se reducen a encontrar las soluciones de ecuaciones de movimento de campos en el volumen que se propagan desde la frontera en el volumen, interactúan y luego regresan a la frontera.

Para poner la teoría a temperatura finita, uno introduce agujeros negros en el volumen con una radiación de Hawking igual a la temperatura deseada en la QFT dual, pero sin modificar las asíntotas del espacio-tiempo. Uno puede todavía usar (E.0.8) para calcular las funciones de correlación a temperatura finita, pero en el caso de tiempo real (funciones de Green retardadas o adelantadas) uno tiene que extender la prescripción para prestar atención a las condiciones de frontera en el horizonte de los campos [15].

Desde el punto de vista de aplicaciones de Materia Condensada, esto es muy útil puesto que nos permite calcular los coeficientes de transporte, tales como σ y η, simplemente resolviendo ecuaciones de movimiento en el fondo dado por el agujero negro. Incluso un simple tratamiento de punto de silla de la teoría gravitatoria nos da ya una dinámica para la CFT que tiene coeficientes de transporte no-nulos y no-singulares, tiene una producción de entropía positiva, y se relaja al equilibrio térmico local. Éstas son unas características que hacen la correspondencia AdS/CFT tan atractiva: no tienen ningún precedente en teorías previas de campo medio de sistemas cuánticos de muchos cuerpos.

Promovido en primer lugar por el trabajo de [16, 17], enfocado ante todo en la dinámica de transporte y coeficientes, la aplicación de AdS/CFT a transiciones de fase cuánticas se ha visto que es una herramienta útil. El principal obstáculo, sin embargo, es la disparidad entre la teorías gauges emergentes típicas en los sistemas de Materia Condensada, que son en su mayor parte U(1) o incluso SU(2), y la aproximación de gran N inevitable en un tratamiento del dual gravitatorio. Los resultados no son predicciones de alta precisión que se pueden comparar ciegamente con el experimento. No obstante pueden ser vistos como proveedores de un conocimiento invaluable por medio de modelos exactamente resolubles de puntos críticos cuánticos y, de forma más importante, ponen a nuestro alcance una nueva herramienta para explorar la fenomenología de estos sistemas.

Es en esta línea de pensamiento donde esta tesis se desarrolla. Pondremos a trabajar a la correspondencia AdS/CFT para estudiar diferentes aspectos de estos puntos críticos cuánticos. En la primera parte usaremos la dualidad para explorar la estructura de los estados fundamentales de puntos críticos con $z = 1$. Lo investigaremos por medio de la entropía de entrelazamiento. Gracias la prescripción holográfica de Ryu y Takayanagi [18], seremos capaces de navegar por las propiedades de la entropía de entrelazamiento para teorías en acoplamiento fuerte, véase el capítulo 2 para un resumen. En particular elucidaremos la

relación entre la localidad de las interacciones y la ley del área en el capítulo 3. En el capítulo 4 exploraremos de forma sistemática los diferentes posibles comportamientos de la entropía de entrelazamiento en duales gravitatorios genéricos con $z = 1$.

En la segunda parte de esta tesis abordaremos un objetivo distinto e iremos a por el estudio de extensiones de la aplicabilidad de la correspondencia AdS/CFT a otros tipos de puntos críticos. Hasta ahora la única clase de fondos gravitatorios que han sido minuciosamente estudiados en la literatura corresponden a teorías con un exponente crítico dinámico $z = 1$. Son precisamente los que son asintóticos a AdS: la invariancia bajo escala consiste en transformaciones que tratan el espacio y el tiempo en plena igualdad. Sin embargo hay otros puntos críticos (más exóticos) con $z \neq 1$. Un ejemplo particular surge como un punto crítico aislado a $T = 0$ en un gas de Fermi no-relativista en tres dimensiones cerca de una resonancia de Feshbach. Este punto fijo tiene [19] una simetría conforme no-relativista (el grupo de Schrödinger) con $z = 2$. Lo que haremos en la segunda parte es el estudio preciso de las recientes construcciones de fondos gravitatorios que implementan el grupo de Schrödinger [3, 4], vease el capítulo 5 para un resumen. En particular estudiaremos su formulación Hamiltoniana (capítulo 6), sus funciones de correlación (capítulo 7) y al final entenderemos en términos de un modelo estadístico simple su termodinámica conocida y que difiere de los fermiones en unitariedad (capítulo 8). Finalmente, en el capítulo 9 ofreceremos un resumen y conclusiones.

El trabajo contenido en esta tesis está basado en los artículos del autor [20, 21, 22, 23, 24].

Appendix F

Resumen y conclusiones generales

[1] En esta tesis hemos estudiado la entropía de entrelazamiento y sistemas no-relativistas invariantes Schrödinger desde la correspondencia AdS/CFT. Este estudio toma lugar dentro del programa mucho más amplio de aplicación de la correspondencia AdS/CFT a la Materia Condensada. Nuestro estudio está directamente conectado a la aplicación de AdS/CFT a la investigación de sistemas cerca de transiciones de fase cuánticas. Por medio de la entropía de entrelazamiento uno puede ganar información acerca de la estructura cuántica de los estados fundamentales en el punto cuántico crítico, como hemos mostrado en la primera parte de esta tesis. En la segunda parte, hemos contribuido al estudio de los duales holográficos de puntos cuánticos críticos invariantes Schrödinger con $z = 2$.

Entropía de Entrelazamiento

La entropía de entrelazamiento nos permite estudiar la estructura de estados fundamentales no-degenerados de sistemas cerca de una transición de fase cuántica o genericamente descritos por QFTs. A partir del escaleo de la entropía de entrelazamiento como función de la escala de longitud de una región bajo consideración, uno puede leer muchas propiedades de la teoría. En particular, en el capítulo 3 vimos cómo la localidad de las interacciones está codificado en la ley del área de la contribución no-universal (o dependiente del tope UV). Por otro lado, en el capítulo 4, vimos cómo la entropía de entrelazamiento renormalizada, o lo que es lo mismo la contribución universal independiente de todo corte UV, codifica la información relativa a la presencia de saltos de masas y el número efectivo de grados de libertad en la teoría. Todos estos análisis fueron hechos en el límite de gran N para sistemas fuertemente acoplados con $z = 1$ por medio del ansatz holográfico de [18].

[1] Traducción al español del capítulo 9 / Spanish translation of chapter 9.

Como resultado del análisis del capítulo 3, argumentamos que la combinación de la simetría de Lorentz más una densidad de estados más o menos habitual a altas energías es suficiente para garantizar una ley del área en la contribución UV a la entropía de entrelazamiento. Encontramos y analizamos dos familias de teorías no-locales fuera de esta categoría: super Yang-Mills no-conmutativo y Little String Theory (LST). Ambos presentan un ley del volumen por debajo de su escala espacial de no-localidad. El primero evade la ley del área debido a su rotura de la simetría de Lorentz por debajo de la escala de no commutatividad. LST está también fuera debido a su densidad de estados inusual correspondiente a un comportamiento de tipo Hagedorn con una temperatura límite por encima de la escala no-commutativa de energía.

La conclusión principal del capítulo 3 es que la entropía de entrelazamiento provee un criterio de localidad en la teoría, i.e. ley del área de la contribución no-universal, y que se puede trazar a la combinación de invariancia Lorentz más una densidad de estados normal a altas energías. Como consecuencia, cualquier teoría no-local violará alguna de estas dos. En particular nuestro análisis respalda la interpretación del dual de espacio-tiempos planos como una teoría no-local debido a su ley del volumen.

En el capítulo 4, aprendimos que de la entropía de entrelazamiento renormalizada uno puede leer las diferentes escalas de la teoría y sus grados de libertad efectivos. Estudiamos de forma sistemática la entropía de entrelazamiento renormalizada para diferentes escenarios genéricos que pueden aparecer en construcciones holográficas asintóticas a AdS. Encontramos que en modelos fenomenológicos (paredes suaves y fuertes) de confinamiento, la entropía de entrelazamiento renormalizada presenta una ley del volumen. Esto está en contraste con modelos bien definidos de Teoría de Cuerdas (paredes resueltas) donde la entropía de entrelazamiento se anula, o de forma equivalente satura. Sólo el último caso está en acuerdo con un análisis en acoplo débil. Por lo tanto interpretamos la ley del volumen como una característica no física de los modelos fenomenológicos.

También obtuvimos que generalmente, y como era de esperar, las geometrías de agujeros negros dan lugar a una contribución extensiva a la entropía de entrelazamiento a temperatura finita. Encontramos, no obstante, un caso donde esta extensividad se mantiene a temperatura cero: aquél de un agujero negro diónico (respaldado por una contrucción de Teoría de Cuerdas). Corresponde a un sistema con un condensado de carga y/o un campo magnético externo a temperatura cero. Este comportamiento es nuevo e insinúa sobre nuevos tipos de puntos críticos cuánticos hasta ahora no identificados desde un análisis de QFT en acoplo débil.

Por último también especulamos sobre una posible modificación de la prescripción holográfica de [18] en la presencia de agujeros negros a temperatura finita. Al incorporar la

posibilidad de superficies mínimas que crucen el horizonte, pensamos que la misma cantidad holográfica dual está ahora midiendo la información mutua. Esto está de acuerdo con una ley del área en ambos lados de la dualidad.

Cerremos comentando algunas cuestiones abiertas relativas a la entropía de entrelazamiento. Una de las cuestiones más acuciantes en todo nuestro análisis y en la prescripción holográfica en sí es que sólo captura las contribuciones dominantes $\mathcal{O}(N_{\text{eff}})$ a la entropía de entrelazamiento. Correcciones subdominantes $1/N_{\text{eff}}$ simplemente no están disponibles. Uno debería intentar extender el ansatz en esta dirección.

También sería interesante extender este análisis a otros sistemas críticos con $z \neq 1$, en particular a los modelos invariantes Schrödinger $z = 2$ y a teorías tipo Lifshitz. Una rápida aplicación del ansatz holográfico en estos modelos sugiere que la ley del área continúa dándose. Sin embargo un análisis más completo y detallado sería deseable. También consideramos una extensión de la prescripción holográfica que incluya la entropía de entrelazamiento topológica. Aunque hubo un intento de abordarlo en [224] creemos que un analisis mucho más detallado es necesario.

AdS/CFT no-relativista

En la segunda parte de esta tesis, hemos estudiado los duales holográficos de teorías de campos invariantes Schrödinger, presentadas por primera vez en [3, 4]. La motivación física principal detrás de ello, es una implementación del punto crítico de los fermiones en unitariedad que presenta precisamente invariancia bajo el grupo de Schrödinger.

En el capítulo 6 analizamos la imagen Hamiltoniana del fondo Sch_{d+3}. Encontramos que a nivel de campos libres en el volumen, la simetría conforme está realizada por medio de una mecánica cuántica conforme para la dirección radial holográfica. De forma más notable la misma mecánica cuántica conforme fue encontrada por medio de una construcción AdS pura. El enfoque Hamiltoniano también nos llevó al ansatz correcto para una métrica que incorpora el efecto de un potencial harmónico externo para el sistema. Encontramos un acuerdo perfecto de la correspondencia estado-operador en la teoría invariante Schrödinger, realizada entre los autoestados de energía en el potencial harmónico y las dimensiones de escaleo de los campos. La misma estructura de autoestados de energía está en acuerdo con los cálculos de gases de átomos fríos en potenciales harmónicos. Esta comparación nos motivó a dar una interpretación física de la dirección radial holográfica como dando cuenta de las excitaciones colectivas del gas. Apoyados en el formalismo Hamiltoniano también dimos algunos modelos heurísticos de otros escenarios donde moleculas pueden formarse.

En el capítulo 7, profundizamos en nuestro análisis del fondo Sch_{d+3} pero desde el punto de vista de las funciones de correlación a n-puntos, a temperatura cero y cero potencial químico. Dimos una fórmula explícita relacionando las funciones escalares a n-puntos a nivel árbol en Sch_{d+3} con la misma función a n-puntos en AdS, como una proyección de las inserciones de operadores a lo largo de la dirección tipo luz implementando el operador número,

$$\langle \phi_1(\bar{x}_1) \dots \phi_n(\bar{x}_n) \rangle_{\mathrm{Sch}}^{(\text{tree level})} = \int \prod_{k=1}^{n} d\xi_k \, e^{-i \sum_{j=1}^{n} (M_j \xi_j)} \langle \phi_1(\bar{x}_1, \xi_1) \dots \phi_n(\bar{x}_n, \xi_n) \rangle_{\mathrm{AdS}}^{(\text{tree level})} \, .$$

Esta fórmula demuestra la equivalencia completa a nivel árbol de la construcción en AdS_{d+3} puro y Sch_{d+3}. Esta equivalencia está apoyada por la implementación desde Teoría de Cuerdas de Sch_5, que es dual a cierto tipo de deformación no-commutativa de $\mathcal{N} = 4$ SYM. A nivel árbol, las funciones de correlación de una teoría no-conmutativa y su versión conmutativa coinciden, salvo factores de fase globales. A nivel de lazos la relación anterior no se mantiene y tenemos que usar el fondo de Sch_{d+3}. Encontramos que a nivel de un lazo con una dirección compacta, tenemos el típico problema de DLCQs y uno necesita regularizar la teoría. Una posibilidad es mediante un potencial químico finito.

Desde la relación a nivel árbol entre las funciones de correlación de AdS y Sch, pudimos calcular las funciones a 2 y 3 puntos a nivel árbol. Comparamos estos resultados con aquellos de una QFT de bosones en unitariedad. Aunque la función a 3-puntos no está completamente determinada por la simetría, encontramos acuerdo salvo por el factor global de normalización como era de esperar. Esto fija la esperanza que la correspondencia puede ponerse a funcionar a nivel árbol.

Finalmente en el capítulo 8 encaramos la versión a temperatura finita y potencial químico finito de Sch_{d+3} disponible en la literatura, el agujero negro Schwarzschild-Sch_{d+3} [170, 169, 164]. En particular investigamos la razón detrás del comportamiento patológico de las funciones termodinámicas, que divergen como una potencia de $T/|\mu|$. Esto es especialmente desconcertante cuando se compara con lo que uno esperaría para los átomos fríos en unitariedad, donde uno no encuentra este comportamiento divergente sino un cambio a la fase superfluida. Dimos una explicación simple en términos de un gas ideal con una torre no-relativista Kaluza-Klein de especies, que reproduce todos los observables termodinámicos del agujero negro dual Schwarzschild-Sch. Nuestro análisis muestra que el agujero negro no-relativista está de hecho contando grados de libertad en todas las $d + 2$ dimensiones del espacio-tiempo y excitando completamente la dirección extra. Concluimos que la fase superfluida no-relativista del sistema físico en d dimensiones va a estar relacionada probablemente con agujeros negros que localizan en la dimensión extra.

De todo este trabajo llegamos a la conclusión que Sch_{d+3} sólo puede verse como un candidato prometedor para describir el punto crítico cuántico de teorías no-relativistas conformes a nivel árbol y a temperatura y potencial químicos nulos. Ahora mismo mucho más trabajo es necesario para poder evaluar la aplicabilidad de las construcciones no-relativistas AdS/CFT actuales para el caso de temperatura y potencial químico finitos, que es donde están las aplicaciones reales a Materia Condensada. Emplazamos la búsqueda de fondos apropriados para temperatura y potencial químicos finitos como uno de los problemas más urgentes a abordadar en el futuro.

Como comentario final, simplemente decir que la aplicación de la correspondencia AdS/CFT, y los métodos holográficos a Materia Condensada, se encuentra es un estadío de pleno desarrollo y todavía en su infancia. Los fenómenos y modelos que han sido tratados incluyen gases de átomos fríos en unitariedad [3, 4], superconductividad [5], superfluidez [6], líquidos cuánticos [7, 8]. La correspondencia AdS/CFT resplandece en aquellos regímenes donde la noción de cuasipartículas o parámetros de orden desaparecen completamente. Sin embargo al mismo tiempo sólo podemos aplicarla con algún tipo de control en situaciones donde grandes cantidades de supersimetría y teorías gauge en el límite de gran N están presentes, que no son precisamente habituales en el laboratorio. Tan pronto como queramos abandonar estos escenarios, o bien perdemos completamente todo poder computacional puesto que terminamos con espacio-tiempos altamente curvados, o bien, simplemente perdemos cualquier control de la teoría cuántica de campos dual al simplemente tomar algún espacio-tiempo puramente ad hoc de forma fenomenológica. No obstante, podemos considerar todas estas construcciones como dándonos una intuición fresca y nueva, e incluso puntos de referencia cuantitativos, a algunos problemas viejos y muy difíciles que la gente hasta ahora sólo ha podido tratar parcialmente por medio de complicadas expansiones y técnicas, de las que uno puede llegar a extraer algún número pero ciertamente ninguna imagen física o intuición. Esperemos que este nuevo camino holográfico realmente abra nuevas vías de pensamiento y traiga el tipo de intuición original necesario para alcanzar nuevos progresos.

Bibliography

[1] J. M. Maldacena, "The large N limit of superconformal field theories and supergravity," Adv. Theor. Math. Phys. **2**, 231 (1998) [Int. J. Theor. Phys. **38**, 1113 (1999)] [arXiv:hep-th/9711200].

S. S. Gubser, I. R. Klebanov and A. M. Polyakov, "Gauge theory correlators from non-critical string theory," Phys. Lett. B **428**, 105 (1998) [arXiv:hep-th/9802109].

E. Witten, "Anti-de Sitter space and holography," Adv. Theor. Math. Phys. **2**, 253 (1998) [arXiv:hep-th/9802150].

[2] P. Kovtun, D. T. Son and A. O. Starinets, "Viscosity in strongly interacting quantum field theories from black hole physics," Phys. Rev. Lett. **94** (2005) 111601 [arXiv:hep-th/0405231].

[3] D. T. Son, "Toward an AdS/cold atoms correspondence: a geometric realization of the Schroedinger symmetry," arXiv:0804.3972 [hep-th].

[4] K. Balasubramanian and J. McGreevy, "Gravity duals for non-relativistic CFTs," arXiv:0804.4053 [hep-th].

[5] S. A. Hartnoll, C. P. Herzog and G. T. Horowitz, "Building a Holographic Superconductor," Phys. Rev. Lett. **101** (2008) 031601 [arXiv:0803.3295 [hep-th]].

[6] C. P. Herzog, P. K. Kovtun and D. T. Son, "Holographic model of superfluidity," arXiv:0809.4870 [hep-th].

[7] H. Liu, J. McGreevy and D. Vegh, "Non-Fermi liquids from holography," arXiv:0903.2477 [hep-th].

[8] M. Cubrovic, J. Zaanen and K. Schalm, "Fermions and the AdS/CFT correspondence: quantum phase transitions and the emergent Fermi-liquid," arXiv:0904.1993 [hep-th].

[9] S. Sachdev, *Quantum Phase Transitions*, Cambridge University Press, Cambridge (1999).

[10] S. A. Hartnoll, "Lectures on holographic methods for condensed matter physics," arXiv:0903.3246 [hep-th].

[11] S. Sachdev and M. Mueller, "Quantum criticality and black holes," arXiv:0810.3005 [cond-mat.str-el].

[12] N. Dorey, "Integrability And The Ads/Cft Correspondence," Class. Quant. Grav. **25** (2008) 214003.

[13] I. R. Klebanov, "TASI lectures: Introduction to the AdS/CFT correspondence," arXiv:hep-th/0009139.

E. D'Hoker and D. Z. Freedman, "Supersymmetric gauge theories and the AdS/CFT correspondence," arXiv:hep-th/0201253.

J. M. Maldacena, "Lectures on AdS/CFT," arXiv:hep-th/0309246.

G. T. Horowitz and J. Polchinski, "Gauge / gravity duality," arXiv:gr-qc/0602037.

[14] S. Coleman, *Aspects of Symmetry*, Cambridge University Press, Cambridge (1985).

[15] D. T. Son and A. O. Starinets, "Minkowski-space correlators in AdS/CFT correspondence: Recipe and applications," JHEP **0209** (2002) 042 [arXiv:hep-th/0205051].

[16] C. P. Herzog, P. Kovtun, S. Sachdev and D. T. Son, "Quantum critical transport, duality, and M-theory," Phys. Rev. D **75** (2007) 085020 [arXiv:hep-th/0701036].

[17] S. A. Hartnoll and P. Kovtun, "Hall conductivity from dyonic black holes," Phys. Rev. D **76**, 066001 (2007) [arXiv:0704.1160 [hep-th]].

S. A. Hartnoll, P. K. Kovtun, M. Muller and S. Sachdev, "Theory of the Nernst effect near quantum phase transitions in condensed matter, and in dyonic black holes," Phys. Rev. B **76** (2007) 144502 [arXiv:0706.3215 [cond-mat.str-el]].

[18] S. Ryu and T. Takayanagi, "Holographic derivation of entanglement entropy from AdS/CFT," Phys. Rev. Lett. **96**, 181602 (2006) [arXiv:hep-th/0603001].

"Aspects of holographic entanglement entropy," JHEP **0608**, 045 (2006) [arXiv:hep-th/0605073].

[19] Y. Nishida and D. T. Son, "Nonrelativistic conformal field theories," Phys. Rev. D **76** (2007) 086004 [arXiv:0706.3746 [hep-th]].

[20] J. L. F. Barbon and C. A. Fuertes, "Holographic entanglement entropy probes (non)locality," JHEP **0804** (2008) 096 [arXiv:0803.1928 [hep-th]].

[21] J. L. F. Barbon and C. A. Fuertes, "A note on the extensivity of the holographic entanglement entropy," arXiv:0801.2153 [hep-th].

[22] J. L. B. Barbon and C. A. Fuertes, "On the spectrum of nonrelativistic AdS/CFT," JHEP **0809** (2008) 030 [arXiv:0806.3244 [hep-th]].

[23] C. A. Fuertes and S. Moroz, "Correlation functions in the non-relativistic AdS/CFT correspondence," arXiv:0903.1844 [hep-th].

[24] J. L. F. Barbon and C. A. Fuertes, "Ideal gas matching for thermal Galilean holography," arXiv:0903.4452 [hep-th].

[25] M. A. Nielsen and I. Chuang, "Quantum Computation and Quantum Communication," Cambridge University Press, Cambridge, 2000.

[26] J. Bell, "Speakable and unspeakable in Quantum Mechanics," Cambridge University Press, Cambridge, 1987.

[27] L. Amico, R. Fazio, A. Osterloh and V. Vedral, "Entanglement in Many-Body Systems," Rev. Mod. Phys. **80** (2008) 517 [arXiv:quant-ph/0703044].

[28] C. H. Bennett, H. J. Bernstein, S. Popescu, and B. Schumacher, "Concentrating Partial Entanglement by Local Operations,| 1996 Phys. Rev. A **53** 2046 [arXiv:quant-ph/9511030].

[29] T. M. Fiola, J. Preskill, A. Strominger and S. P. Trivedi, "Black hole thermodynamics and information loss in two-dimensions," Phys. Rev. D **50**, 3987 (1994) [arXiv:hep-th/9403137].

[30] C. Holzhey, F. Larsen and F. Wilczek, "Geometric and renormalized entropy in conformal field theory," Nucl. Phys. B **424**, 443 (1994) [arXiv:hep-th/9403108].

[31] L. Bombelli, R. K. Koul, J. H. Lee and R. D. Sorkin, "A Quantum Source of Entropy for Black Holes," Phys. Rev. D **34**, 373 (1986).

[32] M. Srednicki, "Entropy and area," Phys. Rev. Lett. **71**, 666 (1993) [arXiv:hep-th/9303048].

[33] C. G. . Callan and F. Wilczek, "On geometric entropy," Phys. Lett. B **333**, 55 (1994) [arXiv:hep-th/9401072].

[34] J. D. Bekenstein, "Black holes and entropy," Phys. Rev. D **7**, 2333 (1973).

[35] S. W. Hawking, "Particle Creation By Black Holes," Commun. Math. Phys. **43**, 199 (1975) [Erratum-ibid. **46**, 206 (1976)].

[36] T. Jacobson, "Black hole entropy and induced gravity," arXiv:gr-qc/9404039.

[37] L. Susskind and J. Uglum, "Black hole entropy in canonical quantum gravity and superstring theory," Phys. Rev. D **50**, 2700 (1994) [arXiv:hep-th/9401070].

[38] V. P. Frolov, D. V. Fursaev and A. I. Zelnikov, "Statistical origin of black hole entropy in induced gravity," Nucl. Phys. B **486**, 339 (1997) [arXiv:hep-th/9607104].

[39] V. P. Frolov and D. V. Fursaev, "Mechanism of generation of black hole entropy in Sakharov's induced gravity," Phys. Rev. D **56**, 2212 (1997) [arXiv:hep-th/9703178].

[40] A. Strominger and C. Vafa, "Microscopic Origin of the Bekenstein-Hawking Entropy," Phys. Lett. B **379**, 99 (1996) [arXiv:hep-th/9601029].

[41] J. M. Maldacena, "Eternal black holes in Anti-de-Sitter," JHEP **0304**, 021 (2003) [arXiv:hep-th/0106112].

[42] R. Brustein, M. B. Einhorn and A. Yarom, "Entanglement interpretation of black hole entropy in string theory," JHEP **0601** (2006) 098 [arXiv:hep-th/0508217].

[43] S. Hawking, J. M. Maldacena and A. Strominger, "DeSitter entropy, quantum entanglement and AdS/CFT," JHEP **0105**, 001 (2001) [arXiv:hep-th/0002145].

[44] R. Emparan, "Black hole entropy as entanglement entropy: A holographic derivation," JHEP **0606** (2006) 012 [arXiv:hep-th/0603081].

[45] K. M. R. Audenaert, J. Eisert, M. B. Plenio, and R. F. Werner, Phys. Rev. A **66**, 042327 (2002).

[46] T. F. Osborne, and M. A. Nielsen, Phys. Rev. A **66**, 032110 (2002)

[47] A. Osterloh, L. Amico, G. Falci, and R. Fazio, Nature **416**, 608 (2002).

[48] G. Vidal, J. I. Latorre, E. Rico and A. Kitaev, "Entanglement in quantum critical phenomena," Phys. Rev. Lett. **90**, 227902 (2003) [arXiv:quant-ph/0211074].

[49] S. K. Foong and S. Kanno, Phys. Rev. Lett. 72, 1148 (1994)

[50] D. N. Page, "Expected Entropy Of A Subsystem," Phys. Rev. Lett. **71** (1993) 1291 [arXiv:gr-qc/9305007].

[51] S. Sen, "Average Entropy of a Subsystem," Phys. Rev. Lett. **77** (1996) 1 [arXiv:hep-th/9601132].

[52] J. Eisert, M. Cramer and M. B. Plenio, "Area laws for the entanglement entropy - a review," [arXiv:0808.3773]

[53] M. B. Hastings, J. Stat. Mech. , P08024. (2007)

[54] I. Peschel, J. Stat. Mech. , P12005 (2004)

[55] N. Schuch, M. M. Wolf, F. Verstraete, and J. I. Cirac, Phys. Rev. Lett. **100**, 030504 (2008).

[56] F. Verstraete, and J. I. Cirac, Phys. Rev. B **73**, 094423 (2006).

[57] U. Schollwöck, Rev. Mod. Phys. **77**, 259 (2005)

[58] S. R. White, Phys. Rev. Lett. **69**, 2863 (1992).

[59] S. Ostlund and S. Rommer, "Thermodynamic Limit Of Density Matrix Renormalization For The Spin-1 Heisenberg Chain," Phys. Rev. Lett. **75**, 3537 (1995) [arXiv:cond-mat/9503107].

[60] J. Dukelsky et al., Europhys. Lett. 43, 457 (1997)

[61] F. Verstraete, A. Weichselbaum, U. Schollwck, J. I. Cirac, and Jan von Delft, "Variational matrix product state approach to quantum impurity models", [arXiv:cond-mat/0504305].

[62] F. Verstraete and J. I. Cirac, "Matrix product states represent ground states faithfully," Physical Review B, 73 **9** (2006), [arXiv:cond-mat/0505140].

[63] D. Perez-Garcia, F. Verstraete, M. M. Wolf, J. I. Cirac, "Matrix Product State Representations," Quantum Inf. Comput. 7, 401 (2007), [arXiv:quant-ph/0608197].

[64] F. Verstraete and J. I. Cirac, "Renormalization algorithms for Quantum-Many Body Systems in two and higher dimensions," arXiv:cond-mat/0407066.

[65] M. B. Hastings, Phys. Rev. B **69**, 104431 (2004)

[66] P. Calabrese and J. L. Cardy, "Entanglement entropy and quantum field theory," J. Stat. Mech. **0406** (2004) P002 [arXiv:hep-th/0405152].

P. Calabrese and J. L. Cardy, "Entanglement entropy and quantum field theory: A non-technical introduction," Int. J. Quant. Inf. **4** (2006) 429 [arXiv:quant-ph/0505193].

[67] M. Cramer and J. Eisert, New J. Phys. **8** 71 (2006).

[68] M. Cramer, J. Eisert, M. B. Plenio, and J. Dreissig, Phys. Rev. A **73**, 012309 (2006).

[69] M. B. Plenio, J. Eisert, J. Dreissig, and M. Cramer, Phys. Rev. Lett. 94, 060503 (2005)

[70] M. Cramer, J. Eisert, and M. B. Plenio, Phys. Rev. Lett. **98**, 220603 (2007).

[71] D. Gioev, and I. Klich, Phys. Rev. Lett. **96**, 100503 (2006)

[72] M. M. Wolf, Phys. Rev. Lett. **96**, 010404 (2006)

[73] W. Li, L. Ding, R. Yu, T. Roscilde, and S. Haas, Phys. Rev. B **74** 073103 (2006).

[74] E. Fradkin and J. E. Moore, "Entanglement entropy of 2D conformal quantum critical points: hearing the shape of a quantum drum," Phys. Rev. Lett. **97** (2006) 050404 [arXiv:cond-mat/0605683].

[75] B. Hsu, M. Mulligan, E. Fradkin, and E. Kim, "Universal entanglement entropy in two-dimensional conformal quantum critical points," Phys. Rev. B **79**, 115421 (2009) [arXiv:0812.0203]

[76] Max A. Metlitski, Carlos A. Fuertes, Subir Sachdev, "Entanglement Entropy in the O(N) model,", [arXiv:0904.4477].

[77] M. M. Wolf, F. Verstraete, M. B. Hastings, J. I. Cirac, "Area laws in quantum systems: mutual information and correlations," Phys. Rev. Lett. 100, 070502 (2008)

[78] M.Haque, O. S. Zozulya, and K. Schoutens, Phys. Rev. Lett. **98** 060401 (2007)

[79] A. Kitaev and J. Preskill, "Topological entanglement entropy," Phys. Rev. Lett. **96**, 110404 (2006) [arXiv:hep-th/0510092].

[80] M. Levin and X. G. Wen, "Detecting Topological Order in a Ground State Wave Function," Phys. Rev. Lett. **96**, 110405 (2006) [arXiv:cond-mat/0510613]

[81] Z. Nussinov, and G. Ortiz, "A symmetry principle for Topological Quantum Order," [arXiv:cond-mat/0702377].

[82] S. Papanikolaou, K. S. Raman, and E. Fradkin, Phys. Rev. B **76**, 224421 (2007).

[83] Xiao-Gang Wen, "Topological Orders in Rigid States." Int. J. Mod. Phys. B4, 239 (1990).

[84] Chetan Nayak, Steven H. Simon, Ady Stern, Michael Freedman, Sankar Das Sarma, "Non-Abelian Anyons and Topological Quantum Computation," [arXiv:0707.1889].

[85] S. Dong, E. Fradkin, R. G. Leigh and S. Nowling, "Topological Entanglement Entropy in Chern-Simons Theories and Quantum Hall Fluids," JHEP **0805** (2008) 016 [arXiv:0802.3231 [hep-th]].

[86] H. Casini and M. Huerta, "A finite entanglement entropy and the c-theorem," Phys. Lett. B **600** (2004) 142 [arXiv:hep-th/0405111].

[87] H. Casini, C. D. Fosco and M. Huerta, "Entanglement and alpha entropies for a massive Dirac field in two dimensions," J. Stat. Mech. **0507** (2005) P007 [arXiv:cond-mat/0505563].

[88] H. Casini and M. Huerta, "Entanglement and alpha entropies for a massive scalar field in two dimensions," J. Stat. Mech. **0512** (2005) P012 [arXiv:cond-mat/0511014].

[89] L. Bombelli, R. K. Koul, J. H. Lee and R. D. Sorkin, "A Quantum Source of Entropy for Black Holes," Phys. Rev. D **34**, 373 (1986).

M. Srednicki, "Entropy and area," Phys. Rev. Lett. **71**, 666 (1993) [arXiv:hep-th/9303048].

P. Calabrese and J. L. Cardy, "Entanglement entropy and quantum field theory: A non-technical introduction," Int. J. Quant. Inf. **4**, 429 (2006) [arXiv:quant-ph/0505193].

[90] A. A. Belavin, A. M. Polyakov and A. B. Zamolodchikov, "Infinite conformal symmetry in two-dimensional quantum field theory," Nucl. Phys. B **241** (1984) 333.

[91] A. B. Zamolodchikov, "Irreversibility of the Flux of the Renormalization Group in a 2D Field Theory," JETP Lett. **43** (1986) 730 [Pisma Zh. Eksp. Teor. Fiz. **43** (1986) 565].

[92] V. E. Hubeny, M. Rangamani and T. Takayanagi, "A covariant holographic entanglement entropy proposal," JHEP **0707** (2007) 062 [arXiv:0705.0016 [hep-th]].

[93] G. 't Hooft, "Dimensional reduction in quantum gravity," arXiv:gr-qc/9310026.

[94] L. Susskind, "The World As A Hologram," J. Math. Phys. **36** (1995) 6377 [arXiv:hep-th/9409089].

D. Bigatti and L. Susskind, "TASI lectures on the holographic principle," arXiv:hep-th/0002044.

[95] R. Bousso, "A Covariant Entropy Conjecture," JHEP **9907** (1999) 004 [arXiv:hep-th/9905177].

[96] D. V. Fursaev, "Proof of the holographic formula for entanglement entropy," JHEP **0609** (2006) 018 [arXiv:hep-th/0606184].

[97] C. R. Graham and E. Witten, "Conformal anomaly of submanifold observables in AdS/CFT correspondence," Nucl. Phys. B **546** (1999) 52 [arXiv:hep-th/9901021].

[98] J. M. Maldacena, "Wilson loops in large N field theories," Phys. Rev. Lett. **80** (1998) 4859 [arXiv:hep-th/9803002].

S. J. Rey and J. T. Yee, "Macroscopic strings as heavy quarks in large N gauge theory and anti-de Sitter supergravity," Eur. Phys. J. C **22** (2001) 379 [arXiv:hep-th/9803001].

[99] M. Headrick and T. Takayanagi, "A holographic proof of the strong subadditivity of entanglement entropy," Phys. Rev. D **76** (2007) 106013 [arXiv:0704.3719 [hep-th]].

[100] T. Hirata and T. Takayanagi, "AdS/CFT and strong subadditivity of entanglement entropy," JHEP **0702**, 042 (2007) [arXiv:hep-th/0608213].

[101] D. V. Fursaev, "Entanglement Entropy in Quantum Gravity and the Plateau Problem," Phys. Rev. D **77**, 124002 (2008) [arXiv:0711.1221 [hep-th]].

[102] V. E. Hubeny and M. Rangamani, "Holographic entanglement entropy for disconnected regions," JHEP **0803**, 006 (2008) [arXiv:0711.4118 [hep-th]].

[103] M. Banados, C. Teitelboim and J. Zanelli, "The Black hole in three-dimensional space-time," Phys. Rev. Lett. **69**, 1849 (1992) [arXiv:hep-th/9204099].

[104] A. Schwimmer and S. Theisen, "Entanglement Entropy, Trace Anomalies and Holography," Nucl. Phys. B **801** (2008) 1 [arXiv:0802.1017 [hep-th]].

[105] S. N. Solodukhin, "Entanglement entropy, conformal invariance and extrinsic geometry," Phys. Lett. B **665** (2008) 305 [arXiv:0802.3117 [hep-th]].

[106] I. R. Klebanov, D. Kutasov and A. Murugan, "Entanglement as a Probe of Confinement," Nucl. Phys. B **796**, 274 (2008) [arXiv:0709.2140 [hep-th]].

[107] T. Nishioka and T. Takayanagi, "AdS bubbles, entropy and closed string tachyons," JHEP **0701**, 090 (2007) [arXiv:hep-th/0611035].

[108] J. M. Maldacena, "The large N limit of superconformal field theories and supergravity," Adv. Theor. Math. Phys. **2**, 231 (1998) [Int. J. Theor. Phys. **38**, 1113 (1999)] [arXiv:hep-th/9711200].

S. S. Gubser, I. R. Klebanov and A. M. Polyakov, "Gauge theory correlators from non-critical string theory," Phys. Lett. B **428**, 105 (1998) [arXiv:hep-th/9802109].

E. Witten, "Anti-de Sitter space and holography," Adv. Theor. Math. Phys. **2**, 253 (1998) [arXiv:hep-th/9802150].

[109] O. Aharony, "A brief review of 'little string theories'," Class. Quant. Grav. **17**, 929 (2000) [arXiv:hep-th/9911147].

[110] M. R. Douglas and N. A. Nekrasov, "Noncommutative field theory," Rev. Mod. Phys. **73**, 977 (2001) [arXiv:hep-th/0106048].

[111] S. Ryu and T. Takayanagi, "Holographic derivation of entanglement entropy from AdS/CFT," Phys. Rev. Lett. **96**, 181602 (2006) [arXiv:hep-th/0603001].

"Aspects of holographic entanglement entropy," JHEP **0608**, 045 (2006) [arXiv:hep-th/0605073].

[112] R. Emparan, "Black hole entropy as entanglement entropy: A holographic derivation," JHEP **0606**, 012 (2006) [arXiv:hep-th/0603081].

S. Solodukhin, "Entanglement entropy of black holes and AdS/CFT correspondence," Phys. Rev. Lett. **97** 201601 (2006) [arXiv:hep-th/0606205].

T. Hirata and T. Takayanagi, "AdS/CFT and strong subadditivity of entanglement entropy," JHEP **0702**, 042 (2007) [arXiv:hep-th/0608213].

V. E. Hubeny, M. Rangamani and T. Takayanagi, "A covariant holographic entanglement entropy proposal," JHEP **0707**, 062 (2007) [arXiv:0705.0016 [hep-th]].

V. E. Hubeny and M. Rangamani, "Holographic entanglement entropy for disconnected regions," arXiv:0711.4118 [hep-th].

[113] N. Itzhaki, J. M. Maldacena, J. Sonnenschein and S. Yankielowicz, "Supergravity and the large N limit of theories with sixteen supercharges," Phys. Rev. D **58**, 046004 (1998) [arXiv:hep-th/9802042].

[114] A. W. Peet and J. Polchinski, "UV/IR relations in AdS dynamics," Phys. Rev. D **59**, 065011 (1999) [arXiv:hep-th/9809022].

[115] I. R. Klebanov and M. J. Strassler, "Supergravity and a confining gauge theory: Duality cascades and chiSB-resolution of naked singularities," JHEP **0008**, 052 (2000) [arXiv:hep-th/0007191].

[116] J. L. F. Barbon, I. I. Kogan and E. Rabinovici, "On stringy thresholds in SYM/AdS thermodynamics," Nucl. Phys. B **544**, 104 (1999) [arXiv:hep-th/9809033].

[117] O. Aharony, M. Berkooz, D. Kutasov and N. Seiberg, JHEP **9810**, 04 (1998) [arXiv:hep-th/9808149].

[118] A. Hashimoto and N. Itzhaki, "Non-commutative Yang-Mills and the AdS/CFT correspondence," Phys. Lett. B **465**, 142 (1999) [arXiv:hep-th/9907166].

J. M. Maldacena and J. G. Russo, "Large N limit of non-commutative gauge theories," JHEP **9909**, 025 (1999) [arXiv:hep-th/9908134].

[119] C. G. Callan, J. A. Harvey and A. Strominger, "Supersymmetric string solitons," [arXiv:hep-th/9112030].

[120] J. M. Maldacena, "Statistical Entropy of Near Extremal Five-branes," Nucl. Phys. B **477**, 168 (1996) [arXiv:hep-th/9605016].

[121] J. L. F. Barbon, C. A. Fuertes and E. Rabinovici, "Deconstructing the Little Hagedorn Holography," JHEP **0709**, 055 (2007) [arXiv:0707.1158 [hep-th]].

[122] N. Arkani-Hamed, A. G. Cohen and H. Georgi, "(De)constructing dimensions," Phys. Rev. Lett. **86**, 4757 (2001) [arXiv:hep-th/0104005].

[123] N. Arkani-Hamed, A. G. Cohen, D. B. Kaplan, A. Karch and L. Motl, "Deconstructing (2,0) and little string theories," JHEP **0301**, 083 (2003) [arXiv:hep-th/0110146].

[124] N. Dorey, "A new deconstruction of little string theory," JHEP **0407**, 016 (2004) [arXiv:hep-th/0406104].

[125] N. Seiberg and E. Witten, "String theory and noncommutative geometry," JHEP **9909**, 032 (1999) [arXiv:hep-th/9908142].

[126] M. Li and Y. S. Wu, "Holography and noncommutative Yang-Mills," Phys. Rev. Lett. **84**, 2084 (2000) [arXiv:hep-th/9909085].

[127] K. Landsteiner and J. Mas, "The shear viscosity of the non-commutative plasma," JHEP **0707**, 088 (2007) [arXiv:0706.0411 [hep-th]].

[128] J. Gomis and T. Mehen, "Space-time noncommutative field theories and unitarity," Nucl. Phys. B **591**, 265 (2000) [arXiv:hep-th/0005129].

L. Alvarez-Gaume, J. L. F. Barbon and R. Zwicky, "Remarks on time-space noncommutative field theories," JHEP **0105**, 057 (2001) [arXiv:hep-th/0103069].

[129] E. Alvarez, J. Conde and L. Hernandez, "Codimension two holography," Nucl. Phys. B **663**, 365 (2003) [arXiv:hep-th/0301123].

J. de Boer and S. N. Solodukhin, "A holographic reduction of Minkowski space-time," Nucl. Phys. B **665**, 545 (2003) [arXiv:hep-th/0303006].

D. Marolf, "Asymptotic flatness, little string theory, and holography," JHEP **0703** (2007) 122 [arXiv:hep-th/0612012].

[130] S. Minwalla, M. Van Raamsdonk and N. Seiberg, "Noncommutative perturbative dynamics," JHEP **0002**, 020 (2000) [arXiv:hep-th/9912072].

[131] H. Casini and M. Huerta, "A finite entanglement entropy and the c-theorem," Phys. Lett. B **600** (2004) 142 [arXiv:hep-th/0405111].

H. Casini, C. D. Fosco and M. Huerta, "Entanglement and alpha entropies for a massive Dirac field in two dimensions," J. Stat. Mech. **0507** (2005) P007 [arXiv:cond-mat/0505563].

H. Casini and M. Huerta, "Entanglement and alpha entropies for a massive scalar field in two dimensions," J. Stat. Mech. **0512** (2005) P012 [arXiv:cond-mat/0511014].

[132] E. Witten, "Anti-de Sitter space, thermal phase transition, and confinement in gauge theories," Adv. Theor. Math. Phys. **2** (1998) 505 [arXiv:hep-th/9803131].

[133] I. R. Klebanov and M. J. Strassler, "Supergravity and a confining gauge theory: Duality cascades and chiSB-resolution of naked singularities," JHEP **0008**, 052 (2000) [arXiv:hep-th/0007191].

[134] N. R. Constable and R. C. Myers, "Exotic scalar states in the AdS/CFT correspondence," JHEP **9911**, 020 (1999) [arXiv:hep-th/9905081].

A. Kehagias and K. Sfetsos, "On asymptotic freedom and confinement from type-IIB supergravity," Phys. Lett. B **456**, 22 (1999) [arXiv:hep-th/9903109].

S. S. Gubser, "Dilaton-driven confinement," arXiv:hep-th/9902155.

[135] J. Polchinski and M. J. Strassler, "Hard scattering and gauge/string duality," Phys. Rev. Lett. **88**, 031601 (2002) [arXiv:hep-th/0109174].

[136] P. Kraus, F. Larsen and S. P. Trivedi, "The Coulomb branch of gauge theory from rotating branes," JHEP **9903**, 003 (1999) [arXiv:hep-th/9811120].

[137] D. J. Gross and H. Ooguri, "Aspects of large N gauge theory dynamics as seen by string theory," Phys. Rev. D **58**, 106002 (1998) [arXiv:hep-th/9805129].

[138] M. Nielsen and I. Chuang, *Quantum Computation and Quantum Information*, Cambridge University Press, 2000.

[139] M. M. Wolf, F. Verstraete, M. B. Hastings and J. I. Cirac, "Area laws in quantum systems: mutual information and correlations," Phys. Rev. Lett. **100**, 070502 (2008) [arXiv:0704.3906 [quant-ph]].

[140] A. Faraggi, L. A. Pando Zayas and C. A. Terrero-Escalante, "Holographic Entanglement Entropy and Phase Transitions at Finite Temperature," arXiv:0710.5483 [hep-th].

[141] A. Chamblin, R. Emparan, C. V. Johnson and R. C. Myers, "Charged AdS black holes and catastrophic holography," Phys. Rev. D **60**, 064018 (1999) [arXiv:hep-th/9902170].

[142] S. W. Hawking and D. N. Page, "Thermodynamics Of Black Holes In Anti-De Sitter Space," Commun. Math. Phys. **87**, 577 (1983).

E. Witten, "Anti-de Sitter space, thermal phase transition, and confinement in gauge theories," Adv. Theor. Math. Phys. **2**, 505 (1998) [arXiv:hep-th/9803131].

[143] S. S. Gubser, C. P. Herzog and I. R. Klebanov, "Symmetry breaking and axionic strings in the warped deformed conifold," JHEP **0409** (2004) 036 [arXiv:hep-th/0405282].

[144] S. Kachru, X. Liu and M. Mulligan, "Gravity Duals of Lifshitz-like Fixed Points," Phys. Rev. D **78** (2008) 106005 [arXiv:0808.1725 [hep-th]].

[145] C. R. Hagen, "Scale and conformal transformations in Galilean-covariant field theory," Phys. Rev. D **5**, 377 (1972).

[146] U. Niederer, "The maximal kinematical invariance group of the free Schrödinger equation," Helv. Phys. Acta **45**, 802 (1972).

[147] M. Taylor, "Non-relativistic holography," arXiv:0812.0530 [hep-th].

[148] S. Weinberg, "The Quantum theory of fields. Vol. 1: Foundations," Cambridge, UK: Univ. Pr. (1995) 609 p.

[149] Y. Nishida and D. T. Son, "Nonrelativistic conformal field theories," Phys. Rev. D **76**, 086004 (2007) [arXiv:0706.3746 [hep-th]].

[150] M. Henkel, "Schrödinger invariance and strongly anisotropic critical systems," J. Stat. Phys **75**, 1023 (1994) [arXiv:hep-th/9310081]

[151] M. Henkel and J. Unterberger, "Schroedinger invariance and space-time symmetries," Nucl. Phys. B **660**, 407 (2003) [arXiv:hep-th/0302187].

[152] M. Luscher and G. Mack, "Global Conformal Invariance In Quantum Field Theory," Commun. Math. Phys. **41**, 203 (1975).

[153] F. Werner and Y. Castin, "The unitary gas in an isotropic harmonic trap: symmetry properties and applications," Phys. Rev. A **74**, 053604 (2006) [cond-mat/0607821].

[154] I. Bloch, J. Dalibard and W. Zwerger, "Many-Body Physics with Ultracold Gases," Rev. Mod. Phys. **80**, 885 (2008) [arXiv:0704.3011 [cond-mat.other]]

[155] S. Giorgini, L. P. Pitaevskii, S. Stringari, "Theory of ultracold Fermi gases," Rev. Mod. Phys. **80**, 1215 (2008) [arXiv:0706.3360 [cond-mat.other]]

[156] D. B. Kaplan, M. J. Savage and M. B. Wise, "A new expansion for nucleon nucleon interactions," Phys. Lett. B **424**, 390 (1998) [arXiv:nucl-th/9801034];

"Two-nucleon systems from effective field theory," Nucl. Phys. B **534**, 329 (1998) [arXiv:nucl-th/9802075].

T. Mehen, I. W. Stewart, M. B. Wise, "Conformal invariance for nonrelativistic field theory." Phys. Lett. **B 474** 145 (2000) [arXiv:hep-th/9910025]

Y. Nishida and D. T. Son, "Nonrelativistic conformal field theories," Phys. Rev. D **76** (2007) 086004 [arXiv:0706.3746 [hep-th]].

[157] Y. Nishida and D. T. Son, "An epsilon expansion for Fermi gas at infinite scattering length," Phys. Rev. Lett. **97** (2006) 050403 [arXiv:cond-mat/0604500].

Y. Nishida and D. T. Son, "Fermi gas near unitarity around four and two spatial dimensions," Phys. Rev. A **75** (2007) 063617 [arXiv:cond-mat/0607835].

[158] P. Nikolić and S. Sachdev, "Renormalization group fixed points, universal phase diagram, and $1/N$ expansion for quantum liquids with interactions near the unitarity limit," Phys. Rev. A **75**, 033608 (2007) [arXiv:cond-mat/0609106].

[159] M. Y. Veillette, D. E. Sheehy, and L Radzihovsky, "Large-N expansion for unitary superfluid Fermi gases," Phys. Rev. A **75**, 043614 (2007) [arXiv:cond-mat/0610798].

[160] D. T. Son, "Toward an AdS/cold atoms correspondence: a geometric realization of the Schroedinger symmetry," Phys. Rev. D **78** (2008) 046003 [arXiv:0804.3972 [hep-th]].

[161] K. Balasubramanian and J. McGreevy, "Gravity duals for non-relativistic CFTs," Phys. Rev. Lett. **101** (2008) 061601 [arXiv:0804.4053 [hep-th]].

[162] O. Aharony, M. Berkooz and N. Seiberg, "Light-cone description of (2,0) superconformal theories in six dimensions," Adv. Theor. Math. Phys. **2** (1998) 119 [arXiv:hep-th/9712117].

[163] C. Duval, G. W. Gibbons and P. Horvathy, "Celestial Mechanics, Conformal Structures, and Gravitational Waves," Phys. Rev. D **43** (1991) 3907 [arXiv:hep-th/0512188].

[164] C. P. Herzog, M. Rangamani and S. F. Ross, "Heating up Galilean holography," JHEP **0811** (2008) 080 [arXiv:0807.1099 [hep-th]].

[165] S. Hellerman and J. Polchinski, "Compactification in the lightlike limit," Phys. Rev. D **59** (1999) 125002 [arXiv:hep-th/9711037].

[166] P. Breitenlohner and D. Z. Freedman, "Positive Energy In Anti-De Sitter Backgrounds And Gauged Extended Supergravity," Phys. Lett. B **115**, 197 (1982).

P. Breitenlohner and D. Z. Freedman, "Stability In Gauged Extended Supergravity," Annals Phys. **144**, 249 (1982).

[167] O. Lunin and J. M. Maldacena, "Deforming field theories with U(1) x U(1) global symmetry and their gravity duals," JHEP **0505** (2005) 033 [arXiv:hep-th/0502086].

[168] E. G. Gimon, A. Hashimoto, V. E. Hubeny, O. Lunin and M. Rangamani, "Black strings in asymptotically plane wave geometries," JHEP **0308**, 035 (2003) [arXiv:hep-th/0306131].

[169] J. Maldacena, D. Martelli and Y. Tachikawa, "Comments on string theory backgrounds with non-relativistic conformal symmetry," JHEP **0810** (2008) 072 [arXiv:0807.1100 [hep-th]].

[170] A. Adams, K. Balasubramanian and J. McGreevy, "Hot Spacetimes for Cold Atoms," JHEP **0811** (2008) 059 [arXiv:0807.1111 [hep-th]].

[171] M. Alishahiha and O. J. Ganor, "Twisted backgrounds, pp-waves and nonlocal field theories," JHEP **0303** (2003) 006 [arXiv:hep-th/0301080].

[172] A. Bergman, K. Dasgupta, O. J. Ganor, J. L. Karczmarek and G. Rajesh, "Nonlocal field theories and their gravity duals," Phys. Rev. D **65** (2002) 066005 [arXiv:hep-th/0103090].

[173] A. Bergman and O. J. Ganor, "Dipoles, twists and noncommutative gauge theory," JHEP **0010** (2000) 018 [arXiv:hep-th/0008030].

[174] K. Dasgupta, O. J. Ganor and G. Rajesh, "Vector deformations of N = 4 super-Yang-Mills theory, pinned branes, and arched strings," JHEP **0104** (2001) 034 [arXiv:hep-th/0010072].

[175] L. Mazzucato, Y. Oz and S. Theisen, "Non-relativistic Branes," JHEP **0904**, 073 (2009) [arXiv:0810.3673 [hep-th]].

[176] D. Yamada, "Thermodynamics of Black Holes in Schroedinger Space," arXiv:0809.4928 [hep-th].

[177] G. T. Horowitz and D. L. Welch, "Duality invariance of the Hawking temperature and entropy," Phys. Rev. D **49** (1994) 590 [arXiv:hep-th/9308077].

[178] P. Kovtun and D. Nickel, "Black holes and non-relativistic quantum systems," Phys. Rev. Lett. **102** (2009) 011602 [arXiv:0809.2020 [hep-th]].

[179] A. Adams, A. Maloney, A. Sinha and S. E. Vazquez, "1/N Effects in Non-Relativistic Gauge-Gravity Duality," arXiv:0812.0166 [hep-th].

[180] M. Rangamani, S. F. Ross, D. T. Son and E. G. Thompson, "Conformal non-relativistic hydrodynamics from gravity," JHEP **0901** (2009) 075 [arXiv:0811.2049 [hep-th]].

[181] S. Bhattacharyya, V. E. Hubeny, S. Minwalla and M. Rangamani, "Nonlinear Fluid Dynamics from Gravity," JHEP **0802**, 045 (2008) [arXiv:0712.2456 [hep-th]].

[182] V. de Alfaro, S. Fubini and G. Furlan, "Conformal Invariance In Quantum Mechanics," Nuovo Cim. A **34** (1976) 569.

[183] G. Burdet, M. Perrin and P. Sorba, "On the automorphisms of real lie algebras," J. Math. Phys. **15** (1974) 1436.

[184] P. Havas and J. Plebanski, "Conformal extensions of the Galilei group and their relation to the Schödinger group," J. Math. Phys. **19** (1978) 482.

[185] J. Gomis, A. Poch and J. M. Pons, "Poincare Wave Equations As Fourier Transforms Of Galilei Wave Equations," J. Math. Phys. **21** (1980) 2682.

J. Gomis and J. M. Pons, "Poincare Transformations And Galilei Transformations," Phys. Lett. A **66** (1978) 463.

[186] C. Duval, G. W. Gibbons and P. Horvathy, "Celestial Mechanics, Conformal Structures, and Gravitational Waves," Phys. Rev. D **43**, 3907 (1991) [arXiv:hep-th/0512188].

C. Duval, P. A. Horvathy and L. Palla, "Conformal symmetry of the coupled Chern-Simons and gauged nonlinear Schrodinger equations," Phys. Lett. B **325** (1994) 39 [arXiv:hep-th/9401065].

C. Duval, P. A. Horvathy and L. Palla, "Conformal properties of Chern-Simons vortices in external fields," Phys. Rev. D **50** (1994) 6658 [arXiv:hep-ph/9405229].

C. Duval, P. A. Horvathy and L. Palla, "Spinors in non-relativistic Chern-Simons electrodynamics," Annals Phys. **249** (1996) 265 [arXiv:hep-th/9510114].

M. Hassaine and P. A. Horvathy, "Field-dependent symmetries of a non-relativistic fluid model," Annals Phys. **282** (2000) 218 [arXiv:math-ph/9904022].

[187] Y. Castin, "Basic theory tools for degenerate Fermi gases," arXiv:cond-mat/0612613.

[188] S. Giorgini, L. P. Pitaevskii, and S. Stringari, "Theory of ultracold atomic Fermi gases," arXiv:0706.3360[cond-mat.other].

[189] I. R. Klebanov and E. Witten, "AdS/CFT correspondence and symmetry breaking," Nucl. Phys. B **556** (1999) 89 [arXiv:hep-th/9905104].

[190] O. Aharony, S. S. Gubser, J. M. Maldacena, H. Ooguri and Y. Oz, "Large N field theories, string theory and gravity," Phys. Rept. **323**, 183 (2000) [arXiv:hep-th/9905111].

[191] A. Galindo, P. Pascual, *Quantum Mechanics I, II*, Springer-Verlag (1990).

[192] M. Banados, A. Gomberoff and C. Martinez, "Anti-de Sitter space and black holes," Class. Quant. Grav. **15** (1998) 3575 [arXiv:hep-th/9805087].

[193] M. Blau, J. Hartong and B. Rollier, "Geometry of Schroedinger Space-Times, Global Coordinates, and Harmonic Trapping," arXiv:0904.3304 [hep-th].

[194] M. Schvellinger, "Kerr-AdS black holes and non-relativistic conformal QM theories in diverse dimensions," JHEP **0812**, 004 (2008) [arXiv:0810.3011 [hep-th]].

[195] K. M. O'Hara *et. al*, "Observation of a strongly interacting degenerate Fermi gas of atoms," Science **298**, 2179 (2002).

C. A. Regal, M. Greiner, and D. S. Jin, "Observation of Resonance Condensation of Fermionic Atom Pairs," Phys. Rev. Lett. **92**, 040403 (2004).

M. Bartenstein *et. al*, "Crossover from a molecular Bose-Einstein condensate to a degenerate Fermi gas," Phys. Rev. Lett. **92**, 120401 (2004).

M. Zwierlein *et. al.*, "Condensation of Pairs of Fermionic Atoms Near a Feshbach Resonance," Phys. Rev. Lett. **92**, 120403 (2004).

J. Kinast *et. al*, "Evidence for superfluidity in a resonantly interacting Fermi gas," Phys. Rev. Lett. **92**, 150402 (2004).

T. Bourdel *et. al*, "Experimental study of the BEC-BCS crossover region in lithium 6," Phys. Rev. Lett. **93**, 050401 (2004).

[196] E. Witten, "Anti-de Sitter space, thermal phase transition, and confinement in gauge theories," Adv. Theor. Math. Phys. **2**, 505 (1998) [arXiv:hep-th/9803131].

[197] J. D. Brown, E. A. Martinez and J. W. . York, "Complex Kerr-Newman geometry and black hole thermodynamics," Phys. Rev. Lett. **66** (1991) 2281.

[198] A. Gonzalez-Arroyo and M. Okawa, "The Twisted Eguchi-Kawai Model: A Reduced Model For Large N Lattice Gauge Theory," Phys. Rev. D **27** (1983) 2397.

T. Eguchi and R. Nakayama, "Simplification Of Quenching Procedure For Large N Spin Models," Phys. Lett. B **122** (1983) 59.

T. Filk, "Divergencies in a field theory on quantum space," Phys. Lett. B **376** (1996) 53.

[199] D. Bigatti and L. Susskind, "Magnetic fields, branes and noncommutative geometry," Phys. Rev. D **62** (2000) 066004 [arXiv:hep-th/9908056].

[200] W. Mueck and K. S. Viswanathan, "Conformal field theory correlators from classical scalar field theory on AdS(d+1)," Phys. Rev. D **58** (1998) 041901 [arXiv:hep-th/9804035].

[201] D. Z. Freedman, S. D. Mathur, A. Matusis and L. Rastelli, "Correlation functions in the CFT(d)/AdS($d+1$) correspondence," Nucl. Phys. B **546**, 96 (1999) [arXiv:hep-th/9804058];

[202] Y. Nishida, "Unitary Fermi gas in the epsilon expansion", [arXiv.org:0703465].

[203] P. Nikolic and S. Sachdev, "Renormalization-group fixed points, universal phase diagram, and 1/N expansion for quantum liquids with interactions near the unitarity limit," Phys. Rev. A **75**, 033608 (2007) [arXiv:cond-mat/0609106].

[204] S. Moroz, S. Floerchinger, R. Schmidt and C. Wetterich, "Efimov effect from functional renormalization", [arXiv.org:0812.0528].

[205] V. Efimov, "Energy levels arising form the resonant two-body forces in a three-body system," Phys. Lett. **33B**, 563 (1970).

[206] M. Y. Veillette, D. E. Sheehy and L. Radzihovsky, "Large-N expansion for unitary superfluid Fermi gases," Phys. Rev. A **75**, 043614 (2007) [arXiv:cond-mat/0610798].

[207] S. Lee, S. Minwalla, M. Rangamani and N. Seiberg, "Three-point functions of chiral operators in D = 4, N = 4 SYM at large N," Adv. Theor. Math. Phys. **2**, 697 (1998) [arXiv:hep-th/9806074].

[208] I. S. Gradshteyn and I. M. Ryzhik, *Table of Integrals, Series, and Products*, 6th edition, 2000. Edited by A. Jeffrey and D. Zwillinger. Academic Press, New York.

[209] J. W. Chen and W. Y. Wen, "Shear Viscosity of a Non-Relativistic Conformal Gas in Two Dimensions," arXiv:0808.0399 [hep-th].

[210] W. D. Goldberger, "AdS/CFT duality for non-relativistic field theory," arXiv:0806.2867 [hep-th].

[211] A. Volovich and C. Wen, "Correlation Functions in Non-Relativistic Holography," arXiv:0903.2455 [hep-th].

[212] A. Akhavan, M. Alishahiha, A. Davody and A. Vahedi, "Fermions in non-relativistic AdS/CFT correspondence," arXiv:0902.0276 [hep-th].

[213] C. R. Hagen, "Scale and conformal transformations in Galilean-covariant field theory," Phys. Rev. D **5**, 377 (1972).

U. Niederer, "The maximal kinematical invariance group of the free Schrödinger equation," Helv. Phys. Acta **45**, 802 (1972).

P. Havas and J. Plebanski, "Conformal extensions of the Galilei group and their relation to the Schödinger group," J. Math. Phys. **19** (1978) 482.

[214] C. P. Herzog, M. Rangamani and S. F. Ross, "Heating up Galilean holography," JHEP **0811**, 080 (2008) [arXiv:0807.1099 [hep-th]].

A. Adams, K. Balasubramanian and J. McGreevy, "Hot Spacetimes for Cold Atoms," JHEP **0811**, 059 (2008) [arXiv:0807.1111 [hep-th]].

[215] J. Maldacena, D. Martelli and Y. Tachikawa, "Comments on string theory backgrounds with non-relativistic conformal symmetry," JHEP **0810**, 072 (2008) [arXiv:0807.1100 [hep-th]].

[216] P. Kovtun and D. Nickel, "Black holes and non-relativistic quantum systems," Phys. Rev. Lett. **102**, 011602 (2009) [arXiv:0809.2020 [hep-th]].

[217] F. L. Lin and S. Y. Wu, "Non-relativistic Holography and Singular Black Hole," arXiv:0810.0227 [hep-th].

M. Rangamani, S. F. Ross, D. T. Son and E. G. Thompson, "Conformal non-relativistic hydrodynamics from gravity," JHEP **0901**, 075 (2009) [arXiv:0811.2049 [hep-th]].

[218] J. Gomis and J. M. Pons, "Poincare Transformations And Galilei Transformations," Phys. Lett. A **66** (1978) 463.

C. Duval, G. W. Gibbons and P. Horvathy, "Celestial Mechanics, Conformal Structures, and Gravitational Waves," Phys. Rev. D **43**, 3907 (1991) [arXiv:hep-th/0512188].

O. Aharony, M. Berkooz and N. Seiberg, "Light-cone description of (2,0) superconformal theories in six dimensions," Adv. Theor. Math. Phys. **2**, 119 (1998) [arXiv:hep-th/9712117].

M. Henkel and J. Unterberger, "Schroedinger invariance and space-time symmetries," Nucl. Phys. B **660** (2003) 407 [arXiv:hep-th/0302187].

[219] J. L. F. Barbon and E. Rabinovici, "Extensivity versus holography in anti-de Sitter spaces," Nucl. Phys. B **545**, 371 (1999) [arXiv:hep-th/9805143].

J. L. F. Barbon, I. I. Kogan and E. Rabinovici, "On stringy thresholds in SYM/AdS thermodynamics," Nucl. Phys. B **544**, 104 (1999) [arXiv:hep-th/9809033].

J. L. F. Barbon, C. A. Fuertes and E. Rabinovici, "Deconstructing the Little Hagedorn Holography," JHEP **0709**, 055 (2007) [arXiv:0707.1158 [hep-th]].

[220] G. T. Horowitz and H. Ooguri, "Spectrum of large N gauge theory from supergravity," Phys. Rev. Lett. **80**, 4116 (1998) [arXiv:hep-th/9802116].

[221] S. W. Hawking and D. N. Page, "Thermodynamics Of Black Holes In Anti-De Sitter Space," Commun. Math. Phys. **87**, 577 (1983).

E. Witten, "Anti-de Sitter space, thermal phase transition, and confinement in gauge theories," Adv. Theor. Math. Phys. **2**, 505 (1998) [arXiv:hep-th/9803131].

[222] Y. Castin, "Basic theory tools for degenerate Fermi gases," arXiv:cond-mat/0612613.

S. Giorgini, L. P. Pitaevskii, and S. Stringari, "Theory of ultracold atomic Fermi gases," arXiv:0706.3360[cond-mat.other].

[223] T. Azeyanagi, W. Li and T. Takayanagi, "On String Theory Duals of Lifshitz-like Fixed Points," arXiv:0905.0688 [hep-th].

[224] A. Pakman and A. Parnachev, "Topological Entanglement Entropy and Holography," JHEP **0807** (2008) 097 [arXiv:0805.1891 [hep-th]].